

## ABSTRACT

Title of Document: SPECIFIC TARGETING OF RPW8 FAMILY PROTEINS TO AND *DE NOVO* BIOGENESIS OF THE EXTRAHAUSTORIAL MEMBRANE IN ARABIDOPSIS CELLS INVADED BY POWDERY MILDEW FUNGUS

Robert Berkey, Doctor of Philosophy, 2013

Directed By: Associate Professor Shunyuan Xiao, Institute for Bioscience and Biotechnology Research & Department of Plant Sciences and Landscape Architecture

The unique plant resistance (R) protein RPW8.1 and RPW8.2 confers broad-spectrum resistance in *Arabidopsis* to all tested isolates of *Golovinomyces* spp. fungi, the casual agents of powdery mildew disease in multiple plant species. RPW8.2 is specifically targeted to the extra-haustorial membrane (EHM) that encases the fungal feeding structure named the haustorium and represents the host-pathogen interface. EHM-localization of RPW8.2 correlates with haustorium-targeted host defense, providing subcellular evidence for the broad-spectrum resistance mediated by RPW8.2.

*RPW8.1* and *RPW8.2* belong to a small gene family in the *Arabidopsis* and *Brassica* lineages. However, the cellular function of the other family members remains to be functionally characterized. Here, I report that all homologs of *RPW8* (designated HR#) examined are EHM-residents, suggesting that the RPW8 family proteins share a common EHM-targeting signal. Moreover, through a reverse genetics approach I show that three *Arabidopsis* homologs, i.e. *AtHR1*, *AtHR2* and *AtHR3*, appear to play a role in salicylic acid-dependent basal resistance against powdery mildew and perhaps other biotrophic pathogens. These results support our hypothesis that the two atypical resistance *R* genes, *RPW8.1* and *RPW8.2* evolved from duplication and functional diversification (enhancement) of a more ancient component of basal immunity in *Arabidopsis* (**Chapter 2**). Furthermore, I provide the first piece of cell biological evidence to suggest that the enigmatic EHM is formed via *de novo* synthesis rather than simple extension and differentiation of the host plasma membrane in the invaded host cell during the biogenesis of the fungal haustorium (**Chapter 3**). I also summarize my contribution to a project that aims to utilize RPW8 as a delivery vehicle to confer novel resistance in other crop species against a variety of fungal or oomycete haustorium-forming pathogens (**Chapter 4**) and ongoing efforts to further dissect the RPW8 defense and trafficking pathways in relation to bioactive phosphoinositides (**Chapter 5**) and to characterize putative interacting or signaling components of RPW8-mediated defense mechanisms against powdery mildew in *Arabidopsis* (**Chapter 6**).

SPECIFIC TARGETING OF RPW8 FAMILY PROTEINS TO AND *DE NOVO*  
BIOGENESIS OF THE EXTRAHAUSTORIAL MEMBRANE IN ARABIDOPSIS  
CELLS INVADDED BY POWDERY MILDEW FUNGUS

By:

Robert Berkey

Dissertation submitted to the Faculty of the Graduate School of the  
University of Maryland, College Park, in partial fulfillment  
Of the requirements for the degree of  
Doctor of Philosophy  
2013

Advisory Committee:  
Associate Professor Shunyuan Xiao, Advisory Chair  
Professor Donald Nuss  
Professor James Culver  
Professor Zhongchi Liu  
Professor Heven Sze, Dean's Representative

© Copyright by  
Robert Berkey  
2013



## Dedication

This dissertation is dedicated to my wife and best friend Katie...

And to my parents for their unconditional love, support, and encouragement.

## Acknowledgements

First and foremost, I would like to thank my mentor Dr. Shunyuan Xiao. Dr. Xiao has not only helped me become the scientist I am today, but has been an amazing mentor to our entire group with his academic, professional, and personal support. His dedication to advancing scientific knowledge is second to none, and I will be forever grateful for his support, teachings, and inspiration.

I would also like to thank all my committee members for their support and advice over the years. The valuable teachings, suggestions, and critiques offered to me have been fruitful during my graduate career and will carry with me moving forward.

I would also like to extend my gratitude to all past and present members of the Xiao laboratory. The Xiao lab quickly became more like a family unit than a collection of scientist co-workers and I couldn't imagine working with another group over the past several years. I would like to thank all the Xiao lab postdocs for their exceptional guidance, patience, and support over the years. Specifically, I would like to acknowledge Wenming Wang, who is an exceptionally skilled scientist who taught me numerous experimental skills and concepts across multiple disciplines. I would also like to thank all other Xiao lab members for their unwavering support and friendship. I know we will always maintain strong relationships and I wish you all the best in your future scientific endeavors.

Lastly, I would like to thank all members of the UMCP and IBBR communities and outside collaborators and colleagues who have offered support to the projects or initiatives in the Xiao lab.

## Table of Contents

Dedication .....	ii
Acknowledgements .....	iii
Table of Contents .....	iv
List of Tables .....	vii
List of Figures .....	viii
List of Abbreviations .....	xi
Chapter 1: Introduction and Literature Review .....	1
Importance of Plant Resistance to Pathogens.....	1
Plant-Innate Immune System .....	2
Overview.....	2
Plant <i>R</i> Genes.....	7
Structural Characteristics of R Proteins.....	7
R-Avr Recognition and Defense Signaling.....	11
Plant-Powdery Mildew Interaction .....	17
Life Cycle of Powdery Mildew.....	17
The Extra-Haustorial Membrane – The Host-Pathogen Interface.....	19
Pre- and Post- Invasion Resistance Mechanisms.....	20
<i>RPW8</i> , a Unique Resistance Gene Locus.....	22
Project Aims & Questions .....	30
Chapter 2: Functional Characterization of <i>RPW8</i> Homologs in <i>Arabidopsis thaliana</i> and <i>Brassica oleracea</i> .....	33
Introduction .....	33
Results .....	35
Overexpression of <i>RPW8</i> Homologs Enhances Resistance to Powdery Mildew.....	35
Genetic Depletion of <i>HR1</i> , <i>HR2</i> , or <i>HR3</i> Results in Enhanced Disease Susceptibility .....	37
<i>RPW8</i> Homologs Are Likely Functionally Redundant .....	40
Expression of <i>HR3</i> by the <i>RPW8.2</i> Promoter Enhances Resistance to Powdery Mildew .....	41
Despite Being Microscopically Undetectable, Expression of HR3-YFP Results in Necrotic Cell Death .....	45
All Examined <i>RPW8</i> Homologs Are Localized to the Extrahaustorial Membrane.....	50
YFP-HR3 is Translocalized to the Callosic Papilla Region via a BFA-sensitive Endosomal Recycling Pathway .....	57
Discussion.....	65
Functional Diversification of <i>RPW8.2</i> from <i>HR3</i> .....	65

RPW8 Family Proteins May Function as Sorting Adaptors?.....	69
Materials & Methods .....	72
Chapter 3: Origin of the Extra-haustorial Membrane (EHM) .....	79
Introduction .....	79
Results .....	82
YFP-HR3 and RPW8.2-RFP Are Colocalized at the EHM .....	82
The EHM Appears to be <i>de novo</i> Synthesized .....	82
Discussion .....	87
Materials & Methods .....	90
Chapter 4: Utilization of RPW8.2 to Target Antimicrobial Cargos to the Host-pathogen Interface.....	91
Introduction .....	91
Results .....	97
RPW8.2 is a Type I Membrane Protein .....	97
Targeting Antimicrobial Cargos to the Host-pathogen Interface .....	104
Engineering a Cargo-Release Mechanism Subsequent to Targeted Delivery.....	107
Discussion .....	114
Materials & Methods .....	119
Chapter 5: Towards Understanding the Mechanisms Underlying EHM-specific Targeting of RPW8 Family Proteins.....	126
Introduction .....	126
Results & Discussion.....	129
A PI(3)P Biosensor is Transiently Enriched at the EHM.....	129
RPW8.2 May Preferentially Bind PI(3)P.....	137
Materials & Methods .....	146
Chapter 6: Initiatives in Other Projects.....	153
I. PLD $\delta$ is Dispensable for RPW8-mediated Resistance But is Essential for Basal Resistance.....	153
Introduction.....	153
Results.....	157
Discussion.....	164
Materials & Methods.....	166
II. ATJ3, a Putative RPW8.2-Interacting Protein, is Required for RPW8-mediated and Basal Resistance.....	168
Introduction.....	168
Results.....	170
Discussion.....	176
Materials & Methods.....	178

Chapter 7: Conclusions & Perspectives.....	180
1. How does this study contribute to our understanding of the functional origin of RPW8? .....	180
2. How does this study contribute to our understanding of the host-pathogen interface? .....	182
3. How does this study contribute to our understanding of the EHM-directed protein/membrane trafficking? .....	183
4. Can RPW8 be used as a delivery vehicle to confer novel resistance against haustorium-forming pathogens? .....	184
References.....	186

## List of Tables

Table 1. Conservation and Diversity of Plant R Proteins.....	9
Table 2. <i>PLA</i> and <i>PLD</i> Isoforms.....	167
Table 3. <i>ATJ2</i> and <i>ATJ3</i> Mutant Lines.....	179

## List of Figures

Figure 1-1.	A “zigzag” Model Illustrating the Output of the Plant Immune System.....	6
Figure 1-2.	Overview of the Signaling Pathways Involved in Plant Defense.....	16
Figure 1-3.	<i>Arabidopsis</i> Haplotypes and Response to Powdery Mildew.....	24
Figure 1-4.	Gene Organization of the Syntenic <i>RPW8</i> Loci from <i>Arabidopsis</i> and <i>Brassica</i> .....	26
Figure 1-5.	<i>RPW8.2</i> is Specifically Localized to the EHM.....	29
Figure 2-1.	Overexpression of <i>RPW8</i> Homologs Enhances Resistance to Powdery Mildew.....	36
Figure 2-2.	Genetic Depletion of <i>HR1</i> , <i>HR2</i> and <i>HR3</i> Enhances Susceptibility to Powdery Mildew.....	39
Figure 2-3.	<i>HR1</i> , <i>HR2</i> and <i>HR3</i> are Likely Functionally Redundant.....	42
Figure 2-4.	Expression of <i>HR3</i> by the <i>RPW8.2p</i> Enhances Resistance to Powdery Mildew.....	44
Figure 2-5.	<i>HR#</i> -YFP Proteins are Undetectable and Expression of <i>HR3</i> -YFP Results in Necrotic Cell Death.....	46
Figure 2-6.	Chimeric R82n- <i>HR3c</i> is Functional While <i>HR3n</i> -R82c Remains Undetectable.....	49
Figure 2-7.	N-terminally Fused <i>RPW8</i> Family Member Proteins are Localized to the Plasma Membrane.....	51
Figure 2-8.	All <i>RPW8</i> Homologs are Localized to the Extrahaustorial Membrane.....	55
Figure 2-9.	YFP- <i>RPW8</i> Homologs Show Focal Accumulation Around the Fungal Penetration Site.....	59
Figure 2-10.	Translocation of YFP- <i>HR3</i> to the Penetration Site is BFA-Sensitive.....	60
Sup-Fig 2-1.	Localization of YFP- <i>HR3</i> to the Penetration Site is BFA-Sensitive.....	62
Sup-Fig 2-2.	The YFP-tagged N-terminal Coiled Coil Domain of <i>AtNRG1.2</i> is Not Localized at the EHM.....	64

Figure 3-1.	The Haustorium of Powdery Mildew .....	81
Figure 3-2.	Schematic Illustration of Three Possible Scenarios of Protein Localization Following Cycloheximide Treatment.....	84
Figure 3-3.	The Extra-haustorial Membrane Appears to be <i>de novo</i> Synthesized.....	85
Figure 4-1.	RPW8 is Targeted to the Host-Pathogen Interface of Other Pathogens.....	93
Figure 4-2.	Strategy for Using RPW8 as a Delivery Vehicle.....	96
Figure 4-3.	Subtilisin Can Cleave YFP from the RPW8-YFP fusion protein <i>in vitro</i> .....	99
Figure 4-4.	RPW8.2 is a Type I Membrane Protein.....	101
Figure 4-5.	RPW8.2-AtPR2 Confers Resistance with a High Cost.....	106
Figure 4-6.	Sp-MTK-RPW8.2 May Confer Resistance with A Lower Cost.....	108
Figure 4-7.	Subtilisin Cleaves YFP-PCS-14-3-3 $\lambda$ <i>in vivo</i> .....	112
Figure 4-8.	SP-YFP-PCS-RPW8.2 Is Expressed But YFP May Be Quenched...	116
Figure 5-1.	Phosphoinositides are Spatial Landmarks of Eukaryotic Cells.....	128
Figure 5-2.	PI(3)P is Transiently Enriched in the EHM Upon Haustorial Differentiation.....	130
Figure 5-3.	The PI(3)P-biosensor is Colocalized with RPW8.2 at the EHM.....	133
Figure 5-4.	Sp-GmPH1 is Secreted to the Extracellular Space.....	136
Figure 5-5.	Putative EHM-targeting Motifs are Conserved Among RPW8 Family Members.....	139
Figure 5-6.	RPW8 Family Members Bind PI(3)P in Lipid Filter Assays.....	140
Figure 5-7.	Scanning Mutants of GST-RPW8.2 for Binding Assays.....	143



Figure 6-1.	Phospholipids are Cleaved by Diverse Phospholipases.....	156
Figure 6-2.	<i>PLD<math>\delta</math></i> is Involved in Basal Immunity Against Powdery Mildew.....	158
Figure 6-3.	<i>PLD<math>\delta</math></i> is Not Required for <i>RPW8</i> -mediated Resistance.....	161
Figure 6-4.	<i>PLD<math>\delta</math></i> is Not an EHM Resident Protein.....	163
Figure 6-5.	<i>ATJ2</i> and <i>ATJ3</i> are Involved in Basal Immunity Against Powdery Mildew.....	171
Figure 6-6.	<i>atj3</i> <i>-/-</i> Does Not Compromise <i>RPW8</i> -EHM Localization.....	174
Figure 6-7.	<i>ATJ3</i> is Involved in Basal Resistance Against <i>Pseudomonas syringae</i> .....	175
Figure 7-1.	A Summary and a Working Model.....	185

## List of Abbreviations

AAs	Amino acids
ABA	Absciscic acid
amiRNA	Artificial micro RNA
<i>At</i>	<i>Arabidopsis thaliana</i>
Avr	Avirulence factors
BAK1	BRI1 ASSOCIATED KINASE
BIK1	<i>BOTRYTIS</i> -INDUCED KINASE 1
BFA	Brefeldin A
<i>Bo</i>	<i>Brassica oleracea</i>
<i>Br</i>	<i>Brassica rapa</i>
CC	Coiled-coil
CHIB	CHITINASE B
CHX	Cycloheximide
CLR	CATERPILLER
CNL	CC domain containing subfamily
COI1	CORONATINE-INSENSITIVE 1
CWA	Cell wall apposition
DAG	Diacylglycerol
DGK	DIACYLGLYCEROL KINASE
EDR	Enhanced disease resistance
EDR1	ENHANCED DISEASE RESISTANCE 1
EDS	Enhanced disease susceptibility
EDS1	ENHANCED DISEASE SUSCEPTIBILITY 1
EDS5	ENHANCED DISEASE SUSCEPTIBILITY 5
EFR	EF-Tu RECEPTOR
EF-Tu	Elongation Factor Tu
EHC	Encasement of the haustorial complex
EHM	Extra-haustorial membrane
EHX	Extra-haustorial matrix
EIN2	ETHYLENE INSENSITIVE 2
EIN3	EHTYLENE INSENSITIVE 3
eLRR	Extracellular leucine-rich repeat
ER	Endoplasmic reticulum
ERF1	ETHYLENE RESPONSE FACTOR 1
ET	Ethylene
ETI	Effector-triggered immunity

ETS	Effector-triggered susceptibility
FLS2	FLAGELLIN SENSITIVE 2
<i>Gc</i>	<i>Golovinomyces cichoracearum</i>
GST	Glutathione S-transferase
HC	Haustorial complex
HEL	HEVEIN-LIKE PROTEIN
<i>Hpa</i>	<i>Hyaloperonospora arabidopsidis</i>
HR	Hypersensitive response
HR#	Homologs of RPW8
Hsp	Heat shock protein
IP <sub>3</sub>	Inositol 1,4,5-trisphosphate
JA	Jasmonic acid
JAZ	Jasmonate ZIM domain
LRR	Leucine-rich repeats
LSCM	Laser scanning confocal microscopy
LSD1	LESION SIMULATING DISEASE 1
MAMP	Microbe-associated molecular patterns
MAPK	Mitogen-activated protein kinases
MS	Murashige and Skoog
<i>Mt</i>	<i>Medicago truncatula</i>
MT	Mutant
MYA	Million years ago
NBS	Nucleotide binding site
NDR1	NON-RACE SPECIFIC DISEASE RESISTANCE PROTEIN 1
NLRs	nucleotide-binding domain, leucine rich containing proteins
NO	Nitric oxide
Nod	Nucleotide-binding oligomerization domain
NP	Native promoter
NPR1	NON-EXPRESSOR OF PR GENES 1
NRG1	N-required gene 1
PA	Phosphatidic acid
PAD4	PHYTOALEXIN DEFICIENT 4
PAM	Periabascular membrane
PAMP	Pathogen-associated molecular patterns
PAPP2C	PHYTOCHROME-ASSOCIATED PROTEIN PHOSPHATE TYPE 2C
PC	Phosphatidylcholine
PCS	Protein cleavage site

PDF	PLANT DEFENSIN PROTEINS
PDF1.2	PLANT DEFENSIN 1.2
PE	Phosphatidylethanolamine
PEN	Penetration resistance genes
PI	Propidium Iodide
PIs	Phosphoinositides
PL#	Phospholipase enzyme
PM	Plasma membrane
PR	Pathogenesis related genes
PRRs	Pattern recognition receptors
PS	Phosphatidylserine
<i>Pst</i> DC3000	<i>Pseudomonas syringae</i> pv. <i>tomato</i> DC3000
PtdIns	phosphatidyl-inositol
PTI	PAMP-triggered immunity
<i>R</i> or <i>R</i>	Resistance gene or protein
RFP	Red fluorescent protein
RLKs	Receptor-like kinases
RLPs	Receptor-like transmembrane proteins
ROS	Reactive oxygen species
RT	Reverse-transcription
SA	Salicylic acid
SAR	Systemic acquired resistance
Sbt	Subtilisin
SCD	Spontaneous cell death
SHL	Spontaneous HR-like cell death
SID2	SALICYLIC ACID INDUCTION DEFICIENT 2
SGT1	Suppressor of G-two allele of SKP1
SNARE	Soluble N-ethylmaleimide-sensitive factor attachment protein receptor
Sp	Signal Peptide
THI2.1	THIONIN 2.1
TIR	Toll and interleukin-1 receptor
TLR	Toll-like receptor
TM	Transmembrane domain
UBC21	Ubiquitin-Conjugating Enzyme 21
WT	Wild-type
YFP	Yellow fluorescent protein

## Chapter 1: Introduction and Literature Review

### Importance of Plant Resistance to Pathogens

Food security is a measure of the assurance that individuals have access to sufficient, safe and nutritious food to maintain a healthy and active life ([World Health Organization, 2012](#)). Unfortunately, it is estimated that nearly 1 billion people globally are suffering from severe hunger and poverty ([Food and Agricultural Organization, 2010](#)). On top of the existing global food security pressures, a growing world population, rising incomes, increasingly scarce resources, changing climates and other concerns are threatening to exacerbate these pressures ([Gates Foundation: Agricultural Development, 2011](#)).

One major food security concern is that on a global scale, 10-15% of crops is lost due to diseases caused by diverse plant pathogens including viruses, bacteria, oomycetes, fungi, and nematodes (Strange and Scott, 2005; Oerke, 2007). In some instances, the effects of plant diseases can be extremely damaging to individuals and regional societies, as exemplified by well-known historic tragedies: the Great Irish Famine of the 1840s which was largely triggered by the devastating potato late blight disease caused by *Phytophthora infestans*, and the Great Bengal Famine of 1943 whose direct cause was the devastation of the regional staple rice crop by *Cochliobolus miyabeanus*. The emergence of highly virulent pathogens again raises the alarm for regional or global food security. For example, Ug99, a new strain of stem rust (*Puccinia graminis* f. sp. *tritici*) discovered in Uganda in 1999 overcomes most resistant wheat cultivars and is rapidly spreading to Asia and other parts of the world. *Magnaporthe oryzae*, a pathogen closely related to the

causal fungus of rice blast (the major rice disease) is now threatening wheat production in South America (Singh et al., 2011; Cruz et al., 2012).

Therefore, the need to protect crops from pathogens to ensure food security has never been more pressing. Because plants have evolved complex immune systems to combat various pathogens, the best strategy to control diseases and mitigate losses involves the utilization of naturally evolved disease resistance genes and mechanisms of plants. As such, understanding the mechanisms of natural resistance through comprehensive molecular genetic and genomic studies is crucial for improving disease resistance of crop plants through genetic engineering technology in combination with classical breeding programs.

## **Plant Innate Immune System**

### **Overview**

Despite their sessile nature and lacking of a somatically adaptive immune system, plants have evolved complex immune systems that can effectively protect them against various microbial pathogens. Preformed physical and chemical barriers such as leaf hairs, cuticles, rigid cell walls, and pre-existing antimicrobial compounds generally function to prevent/reduce microbial invasion. Should invading microbes breach these pre-formed barriers, a complex innate immune system consisting of two mechanistically interconnected branches will be activated to fight against the infection (Nurnberger et al., 2004; Chisholm et al., 2006; Thomma et al., 2011). The first branch is similar to the innate immune system of animals and is elicited upon the recognition of pathogen (or microbe)-associated molecular patterns (PAMPs or MAMPs) by cell surface-localized

pattern recognition receptors (PRRs). PAMPs are pathogen-specific molecules that are highly conserved in pathogens of an entire class and often are required for the survival of the pathogens (Gomez-Gomez and Boller, 2000; Zipfel et al., 2006). For example, flagellin and translation elongation factor-Tu (EF-Tu) of plant pathogenic bacteria are two characterized PAMPs that are recognized by two plasma membrane (PM)-localized PRRs, FLAGELLIN SENSITIVE 2 (FLS2) and EF-TU RECEPTOR (EFR) respectively (Gomez-Gomez and Boller, 2000; Zipfel and Felix, 2005; Zipfel et al., 2006). Both FLS2 and EFR are members of a large receptor-like kinase (RLKs) family that are structurally similar to the toll-like immune receptors (TLRs) of animals (Ronald and Beutler, 2010). PAMP-triggered immunity (PTI) is an evolutionary ancient defense mechanism that protects plants against a plethora of potential pathogens (Nurnberger et al., 2004; He et al., 2006).

The second branch of induced plant innate immunity is activated upon recognition of pathogen effectors by cell-surface receptor-like proteins (RLPs) or intracellular immune receptors belonging to the nucleotide binding site (NBS) leucine-rich-repeat (LRR) superfamily. This branch of immune mechanism is thought to have co-evolved along with host adaption of invading microbes (Chisholm et al., 2006). Faced with selective pressures to survive, invading microbes gradually overcome PTI by delivering effector proteins into plant cells to interfere with the host immune system and cause diseases (Kim et al., 2005; He et al., 2006; Janjusevic et al., 2006; Xiang et al., 2008). To counterattack effector-triggered disease, plants have evolved RLP and NBS-LRR immune receptors which are historically called resistance (R) proteins to specifically detect the presence or activity of the pathogen effectors (called avirulence factors (Avr)

once recognized by R proteins) and trigger defense response referred to as effector-triggered immunity (ETI). ETI or *R*-gene dependent resistance often features an induction of pathogenesis-related (PR) genes, fortification of the cell wall, synthesis of antimicrobial peptides, a localized production of reactive oxygen species (ROS), and in most cases, the hypersensitive response (HR). HR is a form of plant programmed cell death at the site of infection that is analogous to apoptosis in animals (Hammond-Kosack and Jones, 1997; Dangl and Jones, 2001; van Doorn, 2011). In addition to the barrage of local defense responses, plants also possess the ability to defend against subsequent attack in uninfected tissues through the activation of systemic acquired resistance (SAR). SAR is a whole plant resistance response that provides enhanced immunity to secondary infection by a wide range of pathogens (Durrant and Dong, 2004).

Aggressive pathogens suppress ETI through mutation or deletion of the recognized Avr genes and/or development of new effectors that can evade host recognition and subvert ETI. This co-evolutionary struggle between plant hosts and pathogens is illustrated by a four phased “zigzag” model (Jones and Dangl, 2006) (**Figure 1-1**). Evidence suggests that ETI may be mechanistically connected with PTI to fortify the plant innate immune system against evolving pathogens in an “arms-race” model (Kim et al., 2005; He et al., 2006; Jones and Dangl, 2006; Nomura et al., 2006; Shen et al., 2007). For example, one study by Nomura and colleagues showed that HopM1, a conserved effector protein of the bacterial pathogen *Pseudomonas syringae*, targets an immunity-linked protein *AtMIN7* in *Arabidopsis thaliana* for degradation (Nomura et al., 2006). More recently, Nomura and colleagues revealed that not only is *AtMIN7* required for PTI and ETI, but that upon recognition of AvrRpt2, AvrPphB or



HopA1 in Arabidopsis ETI blocks the ability of *Pst DC3000* to destabilize AtMIN7 (Nomura et al., 2011).

PTI is effective against most pathogens and generally operates in all individuals of a plant species because both PRRs and their corresponding PAMPs are highly conserved in plants and (potential) pathogens respectively. In contrast, ETI (i.e. *R*-gene resistance) in most cases is only effective against one or a few strains of a particular pathogen that possesses an Avr protein recognized by an R protein. ETI is also less stable and may be overcome by pathogens in a short period of time (e.g. many resistant cultivars last only 5-10 years in field). As a consequence of the co-evolutionary arms-race between plants and pathogens (**Figure 1-1**), both the *R*-gene loci and *Avr* gene loci are highly polymorphic.

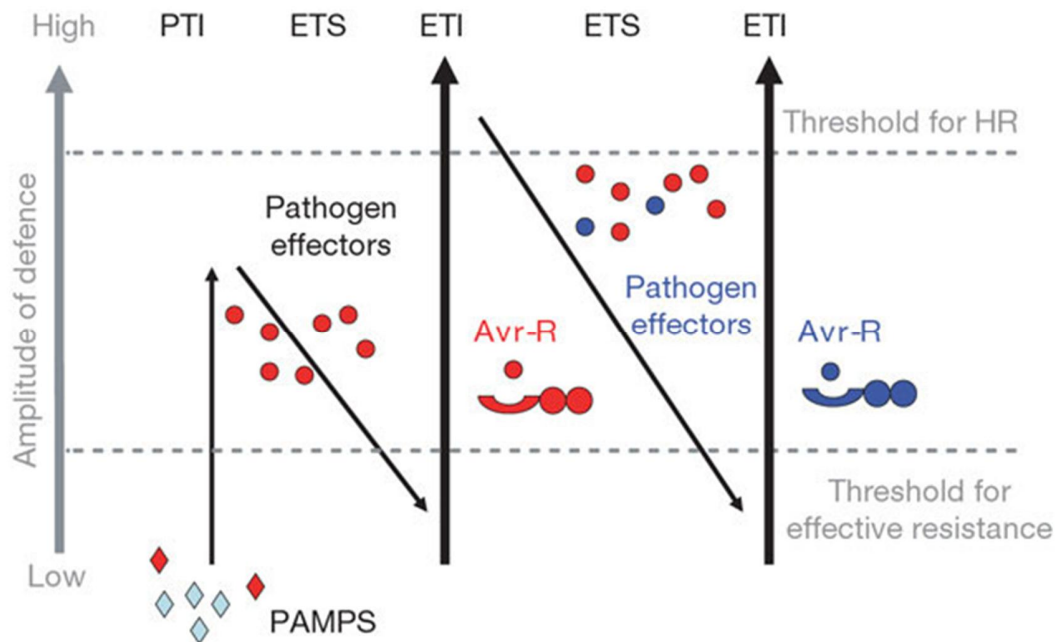


**Figure 1-1. A “zigzag” Model Illustrating the Output of the Plant Immune System.**

This figure is from Jones and Dangl, 2006. The co-evolutionary arms race between plants and pathogens is illustrated by a four phased “zigzag” model. In phase 1, plants detect PAMPs (diamonds) via PRRs to trigger PTI. In phase 2, successful pathogens use effectors to mitigate PTI resulting in ETS (effector-triggered susceptibility). In phase 3, an effector (red circle) is recognized by an R protein, activating effector-triggered immunity (ETI). In phase 4, aggressive pathogens suppress ETI through Avr mutation/deletion (blue circle) and selection favors new plant R proteins that can recognize the newly acquired effector to re-establish ETI. **PAMPS**= pathogenesis-associated molecular patterns; **PTI**= PAMP-triggered immunity; **ETS**= effector-triggered susceptibility; **ETI**= effector-triggered immunity; **Avr**= avirulence proteins; **R**= resistance proteins; **HR**= hypersensitive response.

## **Plant *R* Genes**

In the past 20 years, over 100 plant *R* genes have been isolated from *Arabidopsis* and many other plant species. Most characterized *R* genes are members of the *NBS-LRR* superfamily, suggesting that *NBS-LRR* genes are dedicated to plant innate immunity. Whole genome sequencing revealed that all genomes of higher plants contain a large number of *NBS-LRR* genes as there are ~150 *NBS-LRR* genes in the *Arabidopsis* genome and over 500 in the rice genome (Meyers et al., 2003; Monosi et al., 2004). *NBS-LRR* genes are also found in lower plants such as moss and other non-vascular plants suggesting an ancient origin (Mun et al., 2009; Jupe et al., 2012).













*NBS-LRR* encoding genes are also often clustered within many plant genomes suggesting that duplications of large genome segments and local gene duplications may have contributed to the formation of specific *R* gene clusters in plants (Michelmore and Meyers, 1998; Richly et al., 2002; Meyers et al., 2003). Duplicated *NBS-LRR* genes were probably subjected to selection by various genetic mechanisms, resulting in high levels of intraspecific and interspecific variation (Baumgarten et al., 2003; Kuang et al., 2004; Meyers et al., 2005). Therefore, orthologous relationships are generally difficult to determine because of lineage-specific gene duplications, losses and evolution resulting in family-specific subfamilies (Akita and Valkonen, 2002; Zhou et al., 2004). It is conceivable that the evolution and maintenance of a large and diverse assortment of plant *R* genes among different plant species reflects the capacity that plants have evolved to fight against various pathogens (Xiao et al., 2008).

## **Structural Characterizations of *R* Proteins**

Based on both the deduced structures and/or biochemical functions, plant R proteins can be classified into three different major classes: (1) the NBS-LRR super family, (2) the extracellular (e)LRR-containing RLPs or receptor-like protein kinases (RLKs), and (3) atypical *R* proteins that do not contain an LRR domain (Hammond-Kosack and Jones, 1997; Dangl and Jones, 2001) (**Table 1**). The NBS-LRR class is the largest and can be further divided into two subclasses based on the features of their N-terminus region. One subclass contains an N-terminal TIR domain that shows homology to the *Drosophila* toll and mammalian interleukin-1 (IL-1) receptors and is represented by N from tobacco (Whitham et al., 1994) and L6 from flax (Lawrence et al., 1995) and is called TIR-NBS-LRRs. The other subclass contains a putative coiled coil (CC) domain in the N-terminus and is called CC-NBS-LRRs and is represented by RPS2 and RPM1 from Arabidopsis (Bent et al., 1994; Grant et al., 1995).

eLRR-type proteins play key roles in both plant defense and development by perceiving extracellular signals of pathogen effectors or plant hormones (van der Hoorn et al., 2005). As a representative of the RLP-type R genes, the *Cf* genes of tomato confer resistance against the fungal pathogen *Cladosporium fulvum* (Fritz-Laylin et al., 2005; van der Hoorn et al., 2005). Genetically characterized RLK-type *R* genes include rice *Xa21* and *Xa26* that confer resistance to multiple strains of *Xanthomonas oryzae* pv. *oryzae* (Song et al., 1995; Sun et al., 2004). However, *Xa21* was also recently shown to be a PRR (similar to FLS2) that recognizes Ax21, a PAMP from the *Xanthomonas oryzae* (Lee et al., 2009).

The NBS-LRR R proteins share structural similarity to the intracellular immune receptor proteins of the CATERPILLER (CLR) and Nucleotide-binding oligomerization

R protein Classes	Schematic domain structures <sup>a</sup>	Examples	Predicted functions	References
<b>NBS-LRR</b>		N, L6, RPP5	receptor	(Whitham et al., 1994), (Lawrence et al., 1995), (Parker et al., 1997)
		RPM1, RPS2, I2	receptor	(Bent et al., 1994), (Grant et al., 1995), (Ori et al., 1997)
		RRS1-R	receptor	(Deslandes et al., 2002)
<b>eLRR</b>		CF9, RPP27	receptor	(Jones et al., 1994), (Tor et al., 2004)
		Xa21, Xa26	receptor	(Song et al., 1995), (Sun et al., 2004)
		Ve1, Ve2	receptor	(Kawchuk et al., 2001)
<b>Atypical</b>		Pto, PBS1	host target?	(Martin et al., 1993), (Swiderski and Innes, 2001)
		RPG1	receptor?	(Brueggeman et al., 2002)
		RPW8	haustoria constraint	(Xiao et al., 2001)
		Xa27	?	(Gu et al., 2005)
		Xa13	Sugar transporter	(Chu et al., 2006), (Chen et al., 2010)
		MLO	negative regulator of PCD	(Buschges et al., 1997)
<sup>a</sup> TIR, toll and interleukin-1 receptor; NBS, nucleotide binding site; (e)LRR, (extracellular) leucine rich repeats; CC, coiled coil; Kin, kinase; PEST, protein degradation domain; ECS, endocytosis cell signaling domain; W, WRKY domain; TM, predicted transmembrane helix.				

**Table 1. Conservation and Diversity of Plant R Proteins.**

domain (Nod) protein families (i.e. Nod1, Nod2 and NALP3) which also contain the NBS and LRR domains but differ in the N-terminus (Viala et al., 2004; Ausubel, 2005; Correa et al., 2012). However, unlike plant NBS-LRR proteins (which recognize pathogen effector proteins); animal Nod-like receptors (NLRs) are intracellular PRRs recognizing PAMPs (Martinon and Tschopp, 2005; Kawai and Akira, 2010). Interestingly, the TIR domain is also shared between the TIR-NBS-LRR of plants and animal TLRs and their adaptor proteins: MyD88, MAL, TRIF, TRAM and SARM (O'Neill and Bowie, 2007; Ve et al., 2012). The structural and functional relatedness between the immune receptor proteins of plants and animals suggests that innate immunity between plants and animals evolved through convergent evolution (Yue et al., 2012).

The remaining group of genetically defined plant *R* genes encode structurally diverse proteins that unlikely function as receptors because they lack an LRR domain for ligand perception. One of the most highly studied atypical *R* genes is *Pto* from tomato that confers race-specific resistance to the bacterial pathogen *Pseudomonas syringae* carrying the effectors *AvrPto* or *AvrPtoB* (Martin et al., 1993; Tang et al., 1999). The *Pto* gene encodes a Ser/Thr kinase that is involved in direct recognition of the Avr proteins from *Pseudomonas syringae* (Tang et al., 1999; Eckardt, 2004; Dong et al., 2009) and physically interacts and requires Prf, a CC-NBS-LRR protein for function (Mucyn et al., 2006; Gutierrez et al., 2010). These findings contributed to a better understanding as to how NBS-LRR proteins recognize Avr proteins (see later text). One other atypical *R* gene is *RPW8* from Arabidopsis, which is the subject of this project (see details in later text).

## **R-Avr Recognition and Defense Signaling**

How NBS-LRR receptors recognize specific effector ligands has been the subject of extensive studies in the past 15 years. By studying the interaction specificity between different flax genotypes and different strains of the flax rust pathogen *Melampsora lini*, Flor proposed the “gene-for-gene” hypothesis to interpret the plant-pathogen interaction specificity at the genetic level (Flor, 1956). This hypothesis implies a direct R (receptor) - Avr (ligand) interaction between a specific R protein functioning as the receptor the pathogen-derived Avr protein as the ligand. However while some direct interactions have been documented (Dodds et al., 2006; Kanzaki et al., 2012; Saunders et al., 2012), the majority of known R-Avr interaction pairs fail to show any actual physical interaction (Mackey et al., 2002; Mackey et al., 2003; Ade et al., 2007). Furthermore, one could reason that despite a large number of R genes, plants cannot evolve or maintain the genetic diversity at *R* gene loci to match the abundance of effectors from multiple potential pathogens.

Combined, these facts led to the formation of the indirect R-Avr interaction model, the “guard” hypothesis (Van der Biezen and Jones, 1998; Dangl and Jones, 2001). This model assumes that there is no direct physical interaction between the paired R and Avr, instead the Avr protein targets a host protein(s) as part of its virulence activity and the R protein functions as a "guard" to monitor the status of the Avr-targeted host protein and triggers defense signaling upon detection of the Avr's virulence activity. Strikingly, a recent study on protein interaction networks of the plant-pathogen immune system activated during the interaction between two distinct pathogens, *Pseudomonas syringae* and *Hyaloperonospora arabidopsidis*, and *Arabidopsis* reveals that both pathogens target

an overlapping subset of plant proteins of well-connected cellular hubs of host machinery to suppress host defense and facilitate pathogen fitness (Mukhtar et al., 2011). Mukhtar and colleagues provide evidence that plant immune receptors “guard” these pathogen targeted cellular hubs mostly through indirect interaction with pathogen effectors (Mukhtar et al., 2011).

Pathogens must overcome a series of non-host (or basal) resistant mechanisms including pre-formed defenses and induced responses mediated through PAMP recognition by PRRs. While little is known about the molecular mechanisms that link PRR activation to intracellular signaling, evidence has emerged that additional RLKs, such as the BRI1-ASSOCIATED KINASE (BAK1) and the *BOTRYTIS*-INDUCED KINASE1 (BIK1), are associated with and required for the activation of specific PRRs (Chinchilla et al., 2007; Heese et al., 2007; Nicaise et al., 2009; Zhang et al., 2010; Zhang and Zhou, 2010). Upon recognition, early signaling events lead to ion flux changes in  $K^+$ ,  $Cl^-$ ,  $Ca^{2+}$  and  $H^+$  (Boller and Felix, 2009; Nicaise et al., 2009; Jeworutzki et al., 2010), local or extracellular production of ROS which act as second messengers for HR induction and defense gene expression (Heller and Tudzynski, 2011; O'Brien et al., 2012), cell wall reinforcement (Nuhse, 2012), and activation of mitogen-activated protein kinase (MAPK) and WRKY-type transcription factors that are key regulators of plant defense (Eulgem and Somssich, 2007; Colcombet and Hirt, 2008). Specifically, MPK3, MPK4 and MPK6 have been demonstrated to be rapidly activated in response to PAMPs (Pitzschke et al., 2009).

Downstream of PTI (and ETI) activation, plant hormones including salicylic acid (SA), jasmonic acid (JA) and ethylene (ET) act as central regulators of the plant immune



signaling network (Bari and Jones, 2009; Pieterse et al., 2009; Pieterse et al., 2012) (**Figure 1-2**). Compared to PTI where a MAPK-WRKY signaling cascade is involved (Asai et al., 2002), ETI predominantly engages the SA-signaling pathway for defense activation that has been largely dissected. Upstream of SA accumulation, there appears to be a dichotomous branching where ENHANCED DISEASE SUSCEPTIBILITY 1 (EDS1) and PHYTOALEXIN DEFICIENT 4 (PAD4) are critical for ETI activated by TIR-NBS-LRR proteins whereas NON-RACE SPECIFIC DISEASE RESISTANCE PROTEIN 1 (NDR1) is required for function of many CC-NBS-LRR R proteins (Aarts et al., 1998; Glazebrook, 2001; Wiermer et al., 2005). The genetic components SALICYLIC ACID INDUCTION DEFICIENT 2 (SID2) and ENHANCED DISEASE SUSCEPTIBILITY 5 (EDS5) are required for SA synthesis or accumulation, thus are shared signaling components of both TIR- and CC-NBS-LRR genes. The NON-EXPRESSOR OF PR GENES 1 (NPR1) functions as a master regulator downstream of SA (Cao et al., 1994) and mediates the expression of SA-dependent defense genes in combination with TGA and WRKY transcription factors (Zhang et al., 1999; Despres et al., 2000; Zhou et al., 2000; Wang et al., 2006). Recently, it has also been reported that NPR1 and the NPR1 homologs, NRP3 and NPR4, function as SA receptors (Fu et al., 2012; Wu et al., 2012). SA also engages a feedback amplification loop to increase the defense response and is negatively regulated by several proteins including the putative MAPKKK ENHANCED DISEASE RESISTANCE 1 (EDR1), LESION SIMULATING DISEASE 1 (LSD1) and a calmodulin-binding transcription activator (*AtSR1*) (Dietrich et al., 1994; Frye et al., 2001; Nie et al., 2012). It is important to note that SA-dependent ETI is only effective against biotrophic pathogens that strictly require living host cells to

survive or hemi-biotrophic pathogens that require a short early biotrophic stage for host colonization (Glazebrook, 2001, 2005). For necrotrophic fungal pathogens such as *Alternaria* spp. and *Botrytis* spp., ETI is ineffective as HR accompanying ETI may even facilitate development of disease caused by necrotrophic pathogens (Govrin and Levine, 2000; Mayer et al., 2001). Supporting this notion, a recent paper identified the Arabidopsis NBS-LRR LOV1 protein as the susceptibility determinant for the necrotrophic pathogen *Cochliobolus victoriae* (Lorang et al., 2012).

Compared to ETI against biotrophic or hemi-biotrophic pathogens, mechanisms of plant defense against necrotrophic pathogens are less characterized. Basically, it is known that both the JA- and ET-dependent pathways are engaged for activation of defense against this type of pathogens (**Figure 1-2**). Several JA-dependent antimicrobial proteins including PLANT DEFENSIN1.2 (PDF1.2), THIONIN2.1 (THI2.1), HEVEIN-LIKE PROTEIN (HEL) and CHITINASE B (CHIB) are used to monitor JA-dependent defense responses (Reymond and Farmer, 1998). These JA-responsive genes are induced following activation of the F-box protein CORONATINE-INSENSITIVE 1 (COI1) that interacts with and subsequently degrades jasmonate ZIM domain (JAZ) proteins in an ubiquitin-dependent fashion (Xie et al., 1998; Xu et al., 2002; Chini et al., 2007; Thines et al., 2007; Katsir et al., 2008; Fonseca et al., 2009). In addition, several studies have shown that JA- and ET- signaling are synergistically connected to activate defense gene expression (Penninckx et al., 1998; Thomma et al., 2001; Glazebrook, 2005). For example, *PDF1.2* expression in response to *Alternaria brassicicola* was inhibited in the ETHYLENE INSENSITIVE 2 (EIN2) mutant *ein2* and requires both JA- and ET- signaling for activation (Penninckx et al., 1998; Zarei et al., 2011). Furthermore, the

Arabidopsis transcription factor ETHYLENE RESPONSE FACTOR 1 (ERF1) is a positive regulator of both JA- and ET-signaling and several members of the ERF family play important roles in mediating defense responses (Lorenzo et al., 2003; McGrath et al., 2005). Lastly, ETHYLENE INSENSITIVE 3 (EIN3) and EIN3-like proteins are transcriptional factors of ethylene signaling that act downstream of EIN2 in many plant species and therefore have similar roles in defense mediated via the JA- and ET-signaling pathways (Chang and Shockey, 1999; Hibi et al., 2007; Chen et al., 2009a).



### **Plant-Powdery Mildew Interaction**

Powdery mildew fungi are obligate biotrophic fungal pathogens of the order *Erysiphales* and of the phylum *Ascomycetes*. They are some of the most common, widespread and easily recognizable plant pathogenic fungi that infect approximately 10,000 species of plants belonging to more than 1600 genera except gymnosperms (Agrios, 2005; Huckelhoven and Panstruga, 2011). Wheat, barley, tomato, cucumber, grape, strawberry and apple are among the crop plants of economic importance that suffer from powdery mildew diseases.

Infected plants display white or greyish dusty growth spots consisting of both mycelia (vegetative structures) and conidia (asexual spores) on the surface of leaves and stems of plants and can infect almost any above ground part of the plant. Typically, powdery mildew is visible on the adaxial side of leaves but it can also infect the lower side of leaves. Resulting damage from powdery mildew includes death of host tissue (or the entire plant), defoliation, cosmetic damage (common among ornamentals), weakening of the immune system to other pathogens and reduced yields and quality.

### **Life Cycle of Powdery Mildew**

The life cycle of powdery mildew consists of both asexual and sexual states depending on environmental conditions. The asexual state begins with the landing of conidia or conidiophores on the plant leaf surface. After landing on a leaf surface, fungal spores will uptake low molecular weight molecules from the waxy surface upon the release of an extracellular proteinaceous matrix with esterase and cutinase activity that subsequently directs the formation of the primary germ tubes (Carver et al., 1999;

Nielsen et al., 2000; Wright et al., 2002). Primary germ tubes sense specific topological and hydrophobic features of the leaf surface and produce a “cuticular peg” that penetrates the plant cuticle to anchor the spore and assist in directing germination of the appressorial germ tube (Edwards, 2002; Zhang et al., 2005). The appressorial germ tube is the infection structure that attaches to the leaf surface and produces a penetration peg. The penetration peg pierces through the host cell wall and the resulting cell wall apposition (CWA) (also known as the papillae – see later details) through enzymatic activities and turgor pressure (Zhang et al., 2005; Glawe, 2008). If successful in overcoming non-host resistance, the penetration peg will begin differentiation of the feeding organ, also known as the haustorium in close contact with the host cell cytoplasm for nutrient uptake and delivery of effector proteins into the host cell to subvert defense responses (Staples, 2001; Szabo and Bushnell, 2001; Voegelé and Mendgen, 2003; O'Connell and Panstruga, 2006). The haustorium is separated from the host cell cytoplasm by an interfacial membrane termed the extra-haustorial membrane (EHM) whose origin and biogenesis is virtually unknown.

Conidia of host adapted powdery mildew normally establish colonies consisting of a mycelium network that can produce new spores from conidiophores in 5 days and reach massive production at 8-10 days, resulting in snow-like mildew phenotype (Oshero and May, 2001). New spores are carried away by wind or other mechanical forces onto fresh plant surface, starting a new round of infection.

Sexual reproduction for powdery mildew fungi generally occurs via chasmothecia (formerly cleistothecium) once environmental or nutritional conditions (i.e. availability of host nutrients) becomes less favorable (Agrios, 2005; Glawe, 2008). Sexual reproduction

is initiated by the formation of gametangia (also known as gamocysts) where male and female gametangia are called antheridia (or androgamocysts) and ascogonia (or gynogamocysts) respectively (Braun et al., 2002). Genetic recombination between the male and female gametangia occurs through the establishment of a cytoplasmic connection (also known as plasmogamy) followed by the movement of the antheridia nucleus into the ascogonia (also known as dikaryotization) forming the cleistothecium (Glawe, 2008). The cleistothecium (also known as ascocarps or fruiting bodies) are attached by mycelioid appendages and begin cellular division to form an internal ascus or asci that are also dikaryotic in nature. Asci undergo karyogamy and meiosis to form monokaryotic ascospores which once released can infect other plants (Agrios, 2005; Glawe, 2008).

### **The Extra-Haustorial Membrane - the Host-Pathogen Interface**

As a special type of intracellular hyphae, the haustorium is a collective name for structurally similar feeding organs formed by many plant pathogens including powdery mildew and dikaryotic rust fungi and algae-like oomycetes. It seems likely that fungal and oomycete pathogens independently evolved the haustorium-based pathogenesis strategy. Differentiated haustoria are distinct cellular structures that contain their own cytoplasm, nuclei, mitochondria, cell membrane, cell wall and other organelles and can vary greatly in size and shape depending on the pathogen types (Mehrotra and Aneja, 1990).

Earlier studies revealed that concomitant with the development of the haustorium, a membranous structure distinct from the host cell-wall lining plasma membrane is

formed to encase the invading haustorium (the EHM) (Gil and Gay, 1977; Manners and Gay, 1982). The EHM separates the haustorium from direct contact with the plant cell cytoplasm. Between the EHM and the fungal haustorial cell wall is a gel-like layer enriched in carbohydrates called the extra-haustorial matrix (EHX) that may help protect the fungus from host responses (Green et al., 2002). The entire infectious structure including the haustorium, the EHX and the EHM is referred to as the haustorial complex (HC) (**Figure 3-1**). It is conceivable that the EHM is a critical battleground between the host and the pathogen, and may be modified by both the host and the pathogen for defense and pathogenesis respectively. However, apart from some early descriptive ultrastructural and histobiochemical analyses (Gil and Gay, 1977; Roberts et al., 1993; Soylu, 2004; Koh et al., 2005), the origin/biogenesis and the molecular composition of the EHM and the host-pathogen interaction at the EHM remain virtually uncharacterized.

### **Pre- and Post-Invasion Resistance Mechanisms**

The two layers of resistance mechanisms against biotrophic fungal or oomycete pathogens are referred to as pre- and post-invasion or penetration resistance. For a successful infection, the powdery mildew fungus must breach the cell wall and subsequently establish a functional haustorium inside the plant epidermal cell. Thus, plant resistance to powdery mildew bears spatiotemporal characteristics: i.e. it can be divided into penetration resistance (at the cell wall before haustorium formation; also called pre-invasion resistance) and post-penetration resistance (in the host cell against the haustorium; also called post-invasion resistance). For non- or poorly adapted pathogens, by definition, their infection is typically stopped by penetration resistance. In this



scenario, the fungus fails to break the cell wall and/or the cell wall apposition (the papilla) and lack the formation of (functional) haustoria. For example, penetration resistance as part of non-host resistance prevents infection of barley from wheat powdery mildew, and wheat from barley powdery mildew.

Pre-invasion resistance appears to be associated with dynamic cytoskeletal rearrangements, organelle transport, protein translocation, secretion of defense proteins, focal cell wall remodeling and formation of the callose-enriched papillae at the site of attempted penetration (Hardham et al., 2007; Huckelhoven, 2007; Lipka et al., 2010). The molecular basis of penetration resistance is currently unclear. Fungal chitin- (as a PAMP) triggered immune signaling may play a role in mounting penetration resistance. In recent years, several groups investigated penetration resistance mechanism by using Arabidopsis-barley mildew interaction. Arabidopsis *penetration 1* (*pen1*), (*pen2*) and (*pen3*) mutants with defects in penetration resistance to the non-host mildew *Bgh* have been characterized (Collins et al., 2003b). Results from these studies suggest that there exist at least two separate pathways that contribute to penetration resistance. One involves an exocytosis pathway controlled by PEN1, a plasma membrane anchored syntaxin with a soluble N-ethylmaleimide-sensitive factor attachment protein receptor (SNARE) domain that becomes recruited to the papillae (Collins et al., 2003b; Kwon et al., 2008). The other pathway involves PEN2, which encodes an atypical myrosinase involved in glucosinolate metabolism in defense responses (Lipka et al., 2005; Bednarek et al., 2009; Clay et al., 2009) and PEN3, which encodes a ATP-binding cassette transporter (Stein et al., 2006). Impairment of either or both pathways appears to affect pre-invasion resistance mechanisms against *Bgh* or the pea powdery mildew (*Erysiphe*

*pisi*) on single or double *pen1* and *pen2* mutants, yet barley and pea mildew isolates were unable to breach post-invasion resistance to form functional haustoria (Lipka et al., 2005). Interestingly, the loss of EDS1 or PAD4/SAG101 (another interacting partner of EDS1 like PAD4) in *pen2* or *pen3* mutant backgrounds led to sporulation of the barley and pea mildew in the Arabidopsis mutants, suggesting that the breakdown of post-invasion resistance in Arabidopsis to these non-host pathogens (Lipka et al., 2005; Stein et al., 2006). This finding also suggests that post-invasion resistance against biotrophic fungal pathogens involves SA-dependent defenses since EDS1, PAD4 and SAG101 are characterized components functioning upstream of SA in R-gene mediated resistance. More recently, by using a new mildew isolate *Golovinomyces cichoracearum* Gc-UMSG1 which is a poorly adapt pathogen of Arabidopsis, Wen and colleagues demonstrated that both SA-dependent and SA-independent signaling pathways contribute to post-penetration resistance (Wen et al., 2011). One common subcellular defense activated in post-penetration resistance is the formation of a callosic encasement of the haustorial complex (EHC), which presumably constrains the fungal haustorium (Wen et al., 2011). Well-adapted powdery mildew pathogens, however, probably secrete effectors into host cells and suppress the formation of EHC, thereby developing functional haustoria and establishing colonization. It is conceivable that plants employ NBS-LRR genes to counterattack these aggressive pathogens. Indeed, a number of CC-NBS-LRR R genes that confer post-penetration resistance to adapted mildew have been cloned from barley (Wei et al., 2002) and wheat (Srichumpa et al., 2005).

### ***RPW8*, a Unique Resistance Gene Locus**

The *RPW8* locus from the *Arabidopsis* accession Ms-0 contains two functional genes designated *RPW8.1* and *RPW8.2* (referred to as *RPW8* hereafter unless otherwise specified) that confer broad spectrum resistance to all tested isolates of *Golovinomyces* spp. fungi, the causal agents of powdery mildew disease, with high prevalence and phenotypic plasticity among accessions surveyed (Xiao et al., 1997; Xiao et al., 2001; Gollner et al., 2008). Surprisingly, *RPW8.1* and *RPW8.2* are predicted to encode small atypical R proteins (~18-20 kDa) with a putative N-terminal transmembrane (TM) domain and one or two CC domains (Xiao et al., 2001; Xiao et al., 2004). Thus, *RPW8* represents a unique type of *R* gene featuring a novel protein structure and broad spectrum resistance (Dangl and Jones, 2001; Xiao et al., 2001). A great deal of efforts of the Xiao laboratory has been devoted to understanding the molecular basis of *RPW8*-mediated broad-spectrum mildew resistance.

All tested *Arabidopsis* accessions also contain three closely linked homologs of *RPW8* named *HR1*, *HR2*, and *HR3* with similar predicted protein structures that do not seem to contribute to powdery mildew resistance (Xiao et al., 2001). There are two basic haplotypes at this locus in *Arabidopsis* accessions depending on the presence or the absence of *RPW8*. The first contains the three homologs *HR1/2/3* and *RPW8.1* and *RPW8.2* (the Ms-0-like) and the second contains the three homologs *HR1/2/3* and a fourth homolog, *HR4* which is most similar to *RPW8.1*, in place of *RPW8* (the Col-0 like) (Xiao et al., 2001; Xiao et al., 2004) (**Figure 1-3**). Based on these two major haplotypes, there are two basic types of interactions possible between *Arabidopsis* and powdery mildew (**Figure 1-3**). First, *Arabidopsis* plants that do not express *RPW8* are susceptible to infection (classified by the white, snow-like accumulation on the leaf surface). The

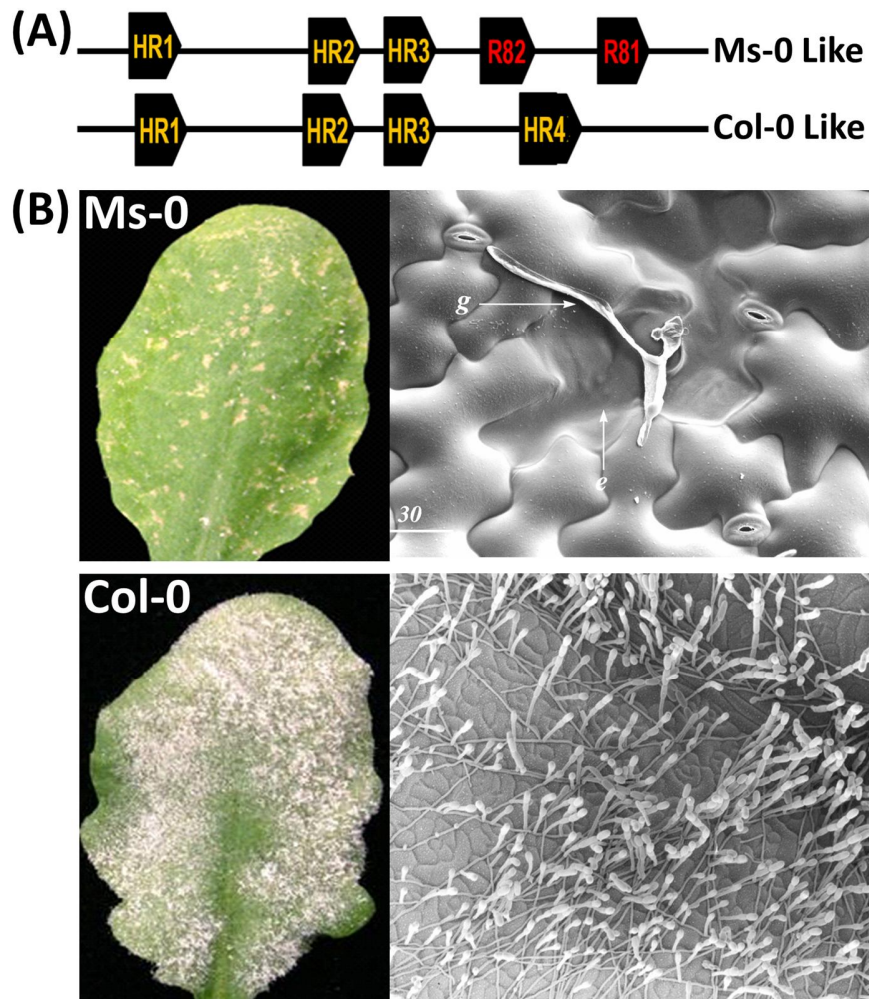


**Figure 1-3. Arabidopsis Haplotypes and Response to Powdery Mildew.**

(A) The schematic gene organization of the complex *RPW8* locus in Ms-0 (resistant) and Col-0 (susceptible) accessions. (B) Scanning electromicrographs are from Xiao et al., 1997. The disease reaction phenotypes of Ms-0 and Col-0 at 8 days after inoculation of *Golovinomyces cichoracearum* (Gc-UCSC1). Note the arrested germinated spore and collapse of the penetrated host epidermal cell in Ms-0 indicative of a HR.

second is an incompatible interaction where *Arabidopsis* plants expressing *RPW8* are resistant to powdery mildew. In this scenario, mycelium expansion is arrested with little or no conidiophores formed after post-invasion resistance is triggered (**Figure 1-3**). Syntenic *RPW8* loci have also been isolated and analyzed from *Arabidopsis lyrata*, *Brassica oleracea* (*Bo*) and *rapa* (*Br*) species (Xiao et al., 2004; Orgil et al., 2007) (**Figure 1-4**). *Arabidopsis lyrata* contains four genes that are apparent orthologs of *AtHR1/2/3* and *AtRPW8.2* (there is no ortholog for *AtRPW8.1* in *A. lyrata*) while *Brassica* spp. contain 4 *RPW8* homologs, *HRa*, *HRb*, *HRc* and *HRd* (on a separate locus in *Brassica rapa* only), that are not definitively orthologous to the *Arabidopsis* genes but share the highest sequence homology to *AtHR3* and *AtHR3* suggesting both lineages evolved from independent duplications of a common *HR3*-like progenitor gene (Xiao et al., 2004). Unlike the paralogs in *A. thaliana* and *A. lyrata*, the *Brassica* paralogs are more highly homologous to each other, which is indicative of a recent origin for this gene cluster (Xiao et al., 2004). Previous evolutionary analysis suggests that *RPW8* is a relatively young *R* gene and its origin followed after the evolution of *Arabidopsis* from the *Brassica* genus but before the speciation of *A. thaliana* from *A. lyrata* and that *RPW8* evolved from an *HR3*-like progenitor gene by duplication and functional diversification (Xiao et al., 2004; Orgil et al., 2007).

Interestingly, *RPW8* family members also share limited sequence amino acid (aa) identity (25-30%) to an ancient clade of CC-NBS-LRR resistance proteins (termed CC<sub>R</sub>-NBS-LRR) that includes *AtNRG1.2* (At5g66910), the *Nicotiana benthamiana* N-required gene 1 (NRG1) and the *Arabidopsis* activated disease resistance gene 1 (ADR1) proteins (Dangl and Jones, 2001; Meyers et al., 2003; Xiao et al., 2008; Collier et al., 2011). The

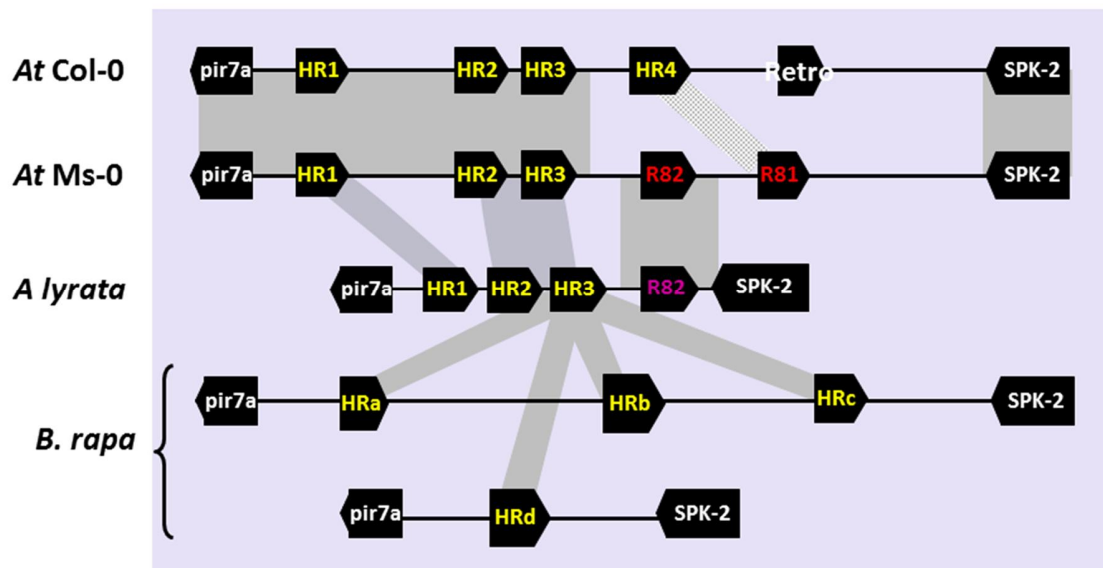


**Figure 1-4. Gene Organization of the Syntenic *RPW8* Loci from *Arabidopsis* and *Brassica*.**

This figure is modified from Xiao et al., 2004. Grey bars/blocks represent the region of highest homology between *RPW8* family members between *Arabidopsis thaliana* Col-0 and Ms-0 accession, *Arabidopsis lyrata*, and *Brassica rapa* plant species. *AtHR4* is most similar to *AtRPW8.1* which is also absent from *Arabidopsis lyrata*. *Brassica* homologs of *RPW8* are most similar to *HR3* suggesting that *HR3* is the putative family progenitor gene. *Brassica* paralogs are also more similar to each other suggesting a recent origin for this gene cluster.

N-terminal domain of CC<sub>R</sub>-NB-LRR proteins is capable of triggering defense responses and therefore functions differently from other canonical CC-NB-LRR proteins that are primarily involved in microbial recognition (Collier and Moffett, 2009; Collier et al., 2011).

Despite having a novel protein structure, RPW8 activates HR and other defense responses via the conserved SA-dependent signaling pathway that is required by TIR-NBS-LRR (Xiao et al., 2003b; Xiao et al., 2005). Loss-of-function mutations in SA-dependent pathway components such as *EDS1*, *PAD4*, *EDS5*, *SGT1*, and *NPR1* compromise *RPW8* defense function (Xiao et al., 2005). Other features of RPW8 signaling include a SA-dependent positive feedback loop for transcriptional amplification of *RPW8* during infection (Xiao et al., 2003b; Xiao et al., 2005) and negative control by *EDR1* a MAPKKK gene (Frye et al., 2001; Xiao et al., 2005). While the molecular mechanisms of *RPW8*-mediated defense are not well understood, interacting partners of RPW8 have been identified. For example, 14-3-3 $\lambda$  (At5g10450) interacts with RPW8 and positively regulates RPW8.2 resistance function and plays a role in enhancing basal resistance in Arabidopsis (Yang et al., 2009). A PHYTOCHROME-ASSOCIATED PROTEIN PHOSPHATE TYPE 2C (PAPP2C) (At1g22280: [AY080735.1](#)) protein also has been shown to interact with and negatively regulate RPW8.2-mediated defense and SA-dependent basal defense against powdery mildew in Arabidopsis and rice (Wang et al., 2012b).

To understand how RPW8 confers broad-spectrum resistance using the same SA-dependent defense pathway, Wang and colleagues investigated the subcellular defense responses activated by RPW8. Interestingly, it was found that expression of RPW8

correlated with i) an enhancement of EHC formation surrounding the haustorial complex and ii) an accumulation of H<sub>2</sub>O<sub>2</sub> at the host pathogen interface (Wang et al., 2009). Similar to the cell-wall apposition or papillae seen in non-host pre-invasion resistance, the EHC (detectable by aniline blue staining) is rich in callose and is rarely formed in *Arabidopsis* Col-0 plants (*RPW8* lacking) when challenged with the adapted powdery mildew *Golovinomyces cichoracearum* UCSC1. However in Ms-0, most haustoria (stained with trypan blue) are surrounded by an EHC and appear shrunk and/or deformed in comparison to those in Col-0 suggesting that the haustorium has been physically constrained by host defenses activated by *RPW8* (Wang et al., 2009). In addition, H<sub>2</sub>O<sub>2</sub> accumulation (detected by DAB staining) in Ms-0 background is detectable inside the haustorial complex when surrounded by an EHC but was rarely seen in the HCs of Col-0 plants (Wang et al., 2009). It is noteworthy that in some cells expressing *RPW8*, H<sub>2</sub>O<sub>2</sub> accumulation spread into the cytoplasm of the invaded epidermal cells and subsequently resulted in cell death. These results demonstrate that *RPW8* enhances both physical and chemical barriers upon the fungal feeding organ to protect the host against colonization.

To understand how *RPW8* achieves broad-spectrum mildew resistance and activates these subcellular defense responses, Wang and colleagues looked at the subcellular localization of *RPW8.2* (Wang et al., 2009). Most interestingly, *RPW8.2* is specifically induced and targeted to the EHM encasing the haustorium upon infection with powdery mildew (*Gc*-UCSC1) (**Figure 1-5**). Consequently, the spatiotemporal targeting of *RPW8.2* and subsequent triggering of defense responses at the host-pathogen interface to constrain fungal haustorium provides a physical explanation for *RPW8*-mediated broad-spectrum mildew resistance (Wang et al., 2009; Wang et al., 2010).



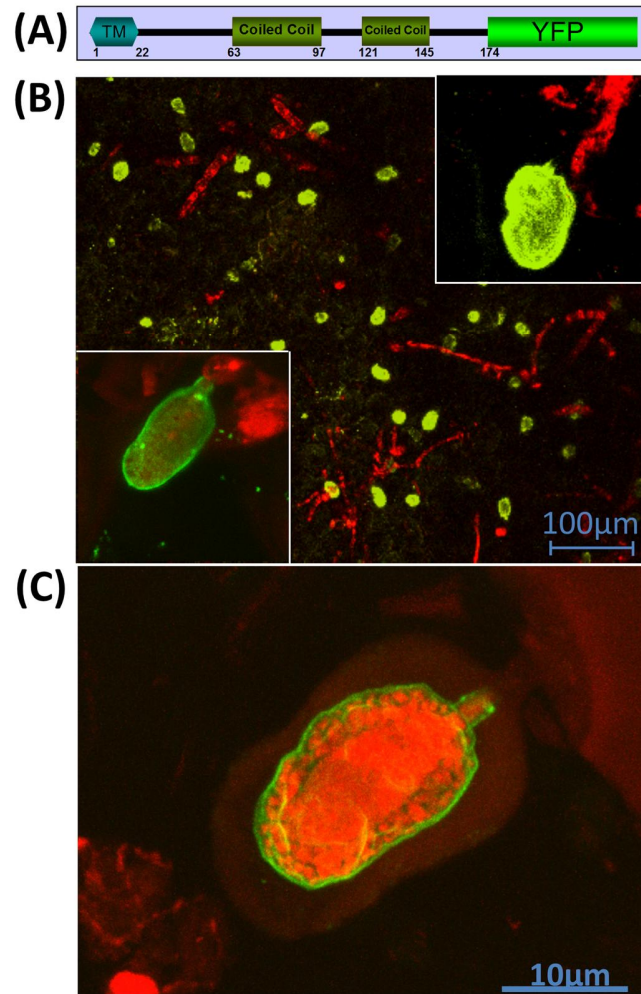


**Figure 1-5. RPW8.2 is Specifically Localized to the EHM.**

Confocal images in (B) and (C) are taken from Wang et al., 2009. (A) A schematic domain structure of RPW8.2 translationally fused to YFP. TM = transmembrane domain.

(B) Col-0 plants expressing RPW8.2-YFP were examined using confocal microscopy at 4dpi with *Gc*-UCSC1. Bright green sphere-like bodies indicate induction and accumulation of RPW8.2-YFP. Note the small fluorescent spots apparently on their way to fuse with the big fluorescent body in the lower left insert. Fungal structures were stained red by propidium iodide (PI). (C) An isolated haustorium from (A) detailing RPW8.2-YFP precisely localized at the EHM.

## **Project Aims & Questions**

Powdery mildew is one of the most widespread and devastating plant pathogens. Despite being one of the most easily recognizable pathogens, powdery mildew (along with other haustorium-forming pathogens causes significant economic and agricultural losses. The overall goal of this project is to understand the functional origin of *RPW8* by characterizing the function of the *RPW8* homologs in *Arabidopsis* and *Brassica*. Moreover, this project is aimed at further dissecting the signaling pathways and molecular mechanisms of *RPW8*-mediated broad-spectrum disease resistance and to use *RPW8* as a delivery vehicle for achieving resistance against haustorium-forming pathogens.

**Aim 1: Determine the molecular functions of multiple *RPW8* homologs in *Arabidopsis* and *Brassica spp.*** *RPW8.1* and *RPW8.2* belong to a small gene family in the *Arabidopsis* and *Brassica* lineages. Interestingly, while the *RPW8* homologs in *Arabidopsis*, specifically *HR1*, *HR2* and *HR3*, are evolutionarily conserved, their cellular functions remains to be functionally characterized. Moreover, our evolutionary studies support the notion that the *RPW8* has evolved from an *HR3*-like progenitor gene (Xiao et al., 2004; Orgil et al., 2007). Therefore, I aim to understand the functional origin of *RPW8* mediated disease resistance by characterizing the function of these homologs (Chapter 2).

**Aim 2: Determine if the *RPW8* homologs in *Arabidopsis* and *Brassica* are EHM-resident proteins.** *RPW8.2* represents the first host protein that is specifically targeted

to the host-pathogen interface (the EHM) whereby it activates a defense response to constrain the fungal haustorium. Because RPW8 likely evolved from duplication and functional diversification of an HR3-like progenitor gene, it is interesting to determine whether the EHM-targeting feature of RPW8.2 is inherited from the more ancient family members or acquired through neofunctionalization in RPW8.2 only. I thus aim to determine the subcellular localization of several RPW8 family members in cells invaded by the haustorium (**Chapter 2**).

**Aim 3: Determine the origin of the extra-haustorial membrane.**

The extra-haustorial membrane represents the critical membrane or interface between the host and pathogen that is presumably modified by both for their benefit. Despite its importance in host-pathogen interactions, little evidence has been presented regarding the function and biogenesis/origin of the EHM. The highly specific localization of RPW8.2 to the EHM together with the absence of plasma membrane proteins in the EHM (Koh et al., 2005) suggests that the EHM is likely of host origin, and distinct from the host PM. However, whether the EHM is derived from the PM or *de novo* synthesized remains to be determined. I aim to take advantage of RPW8.2's unique EHM localization to provide evidence for the origin of the EHM (**Chapter 3**).

**Aim 4: Utilization of RPW8.2 to target antimicrobial cargos to the host-pathogen interface.** RPW8.2 is specifically targeted to the host-pathogen interface of fungal and oomycete pathogens, confers resistance in tobacco against powdery mildew (Xiao et al., 2003a), and enhances basal defense against biotrophic pathogens (Wang et al., 2007).

Therefore, our group devised a unique strategy to target antimicrobial peptides to the host-pathogen interface using RPW8 as a delivery vehicle in an effort to increase resistance in other plant species against haustorium-forming pathogens. In (**Chapter 4**), I highlight my contribution in our group efforts towards developing this strategy to engineer novel resistance against powdery mildew.

**Aim 5: What are the trafficking cue(s) and molecular mechanisms for the specific targeting of RPW8.2 to the EHM?** While RPW8.2 represents the first host protein targeted to the host-pathogen interface, mechanisms of the haustorium-targeted protein/membrane trafficking of RPW8.2 remains unclear. Whether there exists a trafficking cue at the EHM and what this cue might be are particularly intriguing questions. In **Chapter 5**, I highlight my contribution to a group project that aims to investigate whether bioactive phospholipids play any role in polarized protein trafficking and host defense in relation to haustorial invasion.

**Aim 6: Identify novel components of the basal resistance mechanisms regulated by RPW8.** While the identification and functional characterization of a large repertoire of *R* genes has greatly improved our knowledge of plant innate immunity, more work is needed to identify novel regulatory components of *R* proteins to understand how they work to activate resistance. In (**Chapter 6**), I describe my preliminary work towards characterizing the role of a DnaJ type chaperone (ATJ3) and a Phospholipase D (PLD $\delta$ ) in RPW8-mediated and basal resistance against powdery mildew in *Arabidopsis*.

## **Chapter 2: Functional Characterization of RPW8 Homologs in *Arabidopsis thaliana* and *Brassica oleracea***

### **Introduction**

The two homologous *Arabidopsis* *R* genes *RPW8.1* and *RPW8.2* comprise a unique (albeit atypical) type of *R* genes (Dangl and Jones, 2001; Xiao et al., 2001). *RPW8.1* and *RPW8.2* (referred hereafter to as *RPW8* unless otherwise indicated) encode small basic proteins containing an N-terminal TM domain (or signal peptide) and 1-2 CCs. Yet, just like *TIR-NB-LRR* *R* genes, *RPW8* activates EDS1/PAD4- and SA-dependent defense responses including pathogenesis-related (*PR*) genes expression, H<sub>2</sub>O<sub>2</sub> production and accumulation, and localized cell death at the site of infection (i.e. hypersensitive response; HR). However, unlike most *NB-LRR* *R* genes, which often trigger race-specific resistance, *RPW8* confers broad-spectrum resistance in *Arabidopsis* to different powdery mildew species (*Golovinomyces* spp.) with diverse host-ranges. How *RPW8* renders broad-spectrum resistance via a conserved SA-dependent signaling pathway remains an interesting question. Our recent investigation on *RPW8.2*'s subcellular localization reveals a spatiotemporal basis for the broad-spectrum nature of *RPW8*-mediated resistance: *RPW8.2* expression is induced in the fungus-invaded epidermal cell and the *RPW8.2* protein is specifically targeted to the extra-haustorial membrane (EHM) that encases the fungal feeding structure named the haustorium, whereby *RPW8.2* activates defenses to constrain the haustorium (Wang et al., 2009; Wang et al., 2010). Thus, it appears that *RPW8.2* contributes to the broad-spectrum resistance against powdery mildew via activation of haustorium-targeted defense at the EHM—the enigmatic, poorly characterized host-pathogen interfacial membrane.

How RPW8.2 evolved the spatiotemporally controlled subcellular defense against powdery mildew is not known. Our previous studies show that in addition to *RPW8.1* and *RPW8.2*, the *RPW8* locus contains 3-4 homologs of *RPW8* named *HR1* (At3g50450), *HR2* (At3g50460), *HR3*(At3g50470), and *HR4*(At3g50480). The syntenic *RPW8* loci in *Brassica* species also contain 3 homologous genes designated *HRa*, *HRb* and *HRc*. Sequence analysis suggests that the *RPW8* gene family in *Arabidopsis* probably originated from an *HR3*-like progenitor gene (*HR3-p*), with *RPW8.1* and *RPW8.2*, and *HR4* being the newest homologs (Xiao et al., 2004). Whether RPW8.2's defense function and its EHM-targeting properties in particular, have evolved via duplication of *HR3-p* and subsequent neo-functionalization has not been determined. To this end, functional characterization of *HR3* (which most likely has retained the original function of *HR3-p*) and other homologs should be revealing. In this study, we obtained genetic evidence to suggest that *HR1*, *HR2*, and *HR3* in particular, contribute to basal resistance in *Arabidopsis*. Moreover, our cell biological studies indicate that all *RPW8* homologs examined can be targeted to the EHM when ectopically expressed in infected epidermal cells. We thus propose that (i) *HR3* may be a component of basal immunity, (ii) the resistance function of *RPW8.2* (and perhaps *RPW8.1* also) is not an entirely new innovation but rather an enhancement of the existing function of the more ancient progenitor protein *HR3-p*, and (iii) the EHM-targeting properties must have been acquired early in the evolution of the *RPW8* protein family and retained by all members.

## Results

### Overexpression of *RPW8* Homologs Enhances Resistance to Powdery Mildew

To determine if the Arabidopsis *RPW8* homologs are functional in defense against *Golovinomyces cichoracearum* (*Gc*-UCSC1), we generated stable overexpression lines in the Arabidopsis accession Col-0 containing the single gene mutation (glabrous, *gll-1*) (Col-gl). Col-0 lacks *RPW8.1* and *RPW8.2*, and is susceptible to *Gc*-UCSC1 (Xiao, et al., 2001). For each homolog, the genomic sequence of the respective gene including approximately 1000 bp of the 5' UTR/promoter region, (496bp in the case of *HR3*), was placed under control of the *35S* promoter. Independent transgenic lines were passed down to T3 and T4 generations were tested for their disease reactions to powdery mildew. Five to ten independent lines for *35S-HR1*, *35S-HR2* and *35S-HR3*, but not *35S-HR4*, displayed a varied but marked increase in resistance to powdery mildew in comparison to the susceptible, *RPW8*-lacking wild-type (WT) Col-gl (**Figure 2-1A**). Col-0 plants expressing *NahG*, a bacterial gene encoding a SA hydrolase that depletes SA, showed enhanced disease susceptibility (eds) to the pathogen, implying that SA-dependent basal resistance is active in Col-0 wild-type plants (**Figure 2-1A and C**). Disease quantification showed that *35S::HR1*, *35S::HR2*, and *35S::HR3* lines exhibited four-to-five fold reduction in total number of spores produced per milligram of fresh infected leaf tissue, whereas *35S-HR4* lines were as susceptible as Col-gl (**Figure 2-1A and C**). Reverse-transcription (RT)-PCR showed that expression levels of these *RPW8* homologs in the respective transgenic lines were roughly 10-12x higher than those of the endogenous genes in the wild-type plants (**Figure 2-1B**). However, none of the Col-*NahG* plants expressing *35S::HR1*, *35S::HR2* or *35S::HR3* showed an obvious enhanced

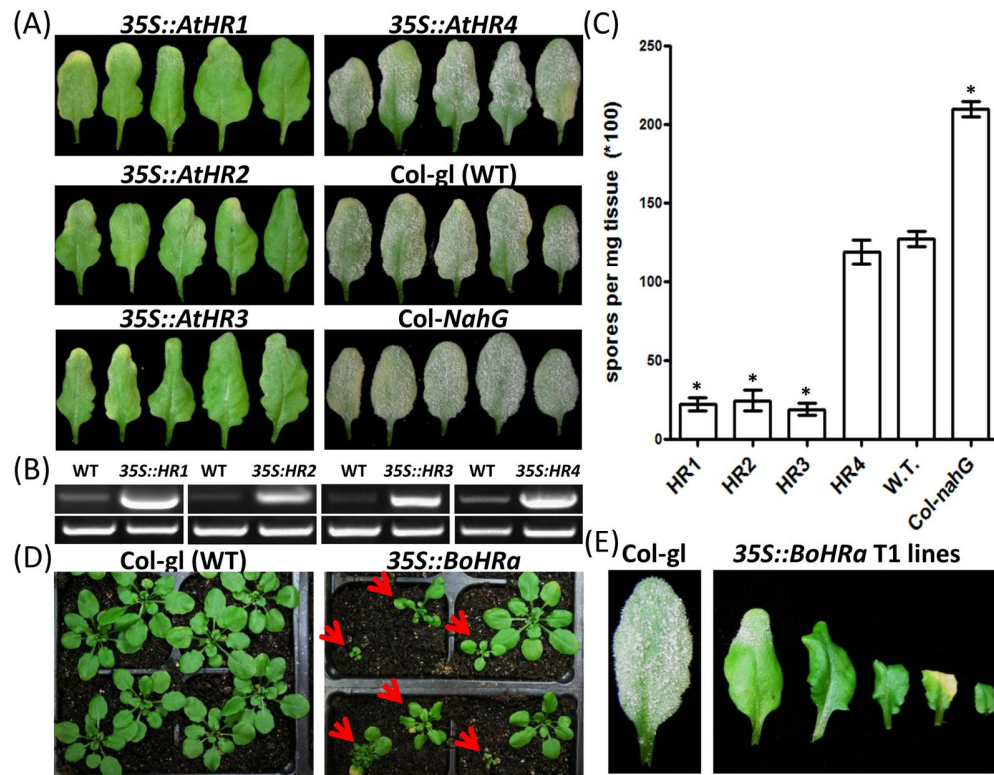


**Figure 2-1. Overexpression of *RPW8* Homologs Enhances Resistance to Powdery Mildew.**

**(A)** Disease reaction phenotypes of representative leaves of T3 Col-gl lines overexpressing *HR1*, *HR2*, *HR3* or *HR4* infected with *Gc-UCSC1*. Col-gl and Col-*nahG* were used as control. Pictures were taken at 12dpi. **(B)** RT-PCR analysis of representative overexpression lines and Col-gl using gene-specific primers (top panels). *UBC21* was used as control (bottom panels). cDNA was synthesized using total RNA prepared from uninfected plants. PCR was done with 24 (*UBC21*) or 30 (other genes) cycles. ImageJ used to estimate band intensities. **(C)** Quantitative assay of disease susceptibility. Data represent means+SE. Asterisks indicate significance at  $P < 0.01$  compared with Col-gl based on Student's t test data represent means  $\pm$  SEM (n=4) from one of three representative experiments. **(D)** Control vs. independent T1 lines expressing *BoHRA*. Distorted growth phenotypes of independent lines indicated by red arrows (>24 tested). **(E)** EDR phenotype for independent 35S::*BoHRA* T1 lines compared to control plants with *Gc-UCSC1* at 12dpi.



mildew resistance (**data not shown**), suggesting that similar to *RPW8.1* and *RPW8.2* (Xiao et al., 2003b; Xiao et al., 2005), these *RPW8* homologs also function via a SA-dependent signaling pathway.

The *Brassica oleracea* genome contains three *RPW8* homologs named *BoHRa*, *BoHRb*, and *BoHRc* and they share >90% sequence identity at the protein level (Xiao et al., 2004). Whether these genes play a role in disease resistance in *B. oleracea* is not known. To test if these *B. oleracea* homologs have similar function as the Arabidopsis *RPW8* homologs, we ectopically expressed *BoHRa* from the 35S promoter in Arabidopsis Col-gl plants. About 12 T1 plants transgenic for 35S::*BoHRa* exhibited stunted and/or distorted growth with varying degrees of necrotic cell death in leaves (**Figure 2-1D**), likely as a result of *BoHRa* overexpression. Upon infection with *Gc*-UCSC1, a noticeable enhanced resistance was observed for those T1 plants (**Figure 2-1E**). Combined, the above results suggest that both *Arabidopsis* and *Brassica* *RPW8* homologs, excluding *HR4*, may be functional genes in conferring basal resistance to powdery mildew.

### **Genetic Depletion of *HR1*, *HR2*, or *HR3* Results in Enhanced Disease Susceptibility**

In order to provide additional evidence for the role of the *RPW8* homologs in basal resistance against powdery mildew, we obtained one or two T-DNA insertion lines from the Arabidopsis Biological Resource Center (ABRC) for *HR1*, *HR2*, or *HR3* (no informative T-DNA lines available for *HR4*) to determine if knocking down or knocking out any of these genes would result in an eds phenotype to powdery mildew infection. The T-DNA insertion positions of these SALK lines were validated (**Figure 2-2A**) and

the mutant alleles were purified by backcrossing to Col-0 once. Subsequent RT-PCR analysis using mildew-infected leaves of the homozygous lines at 3 days post inoculation (dpi) (**Figure 2-2B**) showed that SALK\_093095 had no detectable expression of *HR2* thus is probably *HR2*-null (designated *hr2-ko1*), that SALK\_122954 and WiscDsLox420C08 had no detectable expression of *HR3* thus is probably *HR3*-null (designated *hr3-ko1* and *hr3-ko2*, respectively) and SALK\_056764 had reduced (~10% of the wild-type level) expression of *HR1* thus is *HR1*-knocked down (*hr1-kd1*).

To assess whether *HR1-kd1*, *HR2-ko1*, *HR3-ko1* and *HR3-ko2* have compromised basal resistance to powdery mildew, we first visually monitored the development of the disease phenotypes of these mutant plants along with Col-0 and Col-*NahG*. All of the four T-DNA lines exhibited a small but noticeable increase in fungal mass on the leaf surface in comparison with Col-0, although they were not as susceptible as Col-*NahG* (**Figure 2-2C**). Subsequent quantification of these disease phenotypes showed that plants of these four mutant lines produced approximately 1.4 to 1.5 times of total fungal spores relative to that in Col-0 while Col-*NahG* supported nearly twice as many spores than Col-0 (**Figure 2-2D**). These observations, together with the data from overexpression analyses, indicate that *HR1*, *HR2* and *HR3* are functional genes that contribute to basal resistance to powdery mildew via the conserved SA-dependent signaling pathway.

These results also lend support to our hypothesis that *RPW8* has evolved from *HR3-p* to bolster resistance against aggressive powdery mildew pathogens by enhancing the basal resistance function of *HR3-p* and raise a question as to whether *RPW8*-mediated mildew resistance requires the more ancient function of the *HR3* gene. To address this question, we introduced by crossing *hr3-ko1* into a Col-g1 transgenic line (designated *S5*)

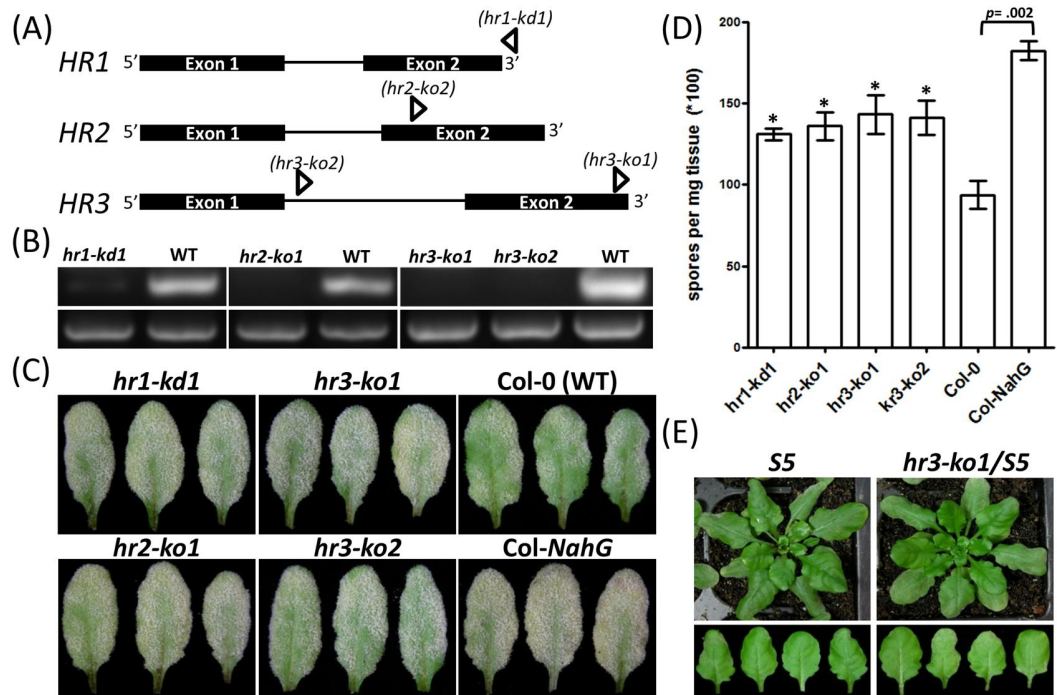


**Figure 2-2. Genetic Depletion of *HR1*, *HR2* and *HR3* Enhances Susceptibility to Powdery Mildew.**

**(A)** Schematic gene structures and location and direction of T-DNA insertion lines for *HR1*, *HR2* and *HR3* (arrowheads). *hr1-kd1*: SALK\_056764 ( $^{+778}$ ACTCAA.. $\blacktriangleleft$ ..CAAATG $^{+789}$ ). *hr2-ko1*: SALK\_093095 ( $^{+582}$ TATGGC.. $\blacktriangleright$ ..CAAGAT $^{+593}$ ). *hr3-ko1*: SALK\_122954 ( $^{+972}$ AAGAAA.. $\blacktriangleright$ ..ACGGAA $^{+983}$ ). *hr3-ko2*: WiscDsLox420C08 ( $^{+361}$ AATTTA.. $\blacktriangleright$ ..AATAGTT $^{+372}$ ). Drawing approximate in scale. **(B)** RT-PCR analysis of T-DNA insertion lines. Top panels (left to right) - *HR1*, *HR2*, or *HR3* using gene-specific primers within Exon 1 upstream of all T-DNA insertions. Bottom panels (all) - *UBC21*. Infected leaves at 3dpi were subjected to RT-PCR (30 cycles). **(C)** Disease phenotypes of infected leaves representative from indicated *kd*, *ko* and control lines at 12dpi. **(D)** Quantitative assay of disease susceptibility. Data represent means  $\pm$  SEM (n=4) from one of three representative experiments. Student's *t* test was used to calculate *P* value for each genotype compared with *Col-0* and *Col-0* compared to *Col-NahG*. (\* =  $p < .05$ ). **(E)** Disease phenotypes of representative *S5* (Col-gl transgenic for *RPW8*) and *hr3-ko1/S5* plants (top) and infected leaves (bottom) at 12dpi. Eight independent F3 *hr3-ko1/S5* lines were tested.

homozygous for a single copy of the 6.2-kb genomic fragment containing both *RPW8.1* and *RPW8.2* and their respective promoters from the Ms-0 accession (Xiao et al., 2003). We challenged F3 progenies that are homozygous for both the *RPW8* transgene and *hr3-ko1* with *Gc*-UCSC1 and found no obvious phenotypic changes in comparison to *S5* plants (**Figure 2-2E**). This result suggests that HR3 (and most likely the other *RPW8* homologs) are not essential for *RPW8*-mediated mildew resistance.

### ***RPW8* Homologs Are Likely Functionally Redundant**

Previously we reported that *HR1*, *HR2*, and *HR3* appear to have been subjected to purifying selection (Xiao et al., 2004; Orgil et al., 2007), implying a functional conservation and redundancy among these three genes. To address this question, we explored an approach to simultaneously silence *HR1*, *HR2* and *HR3* using artificial micro RNA (amiRNA) genes considering that these three genes are tandemly arrayed in a <10kb region, genetic recombination of the T-DNA insertion alleles in the same background would be extremely difficult. We utilized the design principles and web-based tool at <http://wmd3.weigelworld.org/> to find an optimum target site for 21-mer based amiRNA fragments (Schwab et al., 2006). One of the best candidate amiRNA was derived from the middle region of the 2<sup>nd</sup> exon of *HR1*, *HR2*, and *HR3* (**Figure 2-3A**). We introduced this construct (designated *HR1-3ami*) into Col-gl and found that eight of 24 mildew-infected transgenic T1 plants exhibited an eds phenotype at 12dpi (**data not shown**). T2 progenies from four independent T1 lines further tested with *Gc*-UCSC1. These plants showed a similar eds phenotype in comparison to Col-gl plants noticeable at 12dpi (**Figure 2-3B**), which was further validated by quantitative assays (**Figure 2-3C**).

These *HR1-3ami* lines were slightly more susceptible than *hr3-kol* in our multiple infection tests, but the difference between them was not statistically significant. RT-PCR analysis with two representative *HR1-3ami* lines at 2dpi showed that expression levels were reduced to 60-65% for *HR1*, 50-60% for *HR2* and 55-57% for *HR3* of their respective wild-type levels in Col-gl (**Figure 2-3D**), which is in agreement with the eds phenotypes of the *HR1-3ami* lines.

### **Expression of *HR3* by the *RPW8.2* Promoter Enhances Resistance to Powdery Mildew**

Expression of both *RPW8.1* and *RPW8.2* are induced by powdery mildew (Xiao et al., 2003b; Wang et al., 2009). We thus determined if *HR1*, *HR2*, and *HR3* exhibit similar transcriptional regulation. RT-PCR analysis showed that expression of *HR1*, *HR2* and *HR3* before powdery mildew inoculation was detectable at low levels while their expression increased ~2.5-4x at 42 hours post inoculation (hpi) (**Figure 2-4B**), suggesting that the promoters of these three genes are also powdery mildew responsive. We also tested whether expression of *HR3* from the *RPW8.2* promoter (~1.8kb 5' of the ATG start codon of *RPW8.2*) could improve resistance activated by *HR3*. Ten of thirty T1 plants transgenic for *R82p::HR3* showed enhanced disease resistance (edr) to *Gc*-UCSC1 while 3-4 of them also showed spontaneous HR-like cell death (SHL) that could be further accelerated by powdery mildew infection and soon engulf the whole leaf (**Figure 2-4C**). These results indicate that the *RPW8.2* promoter is likely stronger, at least after several dpi, than that of *HR3* which is < 500bp (as the entire intergenic region

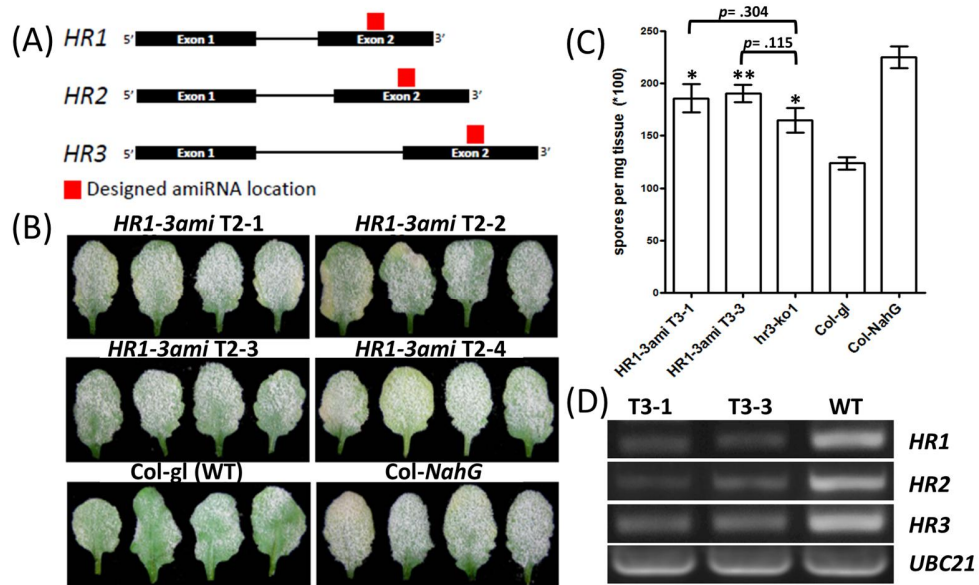


**Figure 2-3. *HR1*, *HR2* and *HR3* are Likely Functionally Redundant.**

**(A)** Schematic illustration of *HR1*, *HR2* and *HR3* with an approximate location of the designed amiRNA 21-mer (TGTTTAGTGTTCATATCGGAC) within the 2<sup>nd</sup> exon of each homolog. **(B)** Disease phenotypes of representative infected leaves from independent T2 lines of *HR1-3ami*/*Col-gl* in comparison to the control lines at 12dpi.

**(C)** Quantitative assay of disease susceptibility. Data represent means  $\pm$  SEM (n=4) from one of three representative experiments. Student's *t* test was used to calculate *P* values for comparisons to *Col-gl* (\* = *p* < .05, \*\* = *p* < .01) and *hr3-ko1* (see bracket values).

**(D)** RT-PCR analysis of two representative *HR1-3ami* lines and a control line for *HR1*, *HR2*, *HR3* and *UBC21* (as indicated). Infected leaves at 2dpi were subjected to RT-PCR (30 cycles).

upstream of the ATG start codon of *HR3* is only 497bp) and probably contributes to RPW8.2's resistance activity in Ms-0.

However, given that RPW8.1 and RPW8.2 share only 40-66% sequence identity at the protein level to HR1, HR2, and HR3 (Xiao et al., 2004), it is likely that protein sequence diversification of RPW8.1 and RPW8.2 from these three homologs mainly explains *RPW8*-mediated resistance. One obvious difference between the two groups of proteins is that RPW8.1 and RPW8.2 had shorter C-tails compared to HR1, HR2 and particularly HR3 (**Figure 2-4A**). We thus wondered if loss of some C-terminal amino acids had contributed to functional enhancement of RPW8.1 and RPW8.2. To get evidence for this speculation, we made an *HR3* mutant gene (*HR3<sup>ΔC165</sup>*) whose product has a truncation of the C-terminal 65 amino acids (AAs) and expressed it from the *RPW8.2* promoter. As shown in (**Figure 2-4B, D and E**), ten of 30 T1 lines transgenic for *RPW8.2p::HR3<sup>ΔC165</sup>* showed similar enhanced mildew resistance compared to *RPW8.2p::HR3* transgenic plants. Interestingly, three independent lines had reduced stature and extensive SHL (**data not shown**). This phenotype is reminiscent of the *S6* line (in Col-gl) that contains multiple copies of *RPW8* (Xiao et al., 2003b). These results suggest that the long C-terminus of HR3 may have a self-inhibitory function and partial loss of this portion in RPW8.1 and RPW8.2 might have been one mechanism for the functional evolution of these two *R* genes.

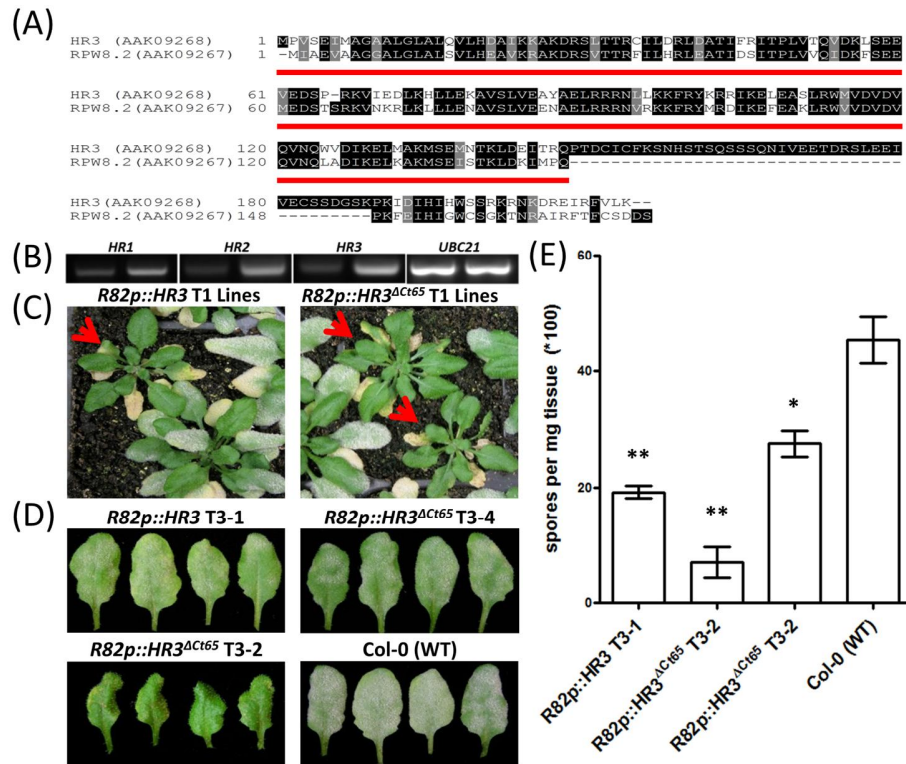


**Figure 2-4. Expression of *HR3* by the *RPW8.2p* Enhances Resistance to Powdery Mildew.**

**(A)** Alignment of *HR3* and *RPW8.2* using ClustalW and shaded using the BOXSHADE server ([http://www.ch.embnet.org/software/BOX\\_form.html](http://www.ch.embnet.org/software/BOX_form.html)). Highest conserved sequence underlined in red. **(B)** RT-PCR analysis for *HR1*, *HR2* and *HR3* and *UBC21* in Col-0 prior to or at 42hpi (30 cycles). **(C)** Independent T1 lines expressing *HR3* (top panel) or *HR3<sup>ΔCt65</sup>* (lower panel) by the *RPW8.2* promoter. Note about 1/3<sup>rd</sup> of T1 plants exhibited SHL and enhanced resistance to powdery mildew (red arrows). **(D)** Representative infected leaves from independent T3 lines in comparison to Col-0 at 10dpi. **(E)** Quantitative assay of disease susceptibility. Data represent means  $\pm$  SEM (n=4) from one of three representative experiments. Student's *t* test was used to calculate *P* values for comparison to Col-0 (\* = *p* < .05, \*\* = *p* < .01).



### **Despite Being Microscopically Undetectable, Expression of HR3-YFP Results in Necrotic Cell Death**

Given that all the RPW8 family members are predicted to contain an N-terminal TM domain and 1-2 coiled-coils, and that HR1, HR2, HR3 appears to be functional genes, it is likely that all of them are EHM-resident proteins. To test this, we thus translationally fused YFP to the C-terminus of HR1, HR2, HR3 and HR4 and placed these fusion genes under control of their respective native promoters (NP) (see Methods). These DNA constructs were introduced in Col-0 and >30 independent T1 transgenic lines were analyzed. Unexpectedly, we were unable to detect any fluorescent signal prior to or post inoculation with *Gc*-UCSC1 in 5-6 week-old plants (**data not shown**). Interestingly, while plants transgenic for *NP::HR1-YFP*, *NP::HR2-YFP*, and *NP::HR4-YFP* appeared phenotypically normal in stature and development, ~55% of plants transgenic for *NP::HR3-YFP* exhibited varying degrees of stunted growth and leaf necrosis (**Figure 2-5A and B** – far left panel). Surprisingly, despite the stunted growth of rosette leaves, these plants seemed to have normal root development (**Figure 2-5B** – middle left panel). These observations suggest that these constructs are likely expressed but the fusion proteins are either toxic (in the case of HR3) and/or rapidly degraded. All transgenic lines for *NP::HR1-YFP*, *NP::HR2-YFP* and *NP::HR4-YFP* are susceptible to powdery mildew (**data not shown**). Notably, *NP::HR3-YFP*-expressing plants appeared less susceptible (or moderately resistant) to *Gc*-UCSC1, as fungal growth was partially suppressed by the necrotic cell death that became exacerbated by mildew infection (**Figure 2-5B** – right panels).

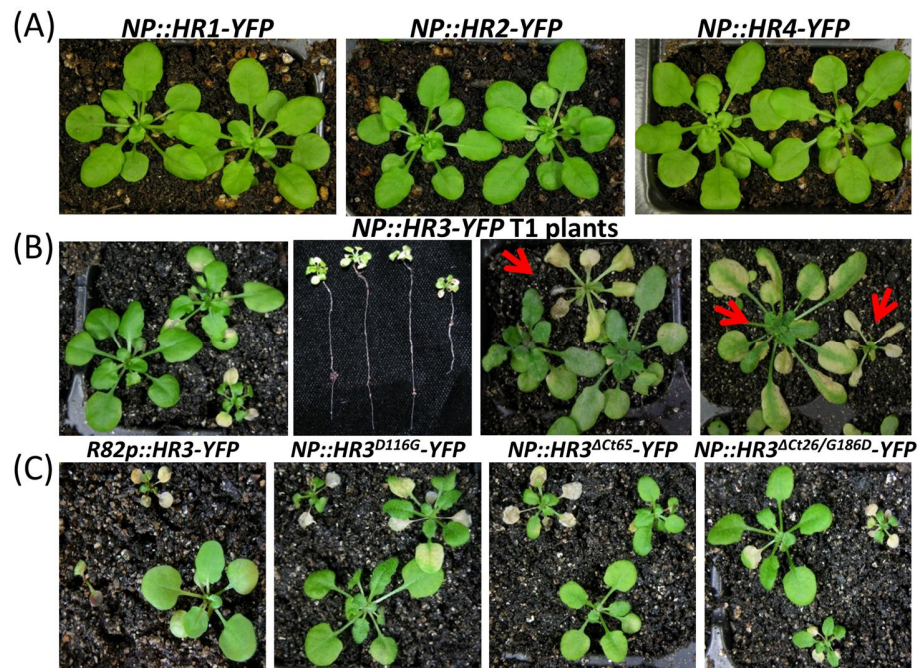


**Figure 2-5. HR#-YFP Proteins are Undetectable and Expression of HR3-YFP**

**Results in Necrotic Cell Death.**

(A) *NP::HR1-YFP*, *NP::HR2-YFP* and *NP::HR4-YFP* transgenic T1 lines (>30 tested) are phenotypically indistinguishable from wild-type plants. (B) Far left panel- Transgenic plants for *NP::HR3-YFP* exhibit varying degrees of i) stunted growth, ii) SHL and iii) leaf necrosis. Middle left panel- normal root development for *NP::HR3-YFP* T1 lines. Right panels- *HR3p::HR3-YFP* lines at 5dpi with *Gc-UCSC1*. Red arrows indicate independent lines experiencing an exacerbation of cell death and leaf necrosis. (C) Cell death phenotypes of Independent T1 lines expressing indicated DNA constructs.

The fact that there was no detectable YFP signal from any of the C-terminally tagged HR1-YFP, HR2-YFP, HR3-YFP and HR4-YFP fusion proteins is in sharp contrast to our early finding concerning RPW8.2-YFP's specific localization in the EHM (Wang et al., 2009). To understand this discrepancy, we first expressed HR3-YFP with the *RPW8.2* promoter in Col-gl. No YFP signal was observed either (**data not shown**) while similar cell death was observed (**Figure 2-5C**). Next, knowing that the aspartate-to-glycine mutation at position 116 (D116G) in RPW8.2 could abolish RPW8.2-triggered HR (Orgil et al., 2007; Wang et al., 2009), we introduced this mutation into HR3 to make *NP::HR3<sup>D116G</sup>-YFP*. Transgenic assays indicated that the D116G mutation could not suppress cell death from HR3-YFP (**Figure 2-5C**) and the fusion protein still remained “invisible” (**data not shown**), suggesting that HR cell death activated by RPW8.2 is mechanistically distinct from the necrotic cell death caused by HR3-YFP. To see if the removal of the presumable self-inhibitory C-terminal 65 AAs of HR3 could alleviate the cell death from HR3-YFP and/or enable substantial accumulation of HR3-YFP, we examined transgenic plants expressing *NP::HR3<sup>ΔCt65</sup>-YFP*. However, no noticeable effect was observed in the T1 transgenic plants (**Figure 2-5C**). Lastly, we made a mutant HR3 in which the encoded product is truncated for the C-terminal 26 AAs and contains the G186D mutation to make an SDDS C-terminus as seen in RPW8.2, such that this mutant HR3<sup>ΔCt26/G186D</sup> structurally resembles RPW8.2 most (**Figure 2-4A**). Unfortunately, no YFP signal was detected from T1 plants transgenic for *NP::HR3<sup>ΔCt26/G186D</sup>-YFP* while similar cell death was readily observed (**Figure 2-5C**). Based on the above results we reasoned that unlike RPW8.2 (Wang et al., 2009), an intact C-terminus may be required for protein stability for HR1, HR2, HR3 and HR4, and

a C-terminal fusion with YFP would make these fusion proteins unstable and/or toxic (in the case of HR3). We also inferred that the N-terminal portion of HR3 (AA<sup>1-148</sup>) must possess the capacity to activate inappropriate cell death if the likely self-inhibitory C-terminus is perturbed, and that this property of HR3 must have been lost in RPW8.2 perhaps as part of its functional diversification from the HR3-p progenitor.

To test the above speculation, we created chimeric domain swap constructs between the N- and C-terminal domains of RPW8.2 and HR3 where the N-terminal domains were defined based on the predicted end of the 2<sup>nd</sup> coiled-coil domain for each protein (HR3<sup>1-147</sup>=HR3n and RPW8.2<sup>1-145</sup>=R82n) using the web-based prediction software (COILS) (Lupas et al., 1991). The C-terminal 66 aa of HR3 (HR3c) were translationally fused to the N-terminal sequence of RPW8.2 and the C-terminal 29 aa of RPW8.2 (R82c) were fused to the N-terminal sequence of HR3, and these chimeric genes were fused with YFP at the C-terminus (**Figure 2-6A**). More than 25 transgenic T1 plants and five T2 lines were examined for each chimeric construct. Interestingly, we found that R82n-HR3c-YFP was functional in defense activation and localized to the EHM induced by *Gc*-UCSC1 in a similar manner as RPW8.2-YFP (**Figure 2-6B&C** – left panels), suggesting that R82n is essential for the stability, defense and targeting properties of RPW8.2 while R82c is dispensable. In contrast, HR3n-R82c-YFP expressed from either the *HR3* or the *RPW8.2* promoter was undetectable (**Figure 2-6C** – right panel), which is consistent with the results from the C-terminally YFP tagged HR3 mutants (**Figure 2-5**). However, T1 plants transgenic for HR3n-R82c-YFP lines did not develop necrotic cell death and stunted phenotypes observed in HR3-YFP transgenic lines and were fully susceptible to *Gc*-UCSC1 (**Figure 2-6B&C** – right panels). This

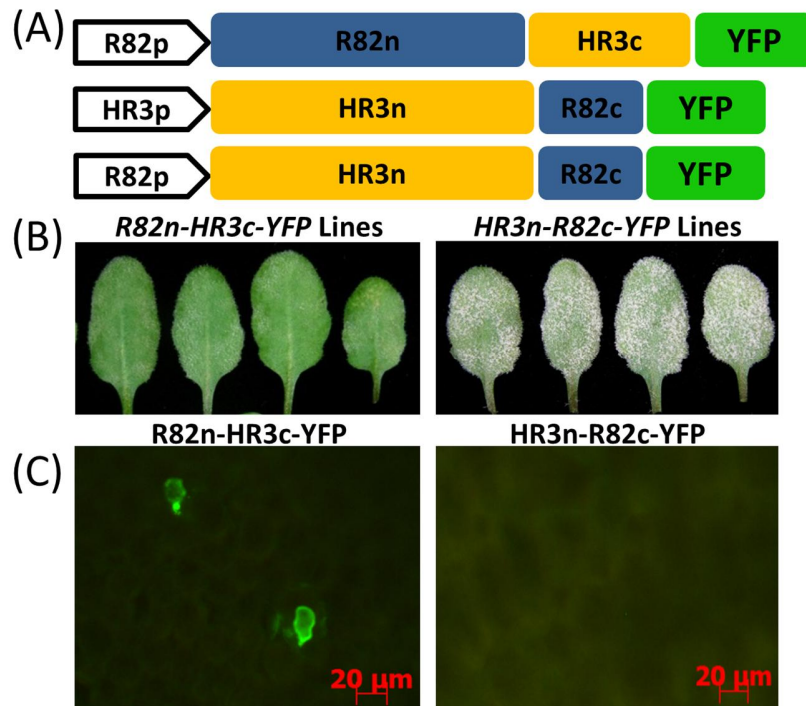


**Figure 2-6. Chimeric R82n-HR3c is Functional While HR3n-R82c Remains Undetectable.**

(A) Schematic drawing of the chimeric R82n-HR3c and HR3n-R82c genes in fusion with YFP driven either by the *RPW8.2* or *HR3* promoter. HR3n=HR3<sup>1-147</sup>, R82n=RPW8.2<sup>1-145</sup>, HR3c=HR3<sup>148-213</sup> and R82c=RPW8.2<sup>146-174</sup>. (B) Phenotypes of the indicated genotypes. Representative leaves from infected plants at 12dpi were shown to reflect the functionality of the DNA constructs. (C) Protein expression and localization analysis. Note that R82n-HR3c-YFP is detected at the EHM, whereas HR3n-R82c-YFP was undetectable.

implies that R82c may be able to suppress HR3n-mediated inappropriate cell death. Alternatively, HR3n-R82c-YFP was very unstable and could not accumulate to a level sufficient for triggering cell death. A more detailed structure-function analysis between HR3 and RPW8.2 is needed to reveal the molecular and evolutionary mechanisms underlying the functional differences between these two related proteins.

### **All Examined RPW8 Homologs Are Localized to the Extrahaustorial Membrane**

From the above analysis, we were unable to determine if the RPW8 homologs are also EHM-resident proteins due to the unknown intrinsic constraints associated with C-terminal YFP tagging. Neither did we succeed in detection of internally YFP-tagged HR3 by microscopy (**data not shown**). Previously we reported that N-terminally YFP tagged RPW8.2 (YFP-RPW8.2), despite its loss of function in defense, was specifically targeted to the EHM in cells invaded by the haustorium (Wang et al., 2010). We thus reasoned that N-terminal YFP-tagging may be used to investigate the subcellular localization of the RPW8 homologs. Therefore, we made DNA constructs in which HR1, HR2, HR3, HR4, and two *B. oleracea* homologs *BoHRA* and *BoHRC*, were individually fused with YFP at their N-termini. These DNA constructs were stably expressed from the 35S promoter in Col-gl. Before infection, YFP signal from each of the six fusion proteins appeared to be distributed in or around the plasma membrane (PM) (**Figure 2-7A**). Interestingly, YFP puncta were observed along the plasma membrane in some lines for all six fusion proteins (see YFP-HR3 and YFP-*BoHRA* as examples) and YFP signal was occasionally found in proximity to the nucleus (see YFP-HR2 and YFP-HR3) (**Figure 2-7A**). To determine if the observed YFP signal was indeed in the PM,

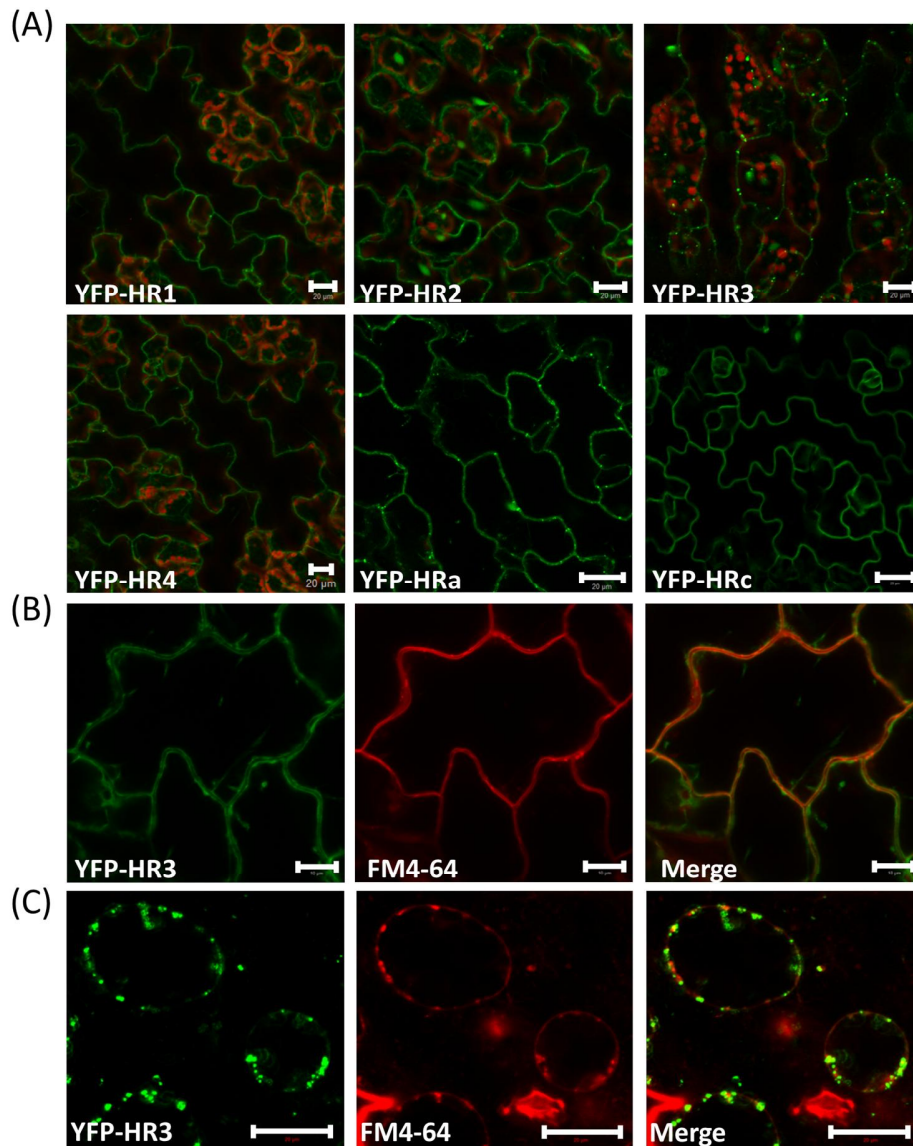


**Figure 2-7. N-terminally Fused RPW8 Family Member Proteins are Localized to the Plasma Membrane.**

**(A)** Localization patterns of N-terminally YFP-tagged RPW8 homologs (excluding BoHRb) stably expressed from 35S in Col-gl. YFP signal was pseudo-colored green while autofluorescent chloroplasts (in some instances) are pseudo-colored red. Bars = 20µm. **(B)** Co-localization between YFP-HR3 and FM4-64. Bars = 20µm. Leaf sections were treated with FM4-64 and imaged at 15-30min after treatment. **(C)** Plasmolysis of

cells expressing *35S::YFP-HR3*. Leaf sections were first stained with FM4-64 for 15-30min and then treated with 1M NaCl for ~2-3min before imaging. Bars = 20µm. Note the YFP puncta align nicely with FM4-64 stained PM.



treated leaf sections of transgenic lines expressing each of the six fusion proteins (YFP-HR3 was shown as a representative) with FM4-64, a lipophilic dye to allow visualization of the PM and other endomembranes, and subsequently added 1M NaCl to induce plasmolysis. We found that the YFP signal in all cases co-localized nicely with the FM4-64 stained PM before and post plasmolysis (**Figure 2-7B and C**), indicating that these YFP-tagged proteins are localized to the PM.

I then challenged these transgenic lines with *Gc*-UCSC1 to examine the localization of these fusion proteins in epidermal cells invaded by haustoria. Interestingly, we found that all of the six YFP-fusion proteins appeared to be preferentially or even exclusively targeted to the EHM in epidermal cells invaded by haustoria (**Figure 2-8A**), similar to our observation with YFP-RPW8.2 (Wang et al., 2010). The EHM-localization of these fusion proteins were confirmed by the precise colocalization between YFP-HR3 and RPW8.2-RFP at the EHM (**Figure 2-8B**). To exclude the possibility that EHM-localization of these fusion proteins was caused by overexpression of these fusion proteins, I also generated transgenic lines expressing YFP-HR1, YFP-HR2, and YFP-HR3 from the *RPW8.2* promoter. As predicted, expression of from these fusion proteins was mostly confined to haustorium-invaded cells and YFP signals were mostly or exclusively found in the EHM (**Figure 2-8C**). All T1 transgenic plants expressing these fusion proteins (>20 for each construct) were as susceptible as Col-gl to *Gc*-UCSC1 (**Figure 2-8C** – right panels), confirming the non-functional nature of these fusion proteins in defense activation. To rule out the possibility that membrane proteins may be targeted by default to the EHM in the haustorium-invaded cells during the biogenesis of the EHM, we expressed two YFP tagged PM-localized membrane

proteins, LTI6b (Koh et al., 2005), and SPY131 (Uemura et al., 2004) in Col-gl from the *RPW8.2* promoter. Both YFP-LTI6b (**data not shown**) and YFP-SYP131 (**Figure 2-8D**) showed exclusive PM localization in haustorium-invaded cells, indicating the EHM-targeting of the YFP-tagged RPW8 homologs is attributable to the properties of these proteins rather than as a consequence of activation of a default EHM-oriented trafficking pathway. Our recent analysis on RPW8.1 also indicates that RPW8.1-YFP can also be targeted to the EHM when expressed from the *RPW8.2* promoter (Wang et al., under review).

Intriguingly, we also noticed that these N-terminally YFP tagged RPW8 homologs showed focal accumulation around the fungal penetration site, where a callosic papilla is formed and is visualized by Sirofluor staining (see Methods) (one representative shown in **Figure 2-9A**). A papilla is part of a cell wall apposition where defense chemicals, including callose ( $\beta$ -1,3-glucan) are deposited in response to fungal penetration (Bushnell and Bergquist, 1975; Aist, 1976; Huckelhoven et al., 1999). This localization pattern is reminiscent of PEN1/SYP121, a syntaxin involved in penetration resistance (which is likely required for a timely assembly of papillae) (Collins et al., 2003a; Assaad et al., 2004; Kwon et al., 2008). To determine the precise localization of YFP-HR3 (as a representative) in relation to papillae, we looked at the invaded cells at higher magnification and found that YFP-HR3 was not always exactly colocalized with callose, as it was more concentrated in the middle and the rim of the bull's eye shape of the callosic papillae (**Figure 2-9B**). These observations suggest that the endogenous HR3 protein and proteins of other RPW8 homologs are targeted to the papillae, whereby they may serve a

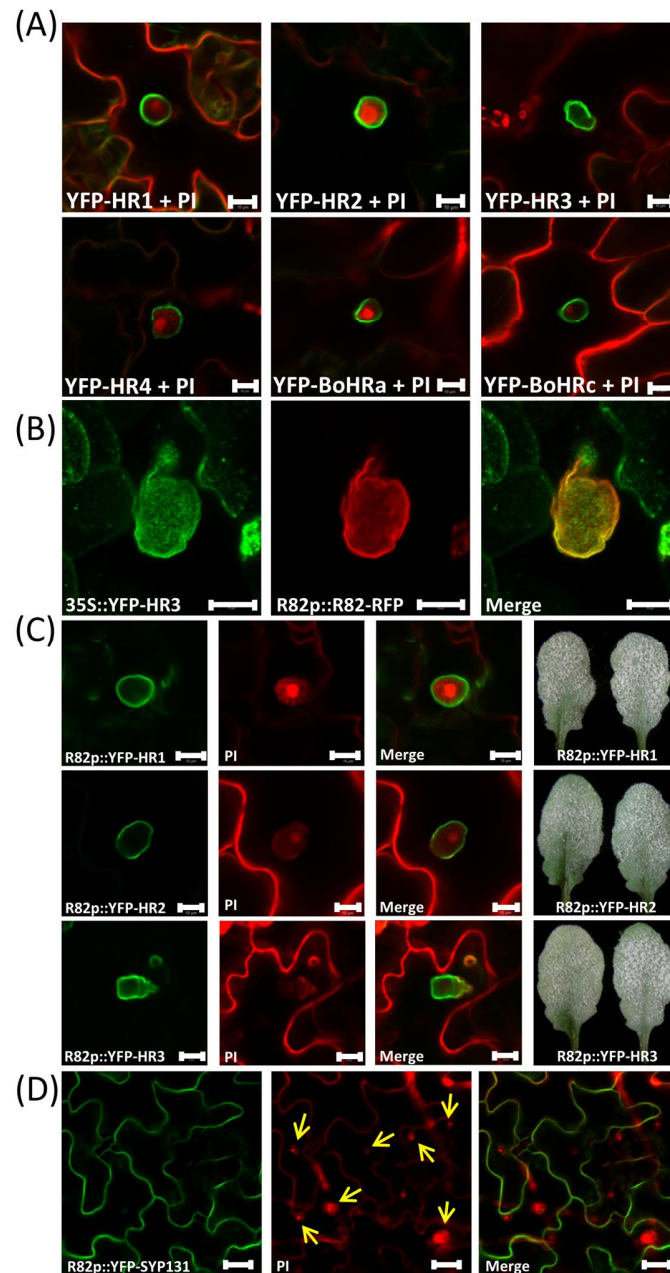


**Figure 2-8. All RPW8 Homologs are Localized to the Extrahaustorial Membrane.**

(A) Representative images showing localization of the indicated YFP fusion proteins. Host PM and fungal haustoria were stained by propidium iodide. Images were taken from infected leaves at 42hpi. Bars = 10 $\mu$ m. (B) Serial images of a representative Z-stack projection showing the colocalization between YFP-HR3 and RPW8.2-RFP at the EHM. Bars = 10 $\mu$ m. (C) Representative images showing the localization of the

indicated fusion protein expressed from the *RPW8.2* promoter (left panels) and representative infected leaves (at 12dpi) for the indicated transgenic lines (right panel). Bars = 10µm. **(D)** Localization of GFP-SYP131 expressed from the *RPW8.2* promoter. Fungal structures were stained by propidium iodide. Yellow arrows indicate differentiating haustoria. Bars = 20µm.

yet-to-be determined cellular function, contributing to basal resistance against powdery mildew as revealed by our earlier genetic results (**Figure 2-1/2/3/4**).

### **YFP-HR3 is Translocalized to the Callosic Papilla Region via a BFA-Sensitive Endosomal Recycling Pathway**

Because powdery mildew-induced YFP-HR3's focal accumulation at the penetration site was not significantly affected by cycloheximide (CHX) treatment (see **Chapter 3**), it is very likely that the PM-localized YFP-HR3 is trans-localized to the papilla via an endosomal recycling pathway. A recent study reveals that focal accumulation of YFP-PEN1 and callose deposition at the fungal penetration site engage a brefeldin A (BFA)-sensitive endosomal recycling pathway (Nielsen et al., 2012). We thus tested if YFP-HR3's localization to the papilla is BFA sensitive. We treated leaves of plants transgenic for *35S::YFP-HR3* and *RPW8.2p::RPW8.2-RFP* with BFA (300  $\mu$ M) and examined the leaf sections at 30 and 45hpi. As expected, YFP-HR3 in control leaves treated with 1% DMSO water solution was found in the PM, the callosic papilla, and the EHM (as shown by precise colocalization with RPW8.2-RFP) (**Figure 2-10A and B; Suppl-Figure 2-1**). However, in BFA-treated leaves, while YFP-HR3 exhibited normal PM and EHM localization and RPW8.2-RFP showed EHM-specific localization, focal accumulation of YFP-HR3 was significantly reduced (~78%) in comparison with that in DMSO control leaves (**Figure 2-10A-C; Suppl-Figure 2-1**). Callose deposition in the papilla showed a similar reduction (~86%), nicely correlating with the reduction of the YFP-HR3 signal in the papilla (**Figure 2-10A-C; Suppl-Figure 2-1**). Based on these observations, we conclude that (i) YFP-HR3's translocalization from the PM to the

papilla is via a BFA-sensitive endosomal recycling pathway that is likely also engaged for callose deposition at the penetration site, and that (ii) EHM-localization of newly synthesized YFP-HR3 and RPW8.2-YFP recruit a BFA-insensitive, most likely the biosynthetic secretory pathway.

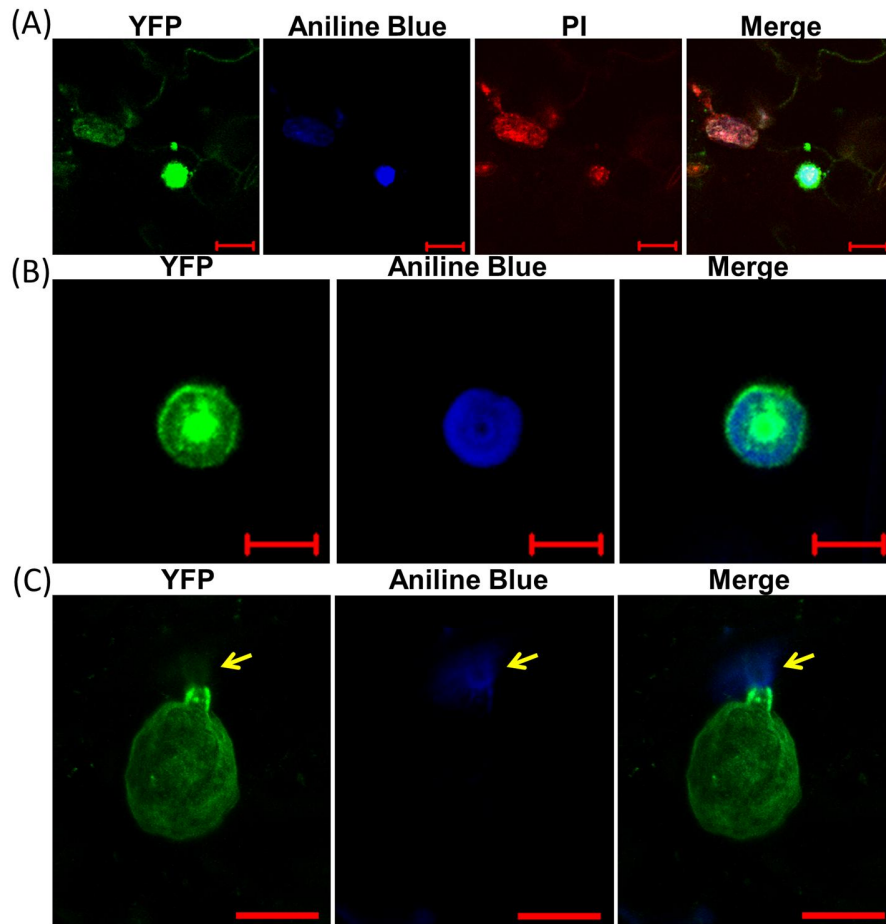


**Figure 2-9. YFP-RPW8 Homologs Show Focal Accumulation Around the Fungal Penetration Site.**

**(A)** An image showing that YFP-HR3 expressed from 35S is localized to the PM and the fungal penetration site where callose and other defense molecules are deposited to form papillae. Callose is visualized by Sirofluor staining. Bars = 20 $\mu$ m. **(B)** A single optical section image showing heterogeneous distribution of YFP-HR3 at the penetration site where callose is deposited. Note the incomplete overlapping between YFP-HR3 and callose. Bars = 5 $\mu$ m. **(C)** A representative Z-stack projection showing that YFP-RPW8 is only in the EHM localization but rarely found in or near the fungal penetration site where callose accumulates ( indicated by an arrow). Bars = 10 $\mu$ m.

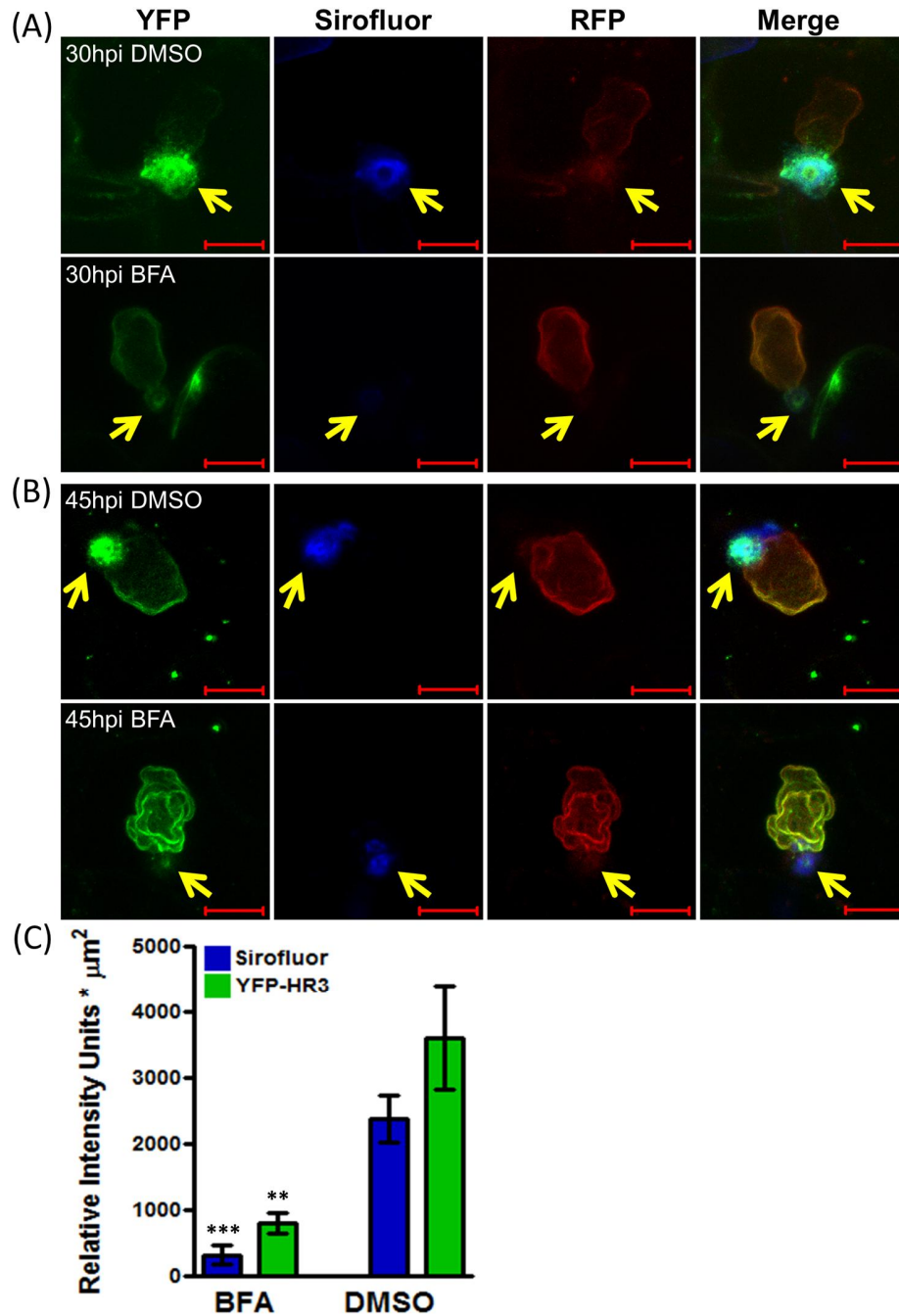
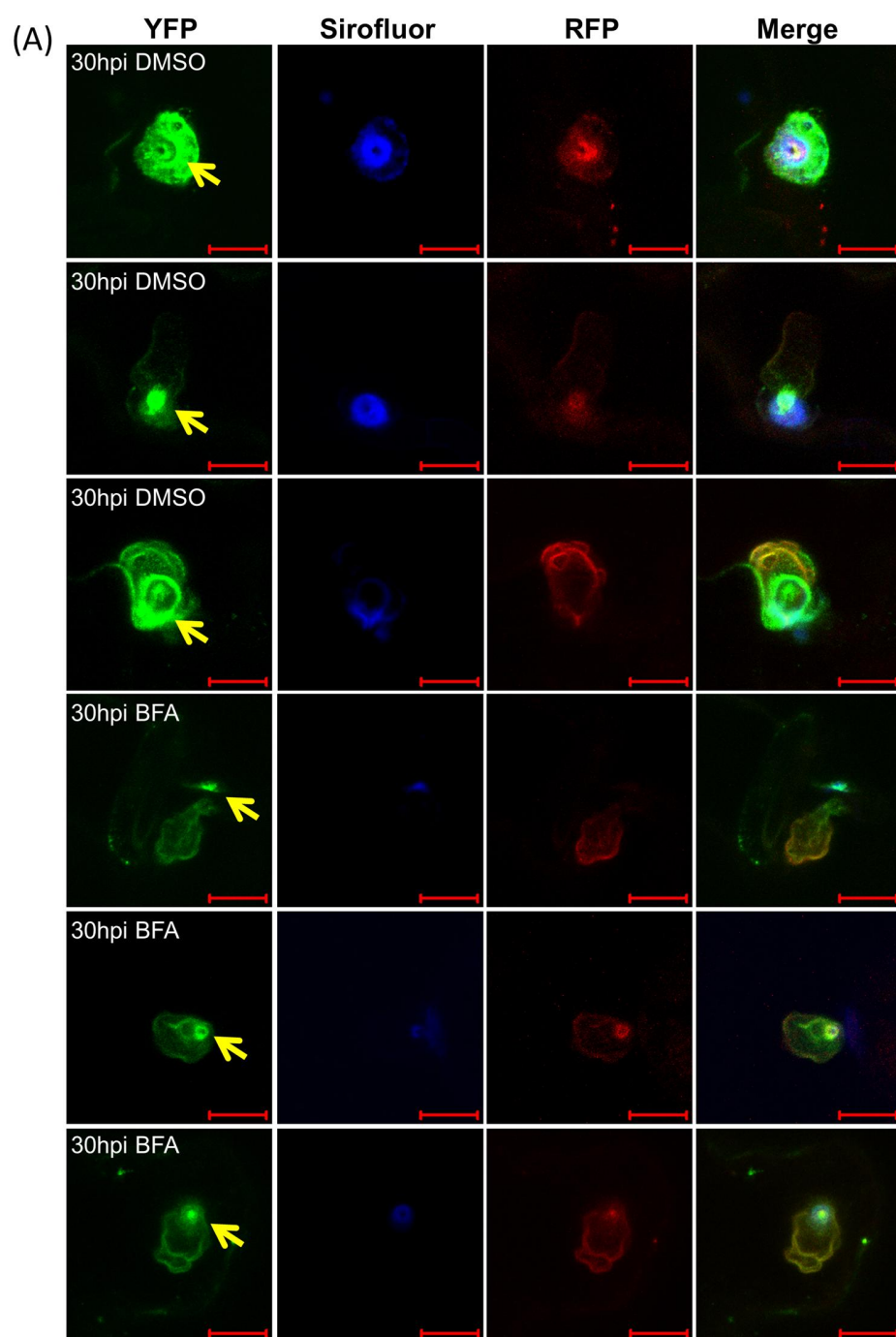


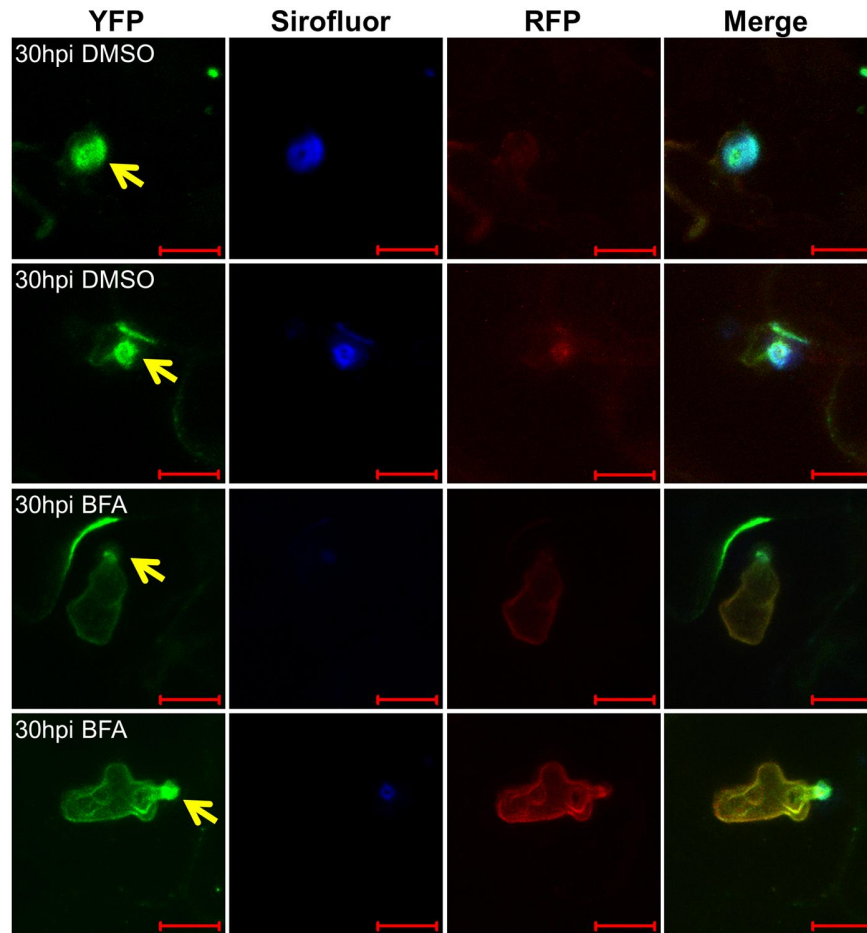
**Figure 2-10. Translocation of YFP-HR3 to the Penetration Site is BFA-Sensitive.**

(A - B) Representative images showing localization of YFP-HR3 to the PM, the papilla, and the EHM in haustorium-invaded cells at 30hpi (A) or 45hpi (B). Detached leaves from plants stably co-expressing *35S::YFP-HR3* and *RPW8.2p::R82-RFP* were treated



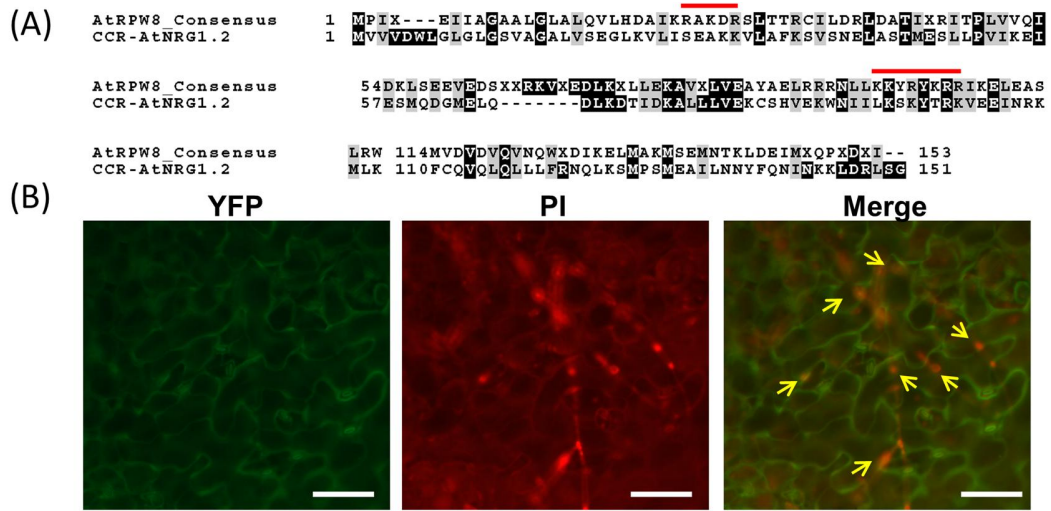
with either 1% DMSO buffer or 300 $\mu$ M BFA at ~6hpi (see Methods). The EHM was highlighted by RPW8.2-RFP and the callose was stained by Sirfluor (indicated by an arrow). Note that both YFP-HR3 and callose were diminished in the papilla due to BFA treatment. Bars = 20 $\mu$ m. **(C)** Quantification of relative fluorescence intensity for YFP-HR3 and Sirofluor-stained callose at the papilla in images captured in **(A)**. Data represent means  $\pm$  SEM (n=6) from one of two independent experiments. Student's *t* test was used to compare the differences between treatments (\*\* =  $p < .01$ , \*\*\* =  $p < .001$ ).





**Suppl-Figure 2-1. Localization of YFP-HR3 to the Penetration Site is BFA-Sensitive.**

**(A)** Additional images showing localization of constitutively YFP-HR3 to the PM, the papilla, and the EHM in haustorium-invaded cells at 30hpi. Detached leaves from plants stably co-expressing *35S::YFP-HR3* and *RPW8.2p::R82-RFP* were treated with either 1% DMSO buffer or 300 $\mu$ M BFA at ~6hpi (see Methods). The EHM was highlighted by RPW8.2-RFP and the callose was stained by Sirofluor and (indicated by an arrow). Bars = 20 $\mu$ m.



**Suppl-Figure 2-2. The YFP-tagged N-terminal Coiled Coil Domain of *AtNRG1.2* is Not Localized at the EHM.**

(A) Alignment of the consensus amino acid sequence of the *AtRPW8* family members and the CC<sub>R</sub> domain of *AtNRG1.2*. The sequences were aligned by ClustalW and shaded using the BOXSHADE server. The two putative EHM-targeting sequences (R/K-X-R/K-X-R/K) for the RPW8 family members are indicated with red lines. The second motif appears to be partially conserved between *AtNRG1.2* and the RPW8 family members.

(B) Localization of CC<sub>R</sub><sup>*AtNRG1.2*</sup>-YFP from mildew-infected leaf epidermal cells expressing 35S::CC<sub>R</sub><sup>*AtNRG1.2*</sup>-YFP. Note that YFP signal was predominantly found in the PM but absent from where the EHM may be present. Fungal structures (red) were visualized by propidium iodide staining (arrows indicate likely fungal penetration sites). Bars = 50µm.

## Discussion

In this study, we have shown that (i) HR3, the presumptive progenitor of the RPW8 family, and other family members play a positive role in basal resistance and that (ii) specific EHM-localization is probably a conserved feature for the RPW8 family. Thus, evolution of RPW8.2 (and RPW8.1)-mediated broad-spectrum mildew resistance represents functional improvement/renovation rather than an entirely new invention from the more ancient family members.

### Functional Diversification of RPW8.2 from HR3

Based on sequence analysis, we previously inferred that RPW8.1 (and HR4) evolved from RPW8.2, and RPW8.2 in turn evolved from duplication and functional diversification from an HR3-like progenitor gene (Xiao et al., 2004). In this study, we found that HR3 and other family members including RPW8.1 (Wang et al., manuscript under review) and two *Brassica oleracea* homologs examined are all likely EHM residents. This suggests that EHM-targeting is a unique feature of subcellular localization originated in an early stage of the evolution of the RPW8 family and has been maintained for millions of years before the separation of Arabidopsis from the *Brassica* lineage. In addition, our genetic data showed that HR1, HR2 and HR3, which are present in all Arabidopsis accessions with very low levels of intraspecific polymorphism (thus are likely under purifying selection) (Xiao et al., 2001; Xiao et al., 2004; Orgil et al., 2007), appear to contribute to basal resistance to powdery mildew (**Figure 2-1 and 2**). Thus, we conclude that RPW8.2's capability in triggering haustorium-targeted defense is not an entirely new innovation, but rather stemmed from

that of HR3. Indeed, the two likely EHM-targeting motifs identified through a comprehensive mutational analysis of RPW8.2 are mostly conserved among the family members (**Suppl-Figure 2-2A**, Wang et al., manuscript under review), and similar to RPW8-mediated resistance, *HR3*-overexpression-mediated enhanced resistance to *Gc*-UCSC1 is also SA-dependent. It is therefore possible that the semi-dominant resistance gene *RPW8.2* has evolved to increase the strength of defense response to counterattack more adapted and aggressive powdery mildew pathogens, whereas *HR1*, *HR2*, and *HR3* may activate basal level of resistance function against less adapted powdery mildew or potentially other haustorium-forming pathogens while minimizing the cost of resistance in the absence of any pathogen that appears to be associated with expression of *RPW8* (Orgil et al., 2007). A critical question then is how RPW8.2-mediated resistance is mechanistically renovated from the original function of HR3. Our present studies provided some insights onto this question. First, while RPW8.2-YFP appears to be mostly functional and accumulates at high levels at the EHM, HR3-YFP is toxic, as reported by a stunted phenotype of transgenic lines (**Figure 2-5**), and unfortunately cannot accumulate to a level detectable in the cells. This suggests that the C-tail of HR3 may serve an auto-inhibitory domain and needs to be intact for proper function/behavior of HR3, whereas this constraint is relaxed for RPW8.2. Interestingly, results from our domain swapping experiments indicate that it is the difference in the N-terminal portion ( $RPW8.2^{Nt1-145}$  and  $HR3^{Nt1-147}$ ) that underlies the major functional diversification between RPW8.2 and HR3. This conclusion was based on our observation that the chimeric protein R82n-HR3c-YFP behaved similarly as RPW8.2-YFP in defense and EHM-targeting whereas HR3n-R82c-YFP did not confer resistance and the protein was not

detectable (**Figure 2-6**). There are 28 non-similar and 14 similar aa substitutions, and two aa insertion/deletion between RPW8.2 and HR3 in the 1-147 aa region. A detailed mutational analysis is needed to nail down the residues that determine the functional divergence. Second, because YFP-RPW8, though not functional in defense activation, is also targeted to the EHM (Wang et al., 2010), we reason that subcellular localization of YFP-HR3 may also faithfully reports that of the native HR3 protein. It is thus worth noting that YFP-HR3 but not YFP-RPW8.2 (**Figure 2-9**), was found in the papillae when expressed either from the *35S* or *RPW8.2* promoter. This suggests that a signal for papillae localization in HR3 might have been lost in RPW8.2. Given that PEN1 and MLO, two genetically defined components involved in penetration resistance also show focal accumulation in papillae (Bhat et al., 2005), whether YFP-HR3's papilla localization correlates with its possible role in penetration resistance against non- or poorly-adapted powdery mildew remains to be an interesting question for future investigation. Lastly, functional improvement of RPW8.2 from HR3 may be partly attributed to the *RPW8.2* promoter, which renders powdery mildew inducible, epidermal cell-specific expression of RPW8.2 (Wang et al., 2009), whereas the HR3 promoter (~500bp 5' sequence between the HR2 stop codon and the HR3 start codon) appears to be weak, as we rarely if ever observed detectable levels of YFP-HR3 from the HR3 promoter (**data not shown**). Supporting this speculation, expression of HR3 from the *RPW8.2* promoter conferred enhanced resistance to powdery mildew (**Figure 2-4**). Thus, functional evolution of RPW8.2 from HR3 probably necessitated DNA sequence diversification at both the 5' regulatory and the coding region for higher efficiency in defense activation while conserving the amino acids for EHM-targeting.

There is also likely functional redundancy among HR1, HR2, and HR3, as evidenced by our observation that the RNAi lines aiming at silencing all the three genes were slightly more susceptible than single knockout or knockdown lines (**Figure 2-3**). However, to what extent these three genes together contribute to basal resistance against powdery mildew and potentially other pathogens is not clear because mutants with simultaneous loss of all the three tandemly-arrayed genes are not available.

*HR4* is the youngest member of the *RPW8* family in *A. thaliana*. It was thought to have evolved from *RPW8.1* via a gene conversion event after a transposon-insertion-mediated deletion of *RPW8.2* in a few Col-0-like accessions that are most susceptible to powdery mildew (Xiao et al., 2004; Orgil et al., 2007). Unlike other family members, (over)expression of *HR4*, *YFP-HR4*, or *HR4-YFP* by the *35S* promoter or the *RPW8.2* promoter (**Figure 2-1; data not shown**) did not alter powdery mildew infection phenotypes. These results suggest that HR4 may not play any positive role in mildew resistance, which is compatible with its occurrence only in accessions with higher mildew susceptibility. Nonetheless, the EHM-targeting feature has apparently been maintained in HR4, implying that either HR4 still plays a role in relation to haustorial invasion or its EHM-targeting feature is purely a relic from its immediate progenitor protein. Interestingly, HR4 is induced upon infection by powdery mildew (Chandran et al., 2009), or *Pseudomonas syringae* (Bricchi et al., 2012), and upon colonization by a beneficial endophytic fungus *Trichoderma atroviride* (Saenz-Mata and Jimenez-Bremont, 2012). How HR4 might contribute to host interaction with multiple microbes remains to be investigated.



### **RPW8 Family Proteins May Function as Sorting Adaptors?**

Now that HR3, the oldest RPW8 family member, appears to be a resistance protein localized at the EHM, one may wonder how HR3 might have functionally originated. BLAST showed that HR3 has the highest homology outside the RPW8 family to the CC domain (designated CC<sub>R</sub> for CC homologous to RPW8) of a group of NB-LRR proteins (CC<sub>R</sub>-NB-LRR) falling into a conserved group represented by the *Nicotiana benthamiana* N-required gene 1 (NRG1) protein and the *Arabidopsis* activated disease resistance gene 1 (ADR1) protein (Xiao et al., 2008; Collier et al., 2011). Both NRG1 and ADR1 are genetically defined as non-canonical NB-LRR proteins that do not function as sensors for pathogen effectors, but rather act as signaling components (Grant et al., 2003; Peart et al., 2005) for immune response, suggesting that they play a more generic and/or likely more ancient function in innate immunity. CC<sub>R</sub>-NB-LRR genes (the ADR1-like clade in particular) are highly conserved in higher plants (Collier et al., 2011). This functional relatedness and sequence homology between HR3 (and other RPW8 family proteins) and CC<sub>R</sub>-NB-LRRs raised a tantalizing question as to how RPW8 family proteins originated in relation to the apparently more ancient CC<sub>R</sub>-NB-LRR proteins. Theoretically, there may be two possibilities: the CC<sub>R</sub> domain of an ancient CC<sub>R</sub>-NB-LRR gene might have spun off the NB-LRR backbone and been maintained initially as a gene encoding a trans-acting CC<sub>R</sub> domain and eventually evolved into the progenitor of the RPW8 family in *Brassicaceae* (Collier et al., 2011). The other possibility is that the RPW8 family genes evolved independently of CC<sub>R</sub>-NB-LRRs through convergent evolution. In both cases, it is possible that the RPW8 family proteins function to activate resistance via exploiting the central immunity machinery governed by NB-LRR proteins

perhaps in a similar manner as the CC<sub>R</sub> domain in the NRG1- and ADR1-like proteins. Indeed, this speculation is supported by the observations that transient expression of RPW8.1 and RPW8.2 (Xiao et al., 2003a), or the CC<sub>R</sub> domain of NRG1-like or ADR1-like Arabidopsis genes in *N. benthamiana* activate cell death (Collier et al., 2011), and that RPW8 activates resistance via the EDS1-dependent pathway (Xiao et al., 2003b; Xiao et al., 2005) that is also engaged for N- and NRG1-mediated resistance to TMV (Liu et al., 2002). Recently, it has been proposed that, in mammalian cells, Toll-like immune receptors (TLRs) recruit sorting adaptors such as MyD88 and TRIF for activation of immune signaling at specific subcellular locales, and the TIR domain is thought to render the sorting capacity (Kagan, 2012). Similarly, different TIR-NB-LRR and CC-NB-LRR proteins have been shown distinct intracellular locations (reviewed by Heidrich et al., 2012), and there has been at least one study that provides experimental evidence to support that the TIR and CC domains of several plant NB-LRR proteins may determine subcellular localization of these NB-LRR proteins (Takemoto et al., 2012). Under this context, the highly specific EHM-localization of the RPW8 family proteins raise a possibility that they may function as sorting adaptors for directing an immune complex to the host-pathogen interface for haustorium-targeted defense. It is also reasonable to speculate that the CC<sub>R</sub> domain of the CC<sub>R</sub>-NB-LRR proteins may provide sorting function for these immunity proteins or an interface for interaction with sorting adaptors such as the RPW8 family proteins. As an initial test, we made and express the CC<sub>R</sub><sup>AtNRG1.2</sup>-YFP fusion construct and expressed it in *N. benthamiana* and Arabidopsis. Although transient overexpression of CC<sub>R</sub><sup>AtNRG1.2</sup>-YFP in *N. benthamiana* activated cell death (**data not shown**) similarly as the CC<sub>R</sub> domain of *AtNRG1.2* (Collier et al., 2011),

we did not observe EHM-localization of  $CC_R^{AtNRG1.2}$ -YFP in Arabidopsis plants stably expressing this fusion protein which appeared to be ubiquitously distributed (**Suppl-Figure 2-3B**). This result is not completely unexpected as only the 2nd of the two putative EHM-targeting signals in RPW8.2 and HR3 (Wang et al., manuscript under review) seems to be partially conserved in the  $CC_R$  domain of *AtNRG1.2* (**Suppl-Figure 2-3A**). This implies that the EHM-targeting feature of the RPW8 family proteins probably evolved independently of the  $CC_R$ -NB-LRR proteins and the sequence conservation between RPW8 family and  $CC_R$ -NB-LRR proteins may mainly hint a connection or related mechanism in defense activation. How exactly RPW8 family proteins activate SA- and EDS1-dependent defense at the host-pathogen interface remains to be determined.

## **Materials & Methods**

### **Plant materials and cultivation**

Arabidopsis accessions Col-0 or its variants, Col-gl (Col-0 containing the glabrous mutation) and Col-*NahG* (Col-0 transgenic for a bacterial SA hydrolase gene) were used for generation of transgenic lines. The Col-gl transgenic line (*S5*) carrying one copy of *RPW8.1* and *RPW8.2* from the Ms-0 accession under control of their native promoters was used as a resistant reference and for crossing with *hr3-kol*. All genetic analyses including crossing, genotyping and phenotyping were conducted in accordance with previous reports (Xiao et al., 2003b; Xiao et al., 2005). Unless otherwise indicated, seeds were sown in Sunshine Mix #1 or Metro-Mix 360 soil (Maryland Plant & Suppliers, Inc, USA) and cold-treated (4 °C for 1-2 days). Seedlings were kept under 22 °C, 75% RH, short-day (8 hrs light at  $\sim 125 \mu \text{mol} \cdot \text{m}^{-2} \cdot \text{sec}^{-1}$ , 16 hrs dark) conditions for 5-6 weeks before pathogen inoculation and/or other treatments.

### **Pathogens strains, inoculation and phenotyping**

Powdery mildew isolate *Golovinomyces cichoracearum* UCSC1 (*Gc*-UCSC1) was maintained on live Col-0 or Col-*NahG* plants for generation of fresh conidia for inoculation purposes. Inoculation, visual scoring, photographing and quantification of disease susceptibility were done as previously described (Xiao et al., 2005). All pathogen infection experiments were repeated at least three times.

### **DNA constructs and generation of transgenic lines**

Overexpression constructs for *HR1*, *HR2*, *HR3* and *HR4* were created following amplification of the genomic sequence including ~1000bp of the 5' UTR/promoter region (496bp in the case of *AtHR3*) from the T20E23 BAC clone obtained from the Arabidopsis Biological Resource Center (ABRC) into the binary vector pKMB downstream of the 35S promoter (Mylne and Botella, 1998). The overexpression construct for *BoHRA* was created following amplification of the genomic sequence from the 25K1 BAC clone using the primers (BoHRatpF: 5' caccATGCCGATTGGTGAGGTTCTTGTA<sup>3'</sup> and BoHRaR: 5' TTCCATTCCACACAACAACAAGA<sup>3'</sup>) (Xiao et al., 2004 ) and inserted downstream of the 35S promoter in the pCXSN binary vector (Chen et al., 2009b).

An artificial miRNA (amiRNA) was constructed according to a published method (Schwab et al., 2006) incorporated into the web-based tool at (<http://wmd3.weigelworld.org/>). The primers for making the *HR1-3ami* are: (HR321-1miR: 5' gaTGTTTAGTGTTTCATATCGGACtctctcttttgattcc<sup>3'</sup>, HR321-2miR: 5' gaGTCCGATATGAACACTAAACAtcaaagagaatcaatga<sup>3'</sup>, HR321-3miR: 5' gaGTACGATATGAACCTCTAAACTtcacaggtcgtgatatg<sup>3'</sup> and HR321-4miR: 5' gaAGTTTAGAGTTCATATCGTACtctacatatattctct<sup>3'</sup>). The amiRNA fragment was digested with *KpnI/BamHI* and cloned into the binary vector pBTEX *KpnI/BamHI* site downstream of the 35S promoter (Frederick et al., 1998).

The pCX-DG TA cloning vector described in (Chen et al., 2009b) was modified by replacing the 35S-GFP fragment upstream of the *ccdB* gene with a ~1.6-kb fragment containing the *RPW8.2* promoter using *EcoRI* digestion and subsequent ligation to make the cloning vector pCX-DG-82p. We used this modified TA cloning vector to express

the full length *AtHR3g* using the primers (BamHR3F:

5'caggatccATGCCGGTTAGTGAGATTATGGCA<sup>3'</sup> and BamHR3R2:

5'gcggatccTCACTTCAAGACAAATCGGATCTCACGGT<sup>3'</sup>) and a truncated version of *AtHR3*, *HR3<sup>ΔCt65</sup>* using the primers (BamHR3F and BamHR3-148R:

5'gcggatccTCATGGTTGACGAGTGATTCATCAAGT<sup>3'</sup>), by the *RPW8.2* promoter.

*Arabidopsis* homologs under control of their native promoters were translationally fused at the C-terminus with YFP using the pPZPYFP23' vector described in (Wang et al., 2007), a modified derivative of pPZP211 (Hajdukiewicz et al., 1994), using the primers: (BamHI-HR1pF: 5'gcggatccGAGCGGTTTGAAGCATCTTGTT<sup>3'</sup> and BamHI-HR1R: 5'gcggatccGAAGATGAACCGGATCTCGTGCT<sup>3'</sup>), (BamHI-HR2pF: 5'gcggatccGCATCTCAATGGACTTTAACAACACCA<sup>3'</sup> and BamHI-HR2R: 5'gcggatccCAAACGAAGCGAATTCCGTGAT<sup>3'</sup>), (BamHI-HR3pF: 5'gcggatccGCTAAAGAGCTAATCTCTTGACCCA<sup>3'</sup> and BamHI-HR3R: 5'gcggatccCTTCAAGACAAATCGGATCTCACGGT<sup>3'</sup>) and (BamHI-HR4pF: 5'gcggatccCATTCGTTGGAGTTGTGTAATGAGGA<sup>3'</sup> and BamHI-HR4R: 5'gcggatccGCCTTCATTTCTTTGATATCGGTCCA<sup>3'</sup>). Derivatives of *NP::HR3-YFP* in the same vector were created using the primers- (HR3-D116GF: 5'TCATTAAGATGGATGGTAGGTGTGGATGTCCAAGTCAAT<sup>3'</sup> and HR3-D116GR: 5'ATTGACTTGGACATCCACACCTACCATCCATCTTAATGA<sup>3'</sup> for *HR3<sup>D116G</sup>* and BamHI-HR3pF and BamHI-HR3R for full transgene amplification), (*HR3<sup>ΔCt65</sup>*: BamHI-HR3pF and BamHR3-148R) and (*HR3-<sup>ΔCt26/G186D</sup>*: BamHI-HR3pF and BamHR3R-SDDS: 5'gcggatccAGAGTCATCACTCGAACATTCAACA<sup>3'</sup>). Additionally, *HR3-YFP*

was also cloned into the pCX-DG-82p vector using the primers (BamHR3F and BglYFPR1: 5'gcagatctCACTTGTACAGCTCGTCCATG<sup>3'</sup>).

Six *Arabidopsis* and *Brassica* homologs were translationally fused to *YFP* at the N-terminus under control of the 35S promoter using the pEarleyGate gateway compatible vector series (Earley et al., 2006). Recombination reactions were completed using pENTR/D-TOPO clones containing the genomic sequences of the respective genes and the pEG104 destination vector using LR recombination. The primers used for amplification from the T20E23 BAC clone for *Arabidopsis* homologs and the 95K1 BAC clone for *Brassica* homologs were: (HR1- HR1tpF: 5'caccATGCCTCTTGTTGAGCTTCTTACAA<sup>3'</sup> and BamHR1R2: 5'cgggatccTCATTTGAAGATGAACCGGATCTCGT<sup>3'</sup>; HR2- HR2tpF: 5'caccATGCCTCTTACCGAGATTATCGCA<sup>3'</sup> and BamHR2R2: 5'cgggatccCTAATTCAAAACGAAGCGAATTCCGT<sup>3'</sup>; HR3- HR3tpF 5'caccATGCCGGTTAGTGAGATTATG<sup>3'</sup> and BamHR3R2; HR4- HR4tpF 5'caccATGCCGATTGCTGAGCTTGCT<sup>3'</sup> and BamHR4R2 5'cgggatccTCATTTATTATGCTTTTCAGATATCTGGG<sup>3'</sup>; BoHRa- BoHRatpF and BoHRaR; BoHRc- BoHRatpF 5'caccATGCCTATTGGTGAGGTTATTGTAGGG<sup>3'</sup> and BoHRcR 5'GAGCATTCATTTTACTTGTTGCTTAA<sup>3'</sup>). Gateway® LR Clonase® II enzyme mix was used to complete the recombination reaction between the entry clones and destination vector (pEG104). Standard published procedures were used for the generation of entry and destination clones.

Chimeric domain swapping constructs between the N- and C- terminal domains of *HR3* and *RPW8.2* were created using *NcoI* adapted primers designed at the end of the 2<sup>nd</sup>

predicted CC domain of each gene. Both domains of HR3 were amplified with the primers (BamHI-HR3pF and NcoHR3-2CCR:

5'caccatggTTGACGAGTGATTTCATCAAGTTTAGTGT<sup>3'</sup> and NcoHR3-CtdF:

5'caccatggCCAAGTGAATGATTTGTTTCAAGAGCA<sup>3'</sup> and BamHR3R2) respectively.

Both domains of RPW8.2 were amplified with the primers (BamR82pF:

5'ttggatccTCACCGAAATTGTTAGTATTCACG<sup>3'</sup> and NcoR82-2CCR:

5'caccatggCATTATTTTGTCAAGTTTAGTGCTGATT<sup>3'</sup> and NcoR82-CtdF:

5'caccatggCCTCAACCGAAGTTTGAAATCCA<sup>3'</sup> and BamR82R2:

5'ttggatccTCAAGAATCATCACTGCAGAAC<sup>3'</sup>) respectively. *HR3p::HR3n-R82c* and

*R82p::R82n-HR3c* chimeric genes were translationally fused to YFP at the C-terminus

under control of either the *HR3* or *RPW8.2* promoter using the previously mentioned

pZPYFP23' homemade vector (Wang et al., 2007). Additionally, *HR3n-R82c-YFP* was

also cloned into the homemade pCX-DG-82p vector using the primers (BamHR3F and BglYFP1).

TA cloning using the modified binary vector pCX-DG-82p was also used for a variety of other constructs including: *YFP-HR1*, *YFP-HR2*, *YFP-HR3*, *YFP-HR4*, *YFP-BoHRA*, *YFP-BoHRC* and *RPW8.2-RFP*. All generated constructs in binary vectors were introduced into *Agrobacterium* strain GV3101 and stable transgenic *Arabidopsis* plants were generated by floral dip (Clough et al., 2000). All materials, sequences and unlisted primers are available upon further request.

## Transcript analysis



RNA extraction and cDNA synthesis were conducted as previously described in (Xiao et al., 2005). DNase treatment of extracted RNA samples was performed with DNase I, amplification grade (Invitrogen: <http://products.invitrogen.com/ivgn/product/18068015>). Endo control transcripts of the *Ubiquitin-Conjugating Enzyme 21 (UBC21)* were amplified using the primers: (UBC21F: 5'GGCATCAAGAGCGCGACTGT<sup>3'</sup> and UBC21R: 5'GCGGCGAGGCGTGTATACAT<sup>3'</sup>).

### **Pharmacological Treatments**

Fully expanded leaves of ~7 week-old *YFP-HR3* or *YFP-HR3/RPW8.2-RFP* Col-gl background plants were detached from the base of the petioles and inserted into sterilized Murashige and Skoog (MS) agar medium in Petri dishes. Detached leaves were inoculated evenly with *Gc*-UCSC1 and at different time points each half leaf was pressure-infiltrated with a blunt end 1 mL plastic syringe with BFA or 1% DMSO solutions at ~6hpi. Leaf sections (~.25 cm<sup>2</sup>) were examined using a Zeiss LSM710 confocal microscope at 36-42hpi following haustorial staining with 0.5% propidium iodide (PI) or FM4-64 solution. BFA treatments were conducted with a 300μM solution of BFA dissolved in a 1% DMSO solution (Nielsen et al., 2012).

### **Other Analyses**

Imaging and laser scanning confocal microscopic (LSCM) imaging was done using either a Zeiss Axio epifluorescence microscope coupled with an HBO 100 microscope illumination system or with a Zeiss LSM710 confocal microscope as

previously described in (Wang et al., 2007; Wang et al., 2009; Wang et al., 2010). All images and videos presented are single optical sections or Z-stack projected of 15-30 images unless otherwise indicated. Relative intensity units  $\times \mu\text{m}^2$  were measured using the Zeiss Zen 2009 Light Edition software for the papillae region using specified regions of interest. The data are represented as mean  $\pm$  standard error of mean (SEM) for (n=6). For FM4-64 staining, detached leaf sections ( $\sim 0.25 \text{ cm}^2$ ) were submerged in  $8.2 \mu\text{M}$  FM4-64 (Molecular Probes) in water for 15-30 minutes. For propidium iodide (PI) staining, detached leaf sections ( $\sim 0.25 \text{ cm}^2$ ) were submerged in 0.5% PI solution for 45-60 minutes then washed briefly (10-15 minutes) in water before imaging. Sirofluor staining of leaf sections for callose was conducted with a  $0.1 \text{ mg ml}^{-1}$  dissolved in a 1% DMSO solution; (Biosupplies, <http://www.biosupplies.com.au/products.htm>). Image data was processed using Zen 2009 Light Edition and Adobe Photoshop CS5. ImageJ gel quantification analysis was used to estimate band intensities (<http://rsb.info.nih.gov/ij/>).

At least three replicates of biological experiments were conducted for all experiments described. Statistical analysis was conducted using Student's *t* test analysis and for data means  $\pm$  SEM ( $n \geq 4$ ) from one replicated experiment.

**Accession Numbers** (<sup>a</sup> Accession number assigned to a gene cluster)

Sequence data from this article can be found in the Arabidopsis Genome Initiative or GenBank/EMBL databases under the following accession numbers: *RPW8.1*/*RPW8.2* [AF273059](#)<sup>a</sup>, *AtHR1* [NM\\_114905](#), *AtHR2* [NM\\_114906](#), *AtHR3* [NM\\_114907](#), *AtHR4* [NM\\_114908](#), *AIHR1*/*AIHR2*/*AIHR3*/*AIHRPW8.2* [AY225591](#)<sup>a</sup>, *BoHRa* [AY225587](#), *BoHRb* [AY225588](#), *BoHRc* [AY225589](#), *BrHRa*/*BrHRb*/*BrHRc* [AY225586](#)<sup>a</sup>, *BrHRd* [AY225590](#).

## Chapter 3: Origin of the Extra-Haustorial Membrane (EHM)

### Introduction

Many plant pathogenic fungi including powdery mildew, dikaryotic rusts and algae-like oomycetes have evolved a similar haustorium-based invasive strategy to colonize their respective plant hosts. This strategy involves the development of appressoria from epicuticular or intercellular hyphae of pathogens for host cell-wall penetration and subsequent differentiation of haustoria - the feeding organs in close contact with the host cell cytoplasm for nutrient uptake (Voegelé et al., 2001; Voegelé and Mendgen, 2003; O'Connell and Panstruga, 2006) (**Figure 3-1**). Apart from stealing photosynthates from plants to establish parasitism, haustoria are also responsible for the delivery of effector proteins from pathogens into host cells to suppress host defense mechanisms (Kim et al., 2005; He et al., 2006; Janjusevic et al., 2006; Xiang et al., 2008; Gimenez-Ibanez et al., 2009) (**Figure 3-1 C**).

Based on earlier electron microscopic observations, the haustorium is thought to be separated from the host cytoplasm by an interfacial membrane termed the extrahaustorial membrane (EHM) that encases the haustorium from the neckband (Hahn and Mendgen, 1992; Roberts et al., 1993) (**Figure 3-1**). The EHM represents the host - pathogen interface and a critical battleground important for both host defense and pathogen pathogenesis. However, the origin and biogenesis and the molecular composition of the EHM are largely unknown. Using monoclonal antibodies raised against isolated haustorial complexes in pea (*Pisum sativum*) infected with *Erysiphe pisi*, Roberts and colleagues detected a ~250 kDa glycoprotein of unknown origin and

structure that was exclusively found in the EHM (Roberts et al., 1993). Conversely, Koh and colleagues found that eight PM-localized proteins were excluded from the EHM during infection of Arabidopsis with *Golovinomyces cichoracearum* (Koh et al., 2005). These observations, together with our recent finding that RPW8.2 is specifically targeted to the EHM but not found in the PM in haustorium-invaded cells (Wang et al., 2009), suggest that the EHM is likely of host origin and distinct from the host PM. However, whether the EHM is formed via PM invagination and subsequent differentiation or via de novo synthesis remains to be an open question.

As described in **Chapter 2**, YFP-HR3 expressed from the 35S promoter is localized to both the PM and the EHM (**Figure 2-7/8**). I reasoned that this unique feature of localization could be useful for investigating the origin and biogenesis of the EHM. I hypothesize that if the EHM originates from the PM via “invagination” and subsequent differentiation of the portion of the PM where the fungal penetration and haustorial differentiation occur, YFP-HR3 already localized at the PM will be found in the EHM at early stages of the biogenesis of the EHM because YFP-HR3 is intrinsically compatible with the EHM and will unlikely be excluded. However, if only newly synthesized YFP-HR3 can be targeted to the EHM, but not PM-localized YFP-HR3, it would indicate that recruitment of proteins (and lipids) for the formation of the EHM probably occurs via the biosynthetic secretory pathway but not from lateral diffusion of the PM. I thus exploited the unique feature of YFP-HR3's subcellular localization to interrogate the origin of the EHM.

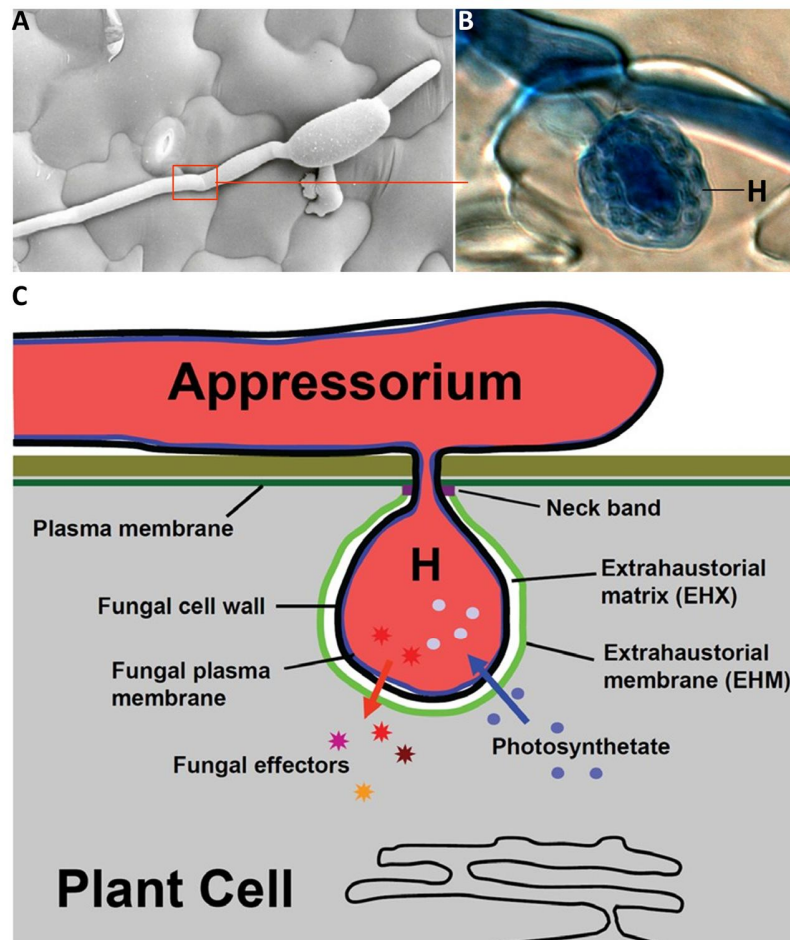


**Figure 3-1. The Haustorium of Powdery Mildew.**

(A-B) A micrograph showing a sporeling of *Gc*-UCSC1 (A) that has developed the first haustorium (H) in an epidermal cell of *Arabidopsis* (B). The fungal hypha and haustorium (H) was stained blue by trypan blue. (C). A cartoon illustrating the composition of the host-pathogen interface and the action of the haustorium modified from Wang et al., 2009.

## Results

### YFP-HR3 and RPW8.2-RFP Are Colocalized at the EHM

In order to unambiguously and instantaneously discern the dynamic localization of YFP-HR3 to the PM, the papilla and the EHM, it is necessary to visualize the EHM and EHM-targeted trafficking in a non-invasive manner. For this purpose, we generated Col-gl plants transgenic for both *35S::YFP-HR3* and *RPW8.2p::RPW8.2-RFP*. In such transgenic plants, the EHM-specific localization of RPW8.2-RFP in mildew-infected cells (rendered by *RPW8.2* promoter) can be used not only to validate and monitor the dynamic EHM-localization of YFP-HR3, but also to provide an ideal spatiotemporal reporter for new protein synthesis in cells undergoing EHM biogenesis (**Figure 3-2**). Indeed, we confirmed that YFP-HR3 was targeted to the EHM as shown by nice colocalization with RPW8.2-RFP at the EHM (**Figure 3-3A**). As described in **Chapter 2**, YFP-HR3 expressed from the *35S* promoter in these dual-reporter transgenic lines was also found in the PM and the papilla in majority of haustorium-invaded cells (**Figure 3-3A**). These transgenic lines were then used for the following experiments to determine whether the EHM is derived from the PM or via *de novo* synthesis.

### The EHM Appears to be *de novo* Synthesized

As illustrated in (**Figure 3-2**), I reasoned that if the EHM is entirely or partially derived from the PM, the existing PM-localized YFP-HR3 in fungus-infected cells whose new protein synthesis is blocked should also be found in the EHM. If not, the opposite is probably true: i.e. the EHM is formed via *de novo* synthesis. I thus employed cycloheximide (CHX) to inhibit protein synthesis of leaf epidermal cells. I first

conducted experiments to determine the minimal concentration of CHX that can completely block new protein (RPW8.2-RFP) synthesis to minimize inhibitory effect of CHX on haustorial differentiation. I infiltrated 0, 1, 10, 25, and 50 $\mu$ M CHX water solution to mildew infected leaves from the base of the abaxial side at ~12hpi when haustoria start to develop. The timing of CHX application is to reduce toxicity of CHX on fungal development and host cell metabolism. I found that leaf infiltration of 25 $\mu$ M CHX could effectively block protein synthesis as reflected by an almost complete lack of YFP signal in the EHM highlighted by FM4-64 when examined between 36 to 48hpi (**Figure 3-3 B**), while the haustorial development appeared to be normal in this time period.

I then used the same method to treat mildew infected leaves of Col-gl plants transgenic for *35S::YFP-HR3* and *RPW8.2p::RPW8.2-RFP*. Results from examination of >50 haustorium invaded cells in each of three duplicated experiments showed that >90% of invaded cells (judged by the presence of YFP-HR3 labeled papillae and formation of haustoria under transmitted white light) completely lacked RPW8.2-RFP at the EHM, and the rest cells had very weak RFP signal at the EHM, indicating effective blockage of protein synthesis. Importantly, while there was a moderate decrease of YFP-HR3 signal in the PM and around the penetration site in the CHX-treated cells compared to buffer control (**Figure 3-3 C-D**), there was no detectable YFP-HR3 signal in the EHM encasing the differentiated haustoria underneath the penetration site (**Figure 3-3 D**). These observations support our hypothesis that the EHM is formed via *de novo* synthesis rather than from simple extension of the PM.

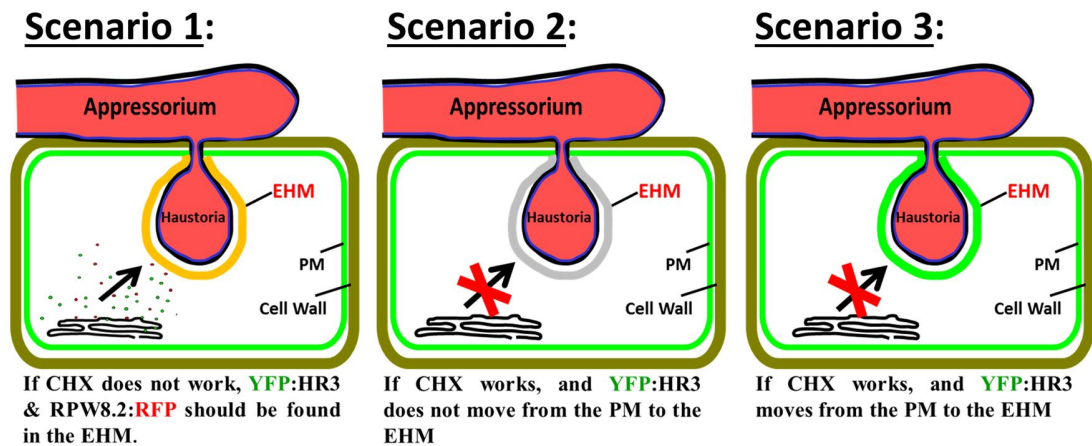


**Figure 3-2. Schematic Illustration of Three Possible Scenarios of Protein**

**Localization Following Cycloheximide Treatment.**

Leaves of transgenic plants co-expressing *35S::YFP-HR3* and *RPW8.2p::RPW8.2-RFP* are to be used for cycloheximide infiltration. Three possible scenarios are described above.



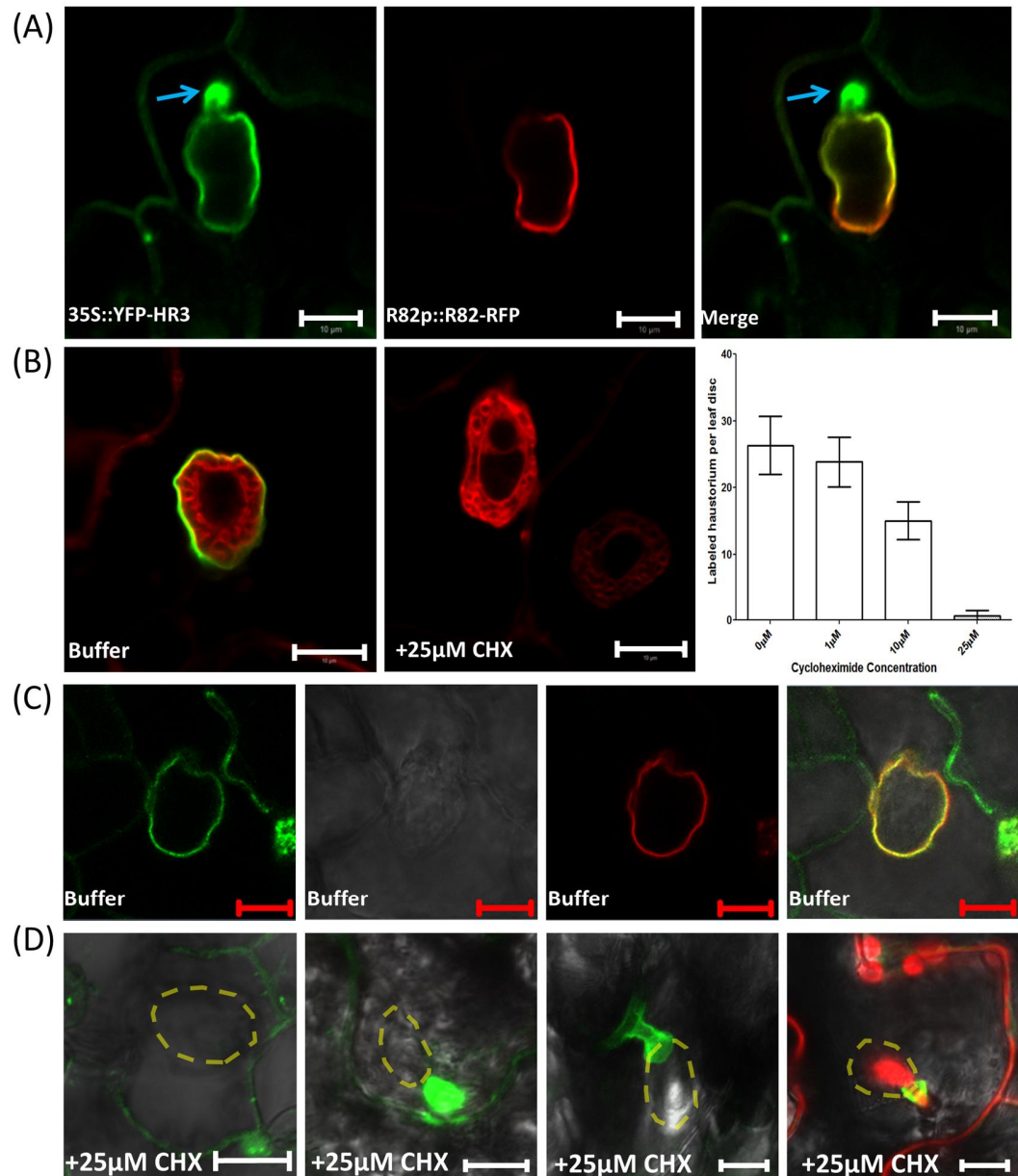


**Figure 3-3. The Extra-haustorial Membrane Appears to be *de novo* Synthesized.**

**(A)** YFP-HR3 and RPW8.2-RFP colocalize at the EHM. A representative image of a single optical section showing localization of YFP-HR3 and RPW8.2-RFP in a haustorium-invaded cell co-expressing 35S::YFP-HR3 and RPW8.2p::RPW8.2-RFP at 42hpi. Papillae localization of YFP-HR3 is indicated by blue arrows. Bars = 10  $\mu$ m. **(B)** Effectiveness of cycloheximide in blocking protein synthesis reported by RPW8.2-YFP.

Representative images showing the presence of RPW8.2-YFP in a cell treated with buffer (left) and the absence of RPW8.2-YFP in a cell treated with 25μM CHX (right).

Haustoria are highlighted by FM4-64 staining (pseudo-colored red). Bars = 10μm. **(C-D)** PM-localized YFP-HR3 is not translocalized to the EHM. Leaves from plants co-expressing *35S::YFP-HR3* and *RPW8.2p::R82-RFP* were treated with buffer **(C)** or 25μM CHX **(D)** at 16hpi. Shown are representative images of single optical sections captured at 36hpi. The haustorium in the far right image of **(D)** was visualized by PI staining. Note, in all cases YFP-HR3 is absent from the presumable EHM (indicated by dashed yellow lines) in CHX-treated cells. Bars = 10μm.

## Discussion

The origin and biogenesis of the EHM is of great interest to researchers in the field because of its apparent importance in understanding the host-pathogen interaction but unfortunately remains largely undetermined. The exclusion of eight PM-localized proteins from the EHM (Koh et al., 2005) and the EHM-specific localization of RPW8.2 (Wang et al., 2009; Wang et al., 2010) suggest that the PM and the EHM are two distinct types of membranes. However, whether the EHM is formed via PM invagination followed by differentiation or it is *de novo* synthesized has not been definitively determined. Here, we take advantage of YFP-HR3's triple localization to the PM, the papillae and the EHM (**Figure 2-7/8/9**) to provide cell biological evidence to support the notion that the EHM is largely *de novo* synthesized.

Our conclusion is based on several observations. First, whereas the existing PM-localized YFP-HR3 could be translocalized to the papillae, it was not found in the EHM during haustorial differentiation from 20 to 48hpi if new protein synthesis was blocked by CHX treatment (**Figure 3-3**). This suggests that the EHM is physically separated from the PM, which is likely imposed by the so-called "neckband" surrounding the neck of the haustorium, observable by electron microscopy (Gil and Gay, 1977). In this case, the "neckband" must form concomitantly with the biogenesis of the haustorium while the EHM is subsequently formed via *de novo* synthesis. However, the timing of EHM synthesis in relation to haustorium formation is unknown. Since RPW8.2-YFP and YFP-HR3 were both detectable at the EHM ~16-18hpi, the EHM must have formed before 16hpi. Second, in (**Chapter 2**), we showed that translocalization of the PM-localized YFP-HR3 to the papillae is likely via a BFA-sensitive endosomal recycling pathway, but

that the delivery of YFP-HR3 and RPW8.2-YFP to the EHM was BFA-insensitive (**Figure 2-10, Suppl-Figure 2-1**). This suggests that the contribution of the endocytic trafficking pathway to the EHM biogenesis may be insignificant because PM-localized YFP-HR3 was not obviously translocalized via this pathway to the EHM in the presence of CHX (and absence of BFA), further supporting a PM-independent origin of the EHM.

*de novo* synthesis of the EHM may also provide crucial advantages for the fungus to establish a functional haustorium within a hostile environment. For example, the fungus may deliver effectors inside the host cell to exert its impact on the molecular composition of the EHM by interfering with host membrane/protein trafficking pathway(s) or by delivering fungal proteins/lipids to directly modify the EHM during biogenesis. On the other hand, *de novo* synthesis of the EHM may be necessary for the host to mount effective post-penetration resistance against the haustorium—the "Achilles' Heel" of powdery mildew. For example, this may give the host cell an opportunity to "build" a novel interfacial membrane as a defense barrier through selective recruitment of lipids and proteins (such as RPW8 family proteins).

The *de novo* synthesis hypothesis is also compatible with the notion that the EHM-oriented membrane/protein trafficking pathway becomes the major default trafficking pathway because of the need for *de novo* synthesis of the EHM while the PM is in a relatively static state. This perhaps offers an explanation for the observations that several tagged membrane proteins (including the syntaxin *PEN1* and the synaptotagmin *SYT1*) when stably or transiently overexpressed in haustorium-invaded plant cells, were found to be localized to the EHM induced by oomycete haustoria (Lu et al., 2012). This result is also in contrast to our finding that GFP-PEN1 and GFP-SYT1 expressed from

their native promoters were not clearly found at the EHM induced by powdery mildew haustoria (Wang et al., 2009; Xiao, unpublished). Additionally, there must be a certain degree of specificity for EHM-targeted trafficking, because we did not observe any EHM localization of the PM-resident protein LTI6b (Cutler et al., 2000) and the syntaxin SYP131 when expressed either from the 35S promoter of the *RPW8.2* promoter (**Figure 2-8D**, Xiao, unpublished data).

A similar situation where polarized membrane/protein trafficking during the biogenesis of the peri-arbuscular membrane (PAM) in *Medicago truncatula* (*Mt*) root cells containing developing arbuscules of the mycorrhizal fungus *Glomus versiforme* has recently been investigated (Pumplin et al., 2012). Based on the observation that PM-localized *Medicago* phosphate transporter 1 (MtPT1) is targeted to the PAM when expressed from the promoter of PAM-specific MtPT4, Pumplin and colleagues proposed that there is transient re-orientation of the host cell's major secretory pathway toward to the PAM during the biogenesis of the arbuscules (Pumplin et al., 2012). However, the PM-resident protein PIP2A was not found in the PAM when expressed from the MTPT4 promoter suggesting that a certain level of specificity for PAM-oriented trafficking still exists (Pumplin et al., 2012). While a specific targeting motif was not identified in MtPT4 for PAM-localization, two short motifs enriched for basic residues have been identified in RPW8.2 and appear to be largely conserved among all RPW8 family members (Wang et al., manuscript under review). Combined, these findings provide an early step toward a better understanding of the biogenesis and molecular composition of the EHM, which is of particular importance for future elucidation of the molecular mechanisms involved in the host cell-haustorium interaction at the interfacial membrane.

## **Materials & Methods**

### **Pharmacological Treatments**

Fully expanded leaves of ~7 week-old *RPW8.2-YFP* or *YFP-HR3/RPW8.2-RFP* Col-gl background plants were detached from the base of the petioles and inserted into sterilized Murashige and Skoog (MS) agar medium in Petri dishes. Detached leaves were inoculated evenly with *Gc*-UCSC1 and at ~12 or 16hpi (as indicated) each half leaf was pressure-infiltrated with a blunt end 1 mL plastic syringe containing 0, 1, 10, 25 or 50  $\mu$ M of cycloheximide (CHX) dissolved in water or buffer (water only). Leaf sections (~.25 cm<sup>2</sup>) were examined using a Zeiss LSM710 confocal microscope at 36-42hpi following staining with 0.5% propidium iodide (PI) or an 8.2 $\mu$ M FM4-64 solution. Detectable *RPW8.2-RFP* signals were used to determine an effective level of CHX to nearly completely inhibit protein synthesis.

### **Other Analysis**

All lines, growth conditions, materials and methods not listed can be found in (Chapter 2).

## **Chapter 4: Utilization of RPW8.2 to Target Antimicrobial Cargos to the Host-pathogen Interface**

### **Introduction**

During the long-time co-evolutionary arms-race between plants and their pathogens, the pathogens often have the upper hand because of their faster multiplication and higher genetic recombination frequency. This is reflected by the fact that *R*-gene dependent resistance of crop cultivars in most cases is overcome by pathogens in a short period of time (5-15 years) (Pavan et al., 2010). Moreover, more and more pathogens have evolved the capacity to suppress the highly conserved SA-dependent defense pathway and become highly virulent on crop plants. Thus, engineering broad-spectrum and durable resistance in crop plants is of special importance to modern agriculture. Tremendous progress in our understanding of the molecular basis of plant resistance and pathogen pathogenesis in the past 20 years has opened a number of novel approaches to create disease-resistant crop cultivars. Those approaches include (i) pyramiding multiple *R* genes or multiple alleles of the same *R* gene into the same genetic background via marker-assisted molecular breeding (for *R* genes at different genomic locations) or transgene technology (for both) (Brunner et al., 2010; Tan et al., 2010; Ferreira et al., 2012); (ii) utilizing PRRs evolved in a specific plant family across family boundaries (Lacombe et al., 2010); (iii) activating ETI via pathogen inducible expression of an *Avr* gene in plants containing the cognate *R* gene for broad-spectrum resistance (Keller et al., 1999); (iv) overexpressing defense signaling components such as *NPRI* (Makandar et al., 2006; Kumar et al., 2012); and (v) targeted modification of host compatibility factors

required for pathogenesis using novel genome editing technology (i.e. TALEN) (Li et al., 2012).

Recent research in the Xiao laboratory revealed that RPW8.2 activates haustorium-targeted (thus broad-spectrum) defense against powdery mildew pathogens by integration of precise EHM-targeting with defense activation (Wang et al., 2009; Wang et al., 2010). Interestingly, although RPW8.2-triggered subcellular defense responses including H<sub>2</sub>O<sub>2</sub> production and enhancement of the formation of the callosic haustorial encasement is SA-dependent, RPW8.2's specific targeting to the EHM does not seem to require SA-signaling (Wang et al., 2009). Moreover, RPW8.2 appears to be also targeted to the EHM induced by the barley powdery mildew *Blumeria graminis* f. sp. *hordei* (*Bgh*) and the oomycete pathogen *Hpa* (Wang et al., 2009) (**Figure 4-1**), and the extra-invasive hyphal membrane (EIHM) induced by a hemi-biotrophic fungi *Colletotrichum higginsianum* (Xiao lab unpublished results). This suggests that there may be a common feature among different types of host-pathogen interfacial membranes that may serve as a trafficking cue for RPW8.2's specific targeting. In addition, RPW8.2 seems to be able to reach the EHM induced by *Gc*-UCSC1 in epidermal cells of cucumber cotyledon leaves when ectopically expressed (Xiao lab unpublished results) implying that the EHM-directed membrane/protein trafficking machinery is conserved in different plant species.

Based on these observations, we reason that it is possible to utilize RPW8.2 as a delivery vehicle to target antimicrobial cargos to the EHM or even the extra-haustorial matrix (EHX) for inducing novel SA-independent broad-spectrum resistance against haustorium-forming fungal and oomycete pathogens. Our endeavor towards this



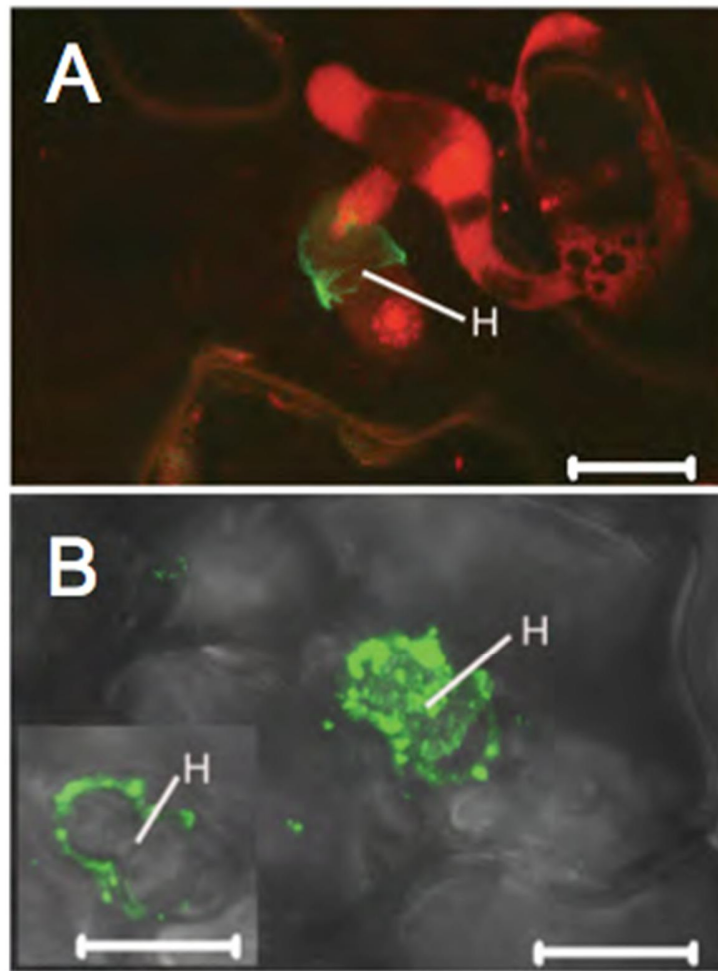


**Figure 4-1. RPW8 is Targeted to the Host-Pathogen Interface of Other Pathogens.**

These images were taken from Wang et al., 2009. **(A)** RPW8.2-YFP is localized to the periphery of haustoria (H) of *Bgh* in epidermal cells of the *eds1-2* mutant in Arabidopsis.

Bars = 10µm. **(B)** Maximum intensity projection of RPW8.2-YFP localized to the periphery of haustoria of *Hpa* in Arabidopsis. Inset is a single optical section showing EHM localization. Bars = 10µm.

potential application of RPW8.2 is a component of a collaborative project funded by the National Science Foundation (NSF) Basic Research to Enable Agricultural Development (BREAD) program. The long-term goal of this project is to engineering novel resistance against fungal and oomycete pathogens in developing country crop plants. Cacao (*Theobroma cacao*), a fruit crop for chocolate production, was selected as the focus crop plant for this project for several reasons: (i) cacao is an economically important cash crop for many developing countries in Africa and South America; (ii) cacao diseases reduce the potential crop yield by an estimated 810,000 tons annually (nearly 30% of world production) and in severe cases cause a near complete yield loss for individual small-holder farmers (Bowers et al., 2001; Ploetz, 2007); and (iii) improving cacao disease resistance via conventional breeding is difficult due to lack of obvious resistance gene resources and other factors (reviewed by Guiltinan et al., 2008).

Specifically, there are three potential strategies for the utilization of RPW8.2 to improve disease resistance in cacao. The first strategy is to express RPW8.2 as a transgene in cacao to see if it can enhance basal resistance cacao to haustorium-forming pathogens. Considering that RPW8 activates resistance to powdery mildew in tobacco (Xiao et al., 2003a) and that cacao is more evolutionarily related to Arabidopsis (~59 MYA) than tobacco (Argout et al., 2011) ([Evolutionary Tree of Plant-based Foods](#)), it is possible that RPW8.2 may be functional in cacao. The second strategy, which constitutes the core of this project, is to use an RPW8.2 mutant version defective in defense activation (RPW8.2<sup>D116G</sup>) that retains EHM-targeting to shuttle a variety of known antimicrobial peptides to the EHM to constrain the haustorium of fungal and oomycete pathogens. The third strategy also utilizes RPW8.2<sup>D116G</sup> to target phosphoinositide (PI)-

binding or degrading proteins to the EHM in an attempt to block host-entry of effector proteins. This is based on a recent exciting finding that RXLR-containing fungal and oomycete effectors bind specific phosphoinositide lipid species for entry into the host cells (Kale et al., 2010).

Here, I summarize our group efforts in testing the second strategy in *Arabidopsis* to engineer novel resistance to powdery mildew and highlight my contributions in (i) determining the membrane topology of RPW8.2, (ii) testing the delivery of antimicrobial cargo peptides to the EHM and their efficacy in conferring mildew resistance in *Arabidopsis* and (iii) engineering a mechanism to release antimicrobial cargo peptides to the extra-haustorial matrix.

**Strategy I**

Use the RPW8 missile directly in crop plants

**Strategy II**

Target antimicrobial peptides to the EHM to kill haustoria

**Strategy III**

Target PI3P-binding or degrading proteins to the EHM to block host-entry of effectors

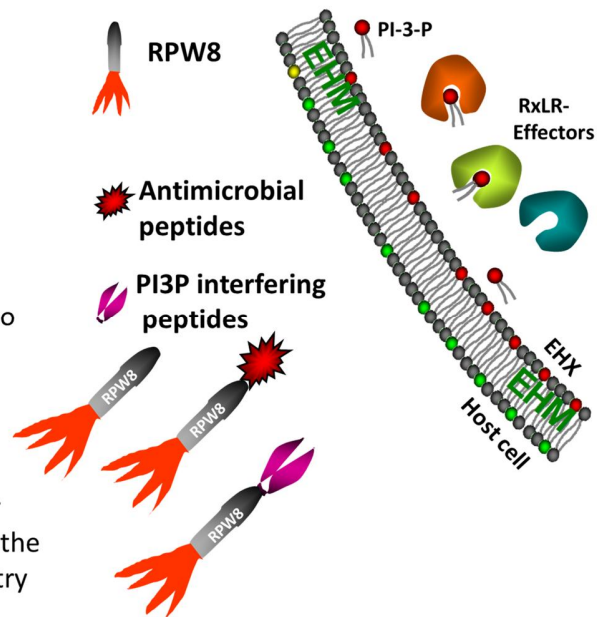


**Figure 4-2. Strategy for Using RPW8 as a Delivery Vehicle.**

A three pronged strategy for utilizing RPW8 to improve resistance against haustorium-forming pathogens.

## Results

### RPW8.2 is a Type I Membrane Protein

The RPW8 family member proteins contain a putative N-terminal transmembrane (TM) domain and are predicted to be Type I membrane proteins by online prediction software available (ie: ConPredII and TMpred) with their C-tails in the cytoplasm (**Figure 4-3A&B**). However, this membrane orientation has not been confirmed.

If RPW8.2 is indeed a type I membrane protein, the C-terminally tagged YFP should be in the cytoplasmic side of the EHM when RPW8.2-YFP is targeted to the EHM. To obtain definitive evidence for clarification of RPW8.2's membrane topology, one method was devised based on the use of a specific protease to cleave YFP as a reporter that is fused at the C-terminus of RPW8.2 spaced with a protease cleavage site (PCS). If YFP signal disappears from the EHM labeled by RPW8.2-PCS-YFP after cleavage, then the C-tail of RPW8.2 must be in the cytoplasm (**Figure 4-3B**). This method, if successful, may also be used to release antimicrobial cargos to appropriate subcellular compartments from the RPW8.2-cargo fusion proteins. To this end, I generated a new *RPW8.2p::RPW8.2-YFP* construct where *RPW8.2* and *YFP* are spaced by a specific protease cleave site (PCS) “EFRAL” that is specifically recognized by an engineered protease known as subtilisin (Sbt) (this fusion construct hereafter is referred to as *R82-PCS-YFP*) kindly provided by Dr. Philip Bryan (IBBR, University of Maryland) (Gallagher et al., 2009). Subtilisins (serine endopeptidases), are proteases initially obtained from the soil bacteria *Bacillus subtilis* and are secreted in large amounts from many *Bacillus* spp. They belong to a group of serine proteases that are physically and chemically well characterized (reviewed in Wells and Estell, 1988).

As a proof of concept, I conducted *in vitro* tests for the ability of purified bacterially expressed Sbt enzyme to cleave the YFP fluorophore from RPW8.2-PCS-YFP expressed *in planta*. Total and microsomal (membranous containing) protein fractions from stable transgenic lines expressing *R82-PCS-YFP* and control plants (Col-0) were extracted at 7dpi with *Gc*-UCSC1. Both total and microsomal fractions from R82-PCS-YFP and Col-0 samples were treated with purified Sbt enzyme and buffer solution and subjected to an incubation period at 37°C for 1 hour. Following treatment with Sbt enzyme, samples were subjected to SDS-PAGE and western blot analysis using YFP specific antibodies (**Figure 4-3C**). As expected, total fractions for Col-0 samples revealed no detectable YFP signal (lane 2) while R82-PCS-YFP samples had weak detectable signals at the approximate size of 47.7 kDa in untreated (lane 3) or buffer-treated only samples (lane 4). Upon the addition of the purified Sbt enzyme (15µM), the R82-PCS-YFP band became undetectable. More convincingly, 80-90% of the full-length protein band was lost in the microsomal fractions of R82-PCS-YFP samples treated with 15µM Sbt while a ~27 kDa band with the same size as YFP seen in the control sample (lane 1). These results suggest that RPW8.2-PCS-YFP expressed *in planta* is recognized and cleaved by Sbt enzyme *in vitro* (**Figure 4-3C**).

In order to determine the topology of RPW8.2 at the EHM, I then prepared RPW8.2-PCS-YFP labeled haustoria from the same transgenic plants infected with *Gc*-UCSC1 at 7dpi. The isolated haustoria were incubated with Sbt (15µM) or buffer for ~1 hr at 37°C and examined under confocal microscopy (**Figure 4-4**). For haustorial samples incubated with buffer, almost all haustoria (>90%) were labeled with YFP signal indicating EHM-localization of RPW8.2-PCS-YFP (**Figure 4-4A**). In contrast, for

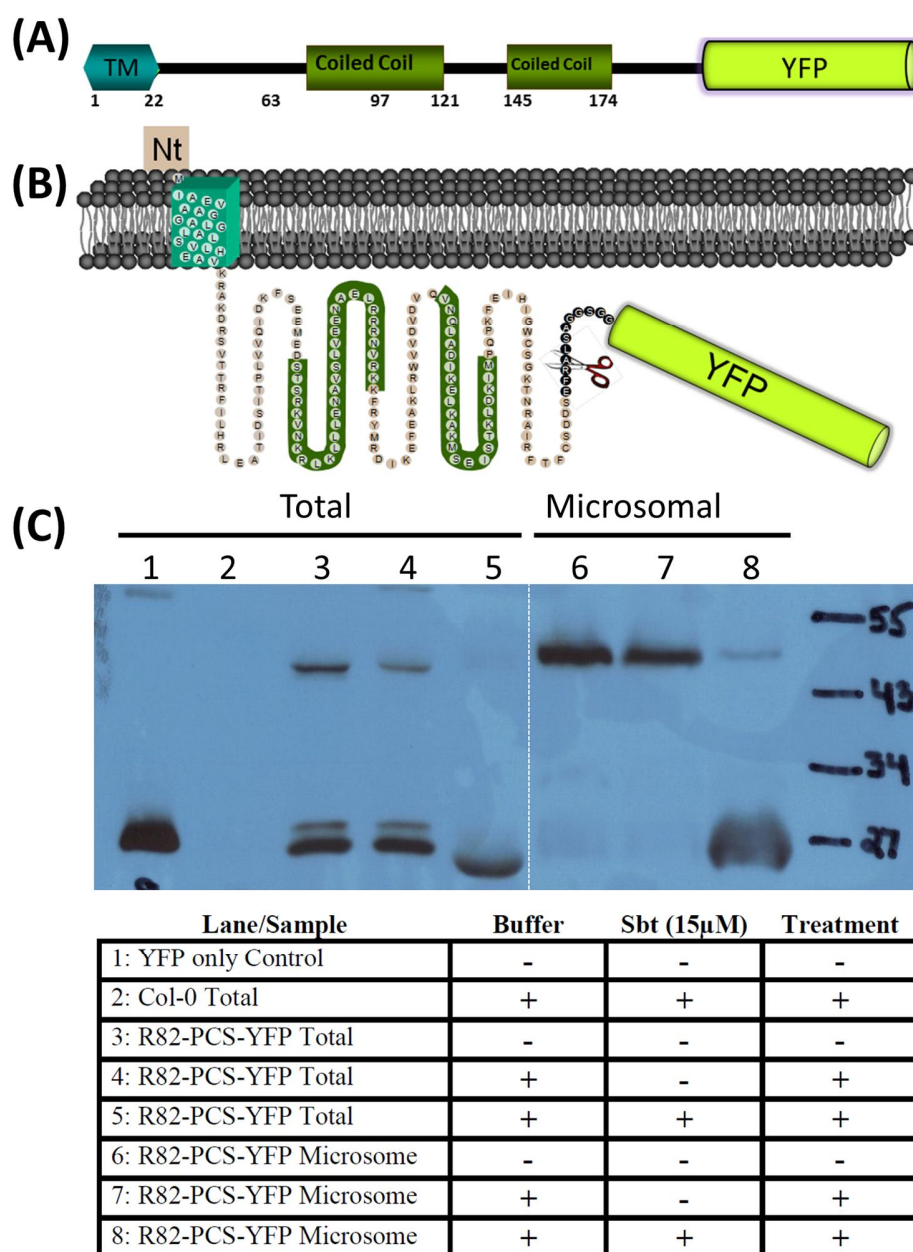


**Figure 4-3. Subtilisin Can Cleave YFP from the RPW8-YFP fusion protein *in vitro*.**

(A) Schematic drawing of RPW8.2 in fusion with YFP at the C-terminus. (B) A cartoon depicting the predicted Type I membrane topology of RPW8.2. The full-length amino acid sequence is listed according to the predicted tertiary structures including the transmembrane domain (TM) and 2 coiled-coil domains. Black circles represent the engineered protein sequence of the protein cleavage site (PCS) -EFRALSAGGSG- while

the scissor represents the Subtilisin (Sbt) enzyme. YFP is the yellow rod. (C) Western blot analysis using anti YFP antibodies for the total and microsomal protein fractions prepared from infected wild-type Col-0 and RPW8.2-PCS-YFP transgenic plants at 7dpi. Total and microsomal fractions were subjected to treatment with or without Sbt (15 $\mu$ M) at 37°C for 1 hour.



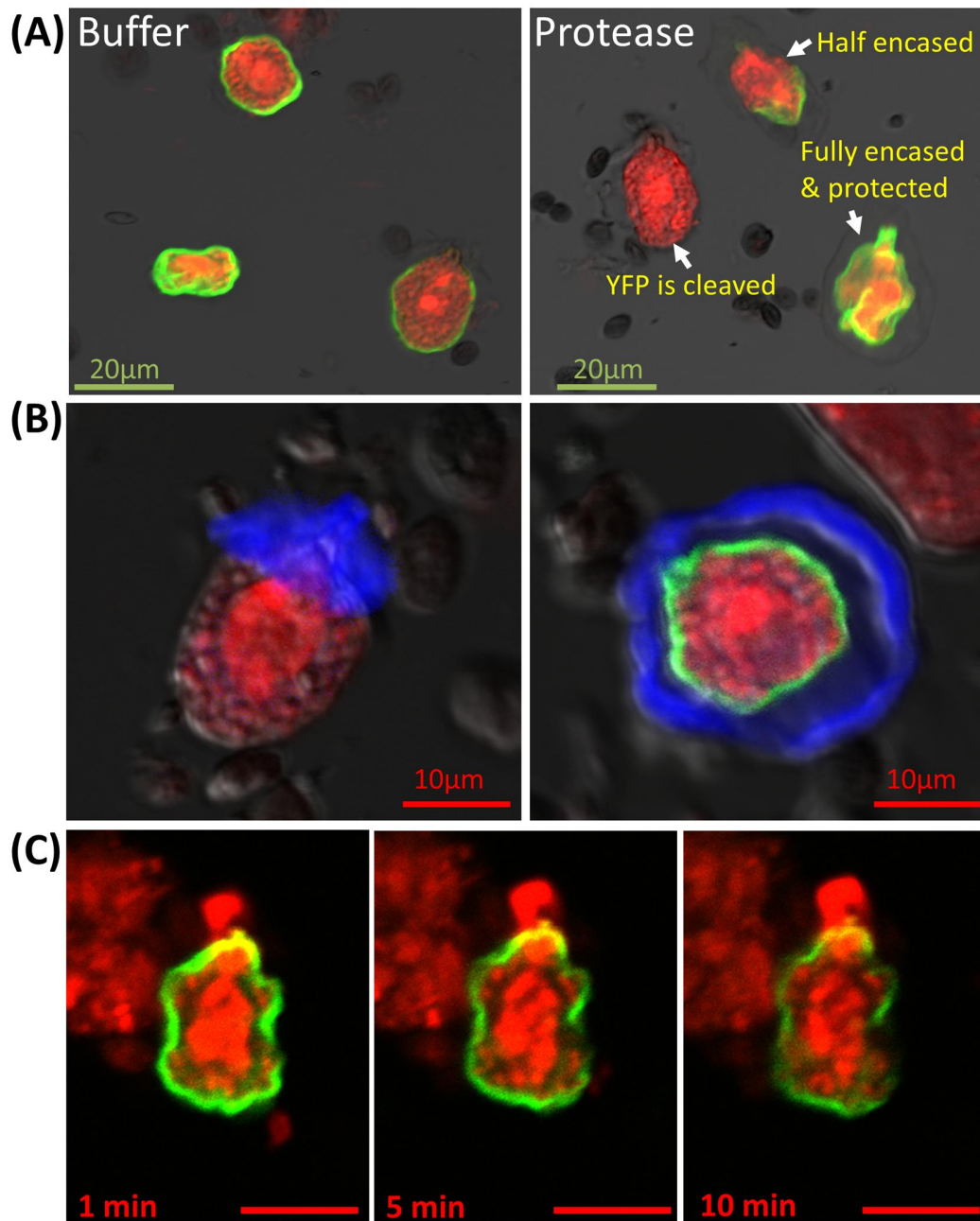


**Figure 4-4. RPW8.2 is a Type I Membrane Protein.**

(A) Haustoria extracted from R82-PCS-YFP transgenic lines at 7dpi with *Gc*-UCSC1 treated with buffer only (left panel) or with subtilisin (Sbt) enzyme (right panel).

Treatment with Sbt results in disappearance of the YFP from R82-PCS-YFP labeled haustoria unless the haustoria are encased. Bars = 20μm. (B) Extracted haustoria from

*R82-PCS-YFP* transgenic lines treated with Sbt and stained with Sirofluor. The callosic encasement may prevent Sbt access to the EHM. Bars = 10µm. **(C)** A single extracted haustoria from *R82-PCS-YFP* transgenic lines treated with Sbt at room temperature. Note YFP signal intensity is reduced within minutes of treatment. Bars = 10µm.

haustorial samples treated with Sbt, a majority (~75%) of haustoria were completely or partially devoid of YFP signal, indicating removal of YFP from RPW8.2-PCS-YFP at the EHM (**Figure 4-4A**). Interestingly, some haustoria (~25%) did retain part or most of the YFP signal after Sbt treatment, but all of these haustoria were either fully or largely encased by a layer enriched for callose as revealed by Sirfluor staining (**Figure 4-4 A & B**). Apparently, the encasement of the haustorial complex (EHC) must have impeded access of Sbt to its substrate, i.e. RPW8.2-PCS-YFP, resulting in the retainment of YFP signal at the EHM. Additionally, a time course experiment with a single isolated haustorium showed diminishment of YFP signal intensity at the EHM in 5-10 min after Sbt treatment at room temperature (**Figure 4-4C**). Collectively, these observations indicate that the C-terminal tail of RPW8.2 must be in the cytoplasmic side of the EHM, supporting the *in silico* prediction that RPW8.2 is a type I membrane protein.

I also attempted to use other methods to determine the membrane topology of RPW8.2. One of these experiments involved the engineering of glycosylation constructs with a putative *N*-glycosylation recognition sequence (NNSS) (Turk et al., 1996) between RPW8.2 and YFP (R82-NNSS-YFP) and YFP and RPW8.2 (YFP-NNSS-R82). Protein glycosylation occurs to specific protein domains of secretory proteins that are localized inside the endoplasmic reticulum (ER) lumen after passage through the translocon. Asparagine-linked oligosaccharides (GlcNAc<sub>2</sub>Man<sub>9</sub>Glc<sub>3</sub>) are transferred onto proteins by the oligosaccharyltransferase (OST) proteins and play an important role in the biosynthesis, folding, trafficking, stabilization and ER translocation of eukaryotic membrane proteins (Johnson and van Waes, 1999; Dempski and Imperiali, 2002; Yan and Lennarz, 2005). While both proteins were detected at the EHM upon *Gc*-UCSC1

infection, western blot analysis with YFP specific antibodies did not reveal a typical discernable shift in protein size of ~2.5kDa upon single glycosylation (Martinez-Gil et al., 2010) (**data not shown**). These results suggests that neither of these proteins were subjected to (or recognized for) *N*-glycosylation upon protein secretion prior to localization to the EHM.

### **Targeting Antimicrobial Cargos to the Host-pathogen Interface**

RPW8.2's ability to localize to the EHM provides a unique opportunity to test if we can target antimicrobial proteins to the host-pathogen interface using RPW8.2 for engineering novel resistance against a variety of haustorium-forming pathogens. Prior to obtaining conclusive evidence on RPW8.2's membrane topology, our group had engineered two T/A cloning vectors (Chen et al., 2009b) that contains RPW8.2<sup>D116G</sup> for making translational fusions of RPW8.2 with antimicrobial or phosphoinositide-binding proteins at both termini of RPW8.2 (**Figure 4-5&6**). Group efforts from Dipti Bendigeri, Xianfeng Ma and myself in the Xiao lab led to the cloning of ~20 RPW8.2-antimicrobial cargos fusion constructs in two orientations (ie: RPW8.2-X or Signal Peptide (Sp)-X-RPW8.2) and stable expression of each of these constructs in Arabidopsis. Cargo proteins include but are not limited to: chitinases (which break down chitin, a major component of fungal and oomycete cell walls) from Arabidopsis and cacao, PR and PLANT-DEFENSIN (PDF) proteins from Arabidopsis, synthetic peptides D4E and D5C that have been tested for disease resistance in crops (reviewed in Cary et al., 2011), PI-binding proteins (2xFYVE (PI3P); PH<sub>FAPP1</sub> (PI4P); PH<sub>PLCδ</sub> (PI4,5P<sub>2</sub>) (Garcia et al., 1995;

Lemmon et al., 1995; Gaullier et al., 1998; Godi et al., 2004) and antimicrobial proteins from moth, honeybee and drosophila.

Stable Arabidopsis lines transgenic for a variety of *RPW8.2<sup>D116G</sup>-Cargo* constructs have been successfully tested for increased resistance to *Gc*-UCSC1. For example, Col-gl lines expressing *RPW8.2<sup>D116G</sup>-PR2* or *RPW8.2<sup>D116G</sup>-PR5* displayed enhanced disease resistance to *Gc*-UCSC1 (**Figure 4-5**). However upon close inspection, this resistance is also associated with accrued host costs in the form of spontaneous and mildew-induced cell death and a stunted phenotype for multiple independent lines (**Figure 4-5**). Based on the topology of *RPW8.2*, it seems likely that the high cost of resistance may be due to overexpression of the transgene and the consequent over-accumulation of the antimicrobial peptides at the cytoplasmic side of the EHM, activating strong resistance to powdery mildew while killing host cells. This situation is analogous to the overexpression of antimicrobial peptides in crop plants that leads to smaller stature, lesion formation and decreased yields overall (Collinge et al., 2008; Islam, 2008; Ceasar and Ignacimuthu, 2012).

On the other hand, preliminary results showed that some *Sp-cargo-RPW8.2<sup>D116G</sup>* fusion constructs may render enhanced resistance to *Gc*-UCSC1 without severe fitness penalty. For example, Col-gl lines transgenic for two *Sp-cargo-RPW8.2<sup>D116G</sup>* constructs in which the antimicrobial cargo gene is either Metchnikowin (Mtk), encoding a novel immune-inducible proline-rich peptide from *Drosophila* with antibacterial and antifungal properties (Levashina et al., 1995), or Magainin (Maga), encoding a peptide with broad-spectrum antimicrobial activity from the African clawed frog *Xenopus laevis* (Zasloff, 1987), showed enhanced resistance to powdery mildew with less pronounced HR and less

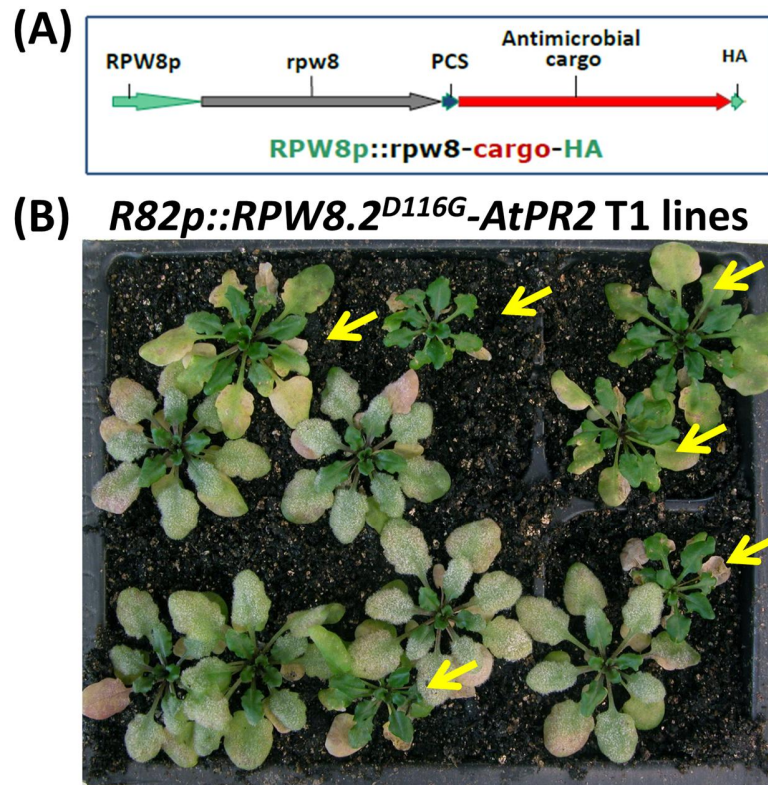


**Figure 4-5. RPW8.2-AtPR2 Confers Resistance with a High Cost.**

(A) Schematic illustration of translational fusion of antimicrobial cargos to the C-terminus of *RPW8.2<sup>D116G</sup>*. *RPW8.2<sup>D116G</sup>* and the antimicrobial cargo is spaced by the protein cleavage site (PCS) that is recognized by subtilisin. (B) Col-gl T1 lines transgenic for *RPW8.2<sup>D116G</sup>-AtPR2* inoculated with *Gc-UCSC1*. The picture was taken at 12dpi. Yellow arrows indicate independent T1 lines with enhanced resistance and experiencing high costs on the plant.

negative impact on plant stature (**Figure 4-6**). Transgenic T1 and T2 lines expressing other Sp-cargo-RPW8.2<sup>D116G</sup> fusion proteins did not show obvious resistance to powdery mildew. For example, Melittin (Meli), an amphipathic cationic peptide from honeybee venom (Wachinger et al., 1998), did not confer resistance when used as a cargo protein (**Figure 4-6C**). These preliminary results imply that targeting some antimicrobial peptides to the pathogen side of the EHM (i.e. the EHX) may confer more cost-effective resistance against powdery mildew. However, more work has to be done before a solid conclusion can be reached.

### **Engineering a Cargo-Release Mechanism Subsequent to Targeted Delivery**

We reasoned that targeted delivery and subsequent release of antimicrobial peptides (enzymes in particular) into the EHX may greatly enhance the efficacy of their antimicrobial activities. Hence, we have conceived such a strategy at the beginning of the NSF-BREAD project.

As depicted in (**Figure 4-5&6**), both the RPW8.2-cargo and cargo-RPW8.2 constructs contain the PCS specifically recognized by the subtilisin enzyme that was used to derive evidence for the membrane topology of RPW8.2. Insertion of the PCS into the cargo fusion constructs is to allow for the specific release of antimicrobial cargos into the EHX by Sbt when the cargo fusion proteins are targeted to the EHM by RPW8.2. This would require that (i) Sbt functions as a protease *in planta*, (ii) Sbt is also targeted by RPW8.2 to the EHM in the same orientation as the antimicrobial cargos, and (iii) Sbt in the Sp-Sbt-PCS-RPW8.2 fusion protein retains protease activity and could release itself off the fusion protein and then cleave antimicrobial cargos off the respective RPW8.2



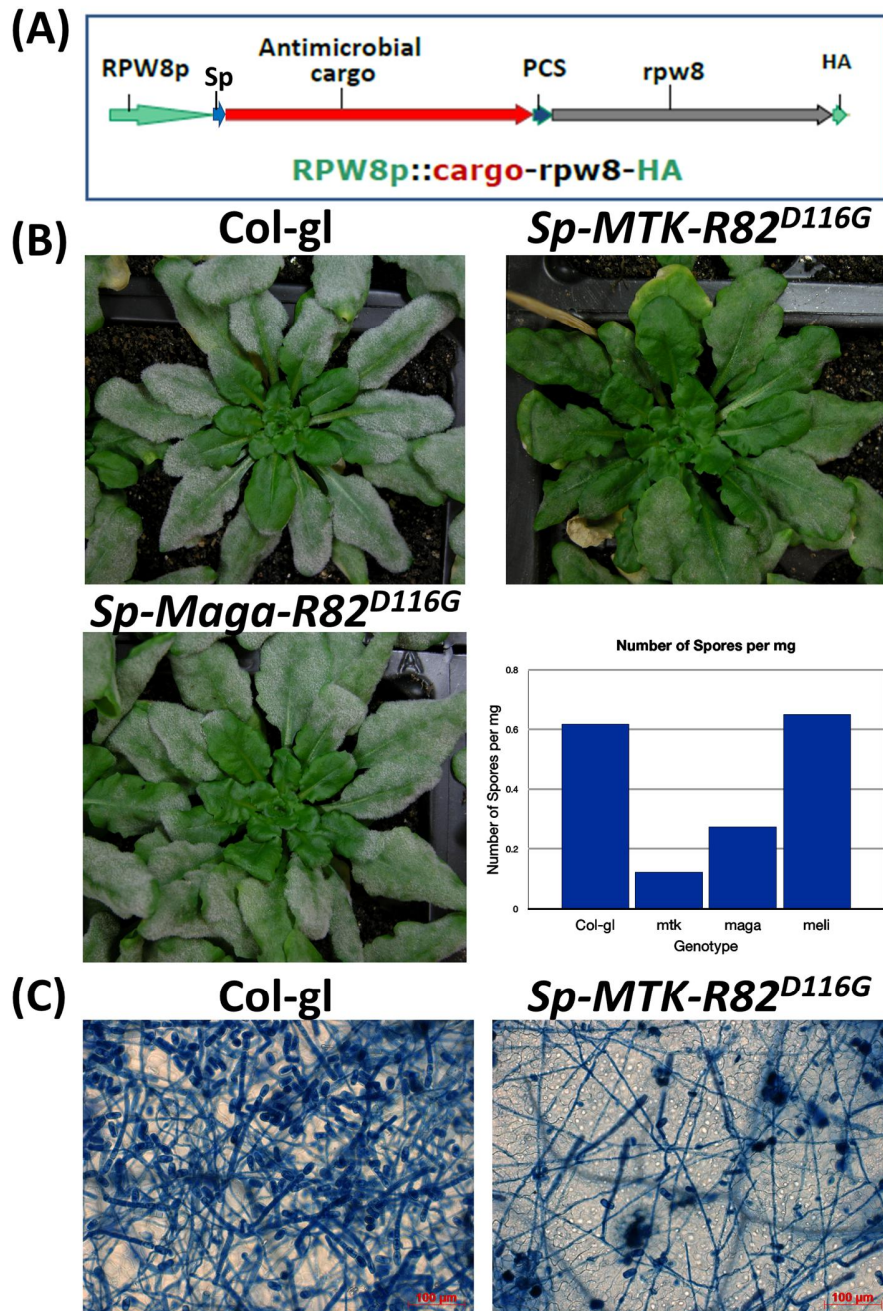


**Figure 4-6. Sp-MTK-RPW8.2 May Confer Resistance with A Lower Cost.**

(A) Schematic illustration of translational fusion of antimicrobial cargos to the N-terminus of *RPW8.2<sup>D116G</sup>*. (B) Infection phenotypes of *Col-gl* wild-type and representative T2 plants expressing Metchnikowin (MTK) or Magainin (Maga) as cargos (X) in *Sp-X-RPW8.2<sup>D116G</sup>* transgenic lines. Pictures were taken at 11dpi. (C)



Disease quantification of plants in **(B)**. Melittin (Meli) cargo lines (not shown in **(B)**) are as susceptible as Col-gl. **(D)** Trypan blue staining of representative leaves between Col-gl and MTK T2 cargo lines reveals a dramatic decrease in fungal mycelia and production of conidiophores (stained in blue) in MTK T2 cargo lines.

fusion proteins. To date, I have obtained some promising preliminary results towards this objective.

To test if plant-expressed Sbt can cleave PCS-site containing plant proteins *in vivo*, I made translational fusion between a conserved regulatory protein 14-3-3 $\lambda$  (At1g22300) from Arabidopsis and YFP spaced with the PCS (35S::*YFP-PCS-14-3-3 $\lambda$* ). I also made the 35S::*Sbt* construct for planta expression of Sbt. These two constructs were transiently expressed individually or in combination in ~4 week-old *N. benthamiana* leaves via agroinfiltration. As shown in (**Figure 4-7A**), whereas YFP-PCS-14-3-3 $\lambda$  alone exhibited a ubiquitous distribution in the transformed leaf epidermal cells, co-expression of YFP-PCS-14-3-3 $\lambda$  and Sbt resulted in a high percentage of cells (~50%) displaying an altered YFP expression pattern where YFP signal was concentrated in concave protrusions of transformed epidermal cells without obvious signal in the nucleus. The change of localization pattern of YFP signal may be caused by Sbt-mediated YFP cleavage although indirect interference on protein localization by Sbt-expression cannot be excluded. It is noteworthy that *N. benthamiana* leaves transiently expressing Sbt alone or in combination with YFP-PCS-14-3-3 $\lambda$  exhibited necrotic cell death that became visible to the naked eye 1-2 days post infiltration (**Figure 4-7B**). This suggests that transient overexpression of the Sbt enzyme is either toxic to the plant cell or activates host cell death machinery. To confirm that the change in YFP expression patterns is caused by Sbt-mediated cleavage, I performed a western blot analysis with the transformed *N. benthamiana* leaf samples using an anti-GFP antibody. As shown in (**Figure 4-7C**), a strong band (~56kDa) corresponding to the YFP-PCS-14-3-3 $\lambda$  fusion protein and a weak band in the size of YFP (~28 kDa) were detected in leaves expressing

YFP-PCS-14-3-3 $\lambda$  alone. In contrast, there was only a faint band for YFP-PCS-14-3-3 $\lambda$  but a strong band for YFP in the leaf samples co-expressing YFP-PCS-14-3-3 $\lambda$  and Sbt. Altogether, these results indicate that the engineered Sbt can be expressed and functions as a protease that is capable of cleaving proteins via the specific PCS *in planta* and comprises the first step of our group efforts towards targeted delivery and release of antimicrobial cargo proteins to the EHx using RPW8.2.

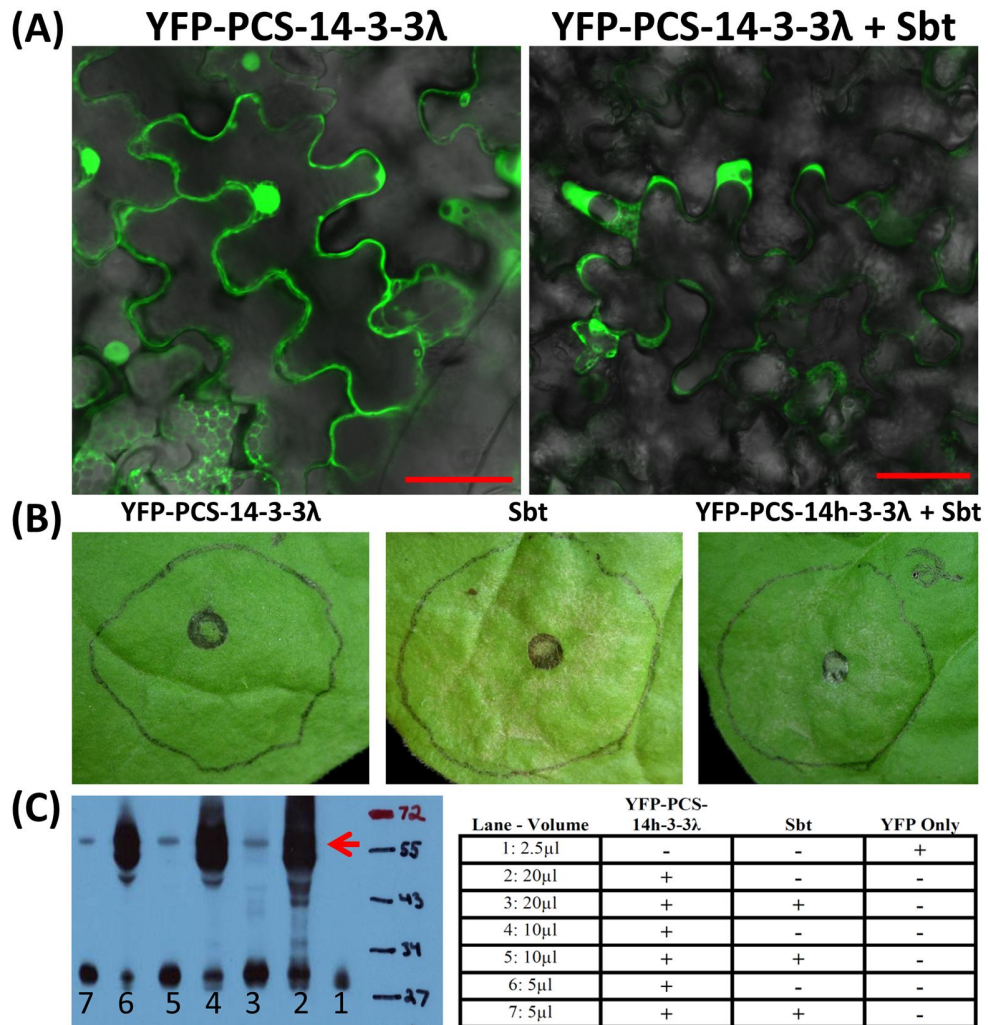


**Figure 4-7. Subtilisin Cleaves YFP-PCS-14-3-3λ *in vivo*.**

**(A)** Single optical sections of *N. benthamiana* leaf epidermal cells transiently expressing YFP-PCS-14-3-3λ alone (left) or YFP-PCS-14-3-3λ together with Sbt (right). Imaging was conducted at ~36 hours post agroinfiltration. Bars = 50μm. **(B)** Leaf sections of *N. benthamiana* transiently expressing the indicated proteins. **(C)** Western blot analysis of total proteins extracted from agroinfiltrated *N. benthamiana* leaf samples. The table on the right details the information about the amount of total protein extracts and the specific proteins under detection. The red arrow indicates the approximate position of the ~56

kDa YFP-PCS-14-3-3 $\lambda$  fusion protein. Note there may be a low level of cleavage of YFP-PCS-14-3-3 $\lambda$  by endogenous proteases of *N. benthamiana* in the absence of Sbt.

## Discussion

A unique feature of RPW8.2-mediated broad-spectrum resistance is the integration of defense activation with a precise subcellular targeting resembling "missile" defense. While the defense component is SA-dependent, the targeting components of RPW8.2 seem to be SA-independent (Wang et al., 2009). Based on this feature, we explored a unique strategy to utilize RPW8.2 for engineering haustorium-targeted and hopefully SA-independent resistance in plants. This strategy centers on the use of a defense-defective, but targeting competent allele of RPW8.2 as a delivery vehicle to shuttle antimicrobial cargo proteins to the extra-haustorial matrix such that more effective resistance against haustorium-forming pathogens may be achieved. However, engineering such a "missile" defense system in plants is not trivial and faces several challenges. My contribution to this exciting project mainly addresses the cargo orientation (relative to the vehicle) and cargo release issues, and has hopefully helped pave the road to future success for this project.

First, because knowing the membrane topology of RPW8.2 is a pre-requisite for targeting antimicrobial cargos to the EHX, I sought a "one stone, two birds" strategy to definitively resolve RPW8.2's membrane orientation. Using Sbt-mediated cleavage of YFP in fusion with RPW8.2, I not only demonstrate that RPW8.2 (and likely all RPW8 family proteins) is a type I membrane protein with its C-tail in the cytoplasmic side of the EHM (**Figure 4-3&4**) but also provide preliminary yet encouraging data for the utility of Sbt for controlled release of antimicrobial cargos at the EHM (**Figure 4-7**).

Second, based on the knowledge I gained for RPW8.2's membrane topology, the Xiao lab selectively fused antimicrobial cargos to the N-terminus of *RPW8.2<sup>D116G</sup>* with a

signal peptide leader in the N-terminus of the cargo-RPW8.2<sup>D116G</sup> fusion proteins to ensure proper secretion and EHM-targeting (**Figure 4-6A**). However, whether the cargos in such an orientation are really targeted to the EH<sub>X</sub> side of the EHM has not been determined. For this purpose, I generated and examined Arabidopsis lines stably expressing SP-YFP-PCS- RPW8.2<sup>D116G</sup>. Interestingly, preliminary results showed that YFP signal from this fusion protein was only detectable as a few punctate spots in some mildew infected epidermal cells (**Figure 4-8**), and in most cases, there was no detectable YFP signal. However, western blot analysis showed that the SP-YFP-PCS-R82 protein is expressed at a similar level as RPW8.2-YFP or YFP-RPW8.2 upon infection with *Gc*-UCSC1 (**Figure 4-8**). One likely interpretation for the above results is that the EH<sub>X</sub> environment is acidic and the YFP fluorophore gets quenched when the YFP fusion protein is targeted to the EH<sub>X</sub> side of the EHM. Our observation that YFP-RPW8.2 (and YFP-HR3) without an N-terminal signal peptide showed normal EHM-localized YFP signal are compatible with this interpretation. However, definitive evidence is needed to make a conclusion that YFP in SP-YFP-PCS- RPW8.2<sup>D116G</sup> expressed in haustorium-invaded cells is indeed targeted to the EH<sub>X</sub> side of the EHM. One promising approach is to use the mCherry-GFP dual fluorescent protein as cargo to report the exact localization of Sp-cargo-RPW8.2 proteins, because mCherry is less pH-sensitive and may be more detectable in the EH<sub>X</sub>.

Third, and perhaps the most challenging task for realizing RPW8.2-guided missile defense is to release the cargo to the EH<sub>X</sub>. Even though I showed that Sbt can function *in planta* to release cargos (YFP as an example) from RPW8.2-PCS-cargo fusion proteins, I have not confirmed (i) whether Sp-Sbt-PCS-RPW8.2<sup>D116G</sup> (for targeting of Sbt

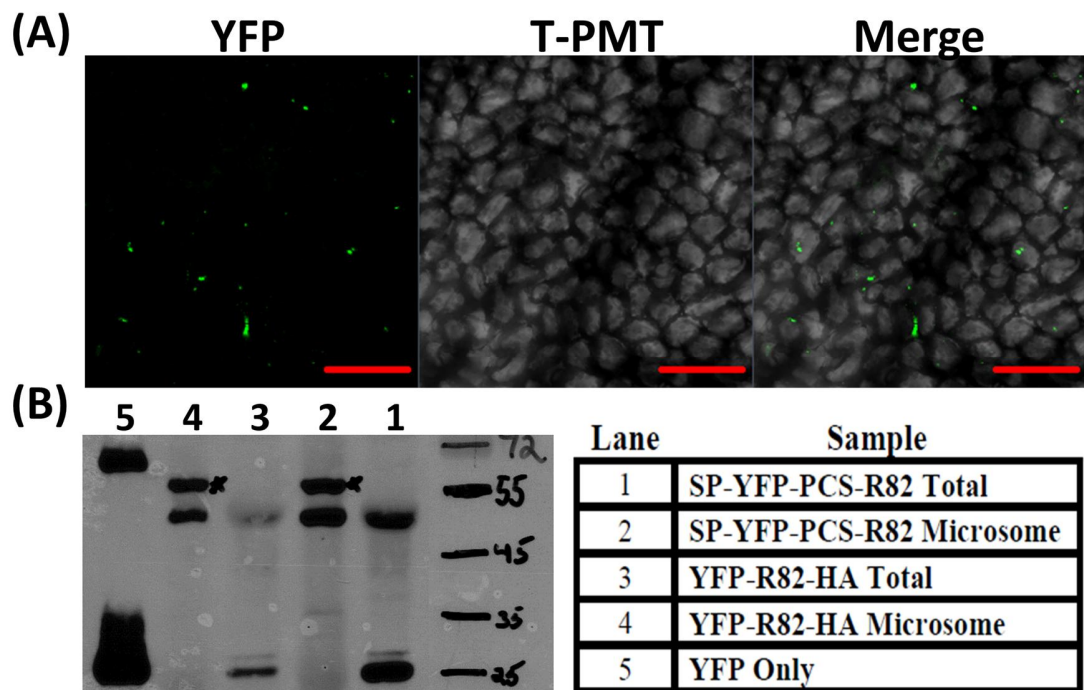


**Figure 4-8. SP-YFP-PCS-RPW8.2 Is Expressed But YFP May Be Quenched.**

**(A)** Representative Z-stack projection of a stable Arabidopsis plant expressing SP-YFP-PCS-R82. Weak YFP signal is detectable in some epidermal cells following *Gc*-UCSC1 infection. Bars = 100 $\mu$ m. **(B)** Western blot analysis with an anti-GFP antibody for the detection of SP-YFP-PCS-R82 in total or membrane fractions of pooled SP-YFP-PCS-R82 T1 lines (lanes 1-2). YFP-R82-HA (lane 3-4) and YFP were used as control (lane 5). Black star indicates SP-YFP-PCS-R82 (lane 2) or YFP-R82-HA protein (lane 4). Both proteins are approximately 57 kDa in size.



to the EHM in the same orientation as Sp-cargo-RPW8.2<sup>D116G</sup>) could function as a protease to release Sbt itself and (ii) then further release antimicrobial cargos from cargo-RPW8 fusion proteins. Recently, I also noted that Arabidopsis plants expressing Sbt exhibited stunted growth and HR-like cell death (**data not shown**) which is in an agreement with my observation that *N. benthamiana* leaves transiently expressing Sbt developed necrotic cell death in (**Figure 4-7B**). Whether secreted Sbt is toxic or capable of triggering plant cells is not known, however I did notice a similar level and timing of cell death for *N. benthamiana* plants expressing Sp-Sbt (**data not shown**). Assuming this is the case for Arabidopsis transgenic plants, modified Sbt with slower or lower protease activity may be used to reduce the negative impact due to Sbt expression.

Lastly, it is worth pointing out that so far only two (Metchnikowin and Magainin) out of > 20 tested antimicrobial cargos in fusion with RPW8.2 at the N-terminus are marginally effective in conferring enhanced resistance against *Gc*-UCSC1. Metchnikowin is from *Drosophila* (Levashina et al., 1995) and Magainin (Maga) is from frog (Zasloff, 1987). None of the antimicrobial proteins from plants showed obvious effect. One possible explanation could be that well-adapted powdery mildew pathogens like *Gc*-UCSC1 may have evolved the ability to detoxify these antimicrobial proteins. Another possibility is that anchoring at the EHM alone without release into the EHX is not sufficient to exert an antifungal effect. Currently, the Xiao lab is co-expressing Sp-Sbt-RPW8.2<sup>D116G</sup> with each of the >20 Sp-cargo-RPW8.2<sup>D116G</sup> constructs to see if it can significantly improve resistance of the respective transgenic Arabidopsis plants against powdery mildew. However, one cannot exclude the possibility that some of these Sp-cargo-RPW8.2<sup>D116G</sup> fusion proteins may not be correctly targeted to the EHX side of the

EHM due to unknown trafficking constraints. Development of a method to determine the precise localization of such Sp-cargo-RPW8.2<sup>D116G</sup> fusion proteins will be very useful for deriving definitive conclusions.

While additional experiments are needed to provide convincing proof-of-concept data for engineering novel resistance via targeted delivery and controlled release of antimicrobial cargos by RPW8.2 to the host pathogen interface in Arabidopsis, I have made five DNA fusion constructs in a binary vector suitable for stable transformation of cacao and these constructs are being used by our collaborator's lab for making transgenic cacao. Such a "missile" defense strategy, once validated, could be potentially used to create crop cultivars or breeding materials with novel resistance against haustorium-forming pathogens.

## **Materials & Methods**

### **Plant materials and cultivation**

Arabidopsis accessions Col-0 or Col-gl were used for generation of all transgenic lines. All genetic analyses for genotyping and phenotyping were conducted in accordance with previous reports (Xiao et al., 2003b; Xiao et al., 2005). Unless otherwise indicated, seeds were sown in Sunshine Mix #1 or Metro-Mix 360 soil (Maryland Plant & Suppliers, Inc, USA) and cold-treated (4 °C for 1-2 days). Seedlings were kept under 22 °C, 75% RH, short-day (8 hrs light at  $\sim 125 \mu \text{mol} \cdot \text{m}^{-2} \cdot \text{sec}^{-1}$ , 16 hrs dark) conditions for 5-6 weeks before pathogen inoculation and/or other treatments.

### **Pathogens strains, inoculation and phenotyping**

Powdery mildew isolate *Golovinomyces cichoracearum* UCSC1 (*Gc*-UCSC1) was maintained on live Col-0 or Col-*NahG* plants for generation of fresh conidia for inoculation purposes. Inoculation, visual scoring, photographing and quantification of disease susceptibility were done as previously described (Xiao et al., 2005).

### **Cloning and Plasmid Construction**

*RPW8.2-PCS-YFP*, *YFP-PCS-RPW8.2* and *YFP-PCS-14-3-3 $\lambda$*  constructs were created using standard PCR amplification strategies coupled with restriction enzyme digestion and T4-mediated ligation. *RPW8.2* and *YFP* were amplified from a previously constructed vector containing *RPW8.2* in fusion with *YFP* (P2Y13) and the PCS sequence was adapted to specific primers used for this amplification. 14-3-3 $\lambda$  was amplified from a Col-0 cDNA sample and used for cloning. The DNA sequence for the

protein cleavage site (PCS) used for amplification was obtained from Dr. Philip Bryan (UMD-IBBR) and is: 5' GAGTTCAGGGCTCTCAGCGCAGGTGGCAGTGGAGGT<sup>3'</sup> and codes for 5' E-F-R-A-L-S-A-G-G-S-G-G<sup>3'</sup>.

For *RPW8.2-PCS-YFP*, the *PCS-YFP* fragment was amplified using the primers (PCS-YFP-F:

5' gaattcAGGGCTCTCAGCGCAGGTGGCAGTGGAGGTATGGTGAGCAAGGGCGA<sup>3'</sup> and BglYFPR1: 5' gcagatcTCACTTGTACAGCTCGTCCATG<sup>3'</sup>) while the *R82*

fragment was amplified using (BamR82F:

5' caccggatccATGATTGCTGAGGTTGCCGCA<sup>3'</sup> and R82-PCS-

R: 5' cctgaattcTCCAGAATCATCACTGCAGAACGTAAA<sup>3'</sup>). Full length *R82-PCS-YFP* was amplified using the primers (BamR82F:

5' caccggatccATGATTGCTGAGGTTGCCGCA<sup>3'</sup> and BglYFPR1:

5' gcagatcTCACTTGTACAGCTCGTCCATG<sup>3'</sup>). For YFP-PCS-RPW8.2, the *PCS-R82* fragment was amplified using the primers (EcoSCSLF:

5' agaattcAGGGCTCTCAGCGCAGGTGGCAGTGGAGGTATGATTGCTGAGGTTGCCGCA<sup>3'</sup> and BamR82R2: 5' ttgatccTCAAGAATCATCACTGCAGAAC<sup>3'</sup>) while the *YFP* fragment was amplified using the primers (BamYFPF1:

5' tcggatccATGGTGAGCAAGGGCGAG<sup>3'</sup> and EcoYFPR:

5' tgaattcTCCGGAATTGTACAGCT<sup>3'</sup>). Full length *YFP-PCS-R82* was amplified using the primers (BamYFPF1: 5' tcggatccATGGTGAGCAAGGGCGAG<sup>3'</sup> and BamR82R2:

5' ttgatccTCAAGAATCATCACTGCAGAAC<sup>3'</sup>). *YFP-PCS-14-3-3λ* was amplified and created in a similar manner using the primers (BamYFPF1:

5' tcggatccATGGTGAGCAAGGGCGAG<sup>3'</sup> and EcoYFPR:

5'tgaattcTCCGGACTTGTACAGCT<sup>3'</sup>) for the *YFP* fragment and the primers (5'agaattcAGGGCTCTCAGCGCAGGTGGCAGTGGAGGTATGGCGGCGACATTAGGCAGA<sup>3'</sup> and Xho14hR: 5'ccgctcgagTCAGGCCTCGTCCATCTGCT<sup>3'</sup>) for the *PCS-14-3-3λ* fragment. Linked *YFP-PCS-14-3-3λ* was amplified using the primers (BamYFPF1: 5'tcgatccATGGTGAGCAAGGGCGAG<sup>3'</sup> and Xho14hR: 5'ccgctcgagTCAGGCCTCGTCCATCTGCT<sup>3'</sup>).

All resulting fragments were digested with the *EcoRI* restriction enzyme according to NEB protocol and linked using the recommended procedures provided for Promega T4 ligation using T4 Ligase (Promega, [Promega T4 Ligase](#)) Both RPW8.2-PCS-YFP and YFP-PCS-RPW8.2 were amplified with ExTaq polymerase (Fischer, [Fischer ExTaq Polymerase](#)) and cloned via T/A cloning into the previously described homemade pCX-DG-82p vector (see **Chapter 2**). YFP-PCS-14-3-3λ was cloned in a similar manner into the 35S driven pCXSN T/A cloning vector (Chen et al., 2009b).

Glycosylation (NNSS) *RPW8.2* constructs were also created using PCR amplification and restriction enzyme linkage strategies. These DNA clones were also inserted via T/A cloning into the pCX-DG-82p vector. 35S::*Sbt* was created by cloning the subtilisin gene from *Bacillus amyloliquefaciens* (Accession Number: [X00165.1](#)) into the pCXSN vector via T/A cloning using the primers (BamSbtF:

5'caccggatccATGGCGAAGTGCGTGTCTTA<sup>3'</sup> and EcoSbtR:

5'tgaattcTGATCCCTGAGCTGCCGCTTCTACGT<sup>3'</sup>). All N-terminal and C-terminal

*RPW8* cargo constructs, including the *SP-YFP-PCS-R82* construct (see **Discussion**) were created using the homemade pCX-DG-82p vector as a backbone. More detailed description for the creation of these cargo vectors, and the resulting cargo constructs are

available upon request as it was a multi-step process that is too lengthy and difficult to list here.

### **Transformation of Arabidopsis and transient expression in *N. benthamiana***

All generated constructs in binary vectors were introduced into *Agrobacterium* strain GV3101 and stable transgenic *Arabidopsis* plants were generated by floral dip (Clough et al., 2000) or transiently expressed by *agrobacterium*-mediated infiltration of 4-5 week old mature *N. benthamiana* leaves (Bendahmane et al., 2002). Fresh GV3101 *agrobacterium* cultures carrying expression constructs were grown O/N at 30°C and washed at least 1 time(s) in 10mM MgCl<sub>2</sub> solution. Cell suspensions were diluted to an approximate OD<sub>600</sub> concentration of 0.4-0.6 and *N. benthamiana* leaves were slowly infiltrated using a needleless syringe on the abaxial side of the leaf.

### **Extraction of Haustoria**

This protocol is modified from the “Isolation of intracellular hyphae by isopycnic centrifugation technique” described in (Pain et al., 1994). Extracted haustoria suspensions were obtained from pooled T2-T4 lines of appropriate transgenic backgrounds between 7-8dpi with *Gc*-UCSC1. Approximately 1-2 total grams of infected leaf tissue was macerated 2x in a conventional kitchen blender in a minimum volume 20-30ml of fresh, chilled haustoria extraction buffer (3-[N-morpholino]-propane sulphonic acid (MOPS) .02M, pH 7.2 containing 0.2M sucrose) for 45-60 seconds. After each 1X blending procedure, macerated plant material was filtered through a 40µm nylon mesh material using vacuum filtration to remove large fragments of plant debris as most mature *Gc*-

UCSC1 haustoria are typically between 15-25 $\mu$ m in size. Final filtrates were centrifuged at 1080  $\times$  g for 15min at 4°C. Pelleted material containing haustoria was resuspended in 2-3ml of haustoria extraction buffer and kept at 4C prior to imaging or further analysis.

### **Subtilisin Treatments**

Purified subtilisin enzyme (isoform S189) was obtained from Dr. Philip Bryan (UMD-IBBR) and directly used in combination with cleavage buffer (10mM NaNO<sub>2</sub>) to analyze the functionality of Sbt in cleaving the PCS. Purified total and membrane protein fractions from RPW8.2-PCS-YFP lines or extracted haustoria were treated with ~15 $\mu$ M Sbt and 10mM NaNO<sub>2</sub> for 45-60min at 37°C and analyzed by Western blot or confocal microscopy. General assay instructions were given through personal communication with Dr. Philip Bryan.

### **Protein Isolation, SDS-PAGE and Western blotting**

Membrane proteins (containing RPW8) were isolated by homogenizing between 0.5-1.0g of fresh leaf material at around 5-8dpi with *Gc*-UCSC1. Leaf material was homogenized in 4-5ml of extraction buffer (50mM Tris, pH 7.5, 50mM NaCl, 1mM EDTA, 1mM DTT, 10% w/v sucrose and .1% protease inhibitor cocktail (Sigma)) using a pre-chilled mortar and pestle. Homogenate samples were filtered through two layers of Miracloth or cheesecloth and centrifuged at 3,000  $\times$  g for 15min at 4°C to remove excess debris. Resulting supernatant fractions were ultracentrifuged at 100,000g for 1hr at 4°C and the resulting membrane pellets were resuspended in approximately 250-350 $\mu$ l of membrane resuspension buffer (20mM Tris, pH 7.5, 50mM NaCl, 1mM EDTA, 1mM

DTT, 10% w/v sucrose and .1% protease inhibitor cocktail (Sigma)). A proportion of the supernatant was also put aside for later analysis on total protein fractions. Isolated total and membrane fractions were mixed with 2x SDS loading buffer and denatured in a 90-95°C water bath for roughly 10-15min and then fractionated by SDS-PAGE on 8-12% w/v polyacrylamide gels for 1.5hr at 110-120V. Following electrophoresis, proteins were electroblotted onto a supported PVDF or nitrocellulose membrane using the Owl semi-dry electroblotting system ([Thermo Scientific](#)) at 15V for 45min. Following electroblotting, membranes were incubated with a 1:5,000 dilution of the primary rabbit monoclonal anti-YFP (Abcam) followed by a 1:20,000 dilution of the goat-anti-rabbit HRP conjugated secondary antibody (Sigma). Immunodetected proteins were visualized using the ECL Advance Western Blotting Detection Kit ([Amersham](#)). Total fractions only of transiently expressed proteins in *N. benthamiana* were isolated in a similar fashion.

### **Other Analyses**

Trypan blue staining for cell death and fungal structures was performed as previously described in (Xiao et al., 2003b). Imaging and laser scanning confocal microscopic (LSCM) imaging was done using either a Zeiss Axioepifluorescence microscope coupled with an HBO 100 microscope illumination system or with a Zeiss LSM710 confocal microscope as previously described in (Wang et al., 2007; Wang et al., 2009; Wang et al., 2010). All images presented are single optical sections or Z-stack projected of 15-30 images unless otherwise indicated. For PI staining, detached leaf sections (~.25 cm<sup>2</sup>) were submerged in 0.5% PI solution for 45-60 minutes then washed



briefly (10-15 minutes) in water before imaging. Alternatively, a final PI concentration of 0.5% was added to extracted haustoria suspensions prior to imaging. Sirofluor staining of leaf sections or extracted haustoria for callose was conducted with a 0.1 mg ml<sup>-1</sup> dissolved in a 1% DMSO solution; (Biosupplies, <http://www.biosupplies.com.au/products.htm>). Image data was processed using Zen 2009 Light Edition and Adobe Photoshop CS5.

## Chapter 5: Towards Understanding the Mechanisms Underlying EHM-specific Targeting of RPW8 Family Proteins

### Introduction

The identification of RPW8 family proteins as EHM-specific residents suggests a host-origin for the EHM and provides the first EHM-specific markers to study the nature of the EHM and the molecular interaction between the host and pathogen. In **Chapter 3**, I provide the first piece of cell biological evidence to suggest that the EHM is *de novo* synthesized upon haustorial differentiation. However, this is only a small albeit the very first step towards molecular characterization of the enigmatic EHM. There are more challenging questions in relation to the biogenesis of the EHM (i.e. the spatiotemporal dynamic protein/lipid composition of the EHM), and why and how RPW8 family proteins are specifically targeted to the EHM. It is conceivable that it may be the lipid composition of the EHM that determines its protein constitution through selective recruitment mechanisms pertaining to specific lipid species that may be (transiently) enriched in the EHM. Based on lipid chemistry and relevant past studies (see below), among a plethora of membrane lipids, phosphoinositides (PIs) are likely candidate lipids that may serve as a spatiotemporal landmarks for the EHM.

PIs are phosphorylated derivatives of the membrane lipid phosphatidyl-inositol (PtdIns) that contain a hydrophobic diacylglycerol (DAG) backbone esterified to a *myo*-inositol 1-phosphate [Ins(1)P] headgroup where three of the five hydroxyl residues (3,4,5) of the inositol ring of PtdIns can be phosphorylated individually or in combination by specific PI kinases to generate seven different varieties of PIs [PI(3)P, PI(4)P, PI(5)P, PI(3,4)P<sub>2</sub>, PI(3,5)P<sub>2</sub>, PI(4,5)P<sub>2</sub>, PI(3,4,5)P<sub>3</sub>] (**Figure 5-1**). All seven varieties of PIs are

detected in animal cells while all but PI(3,4,5)P<sub>3</sub> are detectable in plant cells (Thole and Nielsen, 2008). PIs serve as structural materials of eukaryotic membranes, key regulators of lipid and cell signaling, regulators of membrane trafficking and serve as spatial and temporal markers for subcellular membranes and domains in both animal and plant cells (Behnia and Munro, 2005; Blumental-Perry et al., 2006; Di Paolo and De Camilli, 2006; Thole and Nielsen, 2008; Vicinanza et al., 2008) (**Figure 5-1**). For example in plant cells, PI(3)P has been found to be concentrated in the vacuolar membrane in leaf epidermal cells (Kim et al., 2001; Vermeer et al., 2006), PI(4)P is mainly found in the Golgi apparatus, secretory vesicles, and the PM (Preuss et al., 2006; Vermeer et al., 2009) and PI(4,5)P<sub>2</sub> is found in the cytoplasm and becomes enriched in the PM in response to salt stress or as a gradient at the tip of growing root hairs during cell division (van Leeuwen et al., 2007).

Interestingly, PI(3)P has also been found to be transiently accumulated on the matured phagosomal membranes (Vieira et al., 2001) and host PI metabolism is targeted by intracellular bacterial pathogens of animals to modulate the host PM or vacuolar membranes for host entry and multiplication (Weber et al., 2009). Moreover, as described in **Chapter 4**, host PIs, specifically PI(3)P and PI(4)P are necessary for host uptake of oomycete and fungal effector proteins via binding a conserved RXLR motif that is conserved in the malaria parasite *Plasmodium falciparum* (Kale et al., 2010) (**Figure 4-2**). Combined, these findings suggest that host PIs (i) may serve as landmarks for the interfacial membrane between plant hosts and pathogens and (ii) may be specifically targeted by pathogens or utilized by hosts in the ongoing molecular warfare at the host-pathogen interface.

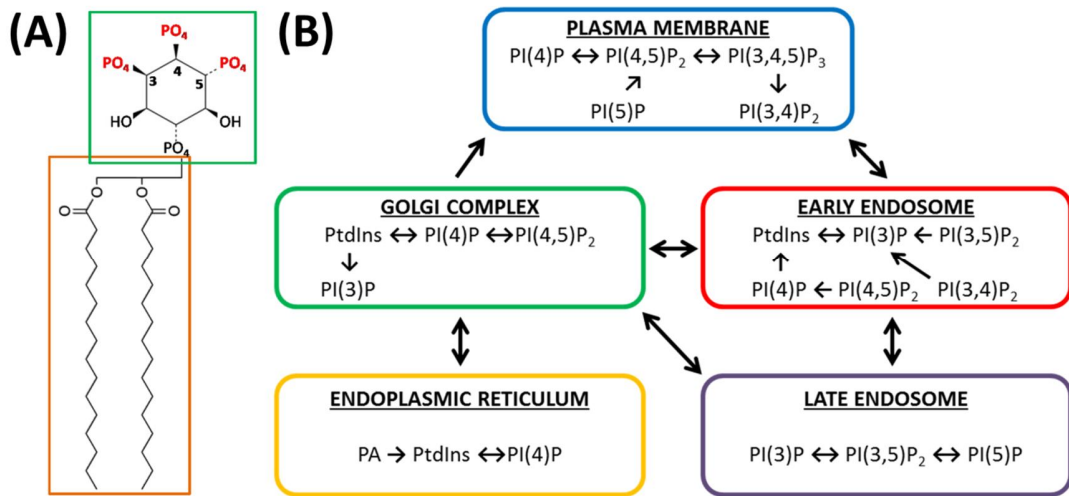


**Figure 5-1. Phosphoinositides are Spatial Landmarks of Eukaryotic Cells.**

**(A)** Structural drawing of phosphoinositides (PI) lipid derivatives. Hydrophobic diacylglycerol (DAG) backbone (orange box) esterified to a myo-inositol 1-phosphate [Ins(1)P] head group (green box) of phosphatidylinositol (PtdIns). Specific hydroxyl groups of the inositol ring at positions 3,4,5 can be phosphorylated individually or in combination to create the 7 different PI species. **(B)** Cartoon representation of the predominant subcellular membrane location of PIs in eukaryotic cells and the rapid interconversion between PI species. Modified from Di Paolo and De Camilli, 2006.

## Results & Discussion

### A PI(3)P Biosensor is Transiently Enriched at the EHM

Based on the above findings, I hypothesize that phosphoinositides may serve a role as (i) lipid landmarks ensuring EHM-directed membrane/protein trafficking (i.e. serving a trafficking cue for EHM-targeting of RPW8.2) and/or (ii) as signaling molecules in the regulation of plant host defense responses. To monitor the spatiotemporal dynamics of phosphoinositides, PI biosensors, which are known protein domains responsible for specific protein-lipid (PI) interactions, are fused to fluorescent tags and used as subcellular reporters of PIs. As such, I created a biosensor for one specific phosphoinositide, PI(3)P, to investigate the spatiotemporal dynamics of PI(3)P in response to powdery mildew and to investigate how the EHM differs from the host PM in terms of PI(3)P.

Specifically, I translationally fused the Arabidopsis PI(3)P binding protein, *AtPH1* ([NP\\_565687](#)) (Dowler et al., 2000), to YFP at both termini and Col-gl plants were transformed with either *RPW8.2p::AtPH1-YFP* and *35S::YFP-AtPH1*. Before inoculation with *Gc*-UCSC1, YFP signal was largely undetectable in *RPW8.2p::AtPH1-YFP* transgenic lines as *RPW8.2p* is a powdery mildew inducible promoter. After inoculation, detectable YFP levels dramatically increased within haustorium-invaded epidermal cells and most importantly, YFP-positive puncta were detected at or near the EHM (**Figure 5-2 A&B**). For *35S::YFP-AtPH1* transgenic lines, a high level of ubiquitously expressed YFP signal was detectable before inoculation in epidermal cells while YFP signal became detectable at or near the EHM following inoculation with

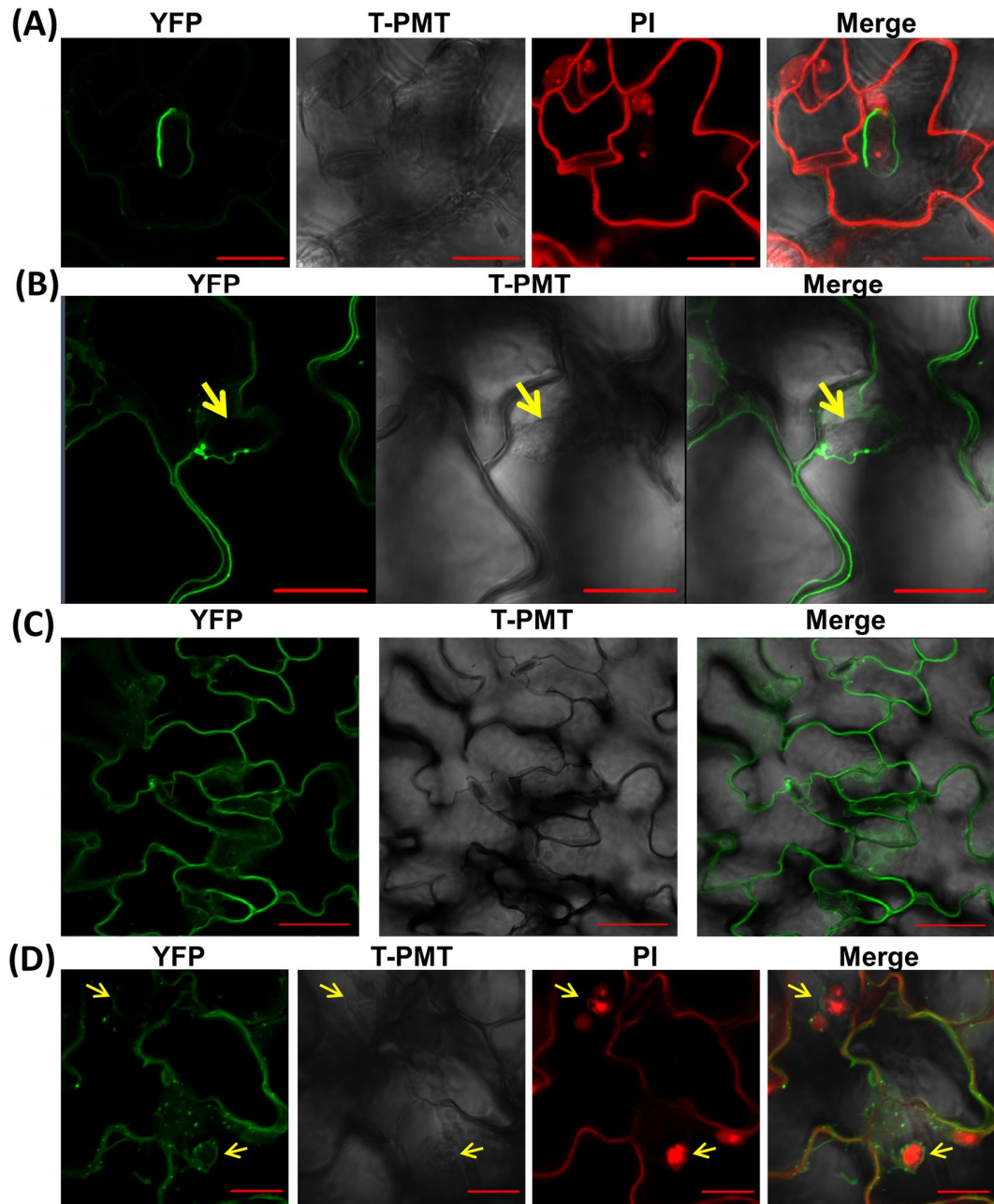


**Figure 5-2. PI(3)P is Transiently Enriched in the EHM Upon Haustorial Differentiation.**

**(A & B)** Representative single optical sections of Col-gl plants expressing *AtPH1*-YFP from the *RPW8.2* promoter. The *AtPH1*-YFP PI(3)P biosensor is transiently enriched at the EHM uniformly or as punctate-like spots around the EHM of differentiated haustoria

at 42hpi. Fungal structures and host PM are stained with PI (red) in **(A)**. Bars = 20µm.

**(C & D)** Representative single optical sections of constitutively expressed YFP-*At*PH1 in epidermal cells before **(C)** and after **(D)** *Gc*-UCSC1 inoculation. Yellow arrows indicate location of haustoria. Bars = 50µm in **(C)** and 20µm in **(D)**.

powdery mildew (**Figure 5-2 C&D**) suggesting that PI(3)P is transiently enriched at the EHM upon haustorial differentiation.

To confirm that *AtPH1*-YFP is indeed localized to the EHM membrane, co-transformation of Col-gl plants with *RPW8.2p::AtPH1-YFP* and *RPW8.2p::RPW8.2-RFP* was conducted. Confocal imaging of these lines strongly suggests that *AtPH1*-YFP is colocalized with RPW8-RFP at the EHM membrane (**Figure 5-3 A&B**). It is noteworthy that while RPW8.2-RFP signal was strongly and uniformly detected at the EHM, *AtPH1*-YFP signal was slightly weaker and occasionally appeared to be enriched at the EHM as puncta-like membrane components suggesting a transient localization to this unique membrane during its biogenesis (**Figure 5-3 A&B**). Moreover, time-lapse imaging used to monitor the movements of vesicles positive for *AtPH1*-YFP revealed that these vesicles were highly mobile and trafficked along cytoplasmic strands throughout the cell and in the periphery of the EHM (**Figure 5-3C**). This pattern is similar to the manner described for another PI(3)P biosensor, YFP-2xFYVE, in response to oomycete haustorium-forming pathogens (Lu et al., 2012). This highly motile movement appears to be bidirectional at the host-pathogen interface, suggesting that endosomal trafficking is active in haustorium-invaded cells between the host cell and the EHM.

I was also interested in testing the extracellular localization of PI(3)P using a biosensor in fusion with the N-terminal secretion signal peptide (Sp). This work is relevant to using PI(3)P-binding proteins to interfere host cell entry of RXLR-containing fungal or oomycete effectors (**Chapter 4**). In short, I obtained a *35S::Sp-GmPH1-mCherry* (PI(3)P) construct from the Tyler group and created transgenic lines in *Arabidopsis* to test its extracellular (extrahaustorial matrix) localization upon powdery



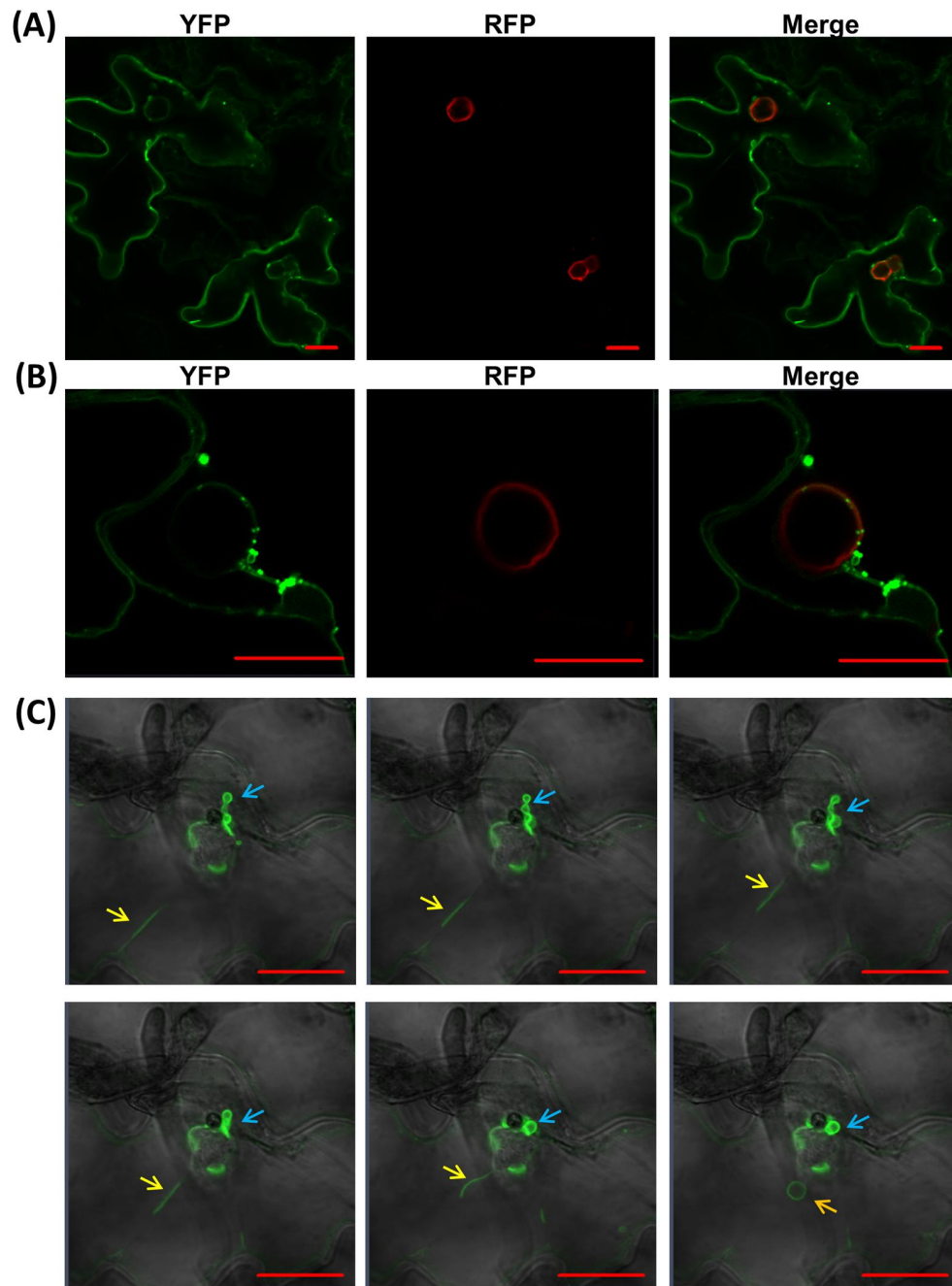


**Figure 5-3. The PI(3)P-biosensor is Colocalized with RPW8.2 at the EHM.**

**(A & B)** *AtPH1*-YFP is colocalized with R82-RFP at the EHM membrane as evident by weak uniform EHM labeling signal **(A & B)** or punctate like vesicles **(B)** at the EHM.

Differentiated haustoria are indicated by RPW8.2-RFP labeling at 42hpi with *Gc*-

UCSC1. Bars = 20 $\mu$ m. **(C)** Single optical sections from a sequential time lapse scan of

the AtPH1-YFP biosensor in a haustoria-invaded epidermal cell. Punctate spots and small vesicle-like structures are highly mobile and move around the host PM, cytoplasmic strands and the EHM suggestive of endocytic recycling between the host and EHM. Yellow arrows indicate cytoplasmic strands moving toward the EHM while blue arrows indicate vesicle-like structures apparently fusing with the EHM. The orange arrow in the last panel indicates a vesicle-like structure moving away from EHM. Bars = 20 $\mu$ m.

mildew infection. I found that this PI(3)P biosensor was homogeneously distributed in the extracellular space (apoplast) of Arabidopsis leaves before powdery mildew infection (**Figure 5-4A**). Upon infection with powdery mildew, I could not detect mCherry signal in the EHX (**Figure 5-4B**). Given that the EHM is *de novo* synthesized and the EHX is probably physically separated from the apoplastic space by the fungal neck band that is analogous in function to the Casparian strip of endodermal cells (Heath, 1976; Gil and Gay, 1977), this result is not surprising as this biosensor does not contain any EHM-targeting signal. To confirm the apoplastic localization, I applied 1M NaCl to the cells and mCherry signal was found in the enlarged apoplastic space as a result of plasmolysis (**Figure 5-4A**). As expected, mCherry signal was also seen in the apoplastic space surrounding the fungal penetration site (papillae region) (**Figure 5-4B**). Similar results were also obtained by Brett Tyler's group using Sp-biosensors and transient expression in *N. benthamiana* challenged with *Hyaloperonospora parasitica* (Brett Tyler, Personal communication).

In an effort to determine if RPW8-mediated resistance and/or EHM-localization could be abrogated by interference with host PI(3)P function or metabolism, I have investigated silencing of a PI(3)P kinase and the use of pharmacological treatments to deplete host PI(3)P levels. While three classes of PI3Ks exist in mammalian species (Wymann and Pirola, 1998), only one class (Type III) exists in plants (Hong and Verma, 1994; Welters et al., 1994) and is homologous to the Vps34p enzyme first identified in *Saccharomyces cerevisiae* (Herman et al., 1992). In Arabidopsis, PI3K is encoded by a single copy gene also known as *AtVPS34* (At1g60490 - [NM\\_104735](#)). Unfortunately, T-DNA insertion mutants have been shown to be gametophyte-lethal and ineffective in

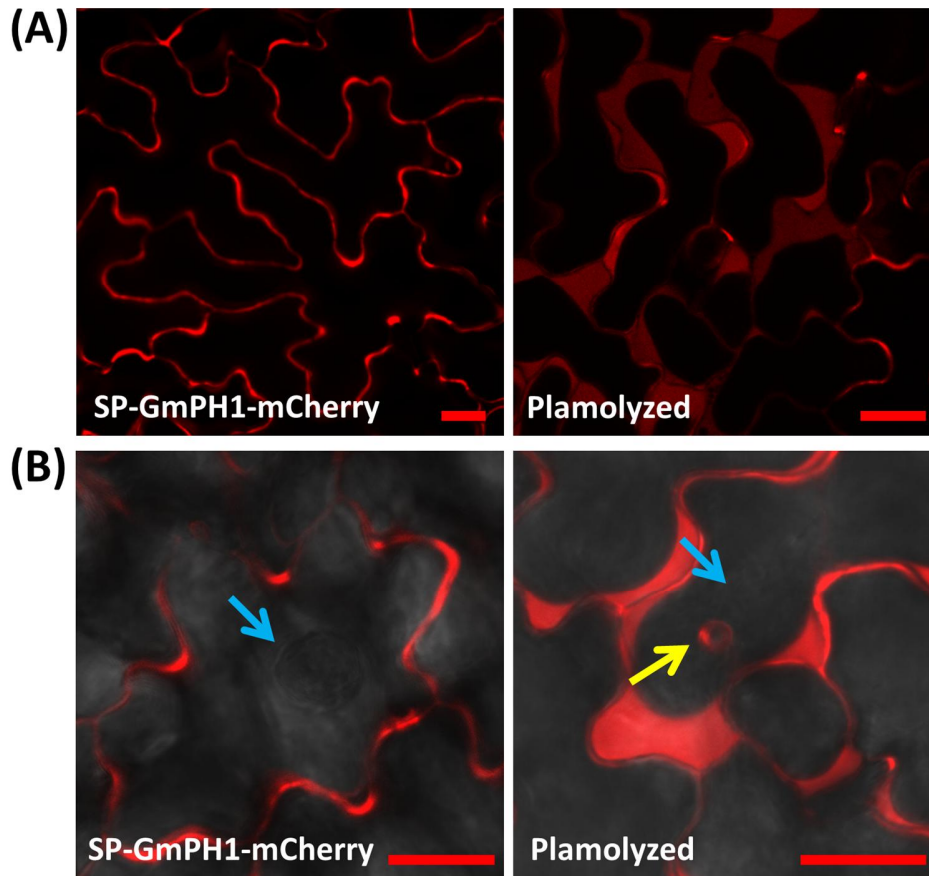


**Figure 5-4. Sp-GmPH1-mCherry is Secreted to the Extracellular Space.**

Leaves of transgenic plants constitutively expressing Sp-*GmPH1*-RFP imaged before **(A)** and after powdery mildew infection **(B)**. Single optical section images of epidermal cells were acquired before (left) and after plasmolysis using 1M NaCl (right). Bars = 50µm in **(A)** and 20µm in **(B)**. Note *GmPH1*-RFP is not detectable in the EHX of fully differentiated haustoria in epidermal cells (blue arrows).

studying molecular functionality of *AtVPS34* (Lee et al., 2008). Therefore, I created amiRNA lines targeting *PI3K* but these plants did not exhibit any obvious phenotypic changes in response to *Gc*-UCSC1 (**data not shown**) as plants with only slightly reduced *PI3K* transcript levels survive and they do not show distinct phenotypes (Lee et al., 2008). For pharmacological treatments, several inhibitors of PI3Ks including Wortmannin, a furanosteroid metabolite of the fungi *Penicillium funiculosum*, and LY294002, a morpholine derivative of quercetin, are commonly used in cell suspension studies. However, infiltration studies of RPW8.2-YFP lines with Wortmannin and LY294002 did not result in a reduction of RPW8 targeting efficiency (**data not shown**) presumably due to the short half-life in tissue culture and transient inhibition of PI3Ks (Okkenhaug and Vanhaesebroeck, 2001) that are insufficient to reduce host PI metabolism.

Overall, these results suggest that host PI(3)P is localized to the EHM and this localization may be a transient event mediated by rapid modification of the EHM by the plant host. In this regard, it will be interesting to test additional lipid biosensors for other PI or bioactive lipid species. Additionally, another future objective will be to determine if host PI(3)P-depletion compromises RPW8.2-EHM targeting efficiency and defense activation at the EHM.

### **RPW8.2 May Preferentially Bind PI(3)P**

Spatiotemporal dynamic distribution of PIs determines protein localizations at specific subcellular localizations (Kher and Worthylake, 2011; Munnik and Nielsen, 2011; Gil et al., 2012). Because PI(3)P is transiently enriched at the EHM, and the

putative RPW8 family EHM-targeting signals are enriched for positively charged amino acid residues (R/K) (Wang et al., under review) (**Figure 5-5**) that are reminiscent of the RXLR domain responsible for PI binding in pathogen effectors (Kale et al., 2010; Bhattacharjee et al., 2012), I speculated that RPW8 family proteins may bind to the negatively charged headgroup of PI(3)P and that this binding may be responsible for EHM localization. To determine potential binding interactions between RPW8 and bioactive lipid species, I purified bacterially expressed GST (glutathione S-transferase) - RPW8.2 fusion protein using the pGEX-4T-1 vector ([GE Healthcare-Life Sciences](#)) modified to contain a gateway cloning cassette (Brett Tyler, Oregon State University) and tested RPW8.2's binding to a variety of lipids using membrane lipid strips ([Echelon](#)). Membrane lipid strips are hydrophobic membranes that have been spotted with 100pmol of 15 different biologically important lipids (**Figure 5-6A**) found in cell membranes and are used to determine whether a protein of interest specifically interacts with any lipid using a protein-lipid overlay assay where bound proteins are detected by Western blotting (see Methods). My initial binding tests using commercialized strips showed that among all seven PIs, phosphatidylethanolamine (PE), phosphatidylcholine (PC), phosphatidylserine (PS) and phosphatidic acid (PA), RPW8.2 seemed to specifically, albeit weakly, bind PI(3)P (**Figure 5-6B**). In a similar protein-lipid overlay assay, no obvious interaction was detected between GST-RPW8.2 and a panel of 15 sphingolipids including sphingosine, ceramide or cholesterol (**data not shown**). As a control, GST alone showed no interaction with any of the spotted lipids (**Figure 5-6B**). I then conducted similar assays with GST-tagged RPW8.1 and HR3 and found that both of these proteins also showed weak but specific binding to PI(3)P, except GST-HR3 which





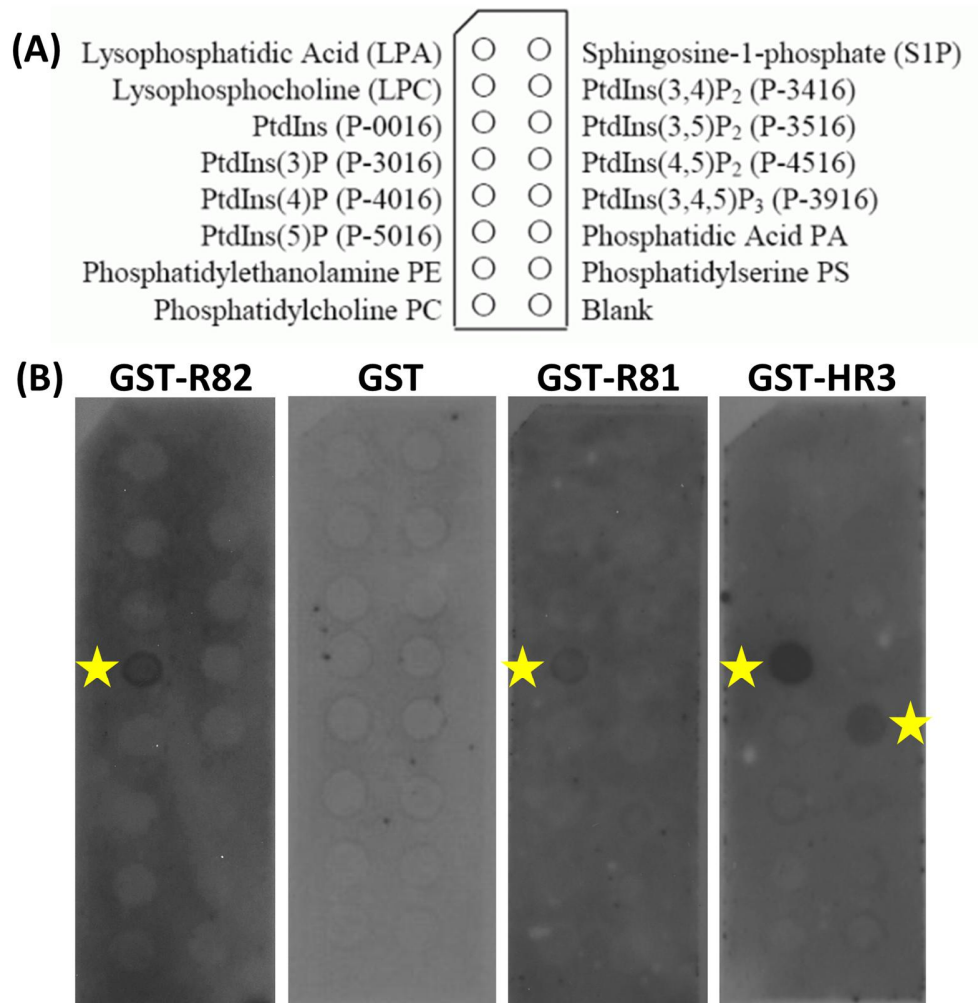


**Figure 5-6. RPW8 Family Members Bind PI(3)P in Lipid Filter Assays.**

**(A)** Commercially available lipid filter strips are hydrophobic membranes that have been spotted with 100pmol of 15 different biologically important lipids found in cell membranes and are used to determine how a protein of interest interacts with these lipids.

**(B)** GST-R82, GST only, GST-R81 and GST-HR3 proteins tested for the binding affinity to the 15 spotted lipids (including PIs) seen in **(A)**. For R82, R81 and HR3, a weak to moderate detectable binding signal is noticed for PI(3,4,5)P<sub>3</sub> (yellow stars). GST control protein does not bind any of the spotted lipids.



also showed weak binding affinity for PI(3,4,5)P<sub>3</sub> (**Figure 5-6B**). However, because PI(3,4,5)P<sub>3</sub> has not been detected in plants, this interaction is unlikely functionally relevant.

This preliminary result was particularly exciting because PI(3)P may be (transiently) enriched at the EHM during its biogenesis as described above (**Figure 5-2/3**) and some RXLR-containing effector proteins bind PI(3)P for host-cell entry (Kale et al, 2012). It is reasonable to hypothesize that one of the two EHM-targeting motifs, or one or more of the several predicted RXLR-like motifs in RPW8.2 (**Figure 5-7A**) may be the PI(3)P binding site(s) and PI(3)P-binding provides a critical cue for EHM-targeting. To validate RPW8.2-PI(3)P binding and then test the above hypothesis, I first made lipid filter strips by spotting commercially available PIs from either ([Echelon](#)) or ([Cayman Chemicals](#)) in a range of concentrations from 200pmol to 12.5pmol on Hybond-C Extra nitrocellulose membrane according to (Kale and Tyler, 2012) for more robust and focused binding assays. In the meantime, I also created 18 GST-RPW8.2 mutant constructs to determine critical residues responsible for the RPW8.2-PI(3)P interaction. These RPW8.2 proteins include existing mutants used for assessing EHM-targeting mutants (Wang et al., under preparation) and additional mutations in RXLR-like motifs (**Figure 5-7B**).

Results from several independent experiments with the homemade lipid filters showed that even though binding between RPW8.2 and PI(3)P was readily detectable, both the RPW8.2 wild-type and various mutant proteins showed binding not only to PI(3)P but also other PIs, such as PI(4)P, PI(5)P and PI(3,5)P<sub>2</sub>. In addition, there was significant variations from experiment to experiment in binding affinity and specificity,

making it extremely difficult to qualitatively gauge RPW8.2's binding to PI(3)P in comparison to other PIs and/or to assess whether any of the mutated motifs shown in **(Figure 5-7 A&B)** had any impact on RPW8.2's binding to PI(3)P **(Figure 5-7C)**.

In an effort to circumvent some of these specificity issues, we began experimentation with a liposome binding assay (see Methods) that provides an experimental system where the protein of interest interacts with the target phospholipid in the context of a membrane-like environment (Kale and Tyler, 2012). In short, binding affinity for a specific phospholipid is measured by incubating purified protein with unilamellar liposomes containing specific phospholipids against unilamellar control liposomes that lack the potential interacting phospholipid. As with the lipid-filter binding assays, results from the initial tests showed that majority of GST-RPW8.2 was detected in the pelleted fraction when incubated with liposomes containing PI(3)P, just as seen with GST-Avh5, a demonstrated PI(3)P binding protein (Kale et al., 2010) as control **(Figure 5-7D)**. However, upon repeated testing, I encountered specificity issues between different PI-containing liposomes and detected similar levels of GST-RPW8.2 WT and GST-RPW8.2 mutant (MT) proteins in the pelleted fraction indicating similar binding to PIs **(data not shown)**. To clarify this, we tested GST-RPW8.2's protein solubility in the liposome incubation buffer (50mM Tris, pH 6.8, 50-100mM KCl) and discovered that GST-RPW8.2 was largely insoluble as a significant proportion of the protein continually precipitated out of solution “mimicking” binding to the liposomes.

In summary, despite promising preliminary results suggesting that RPW8.2 may preferentially/specifically bind PI(3)P, and despite my quite extensive efforts, whether RPW8.2 specifically binds PI(3)P remains to be an unanswered question. Further

challenging work is required to tailor optimization and improvement of the experimental conditions for both lipid filter and liposome assays for RPW8.2, in order to derive unequivocal evidence for making a conclusion as to whether RPW8.2 binds PI(3)P for EHM-targeting.

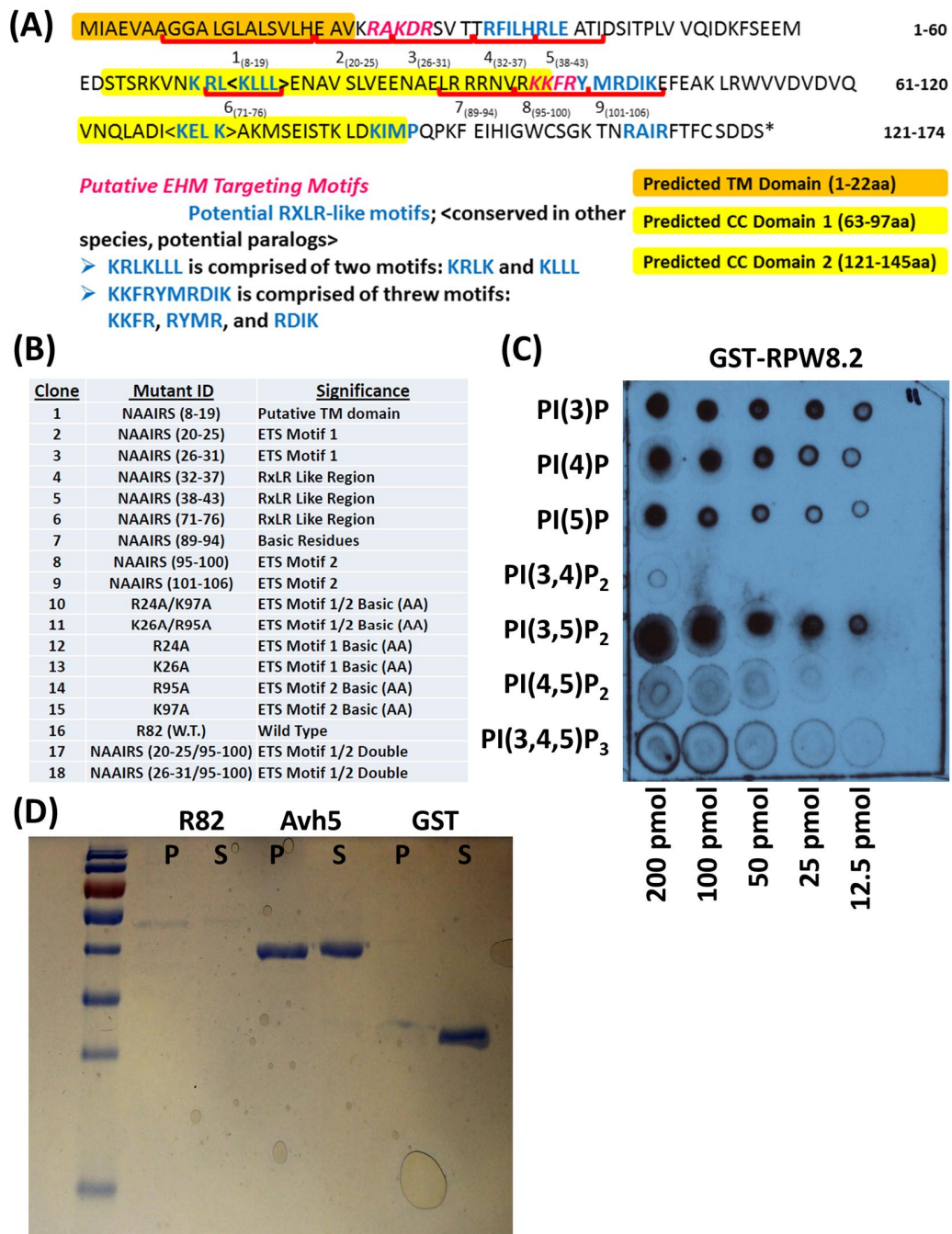


**Figure 5-7. Scanning Mutants of GST-RPW8.2 for Binding Assays.**

**(A)** Protein sequence of RPW8.2 indicating residues of the predicted TM, CC, and the putative EHM-targeting sequences (ETS) (pink font). Red brackets correspond to clones 1-9 and represent the location of 6aa replacements with the amino acid sequence N-A-A-

I-R-S that cover both ETS sites and potential RXLR-like motifs found in other species [blue font] (communication with Brett Tyler). Clones 10-15 represent single or double aa mutations in the positively charged residues in one or two ETS motifs. Clones 17-18 represent double NAAIRS mutation replacements for regions covering both ETS motifs. **(B)** List of clones and and significance. **(C)** Representative homemade lipid filter assay. Note the lack of specificity of GST-RPW8.2 to PI(3)P. **(D)** Liposome blot of GST-R82, GST-Avh5 and GST only control. P = pelleted liposomes (5% PI(3)P containing), S = supernatant.

## **Materials and Methods**

### **Plant materials and cultivation**

Arabidopsis accessions Col-0 or Col-gl were used for generation of all transgenic lines. All generated constructs in binary vectors were introduced into *Agrobacterium* strain GV3101 and stable transgenic Arabidopsis plants were generated by floral dip (Clough et al., 2000). All genetic analyses for genotyping and phenotyping were conducted in accordance with previous reports (Xiao et al., 2003b; Xiao et al., 2005). Unless otherwise indicated, seeds were sown in Sunshine Mix #1 or Metro-Mix 360 soil (Maryland Plant & Suppliers, Inc, USA) and cold-treated (4 °C for 1-2 days). Seedlings were kept under 22 °C, 75% RH, short-day (8 hrs light at  $\sim 125 \mu \text{mol} \cdot \text{m}^{-2} \cdot \text{sec}^{-1}$ , 16 hrs dark) conditions for 5-6 weeks before pathogen inoculation and/or other treatments.

### **Pathogens strains, inoculation and phenotyping**

Powdery mildew isolate *Golovinomyces cichoracearum* UCSC1 (*Gc*-UCSC1) was maintained on live Col-0 or Col-*NahG* plants for generation of fresh conidia for inoculation purposes. Inoculation, visual scoring, photographing and quantification of disease susceptibility were done as previously described (Xiao et al., 2005).

### **Cloning and Plasmid Construction**

The *35S::Sp-GmPHI-mCherry* construct were obtained from Brett Tyler's group (Oregon State University) as part of collaborations. *AtPHI-YFP* and *YFP-AtPHI* constructs were created using standard PCR amplification strategies coupled with restriction enzyme digestion and T4-mediated ligation. *AtPHI* ([At2g29700](#)) was

amplified from a genomic Col-0 DNA sample and used for multiple cloning steps using the standard primers (BamAtPH1-tpF:

5'caccgatccATGGAGAGTATCTGGCGAATCG<sup>3'</sup> and BamAtPH1-R1: 5'

gcggatccCCGCCTGTGATCATAATCGAGA<sup>3'</sup> or EcoAtPH1-R2: 5'

gcgaattcTCACCGCCTGTGATCATAATCGA<sup>3'</sup>). *AtPH1* (no stop) was translationally fused upstream of *YFP* in an *RPW8.2p* driven vector (P2Y3'-6) using traditional BamHI cloning and also shuttled to a 35S driven T/A cloning vector pCXS<sub>N</sub> (Chen et al., 2009b) using the primers (BamAtPH1-tpF: (see above) and BglYFP<sub>R1</sub>:

5'gcagatctCACTTGTACAGCTCGTCCATG<sup>3'</sup>). *YFP-AtPH1* was created by using gateway technology to shuttle an entry vector carrying *AtPH1* (*AtPH1/TOPO*) into the N-terminal YFP destination vector pEG104 (Earley et al., 2006) and then to move YFP-*AtPH1* to the T/A cloning vector pCXS<sub>N</sub> by amplification with the primers (BamYFP<sub>PF1</sub>: 5'TCGGATCCATGGTGAGCAAGGGCGAG<sup>3'</sup> and EcoAtPH1-R2 (see above).

The artificial miRNA (amiRNA) PI3K was constructed according to a published method (Schwab et al., 2006) incorporated into the web-based tool at (<http://wmd3.weigelworld.org/>) and targets the 11<sup>th</sup> out of 17 exon of *PI3K* ([NM\\_104735](#)). The primers for making the *PI3K*<sub>Kami</sub> fragment are: (PI3K aRNA-I:

5'gaTATATTCTGTAATGCCCGCTGtctctctttgtattcc<sup>3'</sup>, PI3K aRNA-II:

5'gaCAGCGGGCATTACAGAATATAtcaaagagaatcaatga<sup>3'</sup>, PI3K aRNA-III:

5'gaCAACGGGCATTACTGAATATTtcacaggtcgatgatg<sup>3'</sup> and PI3K aRNA-IV:

5'gaAATATTCAGTAATGCCCGTTGtctacatatattctt<sup>3'</sup>). The amiRNA fragment was digested with *KpnI/BamHI* and cloned into the binary vector pBTEX *KpnI/BamHI* site downstream of the 35S promoter (Frederick et al., 1998). Following assembly via

overlapping PCR, the amiRNA fragment was also cloned into the pCXSN T/A cloning vector using the primers (amiRNA-F: 5'caccAAACACACGCTCGGACGCAT<sup>3'</sup> and amiRNA-R: 5'CCCCATGGCGATGCCTTA<sup>3'</sup>).

*GST-RPW8.2* WT and MT plasmids were created by gateway technology by cloning the full length cDNA of RPW8.2 WT or MT derivatives into the pENTR/D-TOPO entry vector using the standard primers (R82tpF: 5'caccATGATTGCTGAGGTTGCCGCA<sup>3'</sup> and BamR82R2: 5'TTGGATCCTCAAGAATCATCACTGCAGAAC<sup>3'</sup>). Specific mutant clones were generated by either (i) RNA extraction and cDNA synthesis of mutant RPW8.2-YFP T2 plants used in a mutagenesis analysis by (Wang et al., under review) or (ii) by site-directed overlapping PCR procedures. Entry clones were translationally fused downstream of GST using a modified pGEX-4T-1 vector ([GE Healthcare-Life Sciences](#)) containing a gateway cloning cassette (gift from Brett Tyler's group). All other GST clones including RPW8.1 and HR3 were created in a similar manner. All materials not listed are available upon request.

### **Pharmacological Treatments**

Fully expanded leaves of ~7 week-old *RPW8.2-YFP* Col-gl background plants were detached from the base of the petioles and inserted into sterilized Murashige and Skoog (MS) agar medium in Petri dishes. Detached leaves were inoculated evenly with *Gc*-UCSC1 and at ~16hpi each half leaf was pressure-infiltrated with a blunt end 1 mL plastic syringe containing either 1-50µM Wortmannin dissolved in DMSO or 10-100µM LY294002 dissolved in DMSO and their respective controls (DMSO/water solution).



Leaf sections ( $\sim .25 \text{ cm}^2$ ) were examined using a Zeiss LSM710 confocal microscope at 36-42hpi following staining with 0.5% propidium iodide (PI). Detectable RPW8.2-YFP signal at the EHM was used to determine if either PI3K inhibitor had significant effect on RPW8.2 localization to the EHM.

### **Protein Purification**

Sequence confirmed GST-RPW8.2 WT or MT clones were transfected into either Rosetta Blue (DE3) competent cells ([Rosetta Blue](#)) or BL2.1 Codon Plus competent cells ([BL21 Codon Plus](#)) via heat shock transformation. Single PCR confirmed positive clones were inoculated into a 3-5 mL of O/N Luria Broth (LB) and then into a 100 mL O/N LB culture. 50 mL of 100 mL O/N culture was inoculated into 500 mL without antibiotics and grown to an  $\text{OD}_{600}$  between .4 and .6 and then induced with Isopropyl  $\beta$ -D-1-thiogalactopyranoside (IPTG) at a final concentration between .3 and 1mM. (Note: Standard induction conditions range from 3-5hrs at 37°C, however bacterial cells containing RPW8.2 often experienced accelerated death rates presumably to expression of the RPW8.2 protein. Therefore, cells expressing RPW8.2 were grown at lower temperatures ranging from 16-20°C for longer periods of time with lower IPTG concentrations [ $\sim .3\text{mM}$ ]). Following induction, cells were spun at 7000 rpm for 15 min at 4°C and resuspended in 10-15 mL Cold buffer (50 mM Tris-HCl pH7.5, 150 mM NaCl) with a final .1% protease inhibitor cocktail concentration. Cells were lysed with 2 cycles of sonication and rocked at 4°C in a 1% Triton X-100 solution for 45-60 min. GST- proteins were purified using B-PER GST fusion protein column or spin purification

kits and their respective available protocols at room temperature with minor modifications ([GST Purification Kits](#)).

Protein concentrations were measured using the bicinchoninic acid (BCA) protein assay reagent kit and available protocol from Thermo Scientific ([BCA Assay Kit](#)) and a 562nm plate reader after dialysis into a 1X phosphate buffered saline (PBS) solution as excessive Tris or glutathione remaining in protein elution fractions can drastically alter plate readings.

### **Lipid Filter – Binding Assays**

Lipid filter binding assays were conducted according to protocols provided by Echelon ([Lipid Filter Binding Assay](#)) or by instructions provided by the Brett Tyler laboratory or their published protocol found in (Kale and Tyler, 2012). In short, commercially available or homemade lipid strips are blocked in a PBS-T + 3% bovine serum albumin (BSA) solution for 1 hr at room temperature or O/N at 4°C in a petri dish on a bench top rocker. After blocking, 10-20 mL of fresh PBS-T was added to the filters with ~.5-1.0µg/ml of the protein of interest. Proteins are incubated for 1 hr at room temperature or O/N at 4°C with continual rocking. Following incubation, lipid membranes are washed 3X with PBS-T and following both primary and secondary antibody incubations. Lipid filters were incubated with a 1:7,000 dilution of the primary goat monoclonal anti-GST followed by a 1:20,000 dilution of the rabbit-anti-goat HRP conjugated secondary antibody (Sigma). Immunodetected proteins were visualized using the ECL Advance Western Blotting Detection Kit ([Amersham](#)).

Homemade phosphoinositide lipid filters were created by spotting PIs dissolved in either a chloroform:methanol:water (65:30:8) or chloroform:methanol (65:35) from either ([Echelon](#)) or ([Cayman Chemicals](#)) in a range of concentrations from 200pmol to 12.5pmol on Hybond-C Extra nitrocellulose membrane ([GE Healthcare-Life Sciences](#)). Lipid filters were dried in the dark at room temperature for 1 hour before blocking.

### **Liposome - Binding Assay**

Liposomes were prepared from a suspension of PC, PE, and where appropriate a PI-x-P (5-10%), in chloroform/methanol/water (65:30:8). Lipid mixtures were dried then rehydrated by three cycles of freeze/thawing. Large unilamellar vesicles were formed by extruding the lipid suspension through a 0.1  $\mu$ m filter. After a pre-centrifugation spin of 100,000g for 15 min at 4°C, protein (~1  $\mu$ g/ml) was added to liposomes and incubated for 1 hr at room temperature. Protein-liposome mixtures were centrifuged at 100,000g for 15 min at room temperature and supernatant and pellets were separated before SDS-PAGE analysis. Pellets containing liposome-bound proteins and supernatants containing free proteins were then analyzed by SDS-PAGE. See (Kale and Tyler, 2012) for additional details and troubleshooting tips for liposome binding assays.

### **Other Analyses**

Imaging and laser scanning confocal microscopic (LSCM) imaging was done using either a Zeiss Axio epifluorescence microscope coupled with an HBO 100 microscope illumination system or with a Zeiss LSM710 confocal microscope as previously described in (Wang et al., 2007; Wang et al., 2009; Wang et al., 2010). All

images presented are single optical sections or Z-stack projected of 15-30 images unless otherwise indicated. For PI staining, detached leaf sections ( $\sim 0.25 \text{ cm}^2$ ) were submerged in 0.5% PI solution for 45-60 minutes then washed briefly (10-15 minutes) in water before imaging. Image data was processed using Zen 2009 Light Edition and Adobe Photoshop CS5.

## **Chapter 6: Initiatives in Other Projects**

### **I. PLD $\delta$ is Dispensable for RPW8-mediated Resistance But is Essential for Basal Resistance**

#### **Introduction**

The activation of plant immunity results in a variety of early signaling events including the rapid accumulation of ROS, changes in cellular ion fluxes, activation of protein kinases cascades, cell wall reinforcement, activation of HR, and the induction of defense gene expression (see **Chapter 1**). Likewise, recent reports are beginning to elucidate the importance of lipids and lipid-related molecules including glycerolipids, sphingolipids, fatty acids, oxylipins, jasmonates and sterols in the activation and regulation of plant immunity (reviewed in Shah, 2005; Canonne et al., 2011; Munnik and Nielsen, 2011; Berkey et al., 2012; Chehab and Braam, 2012; Wang et al., 2012a). Specifically, phospholipase enzymes that hydrolyze phospholipids into fatty acids and other lipophilic substances and phospholipid-derived second messengers, such as phosphatidic acid (PA), diacylglycerol (DAG) and inositol 1,4,5-trisphosphate (IP<sub>3</sub>) have also been implicated in a variety of plant signaling events including plant immunity (Laxalt and Munnik, 2002; Munnik and Testerink, 2009).

Phospholipases are a complex group of enzymes that hydrolyze phospholipids in eukaryotic cells. The plant phospholipase family is comprised of multiple members that can be classified according to the positional specificity of their substrate phospholipids (**Figure 6-1**) while sub-group members or isoforms are further distinguishable by their structural, biochemical and physiological characteristics (Wang, 2001; Canonne et al.,

2011). In terms of positional specificity of substrate phospholipids, there are five major classes of plant phospholipases: D (PLD), C (PLC), A<sub>2</sub> (PLA<sub>2</sub>), A<sub>1</sub> (PLA<sub>1</sub>) and B (PLB) (Wang, 2001) (**Figure 6-1**).

Each major class of plant phospholipases has been associated with a variety of subcellular signaling events in response to abiotic and biotic stresses (Wang, 2001; Chen et al., 2011; Wang et al., 2012a). In regards to pathogen stresses, PLAs (A<sub>1</sub> and A<sub>2</sub>) have largely been associated with plant immunity through their involvement in JA and oxylipin biosynthesis through the conversion of phospholipids into lysophospholipids and free fatty acids as precursors for the octadecanoid pathway (Ryu, 2004; Wang, 2004). Interestingly, a non-enzymatic function was recently identified for one secreted PLA<sub>2</sub> enzyme, *AtsPLA2-α* (Froidure et al., 2010). In response to *Pseudomonas syringae* infection, *AtsPLA2-α* is partially localized to the nucleus upon interaction with *AtMYB30* and subsequently leads to the repression of *AtMYB30*-mediated regulation of HR (Froidure et al., 2010). For PLD enzymes, specific isoforms were found to be upregulated in rice in response to *Xanthomonas oryzae* (Young et al., 1996) and in *Arabidopsis* in response to virulent and avirulent strains of *P. syringae* (de Torres Zabela et al., 2002) and ultimately led to an accumulation of PA via the PLD and PLC/DGK (DIACYLGLYCEROL KINASE) pathways (Andersson et al., 2006). Additionally, Krinke and colleagues have shown that phospholipase D activation is an early component of the SA-signaling pathway in *Arabidopsis* cell suspensions (Krinke et al., 2009) and resulting PA has been shown to induce ROS production and the activation of defense-related (Yamaguchi et al., 2005) or ethylene-responsive genes (Testerink et al., 2008). Another recent study by Raho and colleagues shows that nitric oxide (NO) upregulates

the induction of PA production in response to the xylanase PAMP in tomato cells and that PA is required for defense activation (Raho et al., 2011). Likewise, plasma membrane localized PLC enzymes are also involved in plant immunity and have been found to be activated by PAMP recognition that results in an increase in cytosolic IP<sub>3</sub>. Cytosolic IP<sub>3</sub> triggers a release of Ca<sup>2+</sup> from intracellular stores and the formation of PA through DGK (Legendre et al., 1993; van der Luit et al., 2000). More recently, a study by Vossen and colleagues identified specific PLC family members in tomato that are required for Cf-4 HR activation and induce PA accumulation in response to *Cladosporium fulvum* (Vossen et al., 2010; Abd-El-Haliem et al., 2012).

Although evidence is accumulating to suggest a regulatory role for plant phospholipase genes and phospholipase-derived products in plant immune signaling and defense, how phospholipases and/or their products exert regulation on plant immunity remain largely uncharacterized. In addition, there have been no reports concerning the involvement of phospholipase enzymes in resistance against powdery mildew. As my preliminary studies on a possible RPW8.2-phospholipid interaction suggest a potential role of PI(3)P in regulation of RPW8.2's specific targeting to the EHM, I was further prompted to explore if other phospholipids (or their derivatives) play a role in RPW8-mediated resistance via genetic analysis of Arabidopsis mutants defective in several phospholipase genes.

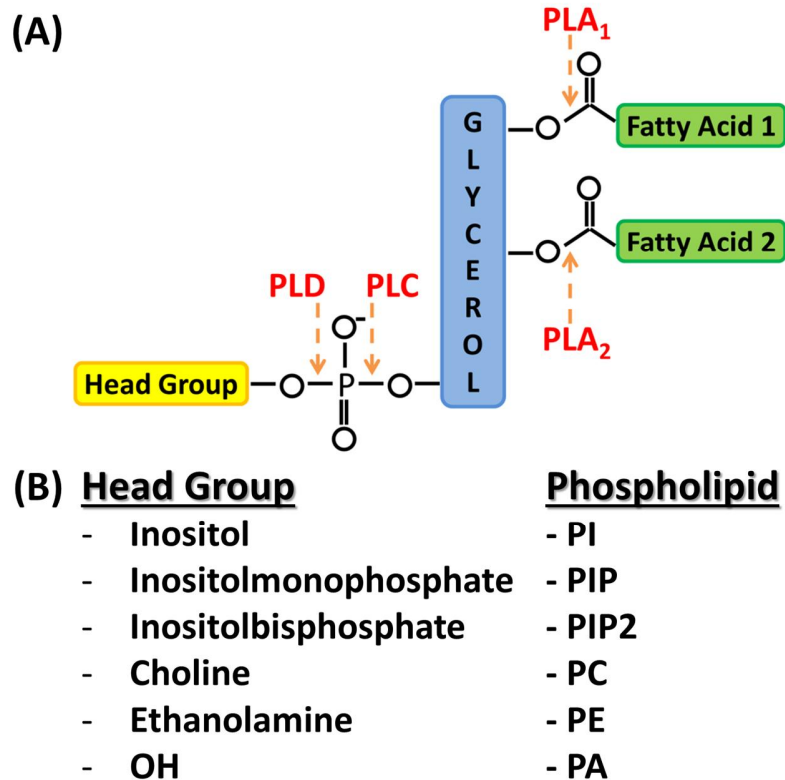


**Figure 6-1. Phospholipids are Cleaved by Diverse Phospholipases.**

**(A)** Schematic representation of a phospholipid molecule with two fatty acyl chains linked to a glycerol backbone and a phosphate group creating the phosphatidyl moiety to which variable head groups are attached. Arrows indicate the cleavage sites of indicated phospholipase enzyme groups. Phospholipase B (not depicted) sequentially removes two fatty acids from phospholipids (PLA<sub>1</sub> and PLA<sub>2</sub> activity combined). **(B)** Several head group varieties and the resulting phospholipids that are subject to phospholipase cleavage are listed. PLA- phospholipase A<sub>(1 or 2)</sub>; PLB- phospholipase B; PLC- phospholipase C; PLD- phospholipase D; PI- phosphatidylinositol; PIP- phosphatidylinositol monophosphate; PIP2- phosphatidylinositol bisphosphate; PC- phosphatidylcholine; PE- phosphatidylethanolamine; PA- phosphatidic acid.



## Results

To determine if any phospholipase genes are involved in powdery mildew resistance in Arabidopsis, I examined the disease reaction phenotypes of 12 T-DNA insertion mutant lines from Dr. Xuemin Wang (University of St. Louis, St. Louis, MO). These T-DNA lines were: *PLD $\alpha$ 1* (At3g15730), *PLD $\beta$ 1* (At2g42010), *PLD $\delta$*  (At4g35790), *PLD $\alpha$ 1 $\delta$*  (double mutant), *pPLAII $\beta$*  (At4g37050), *pPLAII $\delta$*  (At4g37060), *pPLAIII $\delta$*  (At3g63200), *pPLAIII $\alpha$*  (At2g39220), *pPLAII $\alpha$*  (At2g26560), *pPLAIII $\gamma$*  (At4g29800), *pPLAI* (At1g61850) and *pPLAIII $\beta$*  (At3g54950) (see **Table 2**). While the T-DNA insertion lines for the eight phospholipase A isoforms appeared comparable in susceptibility to Col-0 wild-type plants in response to *Gc*-UCSC1 (**data not shown**), two T-DNA mutant lines for PLD isoforms displayed a difference in susceptibility to *Gc*-UCSC1 when compared to Col-0 (**Figure 6-2**). Specifically, I noticed that *pld $\alpha$ 1* *-/-* plants displayed an *edr* phenotype while *pld $\delta$*  *-/-* plants displayed an *eds* phenotype quantitatively similar to the super susceptible Col-*NahG* plants (**Figure 6-2**). Moreover, double mutant *pld $\alpha$ 1* *-/-*; *pld $\delta$*  *-/-* plants were similar to *pld $\alpha$ 1* *-/-* in disease resistance suggesting that *PLD $\alpha$ 1* is functionally epistatic to *PLD $\delta$*  (**Figure 6-2**). Interestingly, *pld $\alpha$ 1* *-/-* lines were also slightly stunted in overall stature with low to moderate levels of detectable SHL compared to other T-DNA lines and Col-0 (**data not shown**).

To confirm the *eds* phenotype of *pld $\delta$*  *-/-* plants, I obtained multiple T2 *PLD $\delta$ p::PLD $\delta$*  complementation lines from Dr. Xuemin Wang's group and purified the *pld $\delta$*  *-/-* background one time by back crossing into Col-0 plants. Once challenged with *Gc*-UCSC1, purified *pld $\delta$*  *-/-* lines remained more susceptible to powdery mildew than

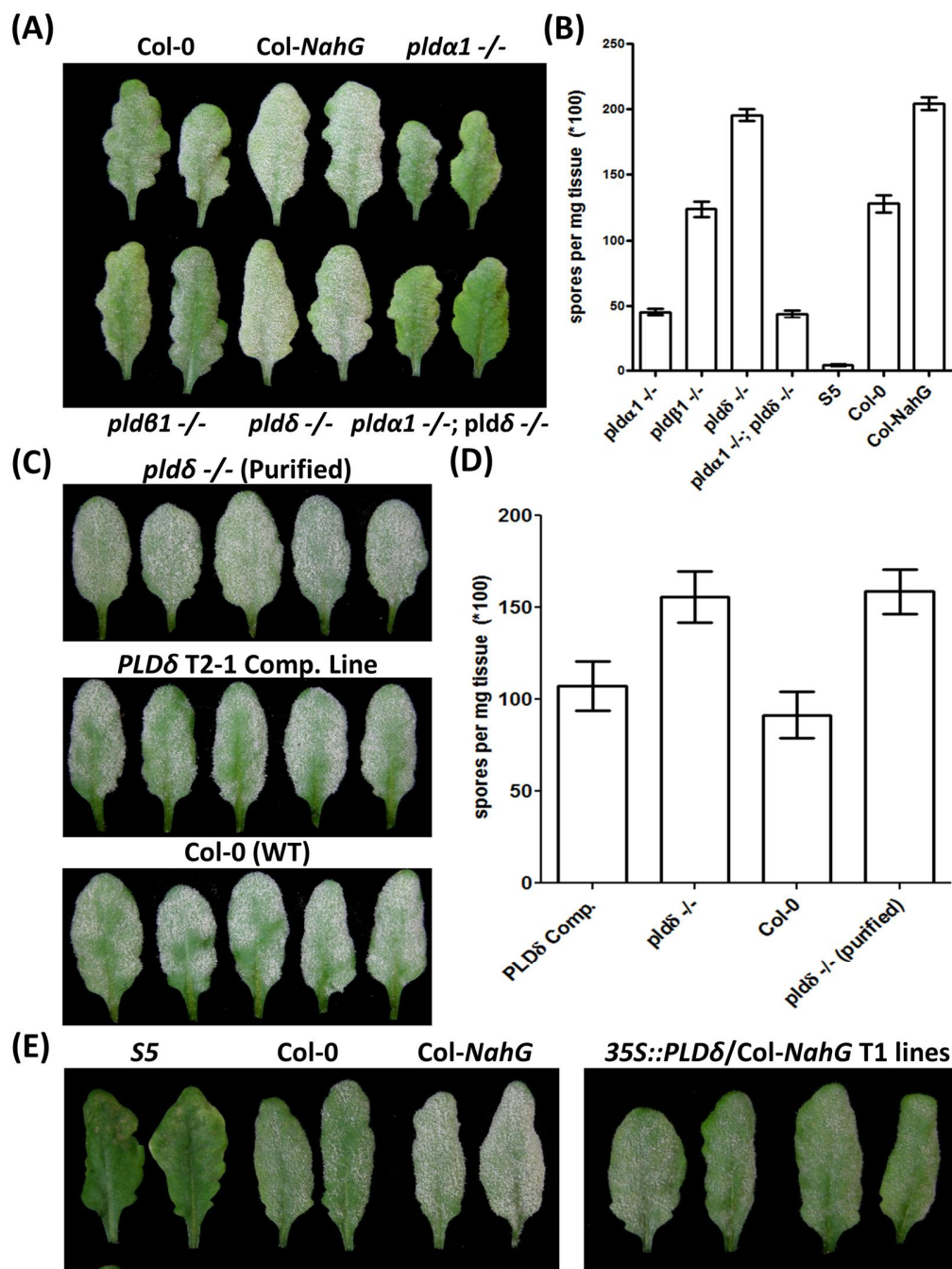


**Figure 6-2. *PLDδ* is Involved in Basal Immunity Against Powdery Mildew.**

**(A)** Phenotypic screen of PLD T-DNA insertion mutant lines in response to powdery mildew. *plda1* <sup>-/-</sup> lines display an enhanced disease resistance to powdery mildew while *pldδ* <sup>-/-</sup> lines display an enhanced susceptibility to *Gc*-UCSC1 at 12dpi. **(B)** Disease

quantification of plants in **(A)** plus *S5* as a resistant control. *pldδ*  $-/-$  lines are quantitatively similar to the highly susceptible Col-*NahG* plants. **(C)** Infection phenotype of representative leaves from *pldδ*  $-/-$  purified lines, a *PLDδ* T2 complementation line and Col-0 plants at 12dpi. **(D)** Disease quantification of plants in **(C)** plus the original *pldδ*  $-/-$  line. **(E)** Representative leaves from control plants (*S5*, Col-0 and Col-*NahG*) and independent T1 lines of *PLDδ* overexpression in Col-*NahG* background.

Col-0 while multiple *PLDδ* complementation lines restored basal resistance to powdery mildew that were quantitatively similar to Col-0 wild-type plants (**Figure 6-2**). Because *PLDδ* appeared to play a positive role in basal resistance against powdery mildew, I also overexpressed *PLDδ* in the SA-deficient Col-*NahG* background. My preliminary results suggest that ectopic expression of *PLDδ* enhances resistance to powdery mildew in Col-*NahG* (**Figure 6-2**). Altogether, these results suggest that *PLDδ* plays a positive role in basal immunity against powdery mildew in Arabidopsis and that *PLDα1* may negatively regulate defense responses against powdery mildew.

To determine if *PLDδ* (or other *PLA/PLD* isoforms) are required for *RPW8*-mediated resistance, I crossed all 12 T-DNA insertion mutant lines into the *S5* background (Col-g1 transgenic for *RPW8*) and selected for homozygous lines. Interestingly, all homozygous F3 progenies of *pldδ* *-/-*/*S5* (and other phospholipase isoforms) were resistant to *Gc*-UCSC1 as *S5* control plants suggesting that *PLDδ* is not required for *RPW8*-mediated defense (**Figure 6-3**). I also transformed all *PLA/PLD* T-DNA insertion mutant lines with *RPW8.2p::RPW8.2-RFP* to examine if *RPW8.2*'s localization to the EHM is compromised in these T-DNA insertion mutant backgrounds. Not surprisingly, *RPW8.2-RFP* was precisely localized to the EHM (**Figure 6-3**) with similar targeting efficiency compared to *RPW8.2-RFP* in control plants (**data not shown**).

In an effort to understand where *PLDδ*'s may function to enhance basal resistance to powdery mildew, I analyzed the subcellular localization of *PLDδ* in epidermal cells invaded by haustoria using *35S::YFP-PLDδ* transgenic lines obtained from Dr. Xuemin Wang. Before powdery mildew inoculation, YFP-*PLDδ* appeared to be ubiquitously

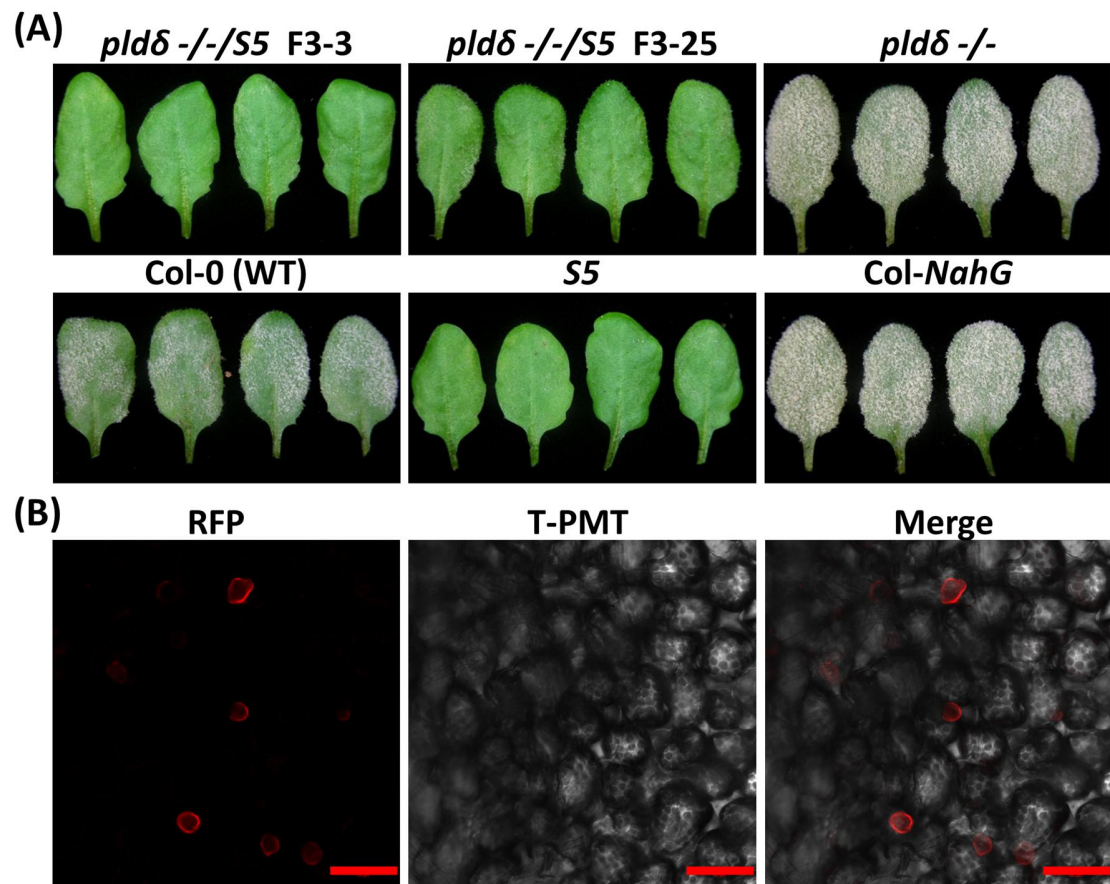


**Figure 6-3. *PLDδ* is Not Required for *RPW8*-mediated Resistance.**

**(A)** Representative leaves of two homozygous *pldδ* <sup>-/-</sup>/S5 F3 lines and control plants (*pldδ* <sup>-/-</sup>, Col-0, S5 and Col-NahG) infected with *Gc*-UCSC1 at 12dpi. **(B)** A single optical section of RPW8.2-RFP EHM-localization in *pldδ* <sup>-/-</sup> background confirming that RPW8.2 trafficking is unaffected in *pldδ* <sup>-/-</sup> background at 48hpi. Bars = 50μm.

expressed at the plasma membrane which is consistent with its reported subcellular localization (Wang and Wang, 2001) (**Figure 6-4**). However, after powdery mildew infection there was no apparent change in the PM localization of YFP-PLD $\delta$  and PI staining of differentiated haustoria reveals that PLD $\delta$  is not an EHM localized membrane protein (**Figure 6-4**). Interestingly, several lines ectopically expressing *YFP-PLD $\delta$*  did however result in an eds phenotype in response to *Gc*-UCSC1 when compared to *35S::YFP* lines (**Figure 6-4**), suggesting a dominant negative effect of YFP-PLD $\delta$  on the endogenous PLD $\delta$ . This result provides additional support to the above conclusion that *PLD $\delta$*  plays a role in basal resistance against powdery mildew.

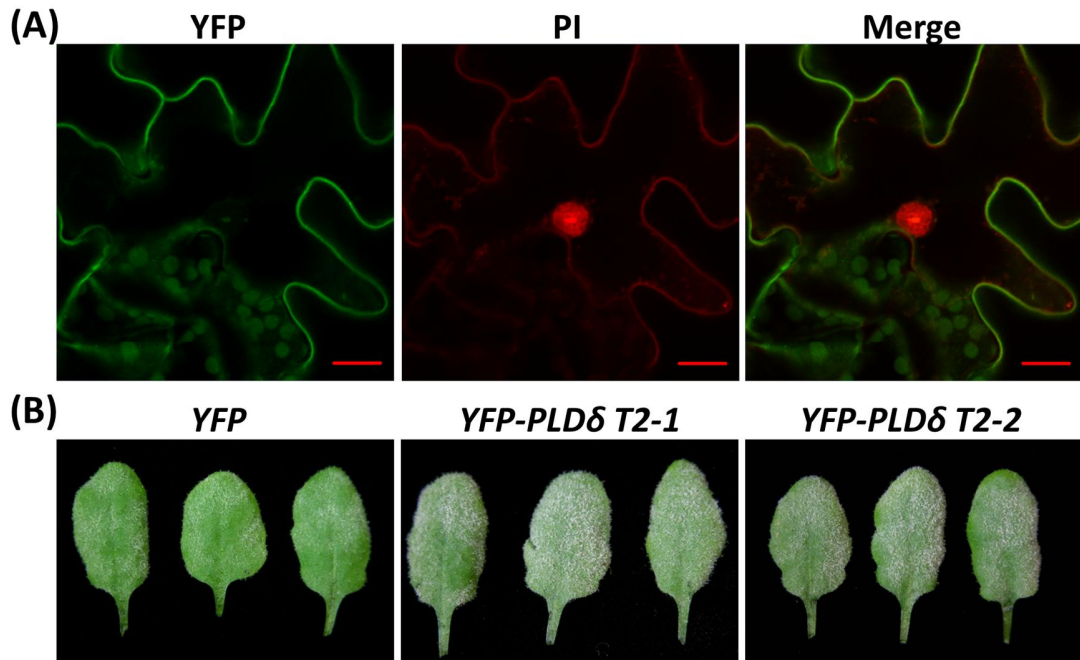


**Figure 6-4. PLD $\delta$  is Not an EHM Resident Protein.**

(A) Representative single optical section of ectopic expression of YFP-PLD $\delta$  in a haustoria invaded epidermal cell at 42hpi. YFP-PLD $\delta$  is only found in the host PM and not the EHM of differentiated haustoria. Bars = 20 $\mu$ m. (B) 35S::YFP-PLD $\delta$  transgenic lines display enhanced susceptibility to powdery mildew. Representative leaves from T2 lines expressing 35S::YFP and 35S::YFP-PLD $\delta$  infected with *Gc*-UCSC1 at 8dpi.

## Discussion

Disease tests of a panel of PLD T-DNA insertion mutants with powdery mildew identified PLD isoforms, *PLD $\alpha$ 1* and *PLD $\delta$*  to be a negative and a positive regulator of basal resistance, respectively. Because the biochemical functions of PLD $\alpha$ 1 and PLD $\delta$  are supposed to be similar (i.e. production of PA from phospholipid substrates), it appears intriguing that these two genes have opposing roles in regulation of basal resistance. One possible explanation is that PLD $\alpha$ 1 and PLD $\delta$  may be localized to different subcellular compartments (Fan et al., 1999) and consequently producing distinct subcellular PA pools that may interact with different target proteins (Hong et al., 2008); thereby inducing differential signaling leading to distinct defense responses. A second possibility is that PLD $\alpha$ 1 and PLD $\delta$  may have different biochemical properties and substrate specificities (Wang, 2001; Wang et al., 2012a) and therefore produce opposing effects on the plant basal resistance pathway. To test the first possibility, we have recently obtained PA biosensor constructs from Dr. Xuemin Wang and are investigating their localization pattern in haustorium-invaded cells. My initial results suggest that these biosensors are ubiquitously expressed with very weak signal or without any signal at the EHM in most cases, suggesting that PA is not a major component at the EHM (**data not shown**). It is worth noting that in a recent report, Uraji and colleagues suggest that while both PLD $\alpha$ 1 and PLD $\delta$  function in ABA (abscisic acid) -induced stomatal closure, their functions are not completely overlapping and that these isoforms respond differently to ABA treatment (Uraji et al., 2012).

Considering that RPW8 activates resistance to powdery mildew by enhancing basal resistance, it is interesting that *PLD $\delta$*  (and other PLA/PLD isoforms) are



dispensable for RPW8-mediated disease resistance or specific targeting to the EHM. Based on these observations, I speculate that (i) either defense activation by RPW8 is PA-independent, unlike the recently identified requirement of PLC enzymes and subsequent PA production for HR activation by Cf-4 in tomato (Vossen et al., 2010; Abd-El-Haliem et al., 2012) or ii) basal PA levels are sufficient for signaling in cells containing RPW8. Taken together, my preliminary results suggest a positive role for PLD $\delta$  and a negative role for PLD $\alpha$ 1 in plant basal immunity, and future genetic work is needed to position *PLD $\alpha$*  and *PLD $\delta$*  in specific signaling pathways of plant disease resistance.

## Materials & Methods

### Plant Lines, Cloning and Plasmid Construction

All T-DNA insertion mutant lines for the listed PLA and PLD isoforms, *PLD* $\delta$  complementation, and *35S::YFP-PLD* $\delta$  lines were obtained from Dr. Xuemin Wang (University of St. Louis, St. Louis, MO). Likewise, agrobacterium cells containing PA biosensor constructs (YFP or CFP) were also obtained from Dr. Xuemin Wang and used to transform Col-gl or RPW8.2-RFP (or YFP) background plants. Col-0 and *S5* (Col-gl transgenic for *RPW8*) plants were used for crossing and purification of the *pld* $\delta$   $-/-$  background. The previously described *RPW8.2::RPW8.2-RFP/pCX-DG* construct was used for agrobacterium-mediated transformation of PLA and PLD T-DNA insertion mutant lines.

The *PLD* $\delta$  overexpression construct (*35S::PLD* $\delta$ ) was created by cloning the full length genomic sequence of *PLD* $\delta$  into the T/A cloning vector pCXSN (Chen et al., 2009b) from a Col-0 gDNA extraction sample. The primers used for amplification of *PLD* $\delta$  were (Bam*PLD* $\delta$ -F: 5' caccggatccATGGCGGAGAAAGTATCGGA<sup>3'</sup> and Eco*PLD* $\delta$ -R: 5' gcgaattcTTACGTGGTTAAAGTGTCAGGAAGA<sup>3'</sup>).

### Other Analysis

All growth conditions, materials and methods not listed have been previously used and described in (**Chapters 2-5**).

### Accession Numbers

Sequence data can be found in the Arabidopsis Genome Initiative or GenBank/EMBL databases under the following gene IDs, accession numbers and SALK IDs:

<b>PLA/PLD Isoform</b>	<b>Gene ID</b>	<b>Accession</b>	<b>SALK Line</b>
<i>PLD<math>\alpha</math>1</i>	At3g15730	<a href="#">NM_112443.2</a>	SALK_053785
<i>PLD<math>\beta</math>1</i>	At2g42010	<a href="#">NM_129765.3</a>	SALK_079133
<i>PLD<math>\delta</math></i>	At4g35790	<a href="#">NM_179171.2</a>	SALK_023247
<i>PLD<math>\alpha</math>1<math>\delta</math></i> (double mutant)	At3g15730/ At4g35790	see above	see above
<i>pPLAII<math>\beta</math></i>	At4g37050	<a href="#">AY099596.1</a>	SALK_142351
<i>pPLAII<math>\delta</math></i>	At4g37060	<a href="#">NM_001204013.1</a>	SALK_090933
<i>pPLAIII<math>\delta</math></i>	At3g63200	<a href="#">NM_116185.1</a>	SALK_029470
<i>pPLAIII<math>\alpha</math></i>	At2g39220	<a href="#">AY062648.1</a>	SALK_040363
<i>pPLAII<math>\alpha</math></i>	At2g26560	<a href="#">NM_128213.3</a>	SALK_059119
<i>pPLAIII<math>\gamma</math></i>	At4g29800	<a href="#">NM_001203937.1</a>	SALK_088404
<i>pPLAI</i>	At1g61850	<a href="#">NM_104867.4</a>	SALK_087152
<i>pPLAIII<math>\beta</math></i>	At3g54950	<a href="#">AY080807.1</a>	SALK_057212

**Table 2. PLA and PLD Isoforms.**

## **II. ATJ3, a Putative RPW8.2-interacting Protein, is Required For RPW8-mediated and Basal Resistance.**

### **Introduction**

In our preliminary studies, we have identified several putative RPW8.2-interactors by yeast-2-hybrid screen using either full-length RPW8.2 or a TM-truncated version, RPW8.2<sub>(NtΔ1-22)</sub>, as bait. One of putative interacting proteins was *ATJ3* (At3g44110: [NM\\_114279.3](#)), a heat shock protein (Hsp40-like) (Zhou and Miernyk, 1999; Li et al., 2005) that contains a highly conserved DnaJ domain found in bacterial, mammalian and plant proteins (Qiu et al., 2006). As one of my initiative projects, I have begun characterizing the role of *ATJ3*, and its closely related homolog, *ATJ2* (At5g22060: [NM\\_122127.2](#)), in plant defense.

DnaJ domain-containing proteins play crucial roles in protein translation, folding, unfolding, translocation and degradation. They primarily work by interacting with and stimulating the ATPase activity of Hsp70s (heat shock proteins) (Fan et al., 2003; Hennessy et al., 2005). While there are no available reports indicating that *ATJ3* (or *ATJ2*) play a role in plant immunity, there is substantial evidence in the field suggesting that Hsp70 and other heat shock proteins (Hsp90 and SGT1 [suppressor of G-two allele of SKP1]) are involved in plant (Hubert et al., 2003; Noel et al., 2007; Meldau et al., 2011) and animal innate immunity (Mayor et al., 2007; Chen and Cao, 2010; van Noort et al., 2012). Moreover, recent reports suggest that plant pathogens target heat shock proteins for virulence or pathogenesis. For example, one recent study suggests that SGT1 contributes to coronatine signaling and *Pseudomonas syringae* disease symptom development in tomato and Arabidopsis (Uppalapati et al., 2011). Likewise, a

*Pseudomonas syringae* effector protein, HopI1, contains a DnaJ domain that is responsible for specific binding to and recruitment of Hsp70 to chloroplasts (Jelenska et al., 2010). This binding not only stimulates Hsp70 ATP hydrolysis activity *in vivo*, but is also responsible for the suppression of SA accumulation and other defense related responses (Jelenska et al., 2007; Jelenska et al., 2010). Another study by Ye and colleagues reveals that the SGT1-Hsp70 complex is up-regulated by *Potato virus X* and contributes to viral accumulation in *N. benthamiana* (Ye et al., 2012).

Collectively, it seems probable that co-chaperone DnaJ proteins like ATJ3 as working partners of other heat shock proteins (Hsp70, Hsp90 and SGT1), may also be involved in regulation plant immunity and/or as potential targets of pathogen effector proteins. To test this speculation, I obtained T-DNA insertion mutant lines for *ATJ3* and its closely related homolog, *ATJ2* (90.3% identity at the protein level), and examined if they play a role in basal and/or *RPW8*-mediated resistance against powdery mildew.

## Results

To determine if either *ATJ3* or *ATJ2* are involved in powdery mildew resistance in *Arabidopsis*, we conducted a screen of T-DNA insertion mutant lines for their disease reactions in comparison with wild-type plants. The T-DNA insertion mutant lines are as follows: *atj3-1* (SALK\_141625), *atj3-2* (SALK\_132923), *atj2-1* (SALK\_012035) and *atj2-2* (SALK\_071563) (**Figure 6-5A**). My preliminary results suggest that both of these genes are involved in basal resistance as representative T-DNA lines for *atj3* *-/-* and *atj2* *-/-* display an enhanced disease susceptibility phenotype in comparison with Col-0 (**Figure 6-5C&D**). Specifically, I found that *atj3-1*, *atj3-2* and *atj2-2* lines appeared more susceptible than wild-type plants and were quantitatively more similar to highly susceptible Col-*NahG* plants (**Figure 6-5C&D**) while *atj2-1* plants were similar to Col-0 (**data not shown**). Subsequent RT-PCR analysis showed that while *atj2-2* lines are knocked out for *ATJ2*, *atj2-1* lines have similar *ATJ2* expression as Col-0 (**Figure 6-5B**) correlating with the respective powdery mildew susceptibility phenotypes. As reported in a recent study, the *ATJ3* transcript was truncated and knockdown in both *atj3-1* and *atj3-2* (Shen et al., 2011).

Interestingly, I also noticed that RPW8-mediated disease resistance was partially abrogated in *atj3-1* *-/-* background compared to resistant *S5* plants (**Figure 6-5C&E**). Moreover, *atj3-1* *-/-*/*S5* plants were generally larger than *S5* plants of the same age suggesting that fitness costs associated with *RPW8* expression (Orgil et al., 2007) are partially relieved (**Figure 6-5E**). Subsequent quantification of *S5* and *atj3-1* *-/-*/*S5* plants reveals that *atj3-1* *-/-*/*S5* are statistically more susceptible than *S5* plants (**Figure 6-5D**). Altogether, these results suggest that both *ATJ2* and *ATJ3* likely play a role in basal

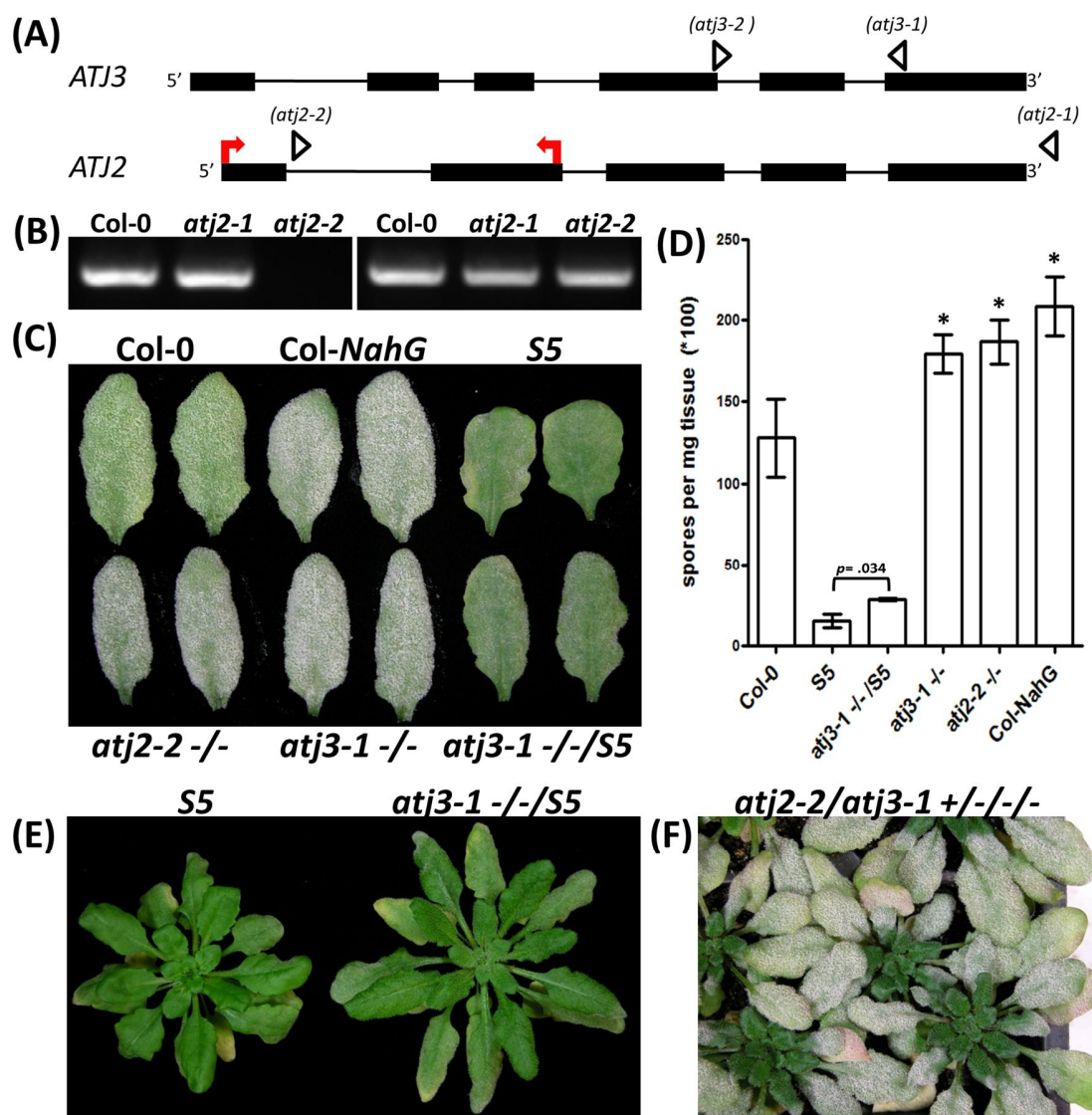


**Figure 6-5. *ATJ2* and *ATJ3* are Involved in Basal Immunity Against Powdery Mildew.**

**(A)** Schematic gene structures and approximate location and direction of T-DNA

insertion lines for *ATJ2* and *ATJ3*. *atj3-1*: SALK\_141625 [6<sup>th</sup> Exon]

(<sup>+1734</sup>CCAAA..◀..GCACT<sup>+1743</sup>), *atj3-2*: SALK\_132923 [4<sup>th</sup> Exon]

(<sup>+1212</sup>CAAGC..▶..AGATG<sup>+1221</sup>), *atj2-1*: SALK\_012035 [3'UTR]

(<sup>+1973</sup>GAAGA..◀..ACCTC<sup>+1982</sup>), *atj2-2*: SALK\_071563 [1<sup>st</sup> Intron]

(<sup>+182</sup>CTCTG..▶..TAAAT<sup>+191</sup>). **(B)** RT-PCR analysis of T-DNA insertion lines. Left

panels - *ATJ2* gene-specific primers indicated in **(A)** by red arrows. Right panels – *UBC21* gene-specific primers. Samples were subjected to RT-PCR (30 cycles). **(C)** Disease phenotypes of representative Col-0, Col-*NahG*, *S5*, *atj2-2* *-/-*, *atj3-1* *-/-* and *atj3-1* *-/-*/*S5* plants at 12dpi with *Gc*-UCSC1 (*atj2-1* and *atj3-2* plants not displayed). **(D)** Quantitative assay of disease susceptibility. Data represent means  $\pm$  SEM (n=4) from one of three representative experiments. Student's *t* test was used to calculate *P* value for each genotype compared with Col-0 and *S5* compared with *atj3-1* *-/-*/*S5*. (\* =  $p < .05$ ). **(E)** Disease phenotypes of representative *S5* and *atj3-1* *-/-*/*S5* plants at 12dpi. **(F)** ~7 week old sesqui *atj2-2* +/-; *atj3-1* *-/-* mutants are viable and are highly susceptible to powdery mildew at 12dpi.



immunity against powdery mildew and may be required for full resistance activated by *RPW8*.

To further explore how *ATJ3* is required for *RPW8*-defense activation or signaling, I investigated whether *RPW8*'s EHM localization was also compromised in *atj3-1 -/-* background. T1 plants expressing *RPW8.2p::RPW8.2-YFP* in *atj3-1 -/-* background had normal EHM localization of *RPW8.2-YFP* upon powdery mildew infection (**Figure 6-6A**). However, we did note that all *RPW8.2-YFP/atj3-1 -/-* T1 lines were fully susceptible to powdery mildew corroborating our results that *ATJ3* is partially required for *RPW8.2* defense activation (**data not shown**). Likewise, we also aimed to investigate the subcellular localization of *ATJ3* and generated Col-0 and *atj3-1 -/-* plants constitutively expressing *YFP-ATJ3* from the *35S* promoter. We found that while *YFP-ATJ3* is ubiquitously expressed in epidermal cells (**Figure 6-6B**), we could not detect *YFP-ATJ3* at the EHM upon infection with powdery mildew (**data not shown**). I also tested whether *atj3-1 -/-* lines were compromised in defense against other pathogens including the virulent bacterial pathogen *Pst DC3000*. Interestingly, my preliminary results suggest that *atj3-1 -/-* plants seemed more susceptible than wild-type plants to bacterial infection as shown by enhanced chlorotic and necrotic symptoms following bacterial spray inoculation (**Figure 6-7A**). Quantification of bacterial growth at 4dpi reveals that *atj3-1 -/-* plants were statistically more susceptible than Col-0 wild-type plants (**Figure 6-7B**). Altogether, it appears likely that *ATJ2* and *ATJ3* are involved in conserved basal resistance mechanisms against multiple plant pathogens.

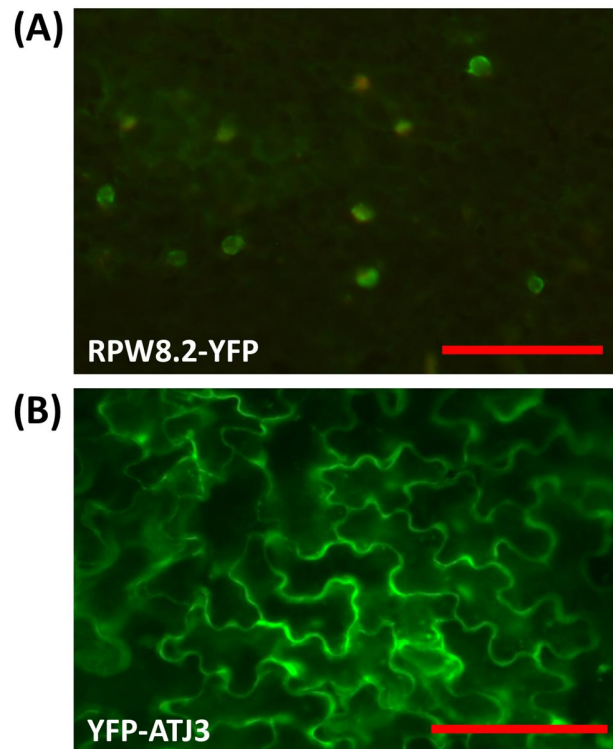


**Figure 6-6. *atj3* <sup>-/-</sup> Does Not Compromise RPW8-EHM Localization.**

**(A)** Single optical section of RPW8.2-YFP localized to the EHM in *atj3-1* <sup>-/-</sup> background at 3dpi with Gc-UCSC1. **(B)** Single optical section of ectopic expression of *YFP-ATJ3* from the *35S* promoter in Arabidopsis. YFP-ATJ3 is ubiquitously expressed in Arabidopsis epidermal cells but is not localized to the EHM (**data not shown**). Bars = 100μm.

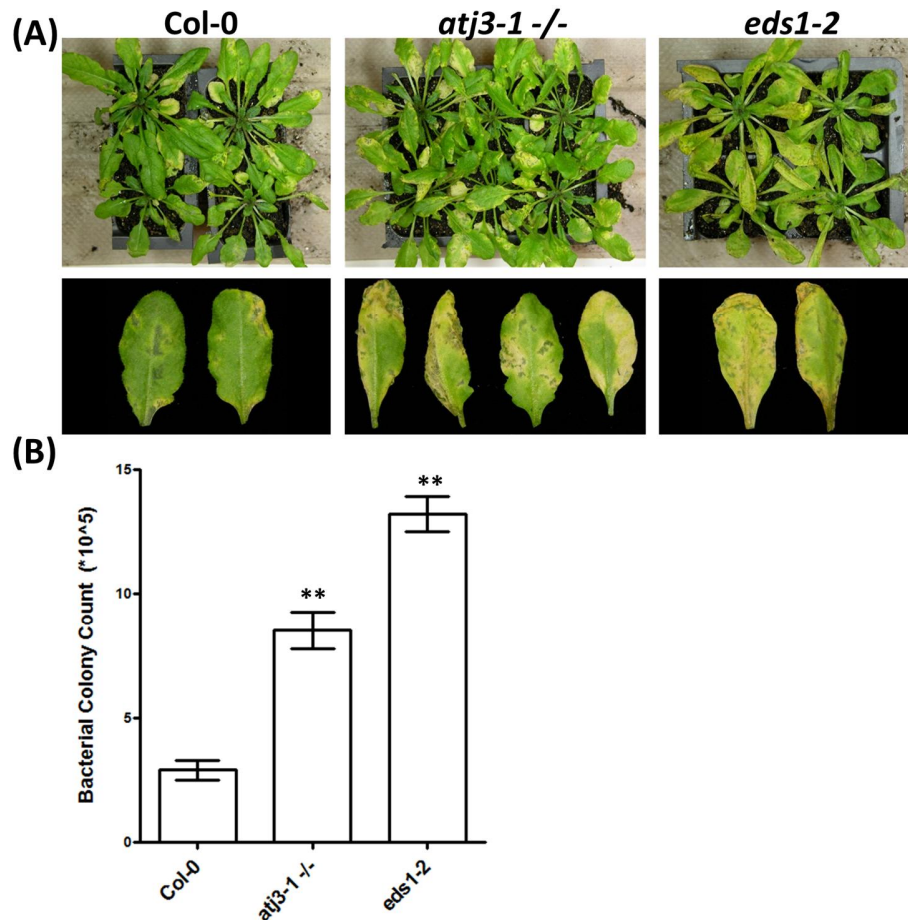


**Figure 6-7. *ATJ3* is Involved in Basal Resistance Against *Pseudomonas syringae*.**

**(A)** Representative whole plant images of Col-0 (left), *atj3-1 -/-* (middle) and *eds1-2* (right) in response to *Pst* DC3000 4dpi. Detached leaf images for each genotype (bottom panels). **(B)** Quantitative assay of disease susceptibility. Data represent means  $\pm$  SEM (n=5) from one of three representative experiments. Student's *t* test was used to calculate *P* value for each genotype compared with Col-0. (\*\* =  $p < .01$ ).

## Discussion

My preliminary results suggest that *ATJ3*, and its closely related homolog *ATJ2*, play a role in basal immunity in *Arabidopsis* against powdery mildew. Moreover, *ATJ3* also appears to be involved in host resistance against bacterial pathogens. Whether or not RPW8.2 interacts with ATJ3 *in vivo* has not been determined. However, the observation that RPW8-mediated mildew resistance is slightly compromised in *atj3-1* *-/-* likely provides genetic evidence for an interaction between RPW8.2 and ATJ3. How ATJ3 may be involved in basal and RPW8-mediated resistance is not known. Given the predicted chaperone function of ATJ3, ATJ3 may play a role in proper folding of RPW8.2. However, because EHM-localization of RPW8.2-YFP did not seem to be affected in *atj3-1* *-/-* plants, it is unlikely that down-regulation of ATJ3 alone affects RPW8.2's trafficking properties. Residual ATJ3 in *atj3-1* *-/-* plants and/or functional redundancy between ATJ3 and ATJ2 may explain partial loss of RPW8-mediated resistance and seemingly normal EHM-localization of RPW8.2-YFP. To address this possibility, I intended to create *atj2/atj3* double mutant. Unfortunately, screening of >96 F2 individuals derived from *atj3-1* *x atj2-2* failed to identify a single double T-DNA mutant. Close examination revealed that ~1/16 young seedlings from the F2 population developed extensive cell death and died shortly after germination, suggesting that the *atj2/atj3* double mutant is seedling lethal (**data not shown**). Initial disease tests showed that F2 individual of the *atj2-2* *+/-; atj3-1* *-/-* genotype (i.e. sesqui mutant) were highly susceptible to powdery mildew (**Figure 6-5F**), supporting the speculation that there is a functional redundancy between ATJ2 and ATJ3. Future efforts are required to determine if RPW8.2 interacts with ATJ3 (and ATJ2) *in vivo*, whether ATJ2 and ATJ3 are required

for classical PTI and ETI, and whether these two chaperones are indeed in complex with Hsp90, Hsp70 and SGT1 to regulate innate immunity in plants and animals.

## Materials & Methods

### Plant Lines, Cloning and Plasmid Construction

All T-DNA insertion mutant lines for *ATJ2* and *ATJ3* were obtained from the Arabidopsis stock center. Col-0, *atj3-1* *-/-* and *S5* (Col-gl transgenic for *RPW8*) plants were used for crossing and/or agrobacterium-mediated transformations. The previously cloned *RPW8.2p::RPW8.2/pPZPYFP23'* (Wang et al., 2007) construct was used for agrobacterium-mediated transformation of *atj3-1* *-/-* lines.

The *35S::YFP-ATJ3* expression construct was created by cloning the full length genomic sequence of *ATJ3* into the pENTR/D-TOPO entry vector and subsequently cloned into the gateway compatible vector pEG104 (Earley et al., 2006) via LR recombination. The primers used for amplification of *ATJ3* from the F26G5 BAC clone sample were (ATJ3tpF: <sup>5'</sup>caccgatccATGTTTCGGTAGAGGACCCTCGA<sup>3'</sup> and EcoATJ3R: <sup>5'</sup>ggaattcT TACTGCTGGGCACATTGCA<sup>3'</sup>).

### Bacterial Spray Inoculation

For bacterial infection, fully expanded rosettes of 7 week old plants (6-12) were sprayed with a bacterial suspension (OD<sub>600</sub> ~ 0.5000) of *Pseudomonas syringae* pv. *tomato* (*Pst*) DC3000 in a 10 mM MgCl<sub>2</sub> solution containing 0.025% Silwet-L77. Quantification of bacterial growth was completed as previously described (Wang et al., 2007).

### Other Analysis

All growth conditions, materials and methods not listed have been previously used and described in (**Chapters 2-5**).

### Accession Numbers

Sequence data can be found in the Arabidopsis Genome Initiative or GenBank/EMBL databases under the following gene IDs, accession numbers and SALK IDs:

Gene/Gene ID	Accession	T-DNA Mutant ID/SALK Line
<i>ATJ2</i> : At5g22060	<a href="#">NM_122127.2</a>	<i>atj2-1</i> /SALK_012035
<i>ATJ2</i> : At5g22060	<a href="#">NM_122127.2</a>	<i>atj2-2</i> /SALK_071563
<i>ATJ3</i> : At3g44110	<a href="#">NM_114279.3</a>	<i>atj3-1</i> /SALK_141625
<i>ATJ3</i> : At3g44110	<a href="#">NM_114279.3</a>	<i>atj3-2</i> /SALK_132923

**Table 3.** *ATJ2* and *ATJ3* Mutant Lines.

## Chapter 7: Conclusions and Perspectives

The major goal of my thesis project was to understand the functional origin of *RPW8* by characterizing the function of the *RPW8* homologs in *Arabidopsis* and *Brassica* and to further dissect the signaling pathways and molecular mechanisms of *RPW8*-mediated broad-spectrum disease resistance. As the project developed, I expanded my thesis studies to include the investigation of the origin and biogenesis of the membranous host-pathogen interface — the extra-haustorial membrane (EHM) and the exploration of utilizing *RPW8* as a delivery vehicle for achieving novel resistance against haustorium-forming pathogens.

Below I summarize the major findings from my thesis and discuss the outstanding questions and future experiments necessary for understanding and engineering haustorium-targeted plant defense mechanisms (see **Figure 7-1**).

### **1. How does this study contribute to our understanding of the functional origin of *RPW8*?**

*RPW8.1* and *RPW8.2* belong to a small gene family in the *Arabidopsis* and *Brassica* lineages. While *RPW8.1* and *RPW8.2* seem to be under positive selection, some *RPW8* homologs, i.e. *HR1*, *HR2* and particularly *HR3*, appear to be under purifying selection for maintaining a conserved, yet unknown function(s) (Xiao et al., 2004; Orgil et al., 2007). Because our previous evolutionary studies indicated that *RPW8* has evolved from an *HR3*-like progenitor gene (Xiao et al., 2004; Orgil et al., 2007), identification of the cellular function of *HR3* and other *RPW8* homologs will not only help understand the



functional origin of RPW8 but also shed light onto the molecular basis of RPW8-mediated broad-spectrum disease resistance.

Here, I report that three homologs in Arabidopsis, *HR1*, *HR2* and *HR3*, play a role in salicylic acid-dependent basal resistance against powdery mildew (**Chapter 2**).

Additionally, the *Brassica oleracea* homolog, *HRa*, is capable of conferring resistance to the well-adapted powdery mildew isolate *Gc*-UCSC1 when heterologously expressed in Arabidopsis (**Chapter 2**). Most interestingly, I also show that all tested homologs of RPW8 are EHM-resident proteins upon haustorial differentiation within invaded Arabidopsis epidermal cells (**Chapter 2**).

Altogether, these results support my hypothesis that *RPW8.1* and *RPW8.2* evolved from duplication and functional diversification (enhancement) of a more ancient component of basal immunity in Arabidopsis and that RPW8-mediated broad-spectrum mildew resistance represents functional improvement/renovation rather than an entirely new invention from the more ancient family members. Moreover, the EHM-targeting of *RPW8.2* is a unique feature that originated during an early evolutionary stage of the RPW8 family and has been maintained before the separation of Arabidopsis and *Brassica*. Therefore, it is plausible that the semi-dominant resistance gene *RPW8.2* has evolved to increase the strength of defense response to counterattack more adapted and aggressive powdery mildew pathogens, whereas *HR1*, *HR2*, and *HR3* may activate basal-level resistance against less adapted powdery mildew or potentially other haustorium-forming pathogens.

However, how exactly *RPW8.2* has evolved in protein sequence from an *HR3*-like progenitor to gain a higher resistance capacity has not been fully determined. Apart

from domain swapping experiments conducted in my thesis studies, a more detailed mutational analysis between RPW8 and HR3 is required for the identification of critical residues or regions that are responsible for the functional diversification. Another critical question for future studies on RPW8-HR3 is how HR3 (and RPW8) exploits the central SA-dependent signaling pathway for basal resistance. Relevant to this question, it is worth mentioning that outside of the RPW8 family, HR3 has the highest homology to the CC domain of a group of non-canonical NB-LRR proteins including NRG1 and ADR1 that primarily function as signaling components rather than sensors for pathogen effectors (Grant et al., 2003; Peart et al., 2005; Collier et al., 2011). This situation is analogous to the function of mammalian sorting adaptors, such as MyD88 and TRIF, that are required for activation of immune signaling at specific subcellular locations by TLR receptors (Kagan, 2012). Therefore, I hypothesize that the RPW8 family proteins may also serve as sorting adaptors of central NB-LRR immune complexes for the activation of resistance at the EHM. Testing this hypothesis requires challenging experiments in the future.

## **2. How does this study contribute to our understanding of the host-pathogen interface?**

Many plant pathogenic fungi and oomycetes have evolved a similar haustorium-based invasive strategy to colonize their respective plant hosts. Despite the importance of the EHM as the host-pathogen interface in defense and pathogenesis, the origin and biogenesis of the EHM remains to be characterized.

The highly specific localization of RPW8.2 to the EHM together with the absence of several plasma membrane proteins in the EHM (Koh et al., 2005) suggests that the EHM is likely of host origin, and distinct from the host PM. In this thesis, by taking advantage of the localization of YFP-HR3 to the host plasma membrane, the papillae, and the EHM, in combination with RPW8.2-RFP as an EHM marker protein, I provide the first piece of cell biological evidence to suggest that the EHM is of host origin and *de novo* synthesized during haustorial differentiation of powdery mildew in invaded plant epidermal cells (**Chapter 3**).

### **3. How does this study contribute to our understanding of the EHM-directed protein/membrane trafficking?**

Specific targeting of RPW8 family proteins to the EHM suggests that there must be a trafficking cue(s) at the EHM that induces/guides EHM-specific protein/membrane transport. In **Chapter 5**, by using a fluorescent lipid biosensor, I provide evidence to suggest that the EHM appears to be transiently enriched for a specific phosphoinositide lipid species, PI(3)P. PI(3)P has been shown to be transiently enriched in the phagosomal membrane in mammalian cells (Vieira et al., 2001) and has recently been shown to mediate the uptake of oomycete and fungal effector proteins (Kale et al., 2010) by plant host cells. I therefore speculate that PI(3)P may serve as a landmark for EHM-identity. As a next step, my preliminary results from initial lipid binding assays suggest RPW8.2 may specifically bind PI(3)P for EHM targeting. However, these results will need confirmation and clarification using more extensive lipid filter-binding and liposome binding assays. A more detailed study of the spatiotemporal dynamics of PI(3)P and

other closely related PI species in plant epidermal cells invaded by haustoria will also be helpful. Future work will also be required to identify the PI(3)P binding site in RPW8.2 and determine if PI(3)P binding indeed provides the trafficking cue for targeting RPW8.2 to the EHM.

#### **4. Can RPW8 be used as a delivery vehicle to confer novel resistance against haustorium-forming pathogens?**

RPW8.2 is specifically targeted to the EHM whereby it activates defense to constrain haustoria of powdery mildew (Wang, et al., 2009). The highly EHM-specific localization of RPW8.2 has inspired the design and testing of a strategy for engineering novel resistance against haustorium-forming pathogens. This strategy involves using RPW8.2 as a delivery vehicle to target antimicrobial peptides to the pathogen side of the EHM for more effective killing of the invading pathogens. Through the introduction of a protease cleavage site (PCS) between RPW8.2 and YFP (as a cargo) and co-expression of the resultant RPW8-PCS-YFP fusion protein and a serine protease subtilisin that specifically recognizes the PCS site, I demonstrate that RPW8.2 is a type I membrane protein and the subtilisin may be used to release antimicrobial cargo protein to the extrahaustorial matrix. Combined with preliminary results from group efforts in testing various antimicrobial proteins in fusion with RPW8.2, my work provides encouraging information for future tests toward targeted delivery and controlled release of antimicrobial cargo proteins to the host-pathogen interface as a novel strategy for fighting against haustorium-forming pathogens.

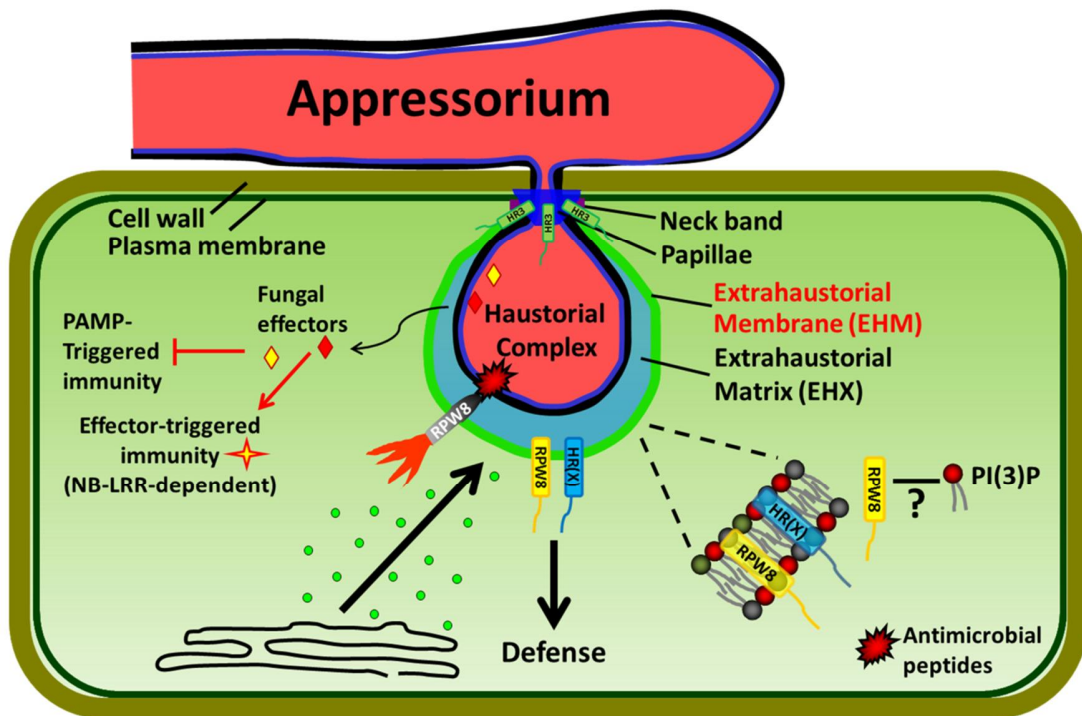


**Figure 7-1. A Summary and a Working Model**

Haustorium-forming pathogens such as powdery mildew differentiate haustoria to secrete fungal effectors to suppress host defense and obtain photosynthate from the host cell. Haustoria are encased the EHM that is of host origin and *de novo* synthesized upon haustorium differentiation. RPW8 family members are type I membrane proteins (as exemplified by RPW8.2) that are targeted to the EHM whereby they activate on-site defense against powdery mildew. The EHM may be enriched for PI(3)P and RPW8.2 may specifically bind PI(3)P. Hence, PI(3)P may provide the trafficking cue for EHM-specific targeting of RPW8. The unique EHM-targeting feature of RPW8 has inspired a strategy in which RPW8 is used as a delivery vehicle to target antimicrobial peptides to the host-pathogen interface, thereby conferring novel resistance against haustorium-forming pathogens.

## References

- Aarts, N., Metz, M., Holub, E., Staskawicz, B.J., Daniels, M.J., and Parker, J.E.** (1998). Different requirements for EDS1 and NDR1 by disease resistance genes define at least two R gene-mediated signaling pathways in Arabidopsis. *Proceedings of the National Academy of Sciences of the United States of America* **95**, 10306-10311.
- Abd-El-Halim, A., Meijer, H.J., Tameling, W.I., Vossen, J.H., and Joosten, M.H.** (2012). Defense activation triggers differential expression of phospholipase-C (PLC) genes and elevated temperature induces phosphatidic acid (PA) accumulation in tomato. *Plant signaling & behavior* **7**, 1073-1078.
- Ade, J., DeYoung, B.J., Golstein, C., and Innes, R.W.** (2007). Indirect activation of a plant nucleotide binding site-leucine-rich repeat protein by a bacterial protease. *Proceedings of the National Academy of Sciences of the United States of America* **104**, 2531-2536.
- Agrios, G.N.** (2005). *Plant pathology*. (Amsterdam ; Boston: Elsevier Academic Press).
- Aist, J.R.** (1976). Papillae and Related Wound Plugs of Plant Cells. *Annual review of phytopathology* **14**, 145-163.
- Akita, M., and Valkonen, J.P.** (2002). A novel gene family in moss (*Physcomitrella patens*) shows sequence homology and a phylogenetic relationship with the TIR-NBS class of plant disease resistance genes. *Journal of molecular evolution* **55**, 595-605.
- Andersson, M.X., Kourtchenko, O., Dangl, J.L., Mackey, D., and Ellerstrom, M.** (2006). Phospholipase-dependent signalling during the AvrRpm1- and AvrRpt2-induced disease resistance responses in *Arabidopsis thaliana*. *The Plant Journal* **47**, 947-959.
- Argout, X., Salse, J., Aury, J.M., Guiltinan, M.J., Droc, G., Gouzy, J., Allegre, M., Chaparro, C., Legavre, T., Maximova, S.N., Abrouk, M., Murat, F., Fouet, O., Poulain, J., Ruiz, M., Roguet, Y., Rodier-Goud, M., Barbosa-Neto, J.F., Sabot, F., Kudrna, D., Ammiraju, J.S., Schuster, S.C., Carlson, J.E., Sallet, E., Schiex, T., Dievart, A., Kramer, M., Gelley, L., Shi, Z., Berard, A., Viot, C., Boccara, M., Risterucci, A.M., Guignon, V., Sabau, X., Axtell, M.J., Ma, Z., Zhang, Y., Brown, S., Bourge, M., Golser, W., Song, X., Clement, D., Rivallan, R., Tah, M., Akaza, J.M., Pitollat, B., Gramacho, K., D'Hont, A., Brunel, D., Infante, D., Kebe, I., Costet, P., Wing, R., McCombie, W.R., Guiderdoni, E., Quetier, F., Panaud, O., Wincker, P., Bocs, S., and Lanaud, C.** (2011). The genome of *Theobroma cacao*. *Nature genetics* **43**, 101-108.
- Asai, T., Tena, G., Plotnikova, J., Willmann, M.R., Chiu, W.L., Gomez-Gomez, L., Boller, T., Ausubel, F.M., and Sheen, J.** (2002). MAP kinase signalling cascade in *Arabidopsis* innate immunity. *Nature* **415**, 977-983.
- Assaad, F.F., Qiu, J.-L., Youngs, H., Ehrhardt, D., Zimmerli, L., Kalde, M., Wanner, G., Peck, S.C., Edwards, H., Ramonell, K., Somerville, C.R., and Thordal-Christensen, H.** (2004). The PEN1 Syntaxin Defines a Novel Cellular Compartment upon Fungal Attack and Is Required for the Timely Assembly of Papillae. *Molecular biology of the cell* **15**, 5118-5129.
- Ausubel, F.M.** (2005). Are innate immune signaling pathways in plants and animals conserved? *Nature immunology* **6**, 973-979.
- Bari, R., and Jones, J.D.** (2009). Role of plant hormones in plant defence responses. *Plant molecular biology* **69**, 473-488.
- Baumgarten, A., Cannon, S., Spangler, R., and May, G.** (2003). Genome-level evolution of resistance genes in *Arabidopsis thaliana*. *Genetics* **165**, 309-319.

- Bednarek, P., Pislewska-Bednarek, M., Svatos, A., Schneider, B., Doubek, J., Mansurova, M., Humphry, M., Consonni, C., Panstruga, R., Sanchez-Vallet, A., Molina, A., and Schulze-Lefert, P.** (2009). A glucosinolate metabolism pathway in living plant cells mediates broad-spectrum antifungal defense. *Science* **323**, 101-106.
- Behnia, R., and Munro, S.** (2005). Organelle identity and the signposts for membrane traffic. *Nature* **438**, 597-604.
- Bendahmane, A., Farnham, G., Moffett, P., and Baulcombe, D.C.** (2002). Constitutive gain-of-function mutants in a nucleotide binding site-leucine rich repeat protein encoded at the Rx locus of potato. *The Plant Journal* **32**, 195-204.
- Bent, A.F., Kunkel, B.N., Dahlbeck, D., Brown, K.L., Schmidt, R., Giraudat, J., Leung, J., and Staskawicz, B.J.** (1994). RPS2 of *Arabidopsis thaliana*: a leucine-rich repeat class of plant disease resistance genes. *Science* **265**, 1856-1860.
- Berkey, R., Bendigeri, D., and Xiao, S.** (2012). Sphingolipids and plant defense/disease: the "death" connection and beyond. *Frontiers in plant science* **3**, 68.
- Bhat, R.A., Miklis, M., Schmelzer, E., Schulze-Lefert, P., and Panstruga, R.** (2005). Recruitment and interaction dynamics of plant penetration resistance components in a plasma membrane microdomain. *Proceedings of the National Academy of Sciences of the United States of America* **102**, 3135-3140.
- Bhattacharjee, S., Stahelin, R.V., Speicher, K.D., Speicher, D.W., and Haldar, K.** (2012). Endoplasmic reticulum PI(3)P lipid binding targets malaria proteins to the host cell. *Cell* **148**, 201-212.
- Blumental-Perry, A., Haney, C.J., Weixel, K.M., Watkins, S.C., Weisz, O.A., and Aridor, M.** (2006). Phosphatidylinositol 4-phosphate formation at ER exit sites regulates ER export. *Developmental cell* **11**, 671-682.
- Boller, T., and Felix, G.** (2009). A renaissance of elicitors: perception of microbe-associated molecular patterns and danger signals by pattern-recognition receptors. *Annual review of plant biology* **60**, 379-406.
- Bowers, J.H., Bailey, B.A., Hebbar, P.K., Sanogo, S., and Lumsden, R.D.** (2001). The Impact of Plant Diseases on World Chocolate Production. *Plant Health Progress*.
- Braun, U., Cook, R., Inman, A., Shin, H., Bélanger, R., Bushnell, W., Dik, A., and Carver, T.** (2002). The taxonomy of the powdery mildew fungi. *The powdery mildews: a comprehensive treatise*, 13-55.
- Bricchi, I., Berteaux, C.M., Occhipinti, A., Paponov, I.A., and Maffei, M.E.** (2012). Dynamics of Membrane Potential Variation and Gene Expression Induced by *Spodoptera littoralis*, *Myzus persicae*, and *Pseudomonas syringae* in *Arabidopsis*. *PloS one* **7**, e46673.
- Brueggeman, R., Rostoks, N., Kudrna, D., Kilian, A., Han, F., Chen, J., Druka, A., Steffenson, B., and Kleinhofs, A.** (2002). The barley stem rust-resistance gene Rpg1 is a novel disease-resistance gene with homology to receptor kinases. *Proceedings of the National Academy of Sciences of the United States of America* **99**, 9328-9333.
- Brunner, S., Hurni, S., Streckeisen, P., Mayr, G., Albrecht, M., Yahiaoui, N., and Keller, B.** (2010). Intragenic allele pyramiding combines different specificities of wheat Pm3 resistance alleles. *The Plant Journal* **64**, 433-445.
- Buschges, R., Hollricher, K., Panstruga, R., Simons, G., Wolter, M., Frijters, A., van Daelen, R., van der Lee, T., Diergaarde, P., Groenendijk, J., Topsch, S., Vos, P., Salamini, F., and Schulze-Lefert, P.** (1997). The barley Mlo gene: a novel control element of plant pathogen resistance. *Cell* **88**, 695-705.
- Bushnell, W.R., and Bergquist, S.E.** (1975). Aggregation of host cytoplasm and the formation of papillae and haustoria in powdery mildew of barley. *Phytopathology* **65**, 310-318.

- Canonne, J., Froidure-Nicolas, S., and Rivas, S.** (2011). Phospholipases in action during plant defense signaling. *Plant signaling & behavior* **6**, 13-18.
- Cao, H., Bowling, S.A., Gordon, A.S., and Dong, X.** (1994). Characterization of an Arabidopsis Mutant That Is Nonresponsive to Inducers of Systemic Acquired Resistance. *The Plant cell* **6**, 1583-1592.
- Carver, T.L.W., Kunoh, H., Thomas, B.J., and Nicholson, R.L.** (1999). Release and visualization of the extracellular matrix of conidia of *Blumeria graminis*. *Mycological research* **103**, 547-560.
- Cary, J.W., Rajasekaran, K., Brown, R.L., Luo, M., Chen, Z.Y., and Bhatnagar, D.** (2011). Developing resistance to aflatoxin in maize and cottonseed. *Toxins* **3**, 678-696.
- Cesar, S.A., and Ignacimuthu, S.** (2012). Genetic engineering of crop plants for fungal resistance: role of antifungal genes. *Biotechnology letters* **34**, 995-1002.
- Chandran, D., Tai, Y.C., Hather, G., Dewdney, J., Denoux, C., Burgess, D.G., Ausubel, F.M., Speed, T.P., and Wildermuth, M.C.** (2009). Temporal global expression data reveal known and novel salicylate-impacted processes and regulators mediating powdery mildew growth and reproduction on Arabidopsis. *Plant physiology* **149**, 1435-1451.
- Chang, C., and Shockey, J.A.** (1999). The ethylene-response pathway: signal perception to gene regulation. *Current opinion in plant biology* **2**, 352-358.
- Chehab, E.W., and Braam, J.** (2012). Jasmonates in Plant Defense Responses. In *Biocommunication of Plants*, G. Witzany and F. Baluška, eds (Springer Berlin Heidelberg), pp. 67-88.
- Chen, G., Snyder, C.L., Greer, M.S., and Weselake, R.J.** (2011). Biology and Biochemistry of Plant Phospholipases. *Critical Reviews in Plant Sciences* **30**, 239-258.
- Chen, H., Xue, L., Chintamanani, S., Germain, H., Lin, H., Cui, H., Cai, R., Zuo, J., Tang, X., Li, X., Guo, H., and Zhou, J.M.** (2009a). ETHYLENE INSENSITIVE3 and ETHYLENE INSENSITIVE3-LIKE1 repress SALICYLIC ACID INDUCTION DEFICIENT2 expression to negatively regulate plant innate immunity in Arabidopsis. *The Plant cell* **21**, 2527-2540.
- Chen, L.Q., Hou, B.H., Lalonde, S., Takanaga, H., Hartung, M.L., Qu, X.Q., Guo, W.J., Kim, J.G., Underwood, W., Chaudhuri, B., Chermak, D., Antony, G., White, F.F., Somerville, S.C., Mudgett, M.B., and Frommer, W.B.** (2010). Sugar transporters for intercellular exchange and nutrition of pathogens. *Nature* **468**, 527-532.
- Chen, S., Songkumarn, P., Liu, J., and Wang, G.L.** (2009b). A versatile zero background T-vector system for gene cloning and functional genomics. *Plant physiology* **150**, 1111-1121.
- Chen, T., and Cao, X.** (2010). Stress for maintaining memory: HSP70 as a mobile messenger for innate and adaptive immunity. *European journal of immunology* **40**, 1541-1544.
- Chinchilla, D., Zipfel, C., Robatzek, S., Kemmerling, B., Nurnberger, T., Jones, J.D., Felix, G., and Boller, T.** (2007). A flagellin-induced complex of the receptor FLS2 and BAK1 initiates plant defence. *Nature* **448**, 497-500.
- Chini, A., Fonseca, S., Fernandez, G., Adie, B., Chico, J.M., Lorenzo, O., Garcia-Casado, G., Lopez-Vidriero, I., Lozano, F.M., Ponce, M.R., Micol, J.L., and Solano, R.** (2007). The JAZ family of repressors is the missing link in jasmonate signalling. *Nature* **448**, 666-671.
- Chisholm, S.T., Coaker, G., Day, B., and Staskawicz, B.J.** (2006). Host-microbe interactions: shaping the evolution of the plant immune response. *Cell* **124**, 803-814.
- Chu, Z., Yuan, M., Yao, J., Ge, X., Yuan, B., Xu, C., Li, X., Fu, B., Li, Z., Bennetzen, J.L., Zhang, Q., and Wang, S.** (2006). Promoter mutations of an essential gene for pollen development result in disease resistance in rice. *Genes & development* **20**, 1250-1255.
- Clay, N.K., Adio, A.M., Denoux, C., Jander, G., and Ausubel, F.M.** (2009). Glucosinolate metabolites required for an Arabidopsis innate immune response. *Science* **323**, 95-101.



- Clough, S.J., Fengler, K.A., Yu, I.C., Lippok, B., Smith, R.K., Jr., and Bent, A.F.** (2000). The Arabidopsis dnd1 "defense, no death" gene encodes a mutated cyclic nucleotide-gated ion channel. *Proceedings of the National Academy of Sciences of the United States of America* **97**, 9323-9328.
- Colcombet, J., and Hirt, H.** (2008). Arabidopsis MAPKs: a complex signalling network involved in multiple biological processes. *The Biochemical journal* **413**, 217-226.
- Collier, S.M., and Moffett, P.** (2009). NB-LRRs work a "bait and switch" on pathogens. *Trends in plant science* **14**, 521-529.
- Collier, S.M., Hamel, L.P., and Moffett, P.** (2011). Cell death mediated by the N-terminal domains of a unique and highly conserved class of NB-LRR protein. *MPMI* **24**, 918-931.
- Collinge, D., Lund, O.S., and Thordal-Christensen, H.** (2008). What are the prospects for genetically engineered, disease resistant plants? *European Journal of Plant Pathology* **121**, 217-231.
- Collins, N.C., Thordal-Christensen, H., Lipka, V., Bau, S., Kombrink, E., Qiu, J.-L., Huckelhoven, R., Stein, M., Freialdenhoven, A., Somerville, S.C., and Schulze-Lefert, P.** (2003a). SNARE-protein-mediated disease resistance at the plant cell wall. *Nature* **425**, 973-977.
- Collins, N.C., Thordal-Christensen, H., Lipka, V., Bau, S., Kombrink, E., Qiu, J.L., Huckelhoven, R., Stein, M., Freialdenhoven, A., Somerville, S.C., and Schulze-Lefert, P.** (2003b). SNARE-protein-mediated disease resistance at the plant cell wall. *Nature* **425**, 973-977.
- Correa, R.G., Milutinovic, S., and Reed, J.C.** (2012). Roles of NOD1 (NLRC1) and NOD2 (NLRC2) in innate immunity and inflammatory diseases. *Bioscience reports* **32**, 597-608.
- Cruz, C.D., Bockus, W.W., Stack, J.P., Tang, X., Valent, B., Pedley, K.F., and Peterson, G.L.** (2012). Preliminary Assessment of Resistance Among U.S. Wheat Cultivars to the Triticum Pathotype of Magnaporthe oryzae. *Plant Disease* **96**, 1501-1505.
- Cutler, S.R., Ehrhardt, D.W., Griffiths, J.S., and Somerville, C.R.** (2000). Random GFP::cDNA fusions enable visualization of subcellular structures in cells of Arabidopsis at a high frequency. *Proceedings of the National Academy of Sciences of the United States of America* **97**, 3718-3723.
- Dangl, J.L., and Jones, J.D.** (2001). Plant pathogens and integrated defence responses to infection. *Nature* **411**, 826-833.
- de Torres Zabela, M., Fernandez-Delmond, I., Niittyla, T., Sanchez, P., and Grant, M.** (2002). Differential expression of genes encoding Arabidopsis phospholipases after challenge with virulent or avirulent Pseudomonas isolates. *MPMI* **15**, 808-816.
- Dempski, R.E., Jr., and Imperiali, B.** (2002). Oligosaccharyl transferase: gatekeeper to the secretory pathway. *Current opinion in chemical biology* **6**, 844-850.
- Deslandes, L., Olivier, J., Theulieres, F., Hirsch, J., Feng, D.X., Bittner-Eddy, P., Beynon, J., and Marco, Y.** (2002). Resistance to Ralstonia solanacearum in Arabidopsis thaliana is conferred by the recessive RRS1-R gene, a member of a novel family of resistance genes. *Proceedings of the National Academy of Sciences of the United States of America* **99**, 2404-2409.
- Despres, C., DeLong, C., Glaze, S., Liu, E., and Fobert, P.R.** (2000). The Arabidopsis NPR1/NIM1 protein enhances the DNA binding activity of a subgroup of the TGA family of bZIP transcription factors. *The Plant cell* **12**, 279-290.
- Di Paolo, G., and De Camilli, P.** (2006). Phosphoinositides in cell regulation and membrane dynamics. *Nature* **443**, 651-657.
- Dietrich, R.A., Delaney, T.P., Uknes, S.J., Ward, E.R., Ryals, J.A., and Dangl, J.L.** (1994). Arabidopsis mutants simulating disease resistance response. *Cell* **77**, 565-577.

- Dodds, P.N., Lawrence, G.J., Catanzariti, A.M., Teh, T., Wang, C.I., Ayliffe, M.A., Kobe, B., and Ellis, J.G.** (2006). Direct protein interaction underlies gene-for-gene specificity and coevolution of the flax resistance genes and flax rust avirulence genes. *Proceedings of the National Academy of Sciences of the United States of America* **103**, 8888-8893.
- Dong, J., Xiao, F., Fan, F., Gu, L., Cang, H., Martin, G.B., and Chai, J.** (2009). Crystal structure of the complex between *Pseudomonas* effector AvrPtoB and the tomato Pto kinase reveals both a shared and a unique interface compared with AvrPto-Pto. *The Plant cell* **21**, 1846-1859.
- Dowler, S., Currie, R.A., Campbell, D.G., Deak, M., Kular, G., Downes, C.P., and Alessi, D.R.** (2000). Identification of pleckstrin-homology-domain-containing proteins with novel phosphoinositide-binding specificities. *The Biochemical journal* **351**, 19-31.
- Durrant, W.E., and Dong, X.** (2004). Systemic acquired resistance. *Annual review of phytopathology* **42**, 185-209.
- Earley, K.W., Haag, J.R., Pontes, O., Oppen, K., Juehne, T., Song, K., and Pikaard, C.S.** (2006). Gateway-compatible vectors for plant functional genomics and proteomics. *The Plant Journal* **45**, 616-629.
- Eckardt, N.A.** (2004). Mechanism of Pto-Mediated Disease Resistance: Structural Analysis Provides a New Model. *The Plant Cell Online* **16**, 2543-2545.
- Edwards, H.H.** (2002). Development of primary germ tubes by conidia of *Blumeria graminis* f.sp. *hordei* on leaf epidermal cells of *Hordeum vulgare*. *Canadian Journal of Botany* **80**, 1121-1125.
- Eulgem, T., and Somssich, I.E.** (2007). Networks of WRKY transcription factors in defense signaling. *Current opinion in plant biology* **10**, 366-371.
- Fan, C.Y., Lee, S., and Cyr, D.M.** (2003). Mechanisms for regulation of Hsp70 function by Hsp40. *Cell stress & chaperones* **8**, 309-316.
- Fan, L., Zheng, S., Cui, D., and Wang, X.** (1999). Subcellular distribution and tissue expression of phospholipase D $\alpha$ , D $\beta$ , and D $\gamma$  in *Arabidopsis*. *Plant physiology* **119**, 1371-1378.
- Ferreira, J.J., Campa, A., Perez-Vega, E., Rodriguez-Suarez, C., and Giraldez, R.** (2012). Introgression and pyramiding into common bean market class fabada of genes conferring resistance to anthracnose and potyvirus. *TAG. Theoretical and applied genetics. Theoretische und angewandte Genetik* **124**, 777-788.
- Flor, H.H.** (1956). The Complementary Genic Systems in Flax and Flax Rust. In *Advances in Genetics*, M. Demerec, ed (Academic Press), pp. 29-54.
- Fonseca, S., Chico, J.M., and Solano, R.** (2009). The jasmonate pathway: the ligand, the receptor and the core signalling module. *Current opinion in plant biology* **12**, 539-547.
- Frederick, R.D., Thilmony, R.L., Sessa, G., and Martin, G.B.** (1998). Recognition specificity for the bacterial avirulence protein AvrPto is determined by Thr-204 in the activation loop of the tomato Pto kinase. *Molecular cell* **2**, 241-245.
- Fritz-Laylin, L.K., Krishnamurthy, N., Tor, M., Sjolander, K.V., and Jones, J.D.** (2005). Phylogenomic analysis of the receptor-like proteins of rice and *Arabidopsis*. *Plant physiology* **138**, 611-623.
- Froidure, S., Canonne, J., Daniel, X., Jauneau, A., Briere, C., Roby, D., and Rivas, S.** (2010). AtsPLA2- $\alpha$  nuclear relocalization by the *Arabidopsis* transcription factor AtMYB30 leads to repression of the plant defense response. *Proceedings of the National Academy of Sciences of the United States of America* **107**, 15281-15286.

- Frye, C.A., Tang, D., and Innes, R.W.** (2001). Negative regulation of defense responses in plants by a conserved MAPKK kinase. *Proceedings of the National Academy of Sciences of the United States of America* **98**, 373-378.
- Fu, Z.Q., Yan, S., Saleh, A., Wang, W., Ruble, J., Oka, N., Mohan, R., Spoel, S.H., Tada, Y., Zheng, N., and Dong, X.** (2012). NPR3 and NPR4 are receptors for the immune signal salicylic acid in plants. *Nature* **486**, 228-232.
- Gallagher, T., Ruan, B., London, M., Bryan, M.A., and Bryan, P.N.** (2009). Structure of a switchable subtilisin complexed with a substrate and with the activator azide. *Biochemistry* **48**, 10389-10394.
- Garcia, P., Gupta, R., Shah, S., Morris, A.J., Rudge, S.A., Scarlata, S., Petrova, V., McLaughlin, S., and Rebecchi, M.J.** (1995). The pleckstrin homology domain of phospholipase C-delta 1 binds with high affinity to phosphatidylinositol 4,5-bisphosphate in bilayer membranes. *Biochemistry* **34**, 16228-16234.
- Gaullier, J.M., Simonsen, A., D'Arrigo, A., Bremnes, B., Stenmark, H., and Aasland, R.** (1998). FYVE fingers bind PtdIns(3)P. *Nature* **394**, 432-433.
- Gil, F., and Gay, J.L.** (1977). Ultrastructural and physiological properties of the host interfacial components of haustoria of *Erysiphe pisi* in vivo and in vitro. *Physiological Plant Pathology* **10**, 1-12.
- Gil, J.E., Kim, E., Kim, I.S., Ku, B., Park, W.S., Oh, B.H., Ryu, S.H., Cho, W., and Do Heo, W.** (2012). Phosphoinositides Differentially Regulate Protrudin Localization through the FYVE Domain. *The Journal of biological chemistry* **287**, 41268-41276.
- Gimenez-Ibanez, S., Hann, D.R., Ntoukakis, V., Petutschnig, E., Lipka, V., and Rathjen, J.P.** (2009). AvrPtoB targets the LysM receptor kinase CERK1 to promote bacterial virulence on plants. *Current biology* **19**, 423-429.
- Glawe, D.A.** (2008). The powdery mildews: a review of the world's most familiar (yet poorly known) plant pathogens. *Annual review of phytopathology* **46**, 27-51.
- Glazebrook, J.** (2001). Genes controlling expression of defense responses in *Arabidopsis*--2001 status. *Current opinion in plant biology* **4**, 301-308.
- Glazebrook, J.** (2005). Contrasting mechanisms of defense against biotrophic and necrotrophic pathogens. *Annual review of phytopathology* **43**, 205-227.
- Godi, A., Di Campli, A., Konstantakopoulos, A., Di Tullio, G., Alessi, D.R., Kular, G.S., Daniele, T., Marra, P., Lucocq, J.M., and De Matteis, M.A.** (2004). FAPPs control Golgi-to-cell-surface membrane traffic by binding to ARF and PtdIns(4)P. *Nature cell biology* **6**, 393-404.
- Gollner, K., Schweizer, P., Bai, Y., and Panstruga, R.** (2008). Natural genetic resources of *Arabidopsis thaliana* reveal a high prevalence and unexpected phenotypic plasticity of RPW8-mediated powdery mildew resistance. *The New phytologist* **177**, 725-742.
- Gomez-Gomez, L., and Boller, T.** (2000). FLS2: an LRR receptor-like kinase involved in the perception of the bacterial elicitor flagellin in *Arabidopsis*. *Molecular cell* **5**, 1003-1011.
- Govrin, E.M., and Levine, A.** (2000). The hypersensitive response facilitates plant infection by the necrotrophic pathogen *Botrytis cinerea*. *Current biology* **10**, 751-757.
- Grant, J.J., Chini, A., Basu, D., and Loake, G.J.** (2003). Targeted activation tagging of the *Arabidopsis* NBS-LRR gene, ADR1, conveys resistance to virulent pathogens. *MPMI* **16**, 669-680.
- Grant, M.R., Godiard, L., Straube, E., Ashfield, T., Lewald, J., Sattler, A., Innes, R.W., and Dangl, J.L.** (1995). Structure of the *Arabidopsis* RPM1 gene enabling dual specificity disease resistance. *Science* **269**, 843-846.

- Green, J.R., Carver, T.L.W., and Gurr, S.J.** (2002). The formation and function of infection and feeding structures (American Phytopathological Society (APS) Press).
- Gu, K., Yang, B., Tian, D., Wu, L., Wang, D., Sreekala, C., Yang, F., Chu, Z., Wang, G.L., White, F.F., and Yin, Z.** (2005). R gene expression induced by a type-III effector triggers disease resistance in rice. *Nature* **435**, 1122-1125.
- Gultinan, M., Verica, J., Zhang, D., and Figueira, A.** (2008). Genomics of *Theobroma cacao*, the Food of the Gods. In *Genomics of Tropical Crop Plants* (P. Moore and R. Ming), pp. 145-170.
- Gutierrez, J.R., Balmuth, A.L., Ntoukakis, V., Mucyn, T.S., Gimenez-Ibanez, S., Jones, A.M., and Rathjen, J.P.** (2010). Prf immune complexes of tomato are oligomeric and contain multiple Pto-like kinases that diversify effector recognition. *The Plant Journal* **61**, 507-518.
- Hahn, M., and Mendgen, K.** (1992). Isolation by ConA binding of haustoria from different rust fungi and comparison of their surface qualities. *Protoplasma* **170**, 95-103.
- Hajdukiewicz, P., Svab, Z., and Maliga, P.** (1994). The small, versatile pPZP family of *Agrobacterium* binary vectors for plant transformation. *Plant molecular biology* **25**, 989-994.
- Hammond-Kosack, K.E., and Jones, J.D.** (1997). Plant Disease Resistance Genes. Annual review of plant physiology and plant molecular biology **48**, 575-607.
- Hardham, A.R., Jones, D.A., and Takemoto, D.** (2007). Cytoskeleton and cell wall function in penetration resistance. *Current opinion in plant biology* **10**, 342-348.
- He, P., Shan, L., Lin, N.C., Martin, G.B., Kemmerling, B., Nurnberger, T., and Sheen, J.** (2006). Specific bacterial suppressors of MAMP signaling upstream of MAPKKK in Arabidopsis innate immunity. *Cell* **125**, 563-575.
- Heath, M.C.** (1976). Ultrastructural and functional similarity of the haustorial neckband of rust fungi and the Casparian strip of vascular plants. *Canadian Journal of Botany* **54**, 2484-2489.
- Heese, A., Hann, D.R., Gimenez-Ibanez, S., Jones, A.M., He, K., Li, J., Schroeder, J.I., Peck, S.C., and Rathjen, J.P.** (2007). The receptor-like kinase SERK3/BAK1 is a central regulator of innate immunity in plants. *Proceedings of the National Academy of Sciences of the United States of America* **104**, 12217-12222.
- Heidrich, K., Blanvillain-Baufume, S., and Parker, J.E.** (2012). Molecular and spatial constraints on NB-LRR receptor signaling. *Current opinion in plant biology* **15**, 385-391.
- Heller, J., and Tudzynski, P.** (2011). Reactive oxygen species in phytopathogenic fungi: signaling, development, and disease. *Annual review of phytopathology* **49**, 369-390.
- Hennessy, F., Nicoll, W.S., Zimmermann, R., Cheetham, M.E., and Blatch, G.L.** (2005). Not all J domains are created equal: implications for the specificity of Hsp40-Hsp70 interactions. *Protein science : a publication of the Protein Society* **14**, 1697-1709.
- Herman, P.K., Stack, J.H., and Emr, S.D.** (1992). An essential role for a protein and lipid kinase complex in secretory protein sorting. *Trends in cell biology* **2**, 363-368.
- Hibi, T., Kosugi, S., Iwai, T., Kawata, M., Seo, S., Mitsuhashi, I., and Ohashi, Y.** (2007). Involvement of EIN3 homologues in basic PR gene expression and flower development in tobacco plants. *Journal of experimental botany* **58**, 3671-3678.
- Hong, Y., Zheng, S., and Wang, X.** (2008). Dual functions of phospholipase D $\alpha$ 1 in plant response to drought. *Molecular plant* **1**, 262-269.
- Hong, Z., and Verma, D.P.** (1994). A phosphatidylinositol 3-kinase is induced during soybean nodule organogenesis and is associated with membrane proliferation. *Proceedings of the National Academy of Sciences of the United States of America* **91**, 9617-9621.

- Hubert, D.A., Tornero, P., Belkhadir, Y., Krishna, P., Takahashi, A., Shirasu, K., and Dangl, J.L.** (2003). Cytosolic HSP90 associates with and modulates the Arabidopsis RPM1 disease resistance protein. *The EMBO journal* **22**, 5679-5689.
- Huckelhoven, R.** (2007). Transport and secretion in plant-microbe interactions. *Current opinion in plant biology* **10**, 573-579.
- Huckelhoven, R., and Panstruga, R.** (2011). Cell biology of the plant-powdery mildew interaction. *Current opinion in plant biology* **14**, 738-746.
- Huckelhoven, R., Fodor, J., Preis, C., and Kogel, K.H.** (1999). Hypersensitive cell death and papilla formation in barley attacked by the powdery mildew fungus are associated with hydrogen peroxide but not with salicylic acid accumulation. *Plant physiology* **119**, 1251-1260.
- Islam, A.** (2008). Fungus Resistant Transgenic Plants: Strategies, Progress and Lessons Learnt. *Plant tissue culture and biotechnology* **16**.
- Janjusevic, R., Abramovitch, R.B., Martin, G.B., and Stebbins, C.E.** (2006). A bacterial inhibitor of host programmed cell death defenses is an E3 ubiquitin ligase. *Science* **311**, 222-226.
- Jelenska, J., van Hal, J.A., and Greenberg, J.T.** (2010). *Pseudomonas syringae* hijacks plant stress chaperone machinery for virulence. *Proceedings of the National Academy of Sciences of the United States of America* **107**, 13177-13182.
- Jelenska, J., Yao, N., Vinatzer, B.A., Wright, C.M., Brodsky, J.L., and Greenberg, J.T.** (2007). A J domain virulence effector of *Pseudomonas syringae* remodels host chloroplasts and suppresses defenses. *Current biology* **17**, 499-508.
- Jeworutzki, E., Roelfsema, M.R., Anschutz, U., Krol, E., Elzenga, J.T., Felix, G., Boller, T., Hedrich, R., and Becker, D.** (2010). Early signaling through the Arabidopsis pattern recognition receptors FLS2 and EFR involves Ca-associated opening of plasma membrane anion channels. *The Plant Journal* **62**, 367-378.
- Johnson, A.E., and van Waes, M.A.** (1999). The translocon: a dynamic gateway at the ER membrane. *Annual review of cell and developmental biology* **15**, 799-842.
- Jones, D.A., Thomas, C.M., Hammond-Kosack, K.E., Balint-Kurti, P.J., and Jones, J.D.** (1994). Isolation of the tomato Cf-9 gene for resistance to *Cladosporium fulvum* by transposon tagging. *Science* **266**, 789-793.
- Jones, J.D., and Dangl, J.L.** (2006). The plant immune system. *Nature* **444**, 323-329.
- Jupe, F., Pritchard, L., Etherington, G.J., Mackenzie, K., Cock, P.J., Wright, F., Sharma, S.K., Bolser, D., Bryan, G.J., Jones, J.D., and Hein, I.** (2012). Identification and localisation of the NB-LRR gene family within the potato genome. *BMC genomics* **13**, 75.
- Kagan, J.C.** (2012). Defining the subcellular sites of innate immune signal transduction. *Trends in immunology* **33**, 442-448.
- Kale, S.D., and Tyler, B.M.** (2012). Identification of lipid-binding effectors. *Methods Mol Biol* **835**, 393-414.
- Kale, S.D., Gu, B., Capelluto, D.G., Dou, D., Feldman, E., Rumore, A., Arredondo, F.D., Hanlon, R., Fudal, I., Rouxel, T., Lawrence, C.B., Shan, W., and Tyler, B.M.** (2010). External lipid PI3P mediates entry of eukaryotic pathogen effectors into plant and animal host cells. *Cell* **142**, 284-295.
- Kanzaki, H., Yoshida, K., Saitoh, H., Fujisaki, K., Hirabuchi, A., Alaux, L., Fournier, E., Tharreau, D., and Terauchi, R.** (2012). Arms race co-evolution of *Magnaporthe oryzae* AVR-Pik and rice Pik genes driven by their physical interactions. *The Plant Journal* **72**, 894-907.
- Katsir, L., Chung, H.S., Koo, A.J., and Howe, G.A.** (2008). Jasmonate signaling: a conserved mechanism of hormone sensing. *Current opinion in plant biology* **11**, 428-435.

- Kawai, T., and Akira, S.** (2010). The role of pattern-recognition receptors in innate immunity: update on Toll-like receptors. *Nature immunology* **11**, 373-384.
- Kawchuk, L.M., Hachey, J., Lynch, D.R., Kulcsar, F., van Rooijen, G., Waterer, D.R., Robertson, A., Kokko, E., Byers, R., Howard, R.J., Fischer, R., and Prufer, D.** (2001). Tomato Ve disease resistance genes encode cell surface-like receptors. *Proceedings of the National Academy of Sciences of the United States of America* **98**, 6511-6515.
- Keller, H., Pamboukdjian, N., Ponchet, M., Poupet, A., Delon, R., Verrier, J.L., Roby, D., and Ricci, P.** (1999). Pathogen-induced elicitor production in transgenic tobacco generates a hypersensitive response and nonspecific disease resistance. *The Plant cell* **11**, 223-235.
- Kher, S.S., and Worthylake, R.A.** (2011). Regulation of ROCKII membrane localization through its C-terminus. *Experimental cell research* **317**, 2845-2852.
- Kim, D.H., Eu, Y.J., Yoo, C.M., Kim, Y.W., Pih, K.T., Jin, J.B., Kim, S.J., Stenmark, H., and Hwang, I.** (2001). Trafficking of phosphatidylinositol 3-phosphate from the trans-Golgi network to the lumen of the central vacuole in plant cells. *The Plant cell* **13**, 287-301.
- Kim, M.G., da Cunha, L., McFall, A.J., Belkadir, Y., DebRoy, S., Dangl, J.L., and Mackey, D.** (2005). Two *Pseudomonas syringae* type III effectors inhibit RIN4-regulated basal defense in *Arabidopsis*. *Cell* **121**, 749-759.
- Koh, S., Andre, A., Edwards, H., Ehrhardt, D., and Somerville, S.** (2005). *Arabidopsis thaliana* subcellular responses to compatible *Erysiphe cichoracearum* infections. *The Plant Journal* **44**, 516-529.
- Krinke, O., Flemr, M., Vergnolle, C., Collin, S., Renou, J.P., Taconnat, L., Yu, A., Burketova, L., Valentova, O., Zachowski, A., and Ruelland, E.** (2009). Phospholipase D activation is an early component of the salicylic acid signaling pathway in *Arabidopsis* cell suspensions. *Plant physiology* **150**, 424-436.
- Kuang, H., Woo, S.S., Meyers, B.C., Nevo, E., and Michelmore, R.W.** (2004). Multiple genetic processes result in heterogeneous rates of evolution within the major cluster disease resistance genes in lettuce. *The Plant cell* **16**, 2870-2894.
- Kumar, V., Joshi, S.G., Bell, A.A., and Rathore, K.S.** (2012). Enhanced resistance against *Thielaviopsis basicola* in transgenic cotton plants expressing *Arabidopsis* NPR1 gene. *Transgenic research* [Epub ahead of print].
- Kwon, C., Neu, C., Pajonk, S., Yun, H.S., Lipka, U., Humphry, M., Bau, S., Straus, M., Kwaaitaal, M., Rampelt, H., El Kasmi, F., Jurgens, G., Parker, J., Panstruga, R., Lipka, V., and Schulze-Lefert, P.** (2008). Co-option of a default secretory pathway for plant immune responses. *Nature* **451**, 835-840.
- Lacombe, S., Rougon-Cardoso, A., Sherwood, E., Peeters, N., Dahlbeck, D., van Esse, H.P., Smoker, M., Rallapalli, G., Thomma, B.P., Staskawicz, B., Jones, J.D., and Zipfel, C.** (2010). Interfamily transfer of a plant pattern-recognition receptor confers broad-spectrum bacterial resistance. *Nature biotechnology* **28**, 365-369.
- Lawrence, G.J., Finnegan, E.J., Ayliffe, M.A., and Ellis, J.G.** (1995). The L6 gene for flax rust resistance is related to the *Arabidopsis* bacterial resistance gene RPS2 and the tobacco viral resistance gene N. *The Plant cell* **7**, 1195-1206.
- Laxalt, A.M., and Munnik, T.** (2002). Phospholipid signalling in plant defence. *Current opinion in plant biology* **5**, 332-338.
- Lee, S.W., Han, S.W., Sriyanum, M., Park, C.J., Seo, Y.S., and Ronald, P.C.** (2009). A type I-secreted, sulfated peptide triggers XA21-mediated innate immunity. *Science* **326**, 850-853.

- Lee, Y., Kim, E.S., Choi, Y., Hwang, I., Staiger, C.J., and Chung, Y.Y.** (2008). The Arabidopsis phosphatidylinositol 3-kinase is important for pollen development. *Plant physiology* **147**, 1886-1897.
- Legendre, L., Yueh, Y.G., Crain, R., Haddock, N., Heinsteins, P.F., and Low, P.S.** (1993). Phospholipase C activation during elicitation of the oxidative burst in cultured plant cells. *The Journal of biological chemistry* **268**, 24559-24563.
- Lemmon, M.A., Ferguson, K.M., O'Brien, R., Sigler, P.B., and Schlessinger, J.** (1995). Specific and high-affinity binding of inositol phosphates to an isolated pleckstrin homology domain. *Proceedings of the National Academy of Sciences of the United States of America* **92**, 10472-10476.
- Levashina, E.A., Ohresser, S., Bulet, P., Reichhart, J.M., Hetru, C., and Hoffmann, J.A.** (1995). Metchnikowin, a novel immune-inducible proline-rich peptide from *Drosophila* with antibacterial and antifungal properties. *European journal of biochemistry / FEBS* **233**, 694-700.
- Li, G.L., Li, B., Liu, H.T., and Zhou, R.G.** (2005). [The responses of AtJ2 and AtJ3 gene expression to environmental stresses in Arabidopsis]. *Zhi wu sheng li yu fen zi sheng wu xue xue bao = Journal of plant physiology and molecular biology* **31**, 47-52.
- Li, T., Liu, B., Spalding, M.H., Weeks, D.P., and Yang, B.** (2012). High-efficiency TALEN-based gene editing produces disease-resistant rice. *Nature biotechnology* **30**, 390-392.
- Lipka, U., Fuchs, R., Kuhns, C., Petutschnig, E., and Lipka, V.** (2010). Live and let die--Arabidopsis nonhost resistance to powdery mildews. *European journal of cell biology* **89**, 194-199.
- Lipka, V., Dittgen, J., Bednarek, P., Bhat, R., Wiermer, M., Stein, M., Landtag, J., Brandt, W., Rosahl, S., Scheel, D., Llorente, F., Molina, A., Parker, J., Somerville, S., and Schulze-Lefert, P.** (2005). Pre- and postinvasion defenses both contribute to nonhost resistance in Arabidopsis. *Science* **310**, 1180-1183.
- Liu, Y., Schiff, M., Marathe, R., and Dinesh-Kumar, S.P.** (2002). Tobacco Rar1, EDS1 and NPR1/NIM1 like genes are required for N-mediated resistance to tobacco mosaic virus. *The Plant Journal* **30**, 415-429.
- Lorang, J., Kidarsa, T., Bradford, C.S., Gilbert, B., Curtis, M., Tzeng, S.C., Maier, C.S., and Wolpert, T.J.** (2012). Tricking the guard: exploiting plant defense for disease susceptibility. *Science* **338**, 659-662.
- Lorenzo, O., Piqueras, R., Sanchez-Serrano, J.J., and Solano, R.** (2003). ETHYLENE RESPONSE FACTOR1 integrates signals from ethylene and jasmonate pathways in plant defense. *The Plant cell* **15**, 165-178.
- Lu, Y.J., Schornack, S., Spallek, T., Geldner, N., Chory, J., Schellmann, S., Schumacher, K., Kamoun, S., and Robatzek, S.** (2012). Patterns of plant subcellular responses to successful oomycete infections reveal differences in host cell reprogramming and endocytic trafficking. *Cellular microbiology* **14**, 682-697.
- Lupas, A., Van Dyke, M., and Stock, J.** (1991). Predicting coiled coils from protein sequences. *Science* **252**, 1162-1164.
- Mackey, D., Holt, B.F., 3rd, Wiig, A., and Dangl, J.L.** (2002). RIN4 interacts with *Pseudomonas syringae* type III effector molecules and is required for RPM1-mediated resistance in Arabidopsis. *Cell* **108**, 743-754.
- Mackey, D., Belkhadir, Y., Alonso, J.M., Ecker, J.R., and Dangl, J.L.** (2003). Arabidopsis RIN4 is a target of the type III virulence effector AvrRpt2 and modulates RPS2-mediated resistance. *Cell* **112**, 379-389.

- Makandar, R., Essig, J.S., Schapaugh, M.A., Trick, H.N., and Shah, J.** (2006). Genetically engineered resistance to Fusarium head blight in wheat by expression of Arabidopsis NPR1. *MPMI* **19**, 123-129.
- Manners, J.M., and Gay, J.L.** (1982). Transport, translocation and metabolism of <sup>14</sup>C-photosynthates at the host-parasite interface of *Pisum sativum* and *Erysiphe pisi*. *New Phytologist* **91**, 221-244.
- Martin, G.B., Brommonschenkel, S.H., Chunwongse, J., Frary, A., Ganai, M.W., Spivey, R., Wu, T., Earle, E.D., and Tanksley, S.D.** (1993). Map-based cloning of a protein kinase gene conferring disease resistance in tomato. *Science* **262**, 1432-1436.
- Martinez-Gil, L., Johnson, A.E., and Mingarro, I.** (2010). Membrane insertion and biogenesis of the Turnip crinkle virus p9 movement protein. *Journal of virology* **84**, 5520-5527.
- Martinon, F., and Tschopp, J.** (2005). NLRs join TLRs as innate sensors of pathogens. *Trends in immunology* **26**, 447-454.
- Mayer, A.M., Staples, R.C., and Gil-ad, N.L.** (2001). Mechanisms of survival of necrotrophic fungal plant pathogens in hosts expressing the hypersensitive response. *Phytochemistry* **58**, 33-41.
- Mayor, A., Martinon, F., De Smedt, T., Petrilli, V., and Tschopp, J.** (2007). A crucial function of SGT1 and HSP90 in inflammasome activity links mammalian and plant innate immune responses. *Nature immunology* **8**, 497-503.
- McGrath, K.C., Dombrecht, B., Manners, J.M., Schenk, P.M., Edgar, C.I., Maclean, D.J., Scheible, W.R., Udvardi, M.K., and Kazan, K.** (2005). Repressor- and activator-type ethylene response factors functioning in jasmonate signaling and disease resistance identified via a genome-wide screen of Arabidopsis transcription factor gene expression. *Plant physiology* **139**, 949-959.
- Mehrotra, R.S., and Aneja, R.S.M.K.R.** (1990). *An Introduction To Mycology*. (South Asia Books).
- Meldau, S., Baldwin, I.T., and Wu, J.** (2011). For security and stability: SGT1 in plant defense and development. *Plant signaling & behavior* **6**, 1479-1482.
- Meyers, B.C., Kaushik, S., and Nandety, R.S.** (2005). Evolving disease resistance genes. *Current opinion in plant biology* **8**, 129-134.
- Meyers, B.C., Kozik, A., Griego, A., Kuang, H., and Michelmore, R.W.** (2003). Genome-wide analysis of NBS-LRR-encoding genes in Arabidopsis. *The Plant cell* **15**, 809-834.
- Michelmore, R.W., and Meyers, B.C.** (1998). Clusters of resistance genes in plants evolve by divergent selection and a birth-and-death process. *Genome research* **8**, 1113-1130.
- Monosi, B., Wisser, R.J., Pennill, L., and Hulbert, S.H.** (2004). Full-genome analysis of resistance gene homologues in rice. *TAG. Theoretical and applied genetics. Theoretische und angewandte Genetik* **109**, 1434-1447.
- Mucyn, T.S., Clemente, A., Andriotis, V.M., Balmuth, A.L., Oldroyd, G.E., Staskawicz, B.J., and Rathjen, J.P.** (2006). The tomato NBARC-LRR protein Prf interacts with Pto kinase in vivo to regulate specific plant immunity. *The Plant cell* **18**, 2792-2806.
- Mukhtar, M.S., Carvunis, A.R., Dreze, M., Eppe, P., Steinbrenner, J., Moore, J., Tasan, M., Galli, M., Hao, T., Nishimura, M.T., Pevzner, S.J., Donovan, S.E., Ghamsari, L., Santhanam, B., Romero, V., Poulin, M.M., Gebreab, F., Gutierrez, B.J., Tam, S., Monachello, D., Boxem, M., Harbort, C.J., McDonald, N., Gai, L., Chen, H., He, Y., Vandenhaute, J., Roth, F.P., Hill, D.E., Ecker, J.R., Vidal, M., Beynon, J., Braun, P., and Dangl, J.L.** (2011). Independently evolved virulence effectors converge onto hubs in a plant immune system network. *Science* **333**, 596-601.
- Mun, J.H., Yu, H.J., Park, S., and Park, B.S.** (2009). Genome-wide identification of NBS-encoding resistance genes in *Brassica rapa*. *Molecular genetics and genomics : MGG* **282**, 617-631.



- Munnik, T., and Testerink, C.** (2009). Plant phospholipid signaling: "in a nutshell". *Journal of lipid research* **50 Suppl**, S260-265.
- Munnik, T., and Nielsen, E.** (2011). Green light for polyphosphoinositide signals in plants. *Current opinion in plant biology* **14**, 489-497.
- Myln, J., and Botella, J.R.** (1998). Binary Vectors for Sense and Antisense Expression of Arabidopsis ESTs. *Plant Molecular Biology Reporter* **16**, 257-262.
- Nicaise, V., Roux, M., and Zipfel, C.** (2009). Recent advances in PAMP-triggered immunity against bacteria: pattern recognition receptors watch over and raise the alarm. *Plant physiology* **150**, 1638-1647.
- Nie, H., Zhao, C., Wu, G., Wu, Y., Chen, Y., and Tang, D.** (2012). SR1, a calmodulin-binding transcription factor, modulates plant defense and ethylene-induced senescence by directly regulating NDR1 and EIN3. *Plant physiology* **158**, 1847-1859.
- Nielsen, K.A., Nicholson, R.L., Carver, T.L.W., Kunoh, H., and Oliver, R.P.** (2000). First touch: An immediate response to surface recognition in conidia of *Blumeria graminis*. *Physiological and Molecular Plant Pathology* **56**, 63-70.
- Nielsen, M.E., Feechan, A., Bohlenius, H., Ueda, T., and Thordal-Christensen, H.** (2012). Arabidopsis ARF-GTP exchange factor, GNOM, mediates transport required for innate immunity and focal accumulation of syntaxin PEN1. *Proceedings of the National Academy of Sciences of the United States of America* **109**, 11443-11448.
- Noel, L.D., Cagna, G., Stuttmann, J., Wirthmuller, L., Betsuyaku, S., Witte, C.P., Bhat, R., Pochon, N., Colby, T., and Parker, J.E.** (2007). Interaction between SGT1 and cytosolic/nuclear HSC70 chaperones regulates Arabidopsis immune responses. *The Plant cell* **19**, 4061-4076.
- Nomura, K., Debroy, S., Lee, Y.H., Pumplin, N., Jones, J., and He, S.Y.** (2006). A bacterial virulence protein suppresses host innate immunity to cause plant disease. *Science* **313**, 220-223.
- Nomura, K., Mecey, C., Lee, Y.N., Imboden, L.A., Chang, J.H., and He, S.Y.** (2011). Effector-triggered immunity blocks pathogen degradation of an immunity-associated vesicle traffic regulator in Arabidopsis. *Proceedings of the National Academy of Sciences of the United States of America* **108**, 10774-10779.
- Nuhse, T.S.** (2012). Cell wall integrity signalling and innate immunity in plants. *Frontiers in plant science* **3**.
- Nurnberger, T., Brunner, F., Kemmerling, B., and Piater, L.** (2004). Innate immunity in plants and animals: striking similarities and obvious differences. *Immunological reviews* **198**, 249-266.
- O'Brien, J.A., Daudi, A., Butt, V.S., and Bolwell, G.P.** (2012). Reactive oxygen species and their role in plant defence and cell wall metabolism. *Planta* **236**, 765-779.
- O'Connell, R.J., and Panstruga, R.** (2006). Tete a tete inside a plant cell: establishing compatibility between plants and biotrophic fungi and oomycetes. *The New phytologist* **171**, 699-718.
- O'Neill, L.A., and Bowie, A.G.** (2007). The family of five: TIR-domain-containing adaptors in Toll-like receptor signalling. *Nature reviews. Immunology* **7**, 353-364.
- Oerke, E.** (2007). Crop Losses to Animal Pests, Plant Pathogens, and Weeds. In *Encyclopedia of Pest Management, Volume II* (CRC Press), pp. 116-120.
- Okkenhaug, K., and Vanhaesebroeck, B.** (2001). New responsibilities for the PI3K regulatory subunit p85 alpha. *Science STKE* **2001**, pe1.

- Orgil, U., Araki, H., Tangchaiburana, S., Berkey, R., and Xiao, S.** (2007). Intraspecific genetic variations, fitness cost and benefit of RPW8, a disease resistance locus in *Arabidopsis thaliana*. *Genetics* **176**, 2317-2333.
- Ori, N., Eshed, Y., Paran, I., Presting, G., Aviv, D., Tanksley, S., Zamir, D., and Fluhr, R.** (1997). The I2C family from the wilt disease resistance locus I2 belongs to the nucleotide binding, leucine-rich repeat superfamily of plant resistance genes. *The Plant cell* **9**, 521-532.
- Osharov, N., and May, G.S.** (2001). The molecular mechanisms of conidial germination. *FEMS microbiology letters* **199**, 153-160.
- Pain, N.A., Green, J.R., Gammie, F., and O'Connell, R.J.** (1994). Immunomagnetic isolation of viable intracellular hyphae of *Colletotrichum lindemuthianum* (Sacc. & Magn.) Briosi & Cav. from infected bean leaves using a monoclonal antibody. *New Phytologist* **127**, 223-332.
- Parker, J.E., Coleman, M.J., Szabo, V., Frost, L.N., Schmidt, R., van der Biezen, E.A., Moores, T., Dean, C., Daniels, M.J., and Jones, J.D.** (1997). The *Arabidopsis* downy mildew resistance gene RPP5 shares similarity to the toll and interleukin-1 receptors with N and L6. *The Plant cell* **9**, 879-894.
- Pavan, S., Jacobsen, E., Visser, R.G., and Bai, Y.** (2010). Loss of susceptibility as a novel breeding strategy for durable and broad-spectrum resistance. *Molecular breeding : new strategies in plant improvement* **25**, 1-12.
- Peart, J.R., Mestre, P., Lu, R., Malcuit, I., and Baulcombe, D.C.** (2005). NRG1, a CC-NB-LRR protein, together with N, a TIR-NB-LRR protein, mediates resistance against tobacco mosaic virus. *Current biology* **15**, 968-973.
- Penninckx, I.A., Thomma, B.P., Buchala, A., Metraux, J.P., and Broekaert, W.F.** (1998). Concomitant activation of jasmonate and ethylene response pathways is required for induction of a plant defensin gene in *Arabidopsis*. *The Plant cell* **10**, 2103-2113.
- Pieterse, C.M., Leon-Reyes, A., Van der Ent, S., and Van Wees, S.C.** (2009). Networking by small-molecule hormones in plant immunity. *Nature chemical biology* **5**, 308-316.
- Pieterse, C.M., Van der Does, D., Zamioudis, C., Leon-Reyes, A., and Van Wees, S.C.** (2012). Hormonal modulation of plant immunity. *Annual review of cell and developmental biology* **28**, 489-521.
- Pitzschke, A., Schikora, A., and Hirt, H.** (2009). MAPK cascade signalling networks in plant defence. *Current opinion in plant biology* **12**, 421-426.
- Ploetz, R.C.** (2007). Cacao diseases: important threats to chocolate production worldwide. *Phytopathology* **97**, 1634-1639.
- Preuss, M.L., Schmitz, A.J., Thole, J.M., Bonner, H.K., Otegui, M.S., and Nielsen, E.** (2006). A role for the RabA4b effector protein PI-4Kbeta1 in polarized expansion of root hair cells in *Arabidopsis thaliana*. *The Journal of cell biology* **172**, 991-998.
- Pumplin, N., Zhang, X., Noar, R.D., and Harrison, M.J.** (2012). Polar localization of a symbiosis-specific phosphate transporter is mediated by a transient reorientation of secretion. *Proceedings of the National Academy of Sciences of the United States of America* **109**, E665-672.
- Qiu, X.B., Shao, Y.M., Miao, S., and Wang, L.** (2006). The diversity of the DnaJ/Hsp40 family, the crucial partners for Hsp70 chaperones. *Cellular and molecular life sciences : CMLS* **63**, 2560-2570.
- Raho, N., Ramirez, L., Lanteri, M.L., Gonorazky, G., Lamattina, L., ten Have, A., and Laxalt, A.M.** (2011). Phosphatidic acid production in chitosan-elicited tomato cells, via both

- phospholipase D and phospholipase C/diacylglycerol kinase, requires nitric oxide. *Journal of plant physiology* **168**, 534-539.
- Reymond, P., and Farmer, E.E.** (1998). Jasmonate and salicylate as global signals for defense gene expression. *Current opinion in plant biology* **1**, 404-411.
- Richly, E., Kurth, J., and Leister, D.** (2002). Mode of amplification and reorganization of resistance genes during recent *Arabidopsis thaliana* evolution. *Molecular biology and evolution* **19**, 76-84.
- Roberts, A.M., Mackie, A.J., Hathaway, V., Callow, J.A., and Green, J.R.** (1993). Molecular differentiation in the extrahaustorial membrane of pea powdery mildew haustoria at early and late stages of development. *Physiological and Molecular Plant Pathology* **43**, 147-160.
- Ronald, P.C., and Beutler, B.** (2010). Plant and animal sensors of conserved microbial signatures. *Science* **330**, 1061-1064.
- Ryu, S.B.** (2004). Phospholipid-derived signaling mediated by phospholipase A in plants. *Trends in plant science* **9**, 229-235.
- Saenz-Mata, J., and Jimenez-Bremont, J.F.** (2012). HR4 Gene Is Induced in the *Arabidopsis*-*Trichoderma atroviride* Beneficial Interaction. *International journal of molecular sciences* **13**, 9110-9128.
- Saunders, D.G., Breen, S., Win, J., Schornack, S., Hein, I., Bozkurt, T.O., Champouret, N., Vleeshouwers, V.G., Birch, P.R., Gilroy, E.M., and Kamoun, S.** (2012). Host protein BSL1 associates with *Phytophthora infestans* RXLR effector AVR2 and the *Solanum demissum* Immune receptor R2 to mediate disease resistance. *The Plant cell* **24**, 3420-3434.
- Schwab, R., Ossowski, S., Riester, M., Warthmann, N., and Weigel, D.** (2006). Highly specific gene silencing by artificial microRNAs in *Arabidopsis*. *The Plant cell* **18**, 1121-1133.
- Shah, J.** (2005). Lipids, lipases, and lipid-modifying enzymes in plant disease resistance. *Annual review of phytopathology* **43**, 229-260.
- Shen, L., Kang, Y.G., Liu, L., and Yu, H.** (2011). The J-domain protein J3 mediates the integration of flowering signals in *Arabidopsis*. *The Plant cell* **23**, 499-514.
- Shen, Q.H., Saijo, Y., Mauch, S., Biskup, C., Bieri, S., Keller, B., Seki, H., Ulker, B., Somssich, I.E., and Schulze-Lefert, P.** (2007). Nuclear activity of MLA immune receptors links isolate-specific and basal disease-resistance responses. *Science* **315**, 1098-1103.
- Singh, R.P., Hodson, D.P., Huerta-Espino, J., Jin, Y., Bhavani, S., Njau, P., Herrera-Foessel, S., Singh, P.K., Singh, S., and Govindan, V.** (2011). The emergence of Ug99 races of the stem rust fungus is a threat to world wheat production. *Annual review of phytopathology* **49**, 465-481.
- Song, W.Y., Wang, G.L., Chen, L.L., Kim, H.S., Pi, L.Y., Holsten, T., Gardner, J., Wang, B., Zhai, W.X., Zhu, L.H., Fauquet, C., and Ronald, P.** (1995). A receptor kinase-like protein encoded by the rice disease resistance gene, Xa21. *Science* **270**, 1804-1806.
- Soylu, S.** (2004). Ultrastructural characterisation of the host-pathogen interface in white blister-infected *Arabidopsis* leaves. *Mycopathologia* **158**, 457-464.
- Srichumpa, P., Brunner, S., Keller, B., and Yahiaoui, N.** (2005). Allelic series of four powdery mildew resistance genes at the Pm3 locus in hexaploid bread wheat. *Plant physiology* **139**, 885-895.
- Staples, R.C.** (2001). Nutrients for a rust fungus: the role of haustoria. *Trends in plant science* **6**, 496-498.
- Stein, M., Dittgen, J., Sanchez-Rodriguez, C., Hou, B.H., Molina, A., Schulze-Lefert, P., Lipka, V., and Somerville, S.** (2006). *Arabidopsis* PEN3/PDR8, an ATP binding cassette transporter,

- contributes to nonhost resistance to inappropriate pathogens that enter by direct penetration. *The Plant cell* **18**, 731-746.
- Strange, R.N., and Scott, P.R.** (2005). Plant disease: a threat to global food security. *Annual review of phytopathology* **43**, 83-116.
- Sun, X., Cao, Y., Yang, Z., Xu, C., Li, X., Wang, S., and Zhang, Q.** (2004). Xa26, a gene conferring resistance to *Xanthomonas oryzae* pv. *oryzae* in rice, encodes an LRR receptor kinase-like protein. *The Plant Journal* **37**, 517-527.
- Swiderski, M.R., and Innes, R.W.** (2001). The Arabidopsis PBS1 resistance gene encodes a member of a novel protein kinase subfamily. *The Plant Journal* **26**, 101-112.
- Szabo, L.J., and Bushnell, W.R.** (2001). Hidden robbers: the role of fungal haustoria in parasitism of plants. *Proceedings of the National Academy of Sciences of the United States of America* **98**, 7654-7655.
- Takemoto, D., Rafiqi, M., Hurley, U., Lawrence, G.J., Bernoux, M., Hardham, A.R., Ellis, J.G., Dodds, P.N., and Jones, D.A.** (2012). N-terminal motifs in some plant disease resistance proteins function in membrane attachment and contribute to disease resistance. *MPMI* **25**, 379-392.
- Tan, M.Y., Hutten, R.C., Visser, R.G., and van Eck, H.J.** (2010). The effect of pyramiding *Phytophthora infestans* resistance genes R Pi-mcd1 and R Pi-ber in potato. *TAG. Theoretical and applied genetics. Theoretische und angewandte Genetik* **121**, 117-125.
- Tang, X., Xie, M., Kim, Y.J., Zhou, J., Klessig, D.F., and Martin, G.B.** (1999). Overexpression of Pto activates defense responses and confers broad resistance. *The Plant cell* **11**, 15-29.
- Testerink, C., Larsen, P.B., McLoughlin, F., van der Does, D., van Himbergen, J.A., and Munnik, T.** (2008). PA, a stress-induced short cut to switch-on ethylene signalling by switching-off CTR1? *Plant signaling & behavior* **3**, 681-683.
- Thines, B., Katsir, L., Melotto, M., Niu, Y., Mandaokar, A., Liu, G., Nomura, K., He, S.Y., Howe, G.A., and Browse, J.** (2007). JAZ repressor proteins are targets of the SCF(COI1) complex during jasmonate signalling. *Nature* **448**, 661-665.
- Thole, J.M., and Nielsen, E.** (2008). Phosphoinositides in plants: novel functions in membrane trafficking. *Current opinion in plant biology* **11**, 620-631.
- Thomma, B.P., Nurnberger, T., and Joosten, M.H.** (2011). Of PAMPs and effectors: the blurred PTI-ETI dichotomy. *The Plant cell* **23**, 4-15.
- Thomma, B.P., Penninckx, I.A., Broekaert, W.F., and Cammue, B.P.** (2001). The complexity of disease signaling in Arabidopsis. *Current opinion in immunology* **13**, 63-68.
- Tor, M., Brown, D., Cooper, A., Woods-Tor, A., Sjolander, K., Jones, J.D., and Holub, E.B.** (2004). Arabidopsis downy mildew resistance gene RPP27 encodes a receptor-like protein similar to CLAVATA2 and tomato Cf-9. *Plant physiology* **135**, 1100-1112.
- Turk, E., Kerner, C.J., Lostao, M.P., and Wright, E.M.** (1996). Membrane topology of the human Na<sup>+</sup>/glucose cotransporter SGLT1. *The Journal of biological chemistry* **271**, 1925-1934.
- Uemura, T., Ueda, T., Ohniwa, R.L., Nakano, A., Takeyasu, K., and Sato, M.H.** (2004). Systematic analysis of SNARE molecules in Arabidopsis: dissection of the post-Golgi network in plant cells. *Cell structure and function* **29**, 49-65.
- Uppalapati, S.R., Ishiga, Y., Ryu, C.M., Ishiga, T., Wang, K., Noel, L.D., Parker, J.E., and Mysore, K.S.** (2011). SGT1 contributes to coronatine signaling and *Pseudomonas syringae* pv. tomato disease symptom development in tomato and Arabidopsis. *The New phytologist* **189**, 83-93.
- Uraji, M., Katagiri, T., Okuma, E., Ye, W., Hossain, M.A., Masuda, C., Miura, A., Nakamura, Y., Mori, I.C., Shinozaki, K., and Murata, Y.** (2012). Cooperative function of PLDdelta and

- PLD $\alpha$ 1 in abscisic acid-induced stomatal closure in Arabidopsis. *Plant physiology* **159**, 450-460.
- Van der Biezen, E.A., and Jones, J.D.** (1998). Plant disease-resistance proteins and the gene-for-gene concept. *Trends in biochemical sciences* **23**, 454-456.
- van der Hoorn, R.A., Wulff, B.B., Rivas, S., Durrant, M.C., van der Ploeg, A., de Wit, P.J., and Jones, J.D.** (2005). Structure-function analysis of cf-9, a receptor-like protein with extracytoplasmic leucine-rich repeats. *The Plant cell* **17**, 1000-1015.
- van der Luit, A.H., Piatti, T., van Doorn, A., Musgrave, A., Felix, G., Boller, T., and Munnik, T.** (2000). Elicitation of suspension-cultured tomato cells triggers the formation of phosphatidic acid and diacylglycerol pyrophosphate. *Plant physiology* **123**, 1507-1516.
- van Doorn, W.G.** (2011). Classes of programmed cell death in plants, compared to those in animals. *Journal of experimental botany* **62**, 4749-4761.
- van Leeuwen, W., Vermeer, J.E., Gadella, T.W., Jr., and Munnik, T.** (2007). Visualization of phosphatidylinositol 4,5-bisphosphate in the plasma membrane of suspension-cultured tobacco BY-2 cells and whole Arabidopsis seedlings. *The Plant Journal* **52**, 1014-1026.
- van Noort, J.M., Bsibsi, M., Nacken, P., Gerritsen, W.H., and Amor, S.** (2012). The link between small heat shock proteins and the immune system. *The international journal of biochemistry & cell biology* **44**, 1670-1679.
- Ve, T., Gay, N.J., Mansell, A., Kobe, B., and Kellie, S.** (2012). Adaptors in toll-like receptor signaling and their potential as therapeutic targets. *Current drug targets* **13**, 1360-1374.
- Vermeer, J.E., Thole, J.M., Goedhart, J., Nielsen, E., Munnik, T., and Gadella, T.W., Jr.** (2009). Imaging phosphatidylinositol 4-phosphate dynamics in living plant cells. *The Plant Journal* **57**, 356-372.
- Vermeer, J.E., van Leeuwen, W., Tobena-Santamaria, R., Laxalt, A.M., Jones, D.R., Divecha, N., Gadella, T.W., Jr., and Munnik, T.** (2006). Visualization of PtdIns3P dynamics in living plant cells. *The Plant Journal* **47**, 687-700.
- Viala, J., Sansonetti, P., and Philpott, D.J.** (2004). Nods and 'intracellular' innate immunity. *Comptes rendus biologies* **327**, 551-555.
- Vicinanza, M., D'Angelo, G., Di Campli, A., and De Matteis, M.A.** (2008). Function and dysfunction of the PI system in membrane trafficking. *The EMBO journal* **27**, 2457-2470.
- Vieira, O.V., Botelho, R.J., Rameh, L., Brachmann, S.M., Matsuo, T., Davidson, H.W., Schreiber, A., Backer, J.M., Cantley, L.C., and Grinstein, S.** (2001). Distinct roles of class I and class III phosphatidylinositol 3-kinases in phagosome formation and maturation. *The Journal of cell biology* **155**, 19-25.
- Voegele, R.T., and Mendgen, K.** (2003). Rust haustoria: nutrient uptake and beyond. *New Phytologist* **159**, 93-100.
- Voegele, R.T., Struck, C., Hahn, M., and Mendgen, K.** (2001). The role of haustoria in sugar supply during infection of broad bean by the rust fungus *Uromyces fabae*. *Proceedings of the National Academy of Sciences of the United States of America* **98**, 8133-8138.
- Vossen, J.H., Abd-El-Haliem, A., Fradin, E.F., van den Berg, G.C., Ekengren, S.K., Meijer, H.J., Seifi, A., Bai, Y., ten Have, A., Munnik, T., Thomma, B.P., and Joosten, M.H.** (2010). Identification of tomato phosphatidylinositol-specific phospholipase-C (PI-PLC) family members and the role of PLC4 and PLC6 in HR and disease resistance. *The Plant Journal* **62**, 224-239.
- Wachinger, M., Kleinschmidt, A., Winder, D., von Pechmann, N., Ludvigsen, A., Neumann, M., Holle, R., Salmons, B., Erfle, V., and Brack-Werner, R.** (1998). Antimicrobial peptides melittin and cecropin inhibit replication of human immunodeficiency virus 1 by suppressing viral gene expression. *The Journal of general virology* **79** ( Pt 4), 731-740.

- Wang, C., and Wang, X.** (2001). A novel phospholipase D of Arabidopsis that is activated by oleic acid and associated with the plasma membrane. *Plant physiology* **127**, 1102-1112.
- Wang, D., Amornsiripanitch, N., and Dong, X.** (2006). A genomic approach to identify regulatory nodes in the transcriptional network of systemic acquired resistance in plants. *PLoS pathogens* **2**, e123.
- Wang, G., Ryu, S., and Wang, X.** (2012a). Plant Phospholipases: An Overview. In *Lipases and Phospholipases*, G. Sandoval, ed (Humana Press), pp. 123-137.
- Wang, W., Devoto, A., Turner, J.G., and Xiao, S.** (2007). Expression of the membrane-associated resistance protein RPW8 enhances basal defense against biotrophic pathogens. *MPMI* **20**, 966-976.
- Wang, W., Wen, Y., Berkey, R., and Xiao, S.** (2009). Specific targeting of the Arabidopsis resistance protein RPW8.2 to the interfacial membrane encasing the fungal Haustorium renders broad-spectrum resistance to powdery mildew. *The Plant cell* **21**, 2898-2913.
- Wang, W., Berkey, R., Wen, Y., and Xiao, S.** (2010). Accurate and adequate spatiotemporal expression and localization of RPW8.2 is key to activation of resistance at the host-pathogen interface. *Plant signaling & behavior* **5**, 1002-1005.
- Wang, W.M., Ma, X.F., Zhang, Y., Luo, M.C., Wang, G.L., Bellizzi, M., Xiong, X.Y., and Xiao, S.Y.** (2012b). PAPP2C interacts with the atypical disease resistance protein RPW8.2 and negatively regulates salicylic acid-dependent defense responses in Arabidopsis. *Molecular plant* **5**, 1125-1137.
- Wang, X.** (2001). Plant Phospholipases. *Annual review of plant physiology and plant molecular biology* **52**, 211-231.
- Wang, X.** (2004). Lipid signaling. *Current opinion in plant biology* **7**, 329-336.
- Weber, S.S., Ragaz, C., and Hilbi, H.** (2009). Pathogen trafficking pathways and host phosphoinositide metabolism. *Molecular microbiology* **71**, 1341-1352.
- Wei, F., Wing, R.A., and Wise, R.P.** (2002). Genome dynamics and evolution of the Mla (powdery mildew) resistance locus in barley. *The Plant cell* **14**, 1903-1917.
- Wells, J.A., and Estell, D.A.** (1988). Subtilisin — an enzyme designed to be engineered. *Trends in biochemical sciences* **13**, 291-297.
- Welters, P., Takegawa, K., Emr, S.D., and Chrispeels, M.J.** (1994). AtVPS34, a phosphatidylinositol 3-kinase of Arabidopsis thaliana, is an essential protein with homology to a calcium-dependent lipid binding domain. *Proceedings of the National Academy of Sciences of the United States of America* **91**, 11398-11402.
- Wen, Y., Wang, W., Feng, J., Luo, M.C., Tsuda, K., Katagiri, F., Bauchan, G., and Xiao, S.** (2011). Identification and utilization of a sow thistle powdery mildew as a poorly adapted pathogen to dissect post-invasion non-host resistance mechanisms in Arabidopsis. *Journal of experimental botany* **62**, 2117-2129.
- Whitham, S., Dinesh-Kumar, S.P., Choi, D., Hehl, R., Corr, C., and Baker, B.** (1994). The product of the tobacco mosaic virus resistance gene N: similarity to toll and the interleukin-1 receptor. *Cell* **78**, 1101-1115.
- Wiermer, M., Feys, B.J., and Parker, J.E.** (2005). Plant immunity: the EDS1 regulatory node. *Current opinion in plant biology* **8**, 383-389.
- Wright, A.J., Thomas, B.J., and Carver, T.L.W.** (2002). Early adhesion of Blumeria graminis to plant and artificial surfaces demonstrated by centrifugation. *Physiological and Molecular Plant Pathology* **61**, 217-226.
- Wu, Y., Zhang, D., Chu, J.Y., Boyle, P., Wang, Y., Brindle, I.D., De Luca, V., and Despres, C.** (2012). The Arabidopsis NPR1 protein is a receptor for the plant defense hormone salicylic acid. *Cell reports* **1**, 639-647.

- Wymann, M.P., and Pirola, L.** (1998). Structure and function of phosphoinositide 3-kinases. *Biochimica et biophysica acta* **1436**, 127-150.
- Xiang, T., Zong, N., Zou, Y., Wu, Y., Zhang, J., Xing, W., Li, Y., Tang, X., Zhu, L., Chai, J., and Zhou, J.M.** (2008). *Pseudomonas syringae* effector AvrPto blocks innate immunity by targeting receptor kinases. *Current biology* **18**, 74-80.
- Xiao, S., Wang, W., and Yang, X.** (2008). Evolution of Resistance Genes in Plants
- Innate Immunity of Plants, Animals, and Humans, H. Heine, ed (Springer Berlin Heidelberg), pp. 1-25.
- Xiao, S., Charoenwattana, P., Holcombe, L., and Turner, J.G.** (2003a). The Arabidopsis genes RPW8.1 and RPW8.2 confer induced resistance to powdery mildew diseases in tobacco. *MPMI* **16**, 289-294.
- Xiao, S., Ellwood, S., Findlay, K., Oliver, R.P., and Turner, J.G.** (1997). Characterization of three loci controlling resistance of Arabidopsis thaliana accession Ms-0 to two powdery mildew diseases. *The Plant Journal* **12**, 757-768.
- Xiao, S., Brown, S., Patrick, E., Brearley, C., and Turner, J.G.** (2003b). Enhanced transcription of the Arabidopsis disease resistance genes RPW8.1 and RPW8.2 via a salicylic acid-dependent amplification circuit is required for hypersensitive cell death. *The Plant cell* **15**, 33-45.
- Xiao, S., Ellwood, S., Calis, O., Patrick, E., Li, T., Coleman, M., and Turner, J.G.** (2001). Broad-spectrum mildew resistance in Arabidopsis thaliana mediated by RPW8. *Science* **291**, 118-120.
- Xiao, S., Emerson, B., Ratanasut, K., Patrick, E., O'Neill, C., Bancroft, I., and Turner, J.G.** (2004). Origin and maintenance of a broad-spectrum disease resistance locus in Arabidopsis. *Molecular biology and evolution* **21**, 1661-1672.
- Xiao, S., Calis, O., Patrick, E., Zhang, G., Charoenwattana, P., Muskett, P., Parker, J.E., and Turner, J.G.** (2005). The atypical resistance gene, RPW8, recruits components of basal defence for powdery mildew resistance in Arabidopsis. *The Plant Journal* **42**, 95-110.
- Xie, D.X., Feys, B.F., James, S., Nieto-Rostro, M., and Turner, J.G.** (1998). COI1: an Arabidopsis gene required for jasmonate-regulated defense and fertility. *Science* **280**, 1091-1094.
- Xu, L., Liu, F., Lechner, E., Genschik, P., Crosby, W.L., Ma, H., Peng, W., Huang, D., and Xie, D.** (2002). The SCF(COI1) ubiquitin-ligase complexes are required for jasmonate response in Arabidopsis. *The Plant cell* **14**, 1919-1935.
- Yamaguchi, T., Minami, E., Ueki, J., and Shibuya, N.** (2005). Elicitor-induced activation of phospholipases plays an important role for the induction of defense responses in suspension-cultured rice cells. *Plant & cell physiology* **46**, 579-587.
- Yan, A., and Lennarz, W.J.** (2005). Unraveling the mechanism of protein N-glycosylation. *The Journal of biological chemistry* **280**, 3121-3124.
- Yang, X., Wang, W., Coleman, M., Orgil, U., Feng, J., Ma, X., Ferl, R., Turner, J.G., and Xiao, S.** (2009). Arabidopsis 14-3-3 lambda is a positive regulator of RPW8-mediated disease resistance. *The Plant Journal* **60**, 539-550.
- Ye, C.M., Kelly, V., Payton, M., Dickman, M.B., and Verchot, J.** (2012). SGT1 is induced by the potato virus X TGBp3 and enhances virus accumulation in *Nicotiana benthamiana*. *Molecular plant* **5**, 1151-1153.
- Young, S.A., Wang, X., and Leach, J.E.** (1996). Changes in the Plasma Membrane Distribution of Rice Phospholipase D during Resistant Interactions with *Xanthomonas oryzae* pv *oryzae*. *The Plant cell* **8**, 1079-1090.

- Yue, J.X., Meyers, B.C., Chen, J.Q., Tian, D., and Yang, S.** (2012). Tracing the origin and evolutionary history of plant nucleotide-binding site-leucine-rich repeat (NBS-LRR) genes. *The New phytologist* **193**, 1049-1063.
- Zarei, A., Korbes, A.P., Younessi, P., Montiel, G., Champion, A., and Memelink, J.** (2011). Two GCC boxes and AP2/ERF-domain transcription factor ORA59 in jasmonate/ethylene-mediated activation of the PDF1.2 promoter in Arabidopsis. *Plant molecular biology* **75**, 321-331.
- Zasloff, M.** (1987). Magainins, a class of antimicrobial peptides from *Xenopus* skin: isolation, characterization of two active forms, and partial cDNA sequence of a precursor. *Proceedings of the National Academy of Sciences of the United States of America* **84**, 5449-5453.
- Zhang, J., and Zhou, J.M.** (2010). Plant immunity triggered by microbial molecular signatures. *Molecular plant* **3**, 783-793.
- Zhang, J., Li, W., Xiang, T., Liu, Z., Laluk, K., Ding, X., Zou, Y., Gao, M., Zhang, X., Chen, S., Mengiste, T., Zhang, Y., and Zhou, J.M.** (2010). Receptor-like cytoplasmic kinases integrate signaling from multiple plant immune receptors and are targeted by a *Pseudomonas syringae* effector. *Cell host & microbe* **7**, 290-301.
- Zhang, Y., Fan, W., Kinkema, M., Li, X., and Dong, X.** (1999). Interaction of NPR1 with basic leucine zipper protein transcription factors that bind sequences required for salicylic acid induction of the PR-1 gene. *Proceedings of the National Academy of Sciences of the United States of America* **96**, 6523-6528.
- Zhang, Z., Henderson, C., Perfect, E., Carver, T.L., Thomas, B.J., Skamnioti, P., and Gurr, S.J.** (2005). Of genes and genomes, needles and haystacks: *Blumeria graminis* and functionality. *Molecular plant pathology* **6**, 561-575.
- Zhou, J.M., Trifa, Y., Silva, H., Pontier, D., Lam, E., Shah, J., and Klessig, D.F.** (2000). NPR1 differentially interacts with members of the TGA/OBF family of transcription factors that bind an element of the PR-1 gene required for induction by salicylic acid. *MPMI* **13**, 191-202.
- Zhou, R., and Miernyk, J.A.** (1999). Cloning and analysis of AtJ3 gene in *Arabidopsis thaliana*. *Acta Botanica Sinica* **41**, 597-602.
- Zhou, T., Wang, Y., Chen, J.Q., Araki, H., Jing, Z., Jiang, K., Shen, J., and Tian, D.** (2004). Genome-wide identification of NBS genes in japonica rice reveals significant expansion of divergent non-TIR NBS-LRR genes. *Molecular genetics and genomics : MGG* **271**, 402-415.
- Zipfel, C., and Felix, G.** (2005). Plants and animals: a different taste for microbes? *Current opinion in plant biology* **8**, 353-360.
- Zipfel, C., Kunze, G., Chinchilla, D., Caniard, A., Jones, J.D., Boller, T., and Felix, G.** (2006). Perception of the bacterial PAMP EF-Tu by the receptor EFR restricts *Agrobacterium*-mediated transformation. *Cell* **125**, 749-760.